Effect of an Intermediate Material Layer on the Lateral Load-Slip Characteristics of Nailed Joints

by

Tomas Plesnik

A thesis submitted to the Faculty of Graduate and Post Doctoral Affairs in partial fulfillment of the requirements for the degree of

Master of Applied Science

in

Civil Engineering

Department of Civil and Environmental Engineering

Carleton University

Ottawa, Ontario

Abstract

The current understanding of the performance of nailed connections within light frame shear walls is limited to situations where sheathing is either in direct contact with framing, or with a small air gap in between the sheathing and framing. Current design standards in Canada conditionally allow the use of shear walls with a layer of gypsum wallboard between the sheathing and framing without compromising shear wall capacity. This type of wall assembly was experimentally tested on 132 tensile specimens replicating nailed connections in shear walls, incorporating intermediate material thicknesses ranging from 0 mm to 38.1 mm of gypsum wallboard or rigid insulation. Finite element and analytical models were created to simulate the performance of a nailed connection, and were validated by the experimental results. Results from this study suggest that adding gypsum or insulation will greatly decrease the capacity and stiffness of the connection.

Acknowledgements

I would like to thank the entire laboratory staff at the Civil Engineering lab at Carleton University for their assistance, training, patience and accommodation with all experimental work done in the summer of 2013, especially Stan Conley and Jason Arnott. This project would not have been possible without their help, the use of the material testing machine, lab time and space.

Experimental work for this project was funded in part by the departments of Civil and Environmental Engineering at both Carleton University and the University of Ottawa.

I would like to thank my supervisors Dr. Jeffrey Erochko at Carleton University and Dr. Ghasan Doudak at the University of Ottawa for their assistance, guidance, advice, encouragement and patience.

I would like to thank my assistant, Jeff Salmon, for helping me construct and test specimens.

I would like to thank my best friend, a source of inspiration, motivation and endless camaraderie during even the darkest times, Eric Kemp.

Finally, I would like to thank my parents Jana and Martin, and my sister Eva for being unwaveringly supportive of all my studies.

Table of Contents

List of Tables

List of Figures

List of Appendices

1. INTRODUCTION

Timber is a highly versatile, renewable and light weight building material used extensively in residential and commercial structures in North America. Timber is differentiated from generic "wood" in that it refers to wood of structural sizes and typically softwood (coniferous) species. Of all timber structures, the majority are characterized as "light frame", which refers to the use of many small-sized, closely spaced members held together by nailing. Light frame structures are typically very lightweight, material efficient, cheap and relatively quick to assemble. They are the dominant form of construction for residential housing and are a growing industry in Canada (CMHC, 2013). A typical light frame structure consists of several structural elements including shear walls, flooring/ceiling/diaphragms, roof systems, partition walls, and foundations. All timber construction in Canada must be designed with and adhere to the Standard for Engineering Design in Wood, CSA-O86 (CSA, 2010).

1.1 Shear Walls

A shear wall is a structural system designed to resist lateral loads such as those caused by wind or earthquakes. In general, shear walls in structures can be built from a variety of materials including masonry, concrete, or timber. For light frame timber construction, the form of a simple, rudimentary shear wall is shown in Figure 1.1. Light frame shear walls consist of sheathing panels which are fastened using common nails to the external side or both sides of timber framing. At a minimum, the most basic framing consists of spaced wall studs secured by top and bottom chords. Shear walls can be sheathed with panels of plywood, oriented strand board (OSB), or gypsum wallboard

(GWB). When a shear wall is loaded in shear, it is loaded in-plane, which results in a high capacity to resist lateral loads. Framing members are loaded axially and in bending, sheathing is loaded in shear and nails are loaded in bending. There is a high degree of redundancy as the applied shear load is distributed to a large number of individual nailed connections. Deformation in a shear wall occurs in several locations: bending in the nails, compression and bending of framing members, rotation of sheathing panels, and shear deflection of the panels. Shear walls, and particularly the nailed connections are designed to be highly ductile and efficient at energy absorption.

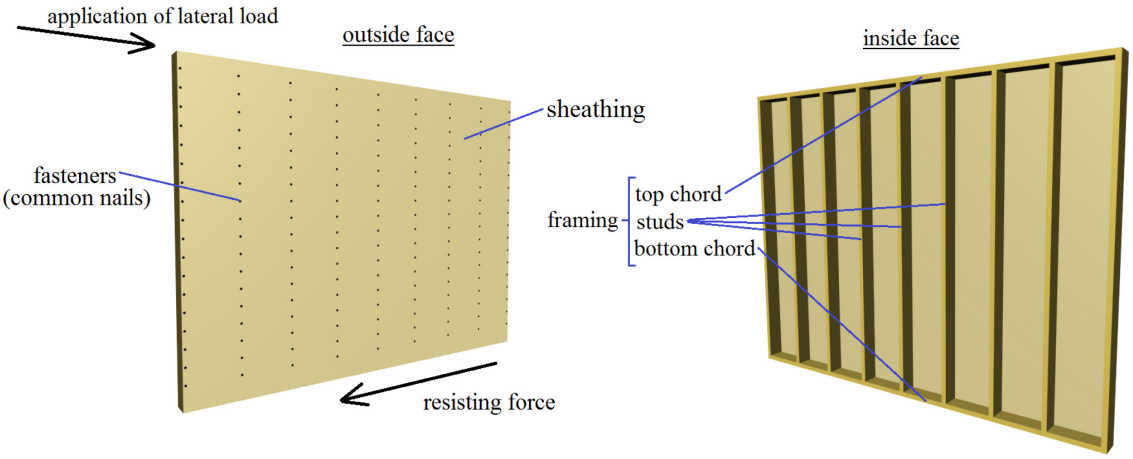

Figure 1.1: Generalized light frame shear wall components

1.2 Intermediate Materials

Nailed connections in light frame shear walls perform at their highest capacity when sheathing is directly in contact with framing. This is not always the case, as the interface may unintentionally open due to member shrinkage or loading-unloading

cycles, thus removing the benefit of interface friction. The sheathing-framing interface may also be intentionally be broken by the decision to introduce intermediate materials.

There are a number of practical reasons why a designer may want to include an intermediate material. The standard for Engineering Design in Wood, CSA-O86 (CSA, 2010) currently allows gypsum wallboard (GWB) as an intermediate material. This type of shear wall design may be useful in the retrofit of existing walls. According to the standard, in a retrofit context, interior walls already sheathed in GWB may potentially be strengthened by the addition of a layer of sheathing (plywood or OSB) overtop of the GWB, without needing to remove the GWB first. In addition to reducing the labor required, this would also have the benefit of increasing the fire resistance of the wall.

Another potentially advantageous intermediate material is rigid insulation. Currently, building technologies exist which feature rigid insulation sandwiched between wall sheathing and framing, such as the Zip-system introduced by Huber Engineered Woods LLC, and shown in Figure 1.2 (Huber, 2012). This system consists of a proprietary sheathing solution, incorporating layers of wall sheathing, insulation and vapor barrier into a single prefabricated element. There are significant advantages in incorporating several building envelope functions into one product in this way, the most significant being a reduction in labor costs. This type of system, being applied continuously on the outer surface of the wall, would provide a continuous, uninterrupted insulation layer which would increase the thermal efficiency of the structure, since thermal bridging through the studs would be mitigated. Currently, some selected Zip-system insulated panels are permitted to be used as sheathing in shear walls in the United States, with reduced specified shear capacity (ICCES, 2013).

Figure 1.2: Zip-system for wall sheathing (Huber, 2012)

1.3 Problem Definition

The current Canadian design standard, *Engineering Design in Wood CSA-O86*, (described in detail in Section 2.1), specifies that sheathing must be fastened (nailed) directly to framing in a light frame shear wall. The exception to this rule is that a 1/2" (12.7 mm) or 5/8" (15.9 mm) GWB layer may exist as an intermediate material between sheathing and framing. This layer is assumed to not compromise the lateral strength or stiffness of the wall, as long as a certain minimum nail penetration is maintained. In this situation, the wall is sheathed in plywood or OSB overtop of a GWB panel. According to the standard, the capacity of such a shear wall is assumed to be equal to that of a shear wall without an intermediate GWB panel (CSA, 2010). To the knowledge of the author, the assumption in the standard has not been directly verified by experiment. The likely assumption is that since GWB is itself permitted to be used as sheathing, its inclusion in a plywood or OSB-sheathed shear wall would not be detrimental, but would rather contribute to shear capacity of the sheathing. The exception permitted by the Canadian

design standard must be tested to ensure the integrity of shear wall designs and by extension ensure general public safety.

Past research in the area of other intermediate materials in nailed connections has been limited to very small intermediate material or air gap thicknesses. In light of this, it would be highly beneficial to quantify and explain the effect of the inclusion of thicker layers of insulation or GWB as intermediate materials.

1.4 Objectives and Methodology

In this study, individual nailed connections of the type found in light frame shear walls were tested, with and without an intermediate layer of GWB of the thicknesses permitted by Canadian design standards (CSA-O86). The results of these tests were analyzed to determine if connections with an intermediate layer of GWB had as much capacity and stiffness as those without one, and by extension, to determine theoretically whether or not shear walls with intermediate GWB panels have as much capacity as those without.

In addition to the test of nailed interfaces with standard thicknesses of GWB, this study also experimentally tested nailed connections of the same type, with intermediate layers of rigid, extruded polystyrene insulation (XPS) of various thicknesses. Similarly, the results of these tests were analyzed to quantify the loss of connection capacity and stiffness that occurs with increasing insulation (gap) thickness.

These two goals were achieved through the experimental testing of specimens that were designed to replicate nailed connections in light frame shear walls. Each specimen was designed for the application of a pure lateral load on 4 nails embedded in two

sheathing strips, on either side of a stud segment. In total, 132 specimens were built and tested in this study. Six identical specimens were built and tested for each combination of sheathing thickness, intermediate material type (GWB or insulation), intermediate material thickness, and nail size considered. In total, there were 9 parameter combinations tested for specimens with GWB as an intermediate material, and 13 parameter combinations tested for specimens with insulation as an intermediate material. For all tests, OSB was used as the primary sheathing material, with SPF (spruce-pine-fir) lumber used to simulate framing.

Finite element and analytical models of nailed connections were adapted from previous models to simulate the nailed connection in question. The finite element model was constructed using the nonlinear modeling software OpenSees and was based on a previous model of a simple nailed connection without intermediate materials by Ni (1997). The analytical model was derived from yield equations of relevant failure modes found by Aune & Patton-Mallory (1986). The analytical model is loosely based on the European Yield Model, used in practice today, and first introduced by Johansen (1949). Both types of models were used to simulate all of the connections tested experimentally, the results of which were compared with experimental values to test their accuracy in predicting connection behavior.

1.5 Thesis Structure

Chapter 2 will begin with a discussion of the process of the design of light frame shear walls in Canada and the design of nailed connections in general. This chapter will then review relevant past literature related to nailed connections with intermediate gaps and

how current design standards were influenced. Finally, specific knowledge gaps are identified and a plan for addressing them is put forward.

Chapter 3 will describe the method used for all of the experimental testing in this study. This chapter will discuss apparatus, instrumentation, data recording, specimen design and preparation, determination of an appropriate testing matrix, and the relevant properties of all materials involved.

Chapter 4 will summarize the results of the experimental testing, and compare load-deformation curves for tests with various intermediate GWB and insulation thicknesses. Following this, the location of the yield point will be calculated using various methods, and curve fitting analysis will be conducted for each case. The chapter will conclude with a comparison of all methods used to calculate connection capacity and stiffness, and quantify the loss in capacity and stiffness as a function of intermediate material type and thickness.

Chapter 5 will begin with a description of the creation, development, testing and use of a finite element model that simulates the types of connections considered in this study. The results of the model are discussed and compared with experimental results using the same methods used in Chapter 4. This chapter will follow with the derivation of an analytical model of the nailed connection. Experimental results, and results from the finite element and analytical models are then compared.

Conclusions and recommendations are provided in Chapter 6

2. LITERATURE REVIEW

This chapter will explain the mechanics and rudimentary design methodology of light frame timber shear walls according to the Canadian standards of timber design. Following this, the origins and development of the Canadian standard in the area of nailed connections will be summarized. A discussion of the contributions from studies that considered the use of interface gaps and intermediate materials between wood members in nailed connections will also be presented. This chapter will also describe finite element models of nailed connections used in past research studies, and will conclude with a statement of motivation for this research, which will specify the current gaps in knowledge that this study will attempt to address.

2.1 Terminology

The following common basic terms are used extensively in this thesis:

SPF: Spruce-Pine-Fir - a term used to describe a collection of Canadian softwood species with similar strength properties

OSB: Oriented Strand Board - a common, inexpensive sheathing material used in light frame construction in North America, consisting of sandwiched layers of wood strands

Plywood: a common sheathing material used in light frame construction in North America, as well as in engineered wood applications and furniture. Plywood consists of several sandwiched layers of thin wood veneer.

GWB: Gypsum wallboard is a panel product made of gypsum plaster pressed between sheets of paper. GWB is most commonly used to line the interior of walls and ceilings, and is colloquially often referred to as drywall.

Insulation or **rigid insulation:** a panel made of extruded (XPS) or expanded (EPS) polystyrene. It is used in construction to provide an uninterrupted barrier to the passage of heat through a building envelope.

Sheathing: any panel material nailed to framing in a light frame wall. When part of a shear wall, sheathing is loaded in an in-plane direction, and therefore is effective in resisting lateral load.

Framing: forms the basis of all light frame walls. Dimensional lumber of a certain structural grade and size is assembled into a frame structure consisting of vertical wall studs, top and bottom chords, as well as other members such as panel blocking, headers and bracing. The most common sizes of lumber used to construct framing are 38x89 mm (2x4") and 38x140 mm (2x6").

Nails or **Common Nails:** The most common structural fastener. Nails considered in this study are common, steel wire nails.

Slip or **Nail Slip**: in the context of nailed connections, refers to the relative displacement between adjacent members in the direction of loading.

2.2 Design of Light Frame Timber Shear Walls

2.2.1 Shear wall capacity

The Canadian timber design standard (CSA, O86) specifies that the capacity of a shear wall segment shall be calculated using expression (2.1):

$$V_{rs} = \phi v_d K_D K_{SF} J_{ub} J_{sp} J_{hd} L_w \qquad (\mathbf{2.1})$$

Where:

ϕ - strength reduction factor for shear walls = 0.7

K_D & K_{SF} are factors that account for load duration and service conditions, respectively

J_{ub} - strength adjustment factor for unblocked shear walls

J_{sp} - species factor for framing material

J_{hd} - hold-down effect factor

L_w - length of the shear wall segment *(m)*

The parameter v_d is the specified shear strength, or base capacity per unit length, as defined by Table 2.1 (Table 9.5.1A in CSA-O86).

From Table 2.1, it can be seen that light frame shear walls can be built in a wide range of capacities. Shear walls can be built from panels with nominal thickness ranging from 7.5 to 15.5 mm, and nails with diameters of 2.84 to 3.66 mm. Note that thin sheathing is not permitted with large nails. Conversely, thick sheathing is not recommended with small nails. These limitations are present because it is necessary for a shear wall to develop full strength in the nails prior to the sheathing failing by localized crushing (pull through). In this way, individual nails are able to effectively absorb energy from cyclic loading on the shear wall (Jones & Fonseca, 2002).

Since the shear wall capacity is dependent on the nail behavior, unnecessarily thick sheathing would have the effect of contributing little additional capacity to the shear wall, while reducing nail penetration. Up to a certain limit, increased nail penetration results in increased resistance to nail pull out.

Table 2.1: Parameter v_d, unit shear strength for light frame shear walls in kN/m (CSA, 2010)

Minimum nominal panel thickness, mm	Minimum nail penetration in framing, mm	Common nail diameter, mm	Nail spacing at panel edges, mm*			
			150	**100**	**75**	**50**
7.5	**31**	**2.84**	4.9	7.3	9.5	12.2
9.5	**31**	**2.84**	5.4	8.2	10.6	13.9
9.5	**38**	**3.25**	6.0	8.7	11.1	14.4
11.0	**38**	**3.25**	6.5	9.5	12.2	15.9
12.5	**38**	**3.25**	7.1	10.3	13.3	17.4
12.5	**41**	**3.66**	8.4	12.5	16.3	20.9
15.5	**41**	**3.66**	9.2	13.9	18.1	23.7

2.2.2 Comments on note 4 in Table 9.5.1A and gypsum wallboard as sheathing

The supplementary note 4 to Table 9.5.1A (Table 2.1 above) in CSA-O86 states:

"For panels applied over 12.7 mm *or* 15.9 mm *gypsum wallboard, the specified shear strength for the same thickness panel applied directly to framing may be used as long as minimum nail penetration (in the framing) is satisfied."* (CSA, 2010)

This exception allows for the use of a 1/2" or 5/8" (12.7 mm or 15.9 mm effective, respectively) layer of GWB as an intermediate material between sheathing and framing. The standard assumes that such a nailed connection would have as much capacity as one without GWB, as long as minimum nail penetration is satisfied. This concept is illustrated in Figure 2.1, in the case of a 3" (76.4 mm) long, 3.66 mm diameter nail. To the author's knowledge, note 4 has not yet been verified using experimental testing.

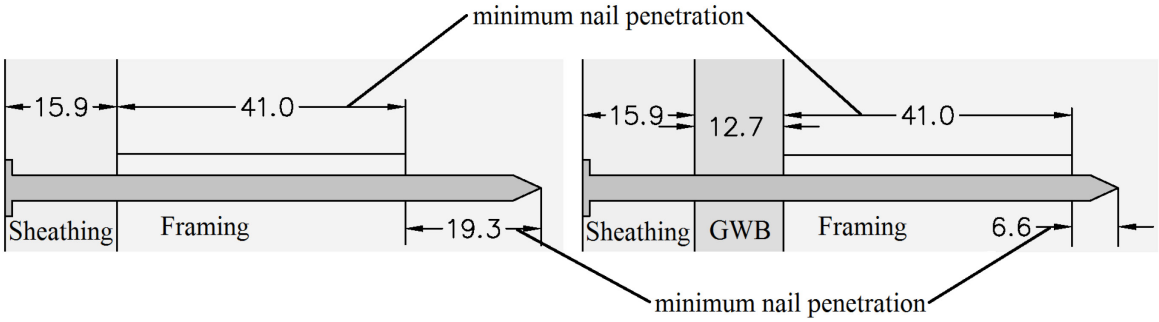

Note: All values are distances in mm

Figure 2.1: Nailed connections in shear walls with equivalent capacity under CSA-O86

The structural standard allows the use of GWB as sheathing. Expression (2.2) is used to calculate the capacity of a shear wall segment sheathed with GWB.

$$V_{rs} = \phi v_d J_{hd} L_W \qquad (\mathbf{2.2})$$

Where:

ϕ, J_{hd}, and L_w are the same as defined for (2.1). The specified shear strength v_d, for walls sheathed with GWB is shown in Table 2.2 (Table 9.5.1B in CSA-O86).

Table 2.2: Parameter v_d, unit shear strength for GWB shear walls in kN/m (CSA, 2010)

Minimum nominal panel thickness, mm	Minimum nail and screw penetration in framing, mm	Wall construction	Panels applied directly to framing*		
			200	**150**	**100**
12.5	**19**	Unblocked	1.2	1.4	1.6
12.5	**19**	Blocked	1.4	1.7	2.1
15.9	**19**	Unblocked	1.5	1.7	2.1
15.9	**19**	Blocked	1.7	2.2	2.5

Although GWB can be used as sheathing, as is seen in Table 2.2, GWB-sheathed shear walls have significantly less capacity than plywood or OSB-sheathed shear walls. An equivalent GWB-sheathed shear wall with identical panel thickness and fastener

spacing will have about 1/5th of the capacity of one built with plywood or OSB sheathing. This is due to the lower strength properties of GWB.

Gypsum (Calcium sulfate dihydrate - $CaSO_4 \cdot 2H_2O$) is a commonly occurring soft rock. The manufacture of gypsum board begins with a slurry of powderized gypsum mineral (FPL, 2010). The slurry is formed into a panel shape and is then sandwiched and cured between two layers of thick paper backing. Additives are often added to the slurry to provide moisture-resistant or fire-resistant properties to the final GWB product. GWB is used most commonly in the interior lining of walls and ceilings, and is more colloquially referred to as drywall (FPL, 2010). GWB is highly brittle, and is dependent on its paper backing to retain integrity and prevent fragmentation. GWB has a typical in-plane compression strength of about 2 MPa.

By contrast, plywood is a laminated panel material made up of multiple layers of veneered wood, with the grain of adjacent layers oriented perpendicular to each other. Plywood is often used in construction sheathing and flooring, and as a component of other engineered wood products such as prefabricated joists and box beams. The structural properties of plywood depend on the quality of the wood plies, quality of the adhesive and the degree to which bonding conditions are controlled (FPL, 2010). The result of this is that plywood has excellent structural properties for use as a sheathing material. Due to the orientation of the fibers, plywood is anisotropic with regard to its in-plane properties, meaning that measured strength and stiffness values differ weather a panel is loaded in its long or short directions.

OSB is another type of structural panel, however it is manufactured from thin wood strands. The strands are long and narrow, having an aspect ratio (length divided by

width) of at least 3. OSB panels are composed of 3 layers of strands, the outer layers with strands that are aligned in the long direction of the panel, and the central layer with strands aligned perpendicularly (in the short direction of the panel). Manufacturing consists of compressing layers of strands together in with water-resistant resin (FPL, 2010). Like plywood, OSB has excellent structural properties for use as a sheathing material, and also like plywood, has anisotropic in-plane properties.

If standard nail sizing is assumed; conventional nail sizing as defined by the Standard Specification for Nails, Spikes and Staples, ASTM-F1667 (ASTM, 2011) and CSA-O86 Table A.10.9.5.2 (CSA, 2010) (listed in Table 2.3), a number of sheathing thickness, nail size and GWB thickness combinations are valid under the assumption of Note 4. These combinations are listed in Table 2.4.

Table 2.3: Standard nail size dimensions (ASTM, F1667) (CSA, 2010)

Nail Diameter		Nail Length		Gauge No.	Dash No.	Common size
(mm)	(in.)	(mm)	(in.)			
2.84	0.113	**50.8**	2.00	11.75	05	***6d***
2.84	0.113	**57.2**	2.25	11.75	06	***7d***
3.25	0.131	**63.5**	2.50	10	07	***8d***
3.25	0.131	**69.9**	2.75	10	08	***9d***
3.66	0.148	**76.2**	3.00	9	09	***10d***
3.66	0.148	**82.6**	3.25	9	10	***12d***
4.06	0.162	**88.9**	3.50	8	11	***16d***

Table 2.4: Component combinations allowed by note 4

Sheathing Panel Thickness (mm)*	GWB Panel Thickness (mm)	Nail Size	Nail Diameter (mm)	Nail Length		Nail Penetration (mm)	Penetration Limit clearance (mm)
				(in.)	(mm)		
9.5	**15.9**	8d	3.25	2.5	63.5	38.1	**0.1**
9.5	**12.7**	8d	3.25	2.5	63.5	41.3	**3.3**
11.1	**12.7**	8d	3.25	2.5	63.5	39.7	**1.7**
12.7	**12.7**	8d	3.25	2.5	63.5	38.3	**0.3**
12.7	**15.9**	10d	3.66	3.0	76.2	47.6	**6.6**
12.7	**12.7**	10d	3.66	3.0	76.2	50.8	**9.8**
15.9	**15.9**	10d	3.66	3.0	76.2	44.4	**3.4**
15.9	**12.7**	10d	3.66	3.0	76.2	47.6	**6.6**

*Actual panel thickness (slightly more than minimum nominal)

2.2.3 Shear wall deformation and ductility

The ductility of a light frame shear wall is a crucial parameter with regards to its function. Shear walls must be ductile enough to absorb the energy caused by lateral loading effects (particularly earthquakes). Deformation of the individual nailed connections between the sheathing and studs provides the ductility of a shear wall. The Standard for Engineering Design in Wood specifies expression (2.3) for calculating the total deflection that a blocked shear wall segment may undergo (CSA, 2010). This is a sum of deflections from 4 contributing sources: bending deflection from the boundary framing elements (studs at either end of the shear wall), shear deflection of the panels (sheathing), nail slip deflection (deformation in individual nails) and rotation of the shear wall due to hold-down deflection.

$$\Delta = \underbrace{\frac{2vH^3}{3EAb}}_{\text{Bending deflection from flanges (boundary framing elements)}} + \underbrace{\frac{vH}{B_v}}_{\text{Shear deflection of the panels forming the webs}} + \underbrace{0.0025He_n}_{\text{Nail slip deflection}} + \underbrace{\frac{H}{b}d_a}_{\text{Rotation of the shearwall due to hold-down deflection}} \qquad (\mathbf{2.3})$$

where;

v - maximum shear due to specified loads at the top of the wall *(N/mm)*

H - Wall height *(mm)*

E - elastic modulus of boundary element *(N/mm^2)* (vertical framing member at shearwall segment boundary)

A - cross-section area of the boundary member *(mm^2)*

b - Wall width *(mm)*

B_v - shear-through-thickness rigidity of the sheathing, *(N/mm)*

e_n - nail deformation *(mm)*

d_a - deflection due to anchorage details *(mm)*

For shear walls without hold-downs:

$$d_a = 2.5dK_m\left[\frac{(vH - P)\frac{s_n}{b}}{n_u}\right]^{1.7} \qquad (\mathbf{2.4})$$

d - nail diameter, *(mm)*

K_m - service creep factor

P - specified uplift restraint force *(N)*

s_n - nail spacing around panel edge *(mm)*

n_u - unit lateral nail strength resistance as calculated using the method in Section 2.2. *(N)*

The nail deformation e_n, for design purposes, as defined by the standard, is calculated based on the load per nail, which is taken as:

$$Load\ per\ nail = v * s$$

Where:

v - maximum shear due to specified loads at the top of the wall (as defined above) *(N/mm)*

s - nail spacing at panel edge (also s_n, as defined above) *(mm)*

Once the load per nail is known, deformation per nail can be calculated using Figure 2.2.

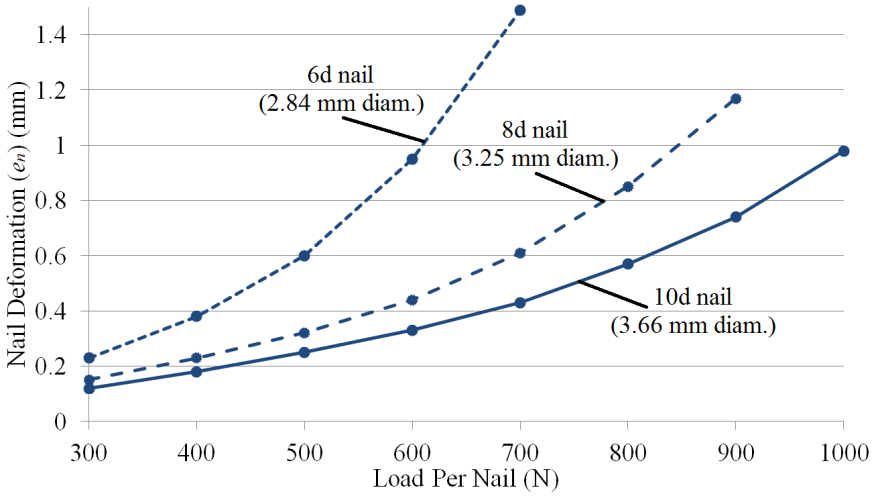

Figure 2.2: Nail deformation e_n for shear wall and diaphragm deflection design from Table A.9.7 in CSA-O86 (CSA, 2010)

2.2.4 Sample shear wall calculation

Using the above method, it is possible to calculate the design capacity and expected deformation of a shear wall. A simple example shear wall segment is considered here. The shear wall consists of three adjacent, vertical sheathing panels, with a height of 8' (2440 mm), width of 12' (3660 mm), framing consisting of 38 x 140 mm No. 1 SPF studs spaced at 16" (406 mm). The sheathing is OSB, with a thickness of 7/16" (nominal thickness of 11.0 mm). The nails are size 10d, with a diameter of 3.66 mm and length of

3" (76.2 mm), spaced at 100 mm at the panel edges and 150 mm at intermediate studs. The shear wall is unblocked and has hold downs. The shear wall is built and used in dry service conditions, all lumber is untreated. For deflection calculation, a specified wind load of 15 kN acts on the wall.

Table 2.5: Sample shear wall calculation (CSA, 2010)

Variable	Value	CSA-O86 clause reference
Capacity Calculation		
K_D - load duration factor	**1.15** (short term)	Table 4.3.2.2
K_{SF} - service condition factor	**1.0** (dry)	Table 10.2.1.5
J_{ub} - strength adjustment factor for unblocked shear walls	**0.8** (given design)	Table 9.4.4
J_{sp} - species factor for framing	**0.8** (for SPF)	Table 9.4.3
J_{hd} - hold-down effect factor	**1.0** (for hold downs)	Clause 9.4.5
L_w - length of shear wall	**3.66 m**	N/A
v_d - unit shear strength	**9.5 kN/m**	Table 9.5.1A
V_r - shear resistance	**25.59 kN**	Clause 9.5.1
Deflection Calculation		
v - maximum shear due to specified loads	**15 kN**	N/A
H - wall height	**2440 mm**	N/A
E - elastic modulus of boundary element (for SPF studs)	**9500 MPa**	Table 5.3.1A
A - cross-section area of the boundary member	**5320 mm^2**	N/A
b - Wall width	**3660 mm**	N/A
B_v - shear-through-thickness rigidity of the sheathing	**11000 N/mm**	Table 7.3C
d, d_F - nail diameter	**3.66 mm**	N/A
K_m - service creep factor	**1.0**	Table A.10.9.3.2
P - specified uplift restraint force	assume **0 kN**	N/A
s_n - nail spacing around panel edge	**100 mm**	N/A
t_1 - head side member thickness	**11.0 mm**	N/A
G - mean relative density	**0.42** for OSB and SPF	Table A10.1
f_2 - embedding strength of main member	**20.23 MPa**	Clause 10.9.4.2
t_2 - length of penetration into point side member	**65.2 mm**	N/A

Table 2.5 Continued

f_3 - embedding strength of main member	**22.24 MPa**	Clause 10.9.4.2
f_y - nail or spike yield strength	**617.0 MPa**	Clause 10.9.4.2
f_1 - embedding strength of structural panel side plates	**27.69 MPa**	Clause 10.9.4.2
n_u - unit lateral nail strength resistance (governing from 6 failure cases)	**700.0 N**	Clause 10.9.4.2
v - maximum specified shear force per unit length	**4.10 N/mm**	N/A
Load per nail	**410 N**	Table A.9.7
e_n - expected nail deformation	**0.187 mm**	Table A.9.7
d_a - deflection due to anchorage details	**1.850 mm**	Clause 9.7.1.1
Δ_{SW} - static deflection at top of shear wall	**3.122 mm**	Clause 9.7.1.1

In the above example, the total expected deflection at the top of the shear wall due to the specified load is 3.12 mm, of this, 1.14 mm (37%) is from the nail slip deflection component. A significant amount of the total deflection in a shear wall occurs due to deformation in individual nails. Repeating the example showed that this increases with the use of smaller nails; identical shear walls built with 6d and 8d nails (which are permitted given the opening assumptions) result in an expected deflection of 4.89 mm and 3.63 mm respectively, of which 50% and 40% of that deflection is attributable to nail slip deflection, respectively. Note that if this example was repeated with a shear wall which had an intermediate layer of GWB, with a thickness of 1/2" or 5/8" (12.7 or 15.9 mm, respectively), the calculation would not change at all and would result in the same shear wall capacity and expected deformation.

2.3 Lateral Loading of Nailed Connections

As was seen in the previous section, the strength of a shear wall depends heavily on individual nailed connections. The nail diameter (nail size), panel material and panel

thickness have the greatest effect on the strength of individual nailed connections subjected to lateral load. The specific capacity to resist lateral load depends on consideration of all applicable failure modes. This concept was first introduced in *Theory of Timber Connections* (Johansen, 1949). Johansen considered dowel connections and bolted connections. In that paper, the contributions from and effects of interface friction, embedment strength of wood and bending strength of the fastener were considered and experimentally tested. The theory assumes that wood behaves in an ideally plastic manner.

Johansen proposed an expression for capacity and fastener bending moment for each failure case: where the fastener yields in bending or where wood material crushes in compression, and this was done for connections with two or three members (single or double shear plane connections, respectively). Figure 2.4 shows a summary of the test cases considered by Johansen, and the first proposed expressions for connection capacity. The following definitions apply for Figure 2.3:

s_H - embedding strength of wood

s_B - modulus of rupture of fastener (resistance to bending)

d - diameter of fastener

l - thickness of outer member(s)

m - thickness of central member

P - connection capacity, maximum load

In the cases of 3-member connections, the main member refers to the central member, and side plates refer to members on either side of the main member.

Failure Case	Force Distribution on Fastener	Load Expression (*P*)	Description
	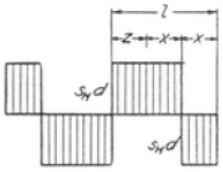	$0.414 s_H l d$	Wood crushing in both members
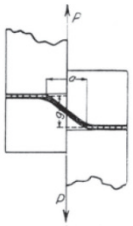	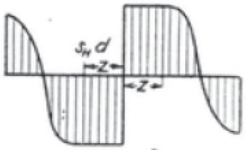	$0.442\sqrt{s_B s_H} d^2$	Fastener yielding
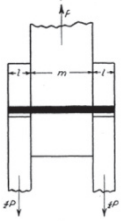	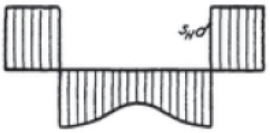	$s_H d m$	Wood crushing only in side plates
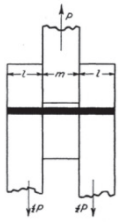	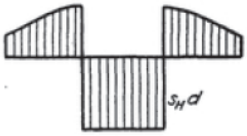	$2 s_H d l$	Wood crushing only in main member
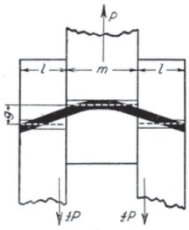	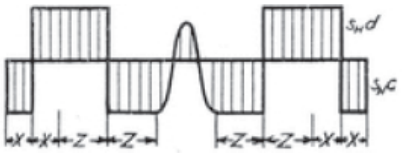	$\left(\frac{1}{4} s_H l^3 + \frac{3}{5} s_H d^2\right) \sqrt{\frac{s_H}{s_B}}$	Fastener yielding only in main member
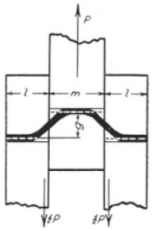	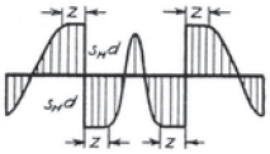	$0.885\sqrt{s_B s_H} d^2$	Fastener yielding in all members

Figure 2.3: Failure modes for connections with dowel fasteners (Johansen, 1949)

This system was subsequently developed further and became what is known as the European Yield Model (EYM). The EYM has been adapted into the Canadian

Standard for Engineering Design in Wood (CSA, 2010), as it has proven to be an accurate and reliable means of predicting the strength of nailed connections. The EYM is widely used in both Europe and North America in the design of fastened timber connections (Pellicane, 1993).

The standard for engineering design in wood has specified the following method, based on the EYM, for calculating the capacity of individual nailed connections. The capacity of a nailed connection is given in expression (2.5). This method differs from that first proposed by Johansen mainly in that it considers the effect of differing embedment properties of each member, while also considering a number of other connection factors such as service conditions, treatment etc.

$$N_r = \phi N_u n_f n_s J_F \qquad (\mathbf{2.5})$$

Where:

ϕ - strength reduction factor for nailed connections = 0.8

$$N_u = n_u(K_D K_{SF} K_T)$$

$$J_F = J_E J_A J_B J_D$$

n_f - number of fasteners in the connection

n_s - number of shear planes per nail or spike (1 for two member connections, 2 for three member connections)

K_D - load duration factor

K_{SF} - service condition factor

K_T - treatment factor

J_E, J_A, J_B and J_D are factors to account for nailing in end grain, toe-nailing, nail clinching, and nailing in diaphragm construction, respectively

n_u - unit lateral resistance, as determined by the 6 possible failure modes illustrated in Figure 2.4, where the following definitions apply:

t_1 - head-side member thickness for two member connections

t_2 - length of penetration into point-side member for two-member connections

f_1 - embedding strength of side plates

f_2 - embedding strength of main member

f_3 - embedding strength of main member where failure is fastener yielding

d_F - nail or spike diameter

f_y - nail or spike yield strength

Failure Case	Load Expression n_u	Visualization	Description
Case A	$f_1 d_F t_1$	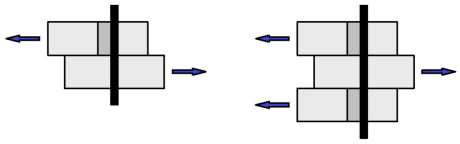	Wood crushing in side plates or member 1
Case B	$f_2 d_F t_2$	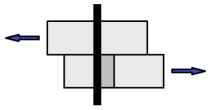	Wood crushing in member 2
Case C	$\frac{1}{2} f_2 d_F t_2$	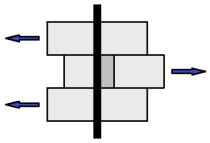	Wood crushing in main member
Case D	$f_1 d_F^2 \left(\sqrt{\frac{1}{6} \frac{f_3}{(f_1 + f_3)} \frac{f_y}{f_1}} + \frac{1}{5} \frac{t_1}{d_F} \right)$	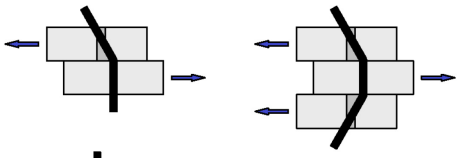	Fastener yielding in member 1 or side plates
Case E	$f_1 d_F^2 \left(\sqrt{\frac{1}{6} \frac{f_3}{(f_1 + f_3)} \frac{f_y}{f_1}} + \frac{1}{5} \frac{t_2}{d_F} \right)$	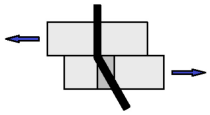	Fastener yielding in member 2
Case F	$f_1 d_F^2 \frac{1}{5} \left(\frac{t_1}{d_F} + \frac{f_2}{f_1} \frac{t_2}{d_F} \right)$	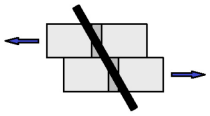	Wood crushing in both members
Case G	$f_1 d_F^2 \sqrt{\frac{2}{3} \frac{f_3}{(f_1 + f_3)} \frac{f_y}{f_1}}$	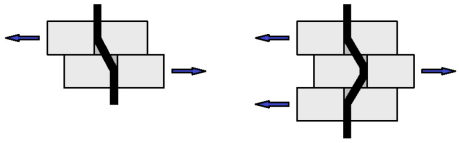	Fastener yielding in all members

Figure 2.4: Failure modes for lateral loading of nailed connections, adapted from clause 10.9.4.2 (CSA, 2010)

2.4 Previous Studies of the Effects of an Interface Gap

In the case of GWB as the intermediate material, previous research has been limited due to the assumed retention of connection capacity and stiffness provided that nail penetration is maintained and allowances for the use of GWB itself as sheathing. In the case of other intermediate materials or no intermediate material (air gap), research has also been limited due to the assumed resultant impractical, detrimental decrease in connection capacity and stiffness. A handful of studies on this topic have been done,

however, and they will be discussed in this subsection. As was mentioned in Section 2.1, the current structural standard does not directly allow for interface gaps, however it does allow for an intermediate layer of GWB via note 4 in Table A9.5.1.

Interface gaps in nailed connections in wood were first investigated by Antonides, Vanderbilt and Goodman (1979). It was found that connections with gaps caused by wood wetting and drying had an equivalent drop in stiffness as those with gaps created by metal shims. The findings from their thesis are summarized by expression (2.6), which was proposed to express the reduction in connection stiffness as a result of an interface gap.

$$\log K = C_a - C_b g \qquad (\mathbf{2.6})$$

where K is connection stiffness *(N/mm)*

g - interlayer gap thickness *(mm)*

C_a and C_b - connection constants

The effect of an interface gap was also considered by Malhotra and Thomas, who considered an air gap between two members of a nailed connection (1985). The premise of their study was to consider the effects of improper nailing, cyclic loading and member shrinkage, which might cause a small separation between nailed members, and thus create an interface gap. This would have the effect of eliminating interface friction. A focus of their study was the consideration of the effect of multiple nails in the connection. The experimental portion of the study was done using metal shims to produce and maintain air gaps of the appropriate size. Air gaps ranging from 0.53 to 1.61 mm were

considered, which are consistent with those that might naturally occur due to the causes listed above. These gap sizes are significantly less than those considered in this study.

Malhotra and Thomas used 3.25 mm diameter nails (size 8d), and eastern spruce lumber for both the point-side and head-side members. For tests with multiple nails, nail spacing was 38 mm. A control case with no interface gap was not considered. Nevertheless, a number of conclusions can be drawn from their results, a sample of which are shown in Figure 2.5. The figure shows the ultimate capacity of connections with the complete range of interface gap thicknesses and numbers of nails in the connections tested (the series number reflects the number of nails in the connection). Malhotra and Thomas differentiated between the ultimate capacity and capacity up to a proportional limit (a point beyond which the load-deformation relationship ceases to be linear). The ultimate capacity is shown in the figure.

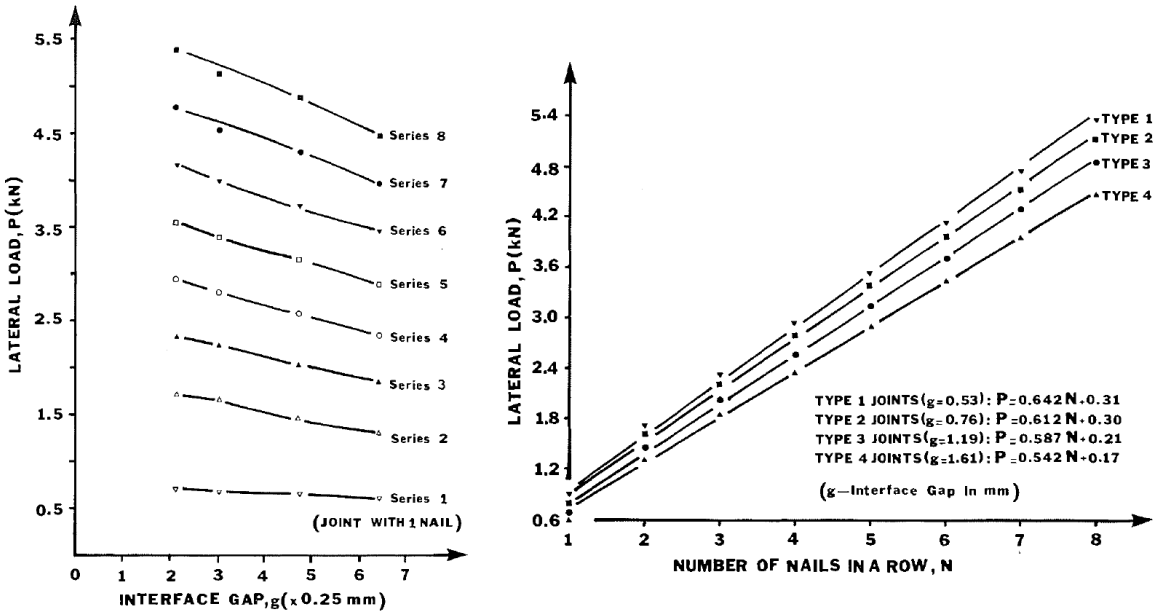

Figure 2.5: Ultimate capacity of connections with interface gaps (Malhotra & Thomas, 1985)

Overall results suggest that connections with an interface gap and multiple nails scale linearly in capacity, similar to ordinary nailed connections with no interface gap. This therefore suggests that results from other single nail or multiple nail tests of connections with interface gaps are applicable in situations where multiple nails are acting simultaneously, such as in light frame shear walls. There appears to be a roughly linearly decreasing trend in the ultimate capacity of approximately 10% per mm of interface gap thickness.

Aune and Patton-Mallory created analytical models based on derived expressions from the European-based yield theory (EYM), for multiple types of nailed connections (1986). Among the types of connections included where those with an intermediate layer of insulation. Four failure modes for connections with an intermediate layer of insulation were considered, are illustrated in Figure 2.6, and are described as follows:

- 3.3A - Steel plate as head side material, where yielding occurs in the point-side member
- 3.4A - Steel plate as head side material, where yielding occurs at the nail head and in the point-side member
- 3.3B - Wood as a head-side material, where yielding occurs in the point-side member
- 3.4B - Wood as a head-side material, where yielding occurs both in the point-side and head-side members.

It is important to note that Aune and Patton-Mallory assumed that, in failure modes 3.3B and 3.4B, head-side and point-side members have equal embedding strength. This is not the case for nails in shear walls, since sheathing materials and framing lumber have different embedment properties. The expressions for ultimate load, F_u, failure cases 3.3A, 3.4A, 3.3B and 3.4B are expressions (2.7) to (2.10), respectively.

$$F_u = f_e\sqrt{e^2 + 4\gamma} - e \qquad (\mathbf{2.7})$$

$$F_u = f_e\left[\sqrt{e^2 + 4\gamma} - e\right] \qquad (\mathbf{2.8})$$

$$F_u = \frac{f_e}{3}\left[2\sqrt{t_1^2 + et_1 + e^2 + 3\gamma} - (t_1 + 2e)\right] \qquad (\mathbf{2.9})$$

$$F_u = \frac{f_e}{2}\left[\sqrt{e^2 + 8\gamma} - e\right] \qquad (\mathbf{2.10})$$

where:

f_e - wood embedding strength *(lb/in)*

e - thickness of intermediate layer of insulation *(inches)*

γ - ratio of nail yield moment *(lb-in)* divided by wood embedding strength

t_1 - thickness of head-side member *(inches)*

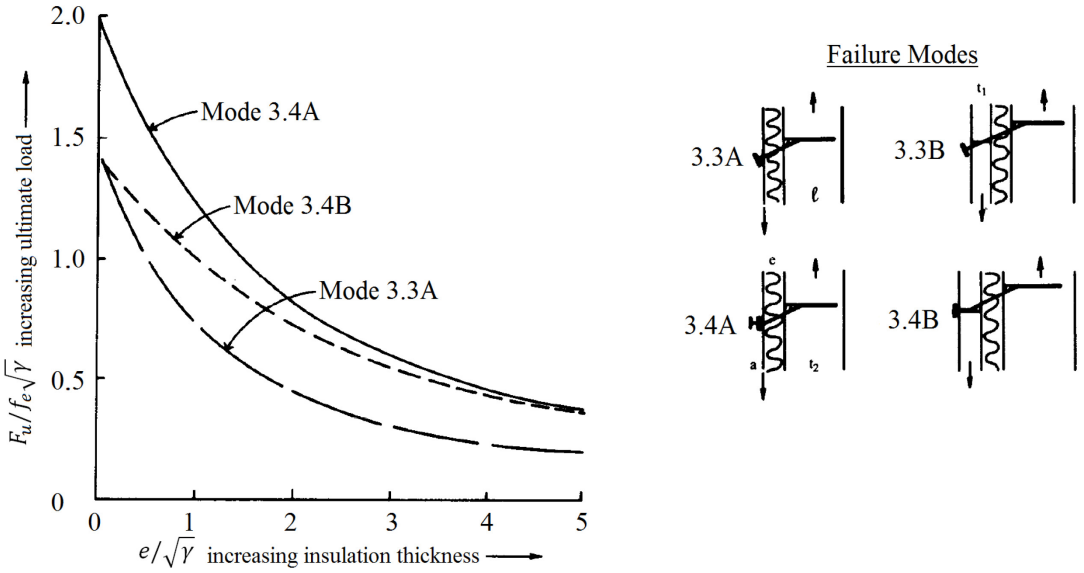

Figure 2.6: Reduction in load due to insulation thickness (Aune & Patton-Mallory, 1986)

The resultant decrease in ultimate load with increasing insulation thickness for failure modes 3.4A, 3.4B and 3.3A are visualized in Figure 2.6, where the connection load and insulation thickness are expressed in terms of generalized parameters. It was found that all failure modes exhibited a significant exponential decay in connection capacity due to an intermediate layer of insulation. It was assumed that the insulation did not contribute to the connection capacity other than to maintain a uniform gap size, and interface friction was ignored.

In *Lateral Load Slip of Nailed Joints* (Pellicane et al., 1991) the effect of multiple parameters on the load-slip response curve of laterally-loaded nailed joints was studied. The parameters considered were the effect of an interface gap between connected members, the sheathing (or head-side member) thickness, and the nail diameter. The

expressions developed were based on a previously developed empirical equation for load-slip by McLain (1975):

$$P = A\ log_{10}(1 + B\Delta)$$

Where P = lateral load, Δ = nail slip, and A, B = empirically derived constants.

This study sought to validate the equation by McLain for a wide range of possible connection types by incorporating correction factors. The following was assumed:

$$A = A_p\left(C_{Ag}C_{At}C_{Ad}\right)$$

$$B = B_p\left(C_{Bg}C_{Bt}C_{Bd}\right)$$

Where the subscripts g, t, and d indicate modification parameters to account for interlayer gap, sheathing (head-side member) thickness, and nail diameter, respectively.

A_p and B_p are the predicted initial values for A and B, respectively. A_p is found using previously determined equations by McLain (1975), one of which is:

$$A_p = 205.3 - \frac{9.813}{SG_S} - \frac{2.221}{SG_M}$$

Where SG_S and SG_M are the specific gravities of the sheathing and framing, respectively. Parameter B_p is determined using the technique developed by Wilkinson (1971).

Correction factors (C_{Ag}, C_{At}, C_{Ad}, C_{Bg}, C_{Bt}, and C_{Bd}) were experimentally determined from 342 load-slip tests.

In the attempt to determine the correction factors for the thickness of an interlayer gap, Pellicane et al. considered a large number of small gap sizes (approximately 30) from 0" to 0.035" (0.89 mm). It was determined that a relationship between correction factor C_{Ag} and gap thickness did not exist and that a constant value of 1.241 fit the

experimental data, consequently, parameter A does not change with interface gap thickness. The result of this is that the load-slip relationship of a connection with an interface gap is affected only by parameter B. Correction factor C_{Bg} showed a distinct declining relationship, shown in Figure 2.7. Regression analysis resulted in the following expression for the correction parameter that accounts for interface gap:

$$C_{Bg} = 10^{(0.284-8.05g)}$$

The parameter C_{Bg} reduces to a very low level (<0.0002) when extrapolated to a larger gap size of 1/2" (12.7mm). By extension, this would cause parameter B to approach zero. Very low values for parameter B result in lower connection capacity and stiffness. Figure 2.7 also shows the effect of parameter C_{Bg} on the load-slip response of a nailed connection for various interface gap sizes, given a hypothetical connection where load-slip parameters A and B are 200 and 100 respectively when there is no interface gap. Since C_{Bg} was not considered for tests beyond an interface gap of 0.035", the method described is not applicable in situations outside of the experimental data points (i.e. for cases where the interface gap is greater than 0.035" or 0.89 mm).

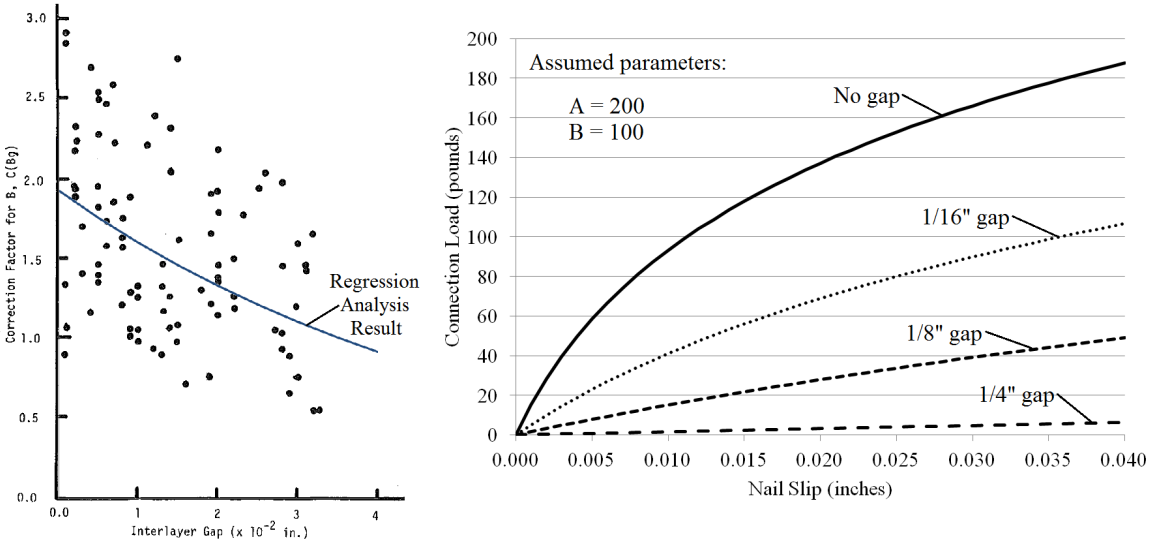

Figure 2.7: Correction factor for interlayer gap thickness (Pellicane et al., 1991)

Since all of these studies only considered very small interface gap sizes, it is difficult to predict the effect on a connection of gaps on the order of 1/2" or larger. If it is assumed that an intermediate layer of insulation contributes negligibly to a connection, then the results from these studies suggest that there may be an immediate and significant drop in capacity with the introduction of any small gap or insulation layer, and that this capacity will continue to decrease with increasing insulation layer thicknesses.

2.4.1 GWB as considered by the structural standard in the United States

The *National Design Specification for Wood Construction* is the standard for engineering design in wood in the United States (AWC, 2012). The part of this standard that considers the design of lateral load resisting systems, such as shear walls, is Section 4: the Special Design Provisions for Wind and Seismic (SDPWS). The counterpart for Table 9.5.1A in CSA-O86, is Table 4.3 in SDPWS, which lists unit capacities for shear wall segments built in various configurations. Table 2.6 shows selected parts of Table 4.3A and 4.3B from SDPWS. It is important to note that SDPWS recognizes the fact that the capacity of a shear wall with an intermediate layer of GWB (described as "Wood Structural Panels Applied over 1/2" or 5/8" Gypsum Wallboard or Gypsum Sheathing Board") may have a lower capacity than that of an equivalent wall without an intermediate layer of GWB. SDPWS allows for the same permissible unit shear capacity for an equivalent wall sheathed over GWB, provided that the next largest common nail size is used, for example; an 8d nail instead of a 6d nail, or a 10d nail instead of an 8d nail.

Also note that an equivalent capacity shear wall, sheathed over GWB, despite using a larger nail, may use thinner sheathing. For example, SDPWS allows for the use of a combination of a (relatively large) 10d nail, with relatively thin, 3/8" nominal sheathing panel thickness over a 5/8" GWB layer, and that this would have the same capacity as a shear wall with smaller 8d nails, with no GWB, but a greater 15/32" sheathing thickness.

Table 2.6: Nominal Unit Shear Capacities for Wood-Frame Shear Walls, v_s (AWC, 2008)

Wood-Based Panels							
Sheathing Material	Minimum nominal panel thickness	Minimum fastener penetration in framing member	Fastener Type & Size Nail (common or galvanized)	Edge fastener spacing			
				6"	**4"**	**3"**	**2"**
Wood Structural Panels-Structural I	5/16"	1-1/4"	**6d**	*400*	*600*	*780*	*1020*
	3/8" 7/16" 15/32"	1-3/8"	**8d**	*460* *510* *560*	*720* *790* *860*	*920* *1010* *1100*	*1220* *1340* *1460*
	15/32"	1-1/2"	**10d**	*680*	*1020*	*1330*	*1740*
Wood Structural Panels-Sheathing	5/16" 3/8"	1-1/4"	**6d**	*360* *400*	*540* *600*	*700* *780*	*900* *1020*
	3/8" 7/16" 15/32"	1-3/8"	**8d**	*440* *480* *520*	*640* *700* *760*	*820* *900* *980*	*1060* *1170* *1280*
	15/32" 19/32"	1-1/2"	**10d**	*620* *680*	*920* *1020*	*1200* *1330*	*1540* *1740*
Plywood Siding	5/16"	1-1/4"	(galvanized) **6d**	*280*	*420*	*550*	*720*
	3/8"	1-3/8"	**8d**	*320*	*480*	*620*	*820*
Wood Structural Panels Applied over 1/2" or 5/8" Gypsum Wallboard or Gypsum Sheathing Board							
Wood Structural Panels-Structural I	5/16"	1-1/4"	**8d**	*400*	*600*	*780*	*1020*
	3/8" 7/16" 15/32"	1-3/8"	**10d**	*560*	*860*	*1100*	*1460*
Wood Structural Panels-Sheathing	5/16" 3/8"	1-1/4"	**8d**	*360* *400*	*540* *600*	*700* *780*	*900* *1020*
	3/8" 7/16" 15/32"	1-3/8"	**10d**	*520*	*760*	*980*	*1280*
Plywood Siding	5/16"	1-1/4"	(galvanized) **8d**	*280*	*420*	*550*	*720*
	3/8"	1-3/8"	**10d**	*320*	*480*	*620*	*820*

Note: tabulated nominal shear capacity for seismic load, v_s (plf - pounds per linear foot of wall)

SDPWS allows for the construction of light frame shear walls sheathed entirely with a layer of GWB, and just as in Table 9.5.1B of CSA-O86, they have a significantly reduced capacity when compared with plywood or OSB sheathed shear walls.

Nominal unit strength capacities found in all tables in SDPWS are based on the adjustment of allowable values in building codes and industry reference documents (AWC, 2008). The document referenced by SDPWS with regard to shear walls built over GWB panels is American Plywood Association (APA) Research Report 154, on wood structural panel shear walls (Tissell, 1993), published by the Engineered Wood Association. Table 2.7 shows the results of experimentation on shear walls built over GWB panels documented in that report.

Table 2.7: Rated sheathing over gypsum wallboard (Tissel, 1993)

Fastener			Sheathing Panel Thickness	GWB Thick-ness	No. of Tests	Ultimate Loads			Target Design Shear	Load Factor
Size	Type	Spacing				Min.	Max.	Avg.		
"Structural I" Sheathing										
10d	Common	4"	3/8"	1/2"	1	-	-	**1863**	**430**	4.3
10d	Common	3"	3/8"	5/8"	2	**1568**	**1634**	**1601**	**550**	2.9
"Rated Sheathing"										
8d	Galvanized box	6"	3/8"	1/2"	1	-	-	**956**	**200**	4.8
8d	Casing	4"	3/8"	1/2"	2	**963**	**1047**	**1005**	**210**	4.8
8d	Common	3"	3/8"	5/8"	2	**1508**	**1559**	**1533**	**390**	3.9

Note: values in bold are in plf (pounds per linear foot)

A total of 8 tests were performed on full sized shear wall specimens sheathed over GWB. It is insufficient to conclude from such a small data set the effects of the introduction of a layer of GWB, particularly when fastener size, fastener type, fastener

spacing and GWB thickness are all variables also tested. For example, when comparing the two test cases with 10d nails and "Structural I" type sheathing, the expected capacity for a shear wall with 3" fastener spacing and a 5/8" intermediate GWB panel is higher than that for a shear wall with 4" fastener spacing, presumably due to the closer nail spacing, however experimentally, the reverse is the case, suggesting that thicker GWB is the cause of the reduced capacity. Note that in the cases involving 1/2" GWB, a higher load (safety) factor is achieved than that for shear walls involving a 5/8" GWB panel. It is possible that this is the case due to less nail penetration as well as an increased separation between the sheathing and framing, leading to greater bending moment in the nails.

The results from this study may have indicated that shear walls built over panels of GWB have a sufficient capacity (and produce a sufficient factor of safety) for this to be an acceptable practice, however they do not discuss the shear stiffness, deformation at capacity nor performance under cyclic loading conditions of such shear walls. Given the limited data set and the number of variables considered, it can also be said that this study does not contribute much to the understanding of such shear walls, other than to suggest that there is some loss occurring due to the introduction of an intermediate GWB layer, regardless of the variation of the other parameters.

The overall differences in structure and assumptions between CSA-O86 and SDPWS indicate that there is a knowledge gap with regard to the specific effect an intermediate layer of GWB would have on the capacity, stiffness, deflection and ductility of a light frame shear wall.

2.5 Finite Element Modeling of Nailed Connections

Finite element models have been successfully used in the past to describe the behavior of nailed connections. These models typically consist of a line of several deformable elements representing the nail, subjected to forces applied by spring elements, which represent reaction embedment forces in the wood members. As far as is known, so far, none of these models have included consideration of an intermediate material between the sheathing and framing.

One of the first published uses of a finite element model to simulate a nailed connection between two wood members was by Ni (1997). Figure 2.8 shows the model used by Ni to simulate a single two-member nailed joint, in which the nail is embedded within two wood layers referred to as the point-side member and head-side member.

This model includes the following components:

- A line of free nodes that are connected with nonlinear beam elements to simulate the behavior of the nail
- Spring elements connected to each nail node to simulate the embedment forces in both the point-side and head-side members
- A fixed base line restricting movement in the head-side member
- A movable base line allowing the point-side member to displace perpendicular to the direction of the nail, to simulate lateral loading
- An additional series of spring elements connected to each nail node to simulate frictional forces between the members and nail (resistance to nail pull out)

- One spring connecting the nail head to a fixed node to simulate the resistance of the nail head to pull through, shown on the far left side of the figure.

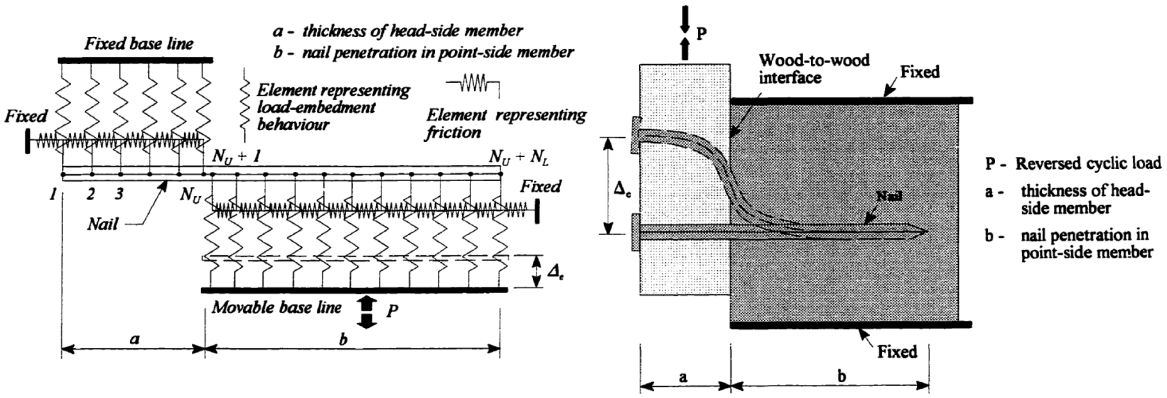

Figure 2.8: First use of a FE model of a nailed connection (Ni, 1997)

The nail elements in Ni's model are 2-dimensional, 3-node beam elements subject to displacement in X & Y directions as well as rotation. All spring elements in Ni's model are 1-dimentional finite elements with stiffness K_{em} and K_{ef}, which are the nonlinear tangential stiffness of the load-embedment relationship of wood, and of the frictional relationship between the shank and wood, respectively. A similar formulation was used for the FE model in this study.

The model used incremental iteration to progress the model using the Newton-Raphson algorithm. It is important to note that this model neglects friction at the interface between the two wood members. Ni has remarked that the model also neglects the relationship between shear and tensile stress within the nail elements, but that this likely has a negligible effect on the result. The nails considered in this study are relatively slender, therefore ignoring this is also a safe assumption.

Ni's model was used in subsequent studies, such as is documented by Chui and Li (2005). Chui and Li adapt the model to consider the effect of the interaction between axial and shear stresses in the fastener in an attempt to more accurately model fasteners of a greater diameter. Ni's model has since typically been adapted for use in cyclic load applications.

More subsequent FE models have been focused on cyclic loading and modeling the hysteretic behavior of shear walls and individual nailed joints. Xu and Dolan developed a finite element model in ABAQUS which was capable of modeling the hysteretic behavior of individual nailed connections with great accuracy (Xu & Dolan, 2009). The nailed connection was based on one previously developed by Foliente (1993), and is shown in Figure 2.9. The figure also compares sample results of experimental monotonic and cyclic loading tests from their study with this type of FE model. Newer FE models in ABAQUS have proved to be highly accurate in predicting connection behavior.

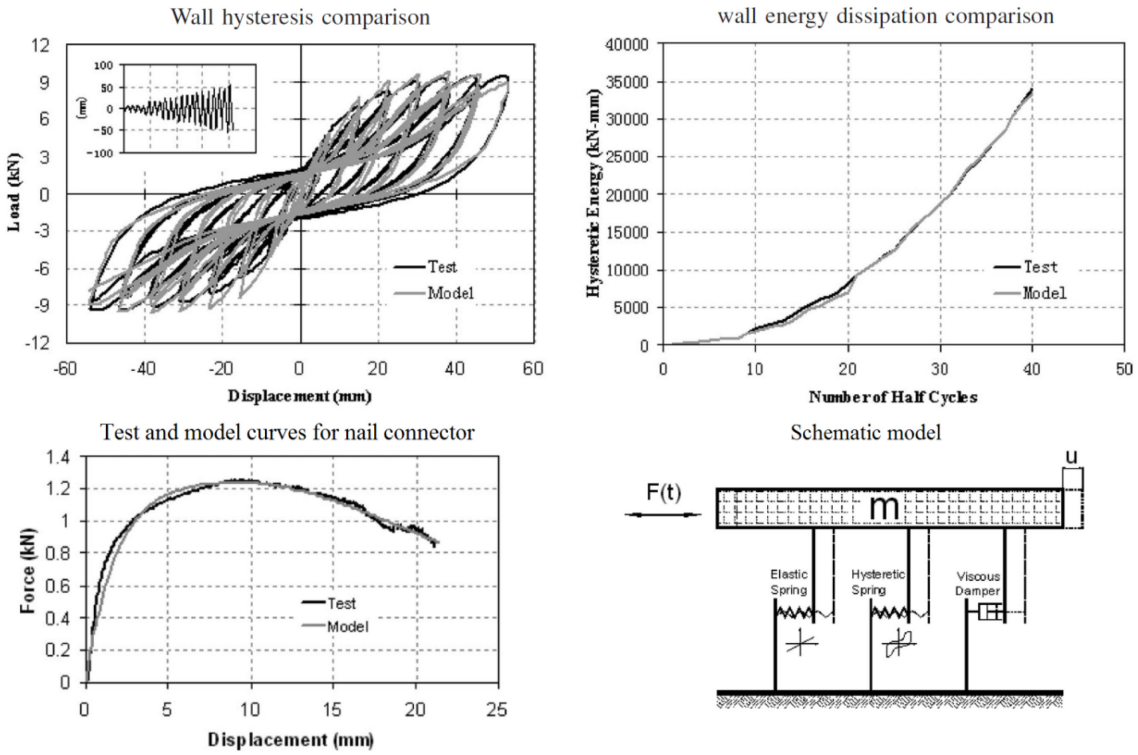

Figure 2.9: Performance of FE nail models in ABAQUS by Xu & Dolan (2009), Model by Foliente (1993)

Another recent finite element model in ABAQUS of a nailed connection in wood with a steel head-side member was developed by Hong and Barrett (2010). This model is shown with its equivalent experimental test in Figure 2.10. This study focused mostly on the embedment properties of the wood. The model was the first successful 3D model of such a nailed connection, and incorporated two distinct wood regions. Localized around the nail is a "wood foundation", a region of transverse isotropic plasticity (with bilinear relationships representing material response in tension, compression and shear), surrounded by a region who's properties depend on only compression. This technique is useful in capturing the change in wood properties as a result of the pre-compression caused by nail driving.

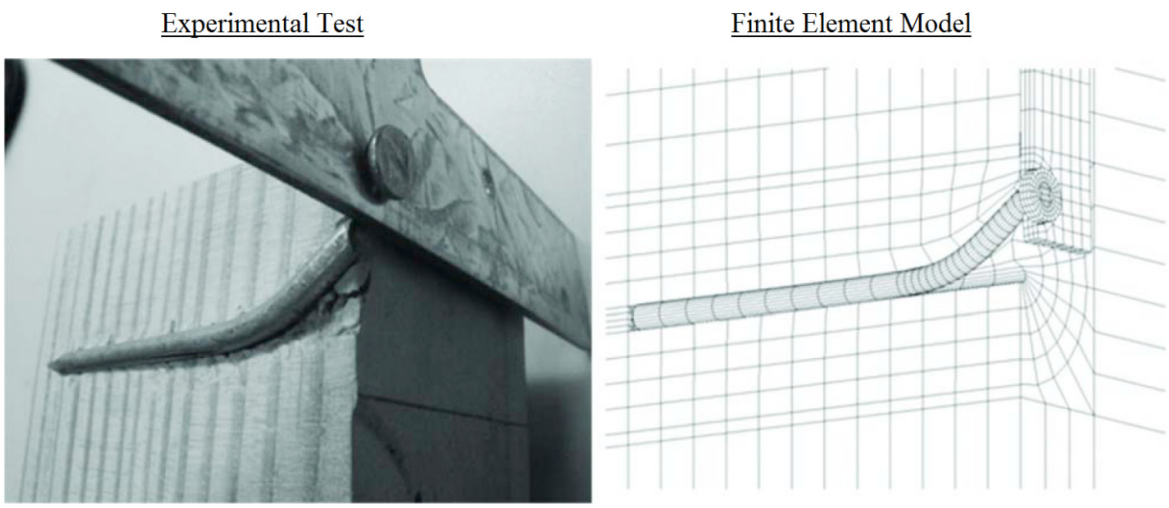

Figure 2.10: FE nail model developed by Hong & Barrett (2010)

Previous FE models of nailed connections have proven to be accurate and useful in capturing the effects of various connection properties. Although no FE models have been developed that incorporate the effects of an intermediate material, such models may be very accurate and relatively easy to develop.

2.6 Motivation

With regard to Note 4 to Table 9.5.1A in CSA-O86, given that the practice of sheathing shear walls with OSB or plywood overtop of a layer of GWB is permitted and common practice, it is evident that thorough experimental testing should be conducted on such connections to determine their behavior. The difference between US and Canadian engineering design standards suggests that there is a significant knowledge gap with regard to this particular type of connection. From this literature review, the following general points emerge:

- GWB is a far weaker material for the purposes of shear wall sheathing than plywood or OSB, however it is permissible for use as sheathing on its own. GWB sheathed shear walls have a significantly reduced capacity over equivalent Plywood or OSB sheathed walls.
- Experimental tests of shear walls sheathed over GWB suggest a reduced capacity of some magnitude.
- Tests into the effect of an interface gap have shown a significant drop in connection capacity with very small gap sizes. Analytical models of nailed connections with large intermediate layers of insulation suggest a continuing drop in connection capacity.
- Experimental tests with larger gap sizes or intermediate insulation have not been done.
- Extensive FE modeling of nailed connections has been done in the past, and such models have proven to be accurate in capturing their behavior.

From the above, it is not clear whether or not a nailed connection with an intermediate layer of GWB, or, by extension, a light frame shear wall with an intermediate GWB panel will perform as well as one without GWB, or indeed, whether these connections will satisfy the intent of the standards. The purpose of this study is to experimentally test specifically the type of nailed connection permitted by Note 4, and evaluate the results to determine the capacity and stiffness of nailed connections with an intermediate layer of GWB.

In the area of other possible intermediate materials or interface gaps (not GWB), it is clear that experimental data is also limited particularly when larger gap sizes are considered. It will be the goal of this study to also experimentally test nailed connections with intermediate layers of insulation of various thicknesses, in order to establish relationships between strength properties (capacity and stiffness) with intermediate material thickness (or equivalent gap thickness, if zero insulation embedment strength is assumed). From here, it will be possible to judge if an intermediate layer of insulation located between sheathing and framing can be of any use to a light frame structure without seriously compromising the capacity of the individual nailed shear wall connections.

With regard to connection modeling, it has been shown in the past that both analytical models based on the European Yield Model (EYM) and FE models can be reliable and accurate, however models of specifically the type of connection considered above have thus far not been made. This study will create both types of model and compare them with the results from experimentation, to further understand the nature and effects of interface gaps and intermediate materials.

3. EXPERIMENTAL SETUP

This chapter will describe all materials used in this study: lumber, sheathing, nails and intermediate materials (gypsum wallboard and extruded polystyrene insulation), providing reasoning for material selection, the standards that were used to certify each material, and the checks that were performed on these materials to verify their adherence to standards.

This chapter also describes the means by which the experimental portion of this study was conducted. Preparation consisted of the following steps:

1. Design and testing of a mounting mechanism for attachment to a load frame
2. Design, construction and preliminary (pilot) testing of a specimen that could apply lateral loads on nails embedded in multiple materials, replicating a typical light frame shear wall nailed joint
3. Design of a mechanism to measure displacement in the nailed connection
4. Determination of which specific nail sizes, sheathing thicknesses and intermediate material thicknesses would be tested.

Following discussion of this, testing matrixes are presented.

3.1 Materials

3.1.1 Framing lumber

Spruce-pine-fir (SPF) lumber is a very common lumber species used in eastern Canada, and due to its availability and widespread use, it was selected for use in this study. The grade of lumber chosen was SPF no. 2 and better because it is a representative

grade used in light frame shear wall construction. The size of lumber chosen was 2x6" (38 x 140 mm) as this is the generally accepted minimum size allowed in exterior wall construction in Canada to accommodate the common minimum insulation thickness. A 140 mm stud width was also the optimal choice for the tested specimens because it allowed for two 16d-size nails to be driven on opposite sides of the stud without risk of interference.

The studs were cut into 1' (30.5 cm) lengths for the construction of tested specimens, and then left for several days to dry before assembly. The moisture content of each stud segment was measured to verify that they had reached moisture equilibrium. Density measurements were also made for each tested stud segment to determine the specific gravity. The results from moisture content and density measurements on all stud segments can be found in Appendix A. Figures 3.1 and 3.2 show the distribution of moisture content and specific gravity of all tested stud sections, respectively.

Moisture content was calculated using a Moore Canada solid state moisture detector model RC-IC, made by Delmhorst Instrument Company. As is referred to in the Standard Test Method for Laboratory Standardization and Calibration of Hand-Held Moisture Meters (ASTM, 2013), specimens were conditioned to an ambient temperature of 25^{o}C, at which all moisture content testing was conducted. As is required by the standard and usage guidelines of the moisture detector, correction factors were applied to compensate for temperature and wood species.

Density was calculated using a method consistent with Test Method A as described by the Standard Testing Methods for Specific Gravity of Wood and Wood Based Materials (ASTM, 2007).

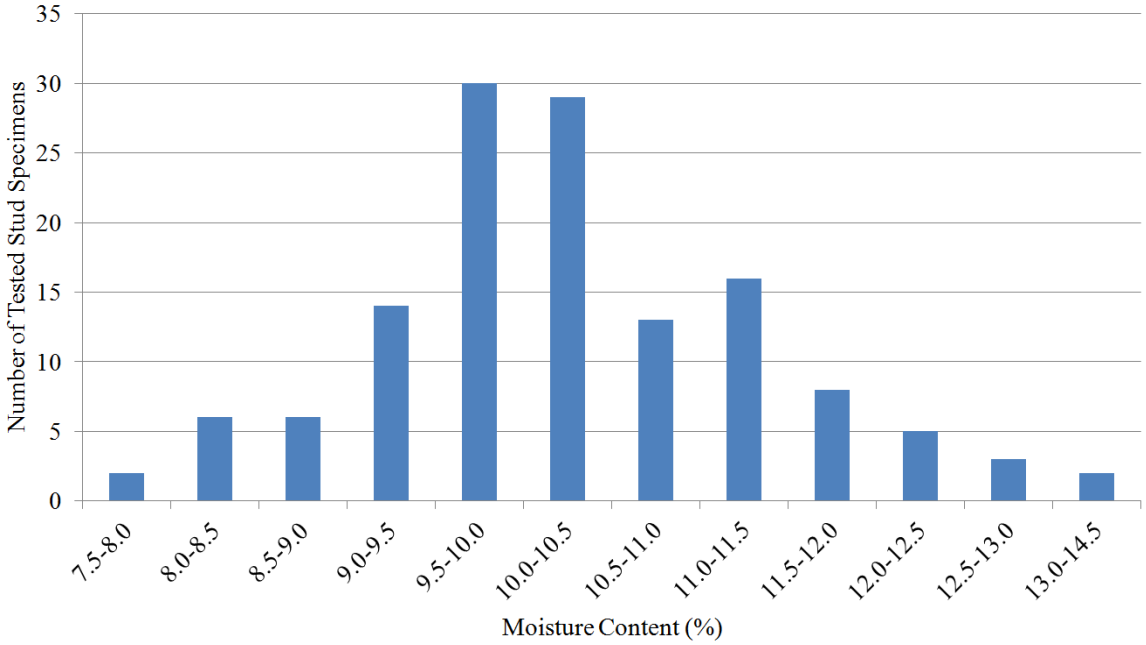

Figure 3.1: Distribution of equilibrium moisture content of tested stud sections

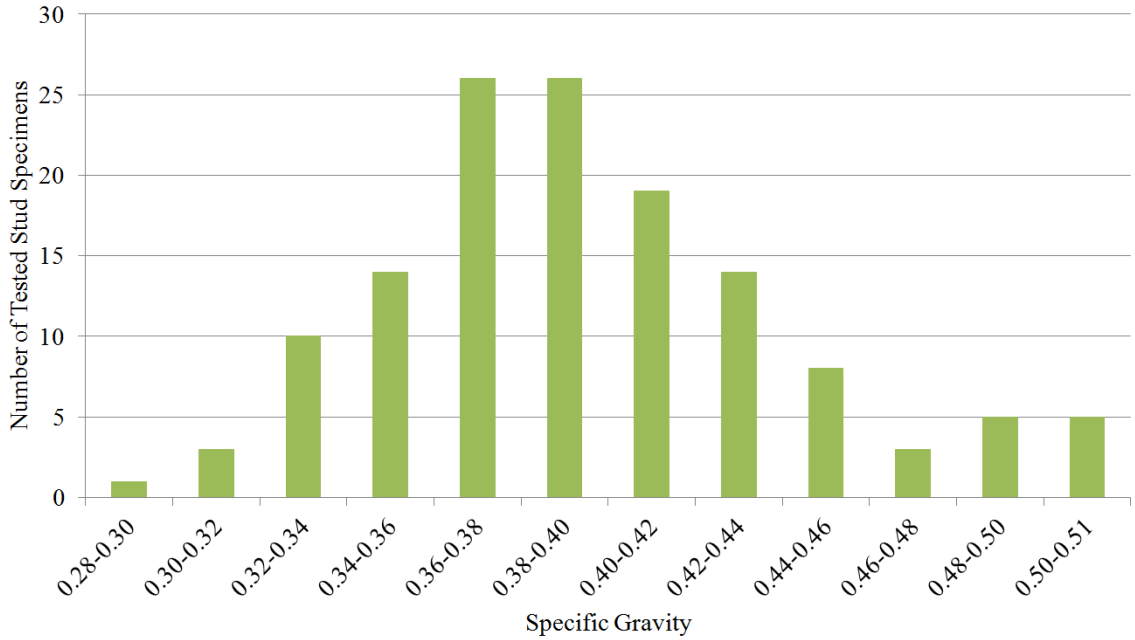

Figure 3.2: Distribution of specific gravity of tested stud sections

Table 3.1: Results from moisture content and density testing

	Minimum Recorded	Maximum Recorded	Mean	COV
Moisture Content (%)	7.9	15.7	10.3	0.115
Specific Gravity	0.299	0.508	0.395	0.117

Results from moisture content and density tests are summarized in Table 3.1. The limit on moisture content to maintain dry service conditions is 19%, therefore the lumber in all tests can be considered dry, and was deemed acceptable. The mean specific gravity of the lumber is slightly less than the assumed design value for SPF of 0.42.

3.1.2 Sheathing

Oriented strand board (OSB) was obtained from the manufacturer Norbord Inc. As will later be discussed in Section 3.6, sheets of thickness 7/16" (11.1 mm) and 5/8" (15.9 mm) were obtained and cut into strips of size 4" x 24" (102 x 610 mm) using a table saw. The orientation of the sheathing strips was in line with the short dimension of the full sheathing panel. This orientation was chosen so that when the strips are loaded in tension, the weak axis properties of the OSB would be in effect. The standard of Construction Sheathing (CSA, 2012) lists structural requirements for various types of sheathing including OSB. Adherence of the selected material to this standard was verified by consulting technical specifications from the manufacturer. Figure 3.3 shows sheathing strips after being cut, prior to specimen assembly.

Figure 3.3: Sheathing strips prior to specimen assembly

3.1.3 Nails

There exist many nail types to fulfill a variety of structural roles. The standard accepted nail for timber construction of the type considered in this study is the steel common wire nail. As can be seen from Figure 3.4, common nails have a round, smooth shank, flat, round head and ridges along the length of the shank that begin near the head and extend 10-20 mm along the shank.

The standard specification for Driven Fasteners: Nails, Spikes, and Staples (ASTM, 2013) describes the physical characteristics of common nails used in construction, as well as dimensional and material requirements. Table 3.2 lists physical requirements for those common nail sizes chosen for this study.

Figure 3.4: Common wire nails, from top to bottom, sizes: 16d, 10d, 8d, 6d

Table 3.2: Physical characteristics of common nails of the sizes used (ASTM, 2013)

Size	Nail Length		Shank Diameter		Head Diameter		Mass		Bending Yield Strength	
	inches	mm	inches	mm	inches	mm	nails/lb	grams	psi	MPa
6d	2.0	50.8	0.113	2.87	0.266	6.76	150	3.02	100,000	689.5
8d	2.5	63.5	0.131	3.33	0.281	7.14	100	4.54	100,000	689.5
10d	3.0	76.2	0.148	3.76	0.312	7.92	66	6.87	90,000	620.5
16d	3.5	88.9	0.162	4.11	0.344	8.74	47	9.65	90,000	620.5

Note that the standard for Engineering Design in Wood (CSA, 2010), clause A.9.5.1.1, lists its own requirements regarding the yield strength of common nails of a non standard diameter for use in shear walls, as follows:

- 635 MPa for nails 2.64 to 3.25 mm in diameter (size 6d, 8d)
- 615 MPa for nails 2.95 to 3.66 mm in diameter (size 8d, 10d)

No requirement exists for nails of the 16d size, as that is not a standard size for use in shear walls. A center point bending test was conducted on representative nail specimens for the purpose of verifying bending yield strength, the method and results of which are discussed in Chapter 4.

Dimensional Measurements

The Standard Specification for Driven Fasteners: Nails, Spikes, and Staples (ASTM, 2013) also requires that construction nails satisfy dimensional tolerances, described as follows:

- Length tolerance of ±1/16" (1.59 mm) for nails of length 1" to and including 2.5" *(6d, 8d)*
- Length tolerance of ±3/32" (2.38 mm) for nails of length 2.5" to 7" *(10d)*
- Shank diameter tolerance of ±0.004in (0.10 mm) for diameters greater than 0.076" (1.93mm) *(all sizes)*
- Head diameter tolerance of ±10% of the nominal head diameter
- Also for head diameter, long axis diameter shall not exceed short axis by more than 20%

20 nails from each size were selected randomly for these dimensional measurements, the results of which are presented in Appendix B. All nails passed all tests, with the exception of a single 10d nail that failed the length test by being slightly too long. Based on these measurements, the chosen nails were deemed suitable for experimental testing. The Standard also lists compositional and ductility requirements for

all common nails (ASTM, 2013), however verification of these requirements was beyond the means and scope of this study.

3.1.4 Gypsum wallboard

Two gypsum wallboard thicknesses were used in this study: 1/2" (12.7 mm) and 5/8" (15.9 mm). Both panels were manufactured by Georgia Pacific Incorporated. The 1/2" panel was ToughRock Mold-Guard^{TM} brand gypsum board, and the 5/8" panel was ToughRock Fireguard-X^{TM} brand gypsum board. Both panels were type-X rated for fire resistance, which is typical of exterior walls. The Standard Specification for Gypsum Board (ASTM, 2013) lists structural properties and various mechanical requirements for gypsum boards such as those used in this study. Adherence to this standard was verified by consulting the manufacturer's specifications. Note that the two brands of GWB selected for this study have identical strength properties when comparing panels of the same thickness.

The Standard Test Methods for Physical Testing of Gypsum Panel Products (ASTM, 2012) specifies the method and apparatus needed to test gypsum boards. The means to perform these tests was not available nor was performing these tests within the scope of this study.

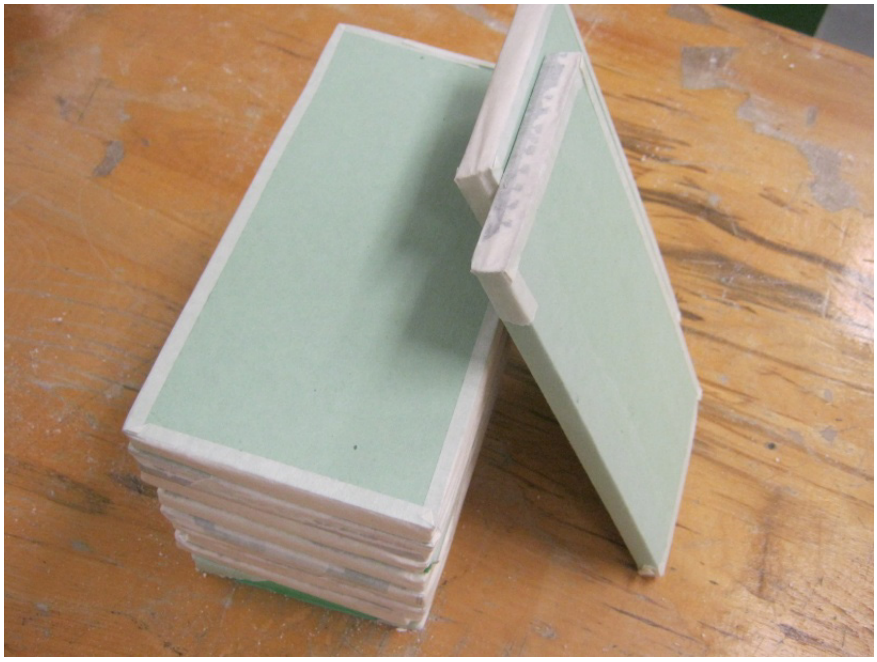

Figure 3.5: Gypsum wallboard segments prior to specimen assembly

In preparation for testing, the gypsum panels were split into segments 4" x 8" (102 x 203 mm) in size. Plain masking or painter's tape was used around the edges for safety reasons and to prevent material fragmentation, as shown in Figure 3.5.

3.1.5 Insulation

The insulation used in this study was Formular® C-300 Extruded Polystyrene (XPS) Rigid Insulation, manufactured by Owens Corning Corporation. A 1" (25.4 mm) thick, 24" x 96" (610 x 2438 mm) sheet was obtained and cut using a crafting knife into the correct sizes and thicknesses. In the test case of a specimen with a 1.5" (38.1 mm) layer of insulation, a 1" layer was combined with a 1/2" layer. The Standard Specification for Rigid, Cellular Polystyrene Thermal Insulation (ASTM, 2012) specifies mechanical properties of rigid insulation organized by type. This brand of insulation is type 4, meaning that it has a compressive strength of approximately 210 kPa, a compressive

modulus of 9.3 MPa, flexural strength of 415 kPa and thermal resistance (R-value) of 5.0 per inch of thickness. It was chosen as a representative sample of the rigid insulations typically available. Mechanical properties were verified using the manufacturer product data sheet, however were not tested as that was beyond the scope of this study.

3.2 Specimen Design

The central question posed by this study is the assessment of how an intermediate material between wall studs and sheathing effects the lateral resistance of a nailed connection. This required the design of a representative test specimen of a nailed connection within a light frame shear wall. The study by Wang (2009), included experimentation of a similar nature in that it required a means by which lateral load could be applied to nails by a load frame. Such a machine is limited to applying loads only in tension or compression. The basic mechanism of this design was adapted to serve the requirements of this study.

A general schematic of the test specimen design is shown in Figure 3.6. Two specimen holding brackets are fitted into both the top and bottom ends of the load frame (which will be discussed further in Section 3.3). Two stud sections are rigidly affixed to these brackets by means of 4 wood screws. These stud sections are referred to as the tested stud, which is located at the top, and dummy stud, which is located at the bottom. The reason for this orientation, with the tested stud located at the top, is to simplify installation and improve visibility of all important parts during each test.

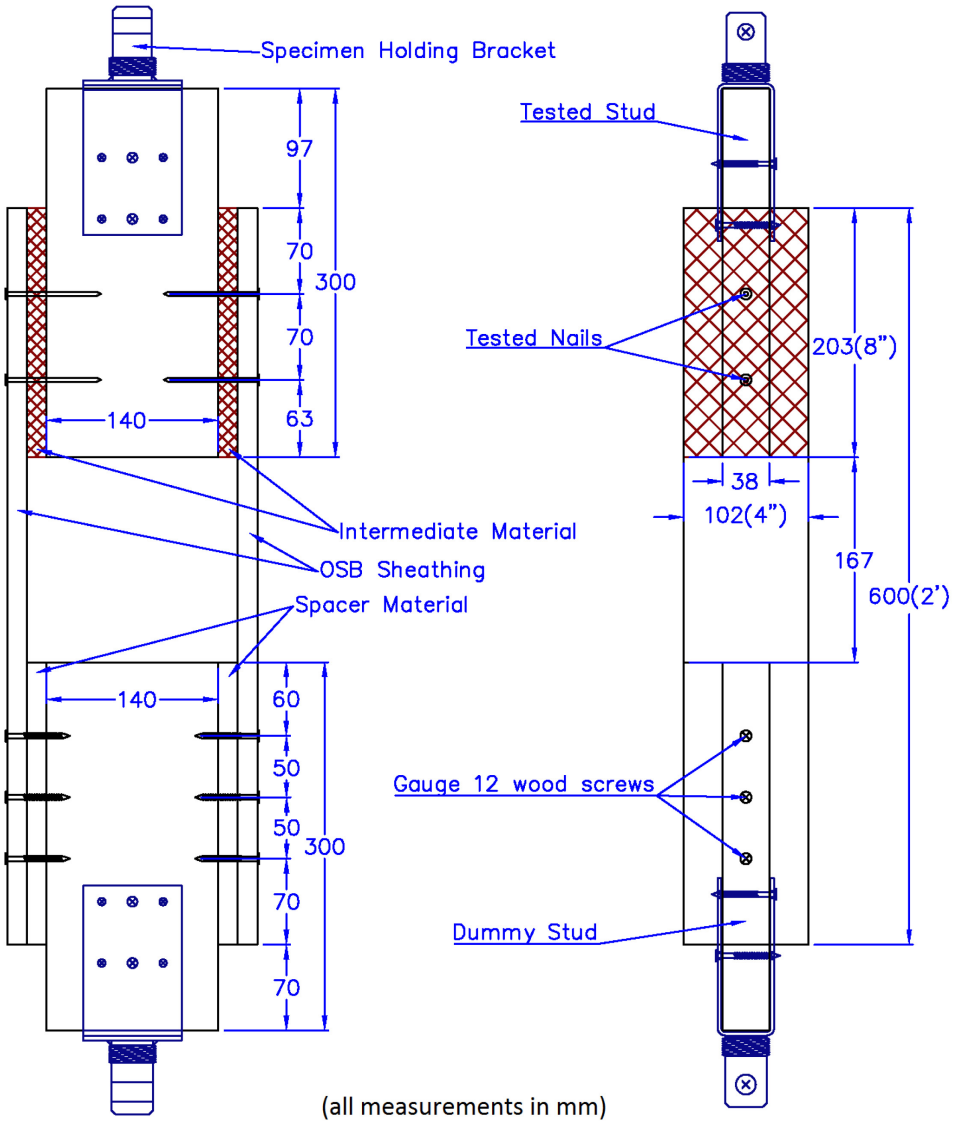

Figure 3.6: Basic specimen design

Two layers of intermediate material (gypsum wallboard or rigid insulation) are sandwiched between the tested stud and two strips of oriented strand board (OSB) sheathing, using four common nails. Two nails were used to secure each strip instead of one because this created a more stable configuration.

Both sheathing strips are attached to the bottom dummy stud using six wood screws (gauge 12). The size and number of screws was selected to create an overdesigned

connection that will not fail nor yield during a test. To ensure pure shear loading on the nails and to rigidify the dummy end, a rigid material was used to separate the lower end of the sheathing strips from the dummy stud. This spacer material was of the same thickness as the tested intermediate material. For the cases where gypsum wallboard was as the intermediate material, another two segments of gypsum wallboard were used as a spacer (use of GWB in the dummy end did not cause any connection problems, as the wood screw connection was overdesigned). For the cases where insulation was used as the intermediate material, blocks of SPF of the appropriate size were used.

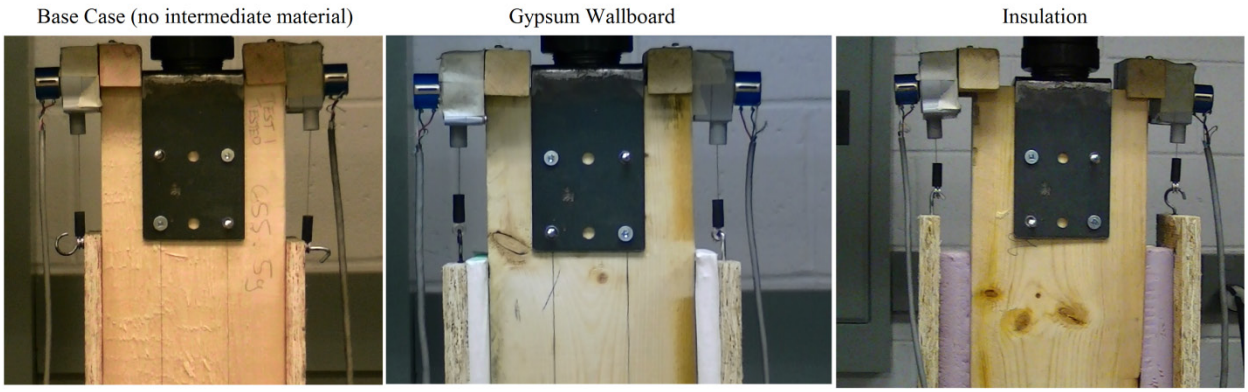

Figure 3.7: Assembled specimens prior to testing

Glue was used in the study by Wang (2009) to secure the connection on the dummy end. Glue was not used in this study, as this allowed for the potential re-use of dummy studs, sped up specimen assembly and disassembly, and preserved sheathing strips for post-test measurement. Given the way that nail slip is measured (as will be discussed in Section 3.3), it does not matter if a small amount of displacement occurs in the dummy end.

A simple wooden jig was created to aid in the assembly of the tested specimens. The 6 wood screws used for the attachment of the dummy end used pre-drilled holes to avoid splitting and to simplify construction.

It was decided that all specimens would be tested in tension, rather than compression, as this eliminates the risk of buckling in the specimen, which would not be present in a full sized light frame shear wall. Given the specimen design, loading in either direction should theoretically produce the same effect on the tested nails.

3.2.1 Specimen sizing

The largest nail that can be used in a lumber section consisting of 2" nominal size in width (38 mm), in accordance with the standard for Engineering Design in Wood, has a diameter of 4.23 mm to avoid splitting (CSA, 2010). Therefore, 16d nails (with a diameter of 4.06 mm) were selected as the largest nail to be used in this study. Following from this, the length of the tested stud was selected to accommodate a pair of size-16d nails on each side such that splitting does not occur. Spacing between the 4 bracket screws, and between the top wood screws and the top of the specimen was selected in accordance with the minimum requirements provided by the design standard. To take account of all spacing requirements, the final length of each stud segment was selected as 12" (305 mm), which included a small amount of clearance.

The width of the sheathing strips was selected as 4" (102 mm) to provide appropriate clearances, reduce any local effect due to interaction with the free edge, and to better replicate a continuous OSB panel. The length of sheathing strips was selected to

be 24" (600 mm), to accommodate attachment to both the tested and dummy ends of the specimen.

3.3 Bracket

A bracket was created to connect the top and bottom of the specimen to the load frame. The bracket was designed to fit securely within the crosshead of the load frame to create a fixed connection. 60 ksi (414 MPa) steel was used to manufacture the bracket. Plate thickness and welds were overdesigned to withstand the maximum possible load on any of the specimens without yielding. Figure 3.3 shows a schematic and a photo of this bracket. Four of the holes in the bracket plates are sized and arranged to accommodate 4 guage-12 wood screws with conical heads into the ends of the 2x6" studs. Wood screw size, predrilled hole size and hole spacing was designed to prevent splitting at maximum possible load.

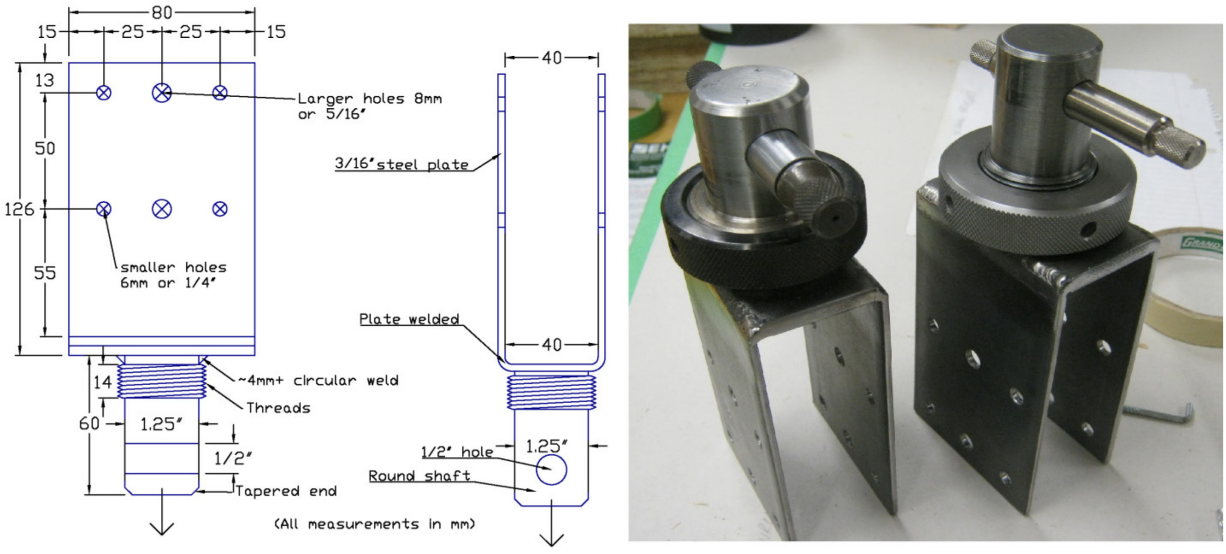

Figure 3.8: Specimen mounting brackets schematic and photo

3.4 Displacement Measurement

Although the load frame used for this study (described in Section 3.5), is capable of recording crosshead displacement to a high degree of accuracy, it was apparent that the entire test assembly would invariably experience additional deformation that is external to the nailed connection that was tested, including:

- Deformation in tension of all materials not part of the nailed connection: sheathing, tested and dummy stud segments, mounting bracket
- Movement between the mounting bracket and stud segments due to the oversized holes in the bracket
- Movement in the wood screw connection between the sheathing strips and dummy studs

For these reasons, it was decided that the nailed connection shear displacement should be measured directly. A pilot test was conducted using 2 LVDTs mounted on either side of the tested stud, recording displacement on the ends of the sheathing strips. As the test proceeded, approximately half of the way into the test, sheathing strips began to separate away from the tested stud as the nails began pulling out. This eventually caused the ends of the LVDTs to slip off mounts on the ends of the sheathing strips, making it impossible to get any further readings.

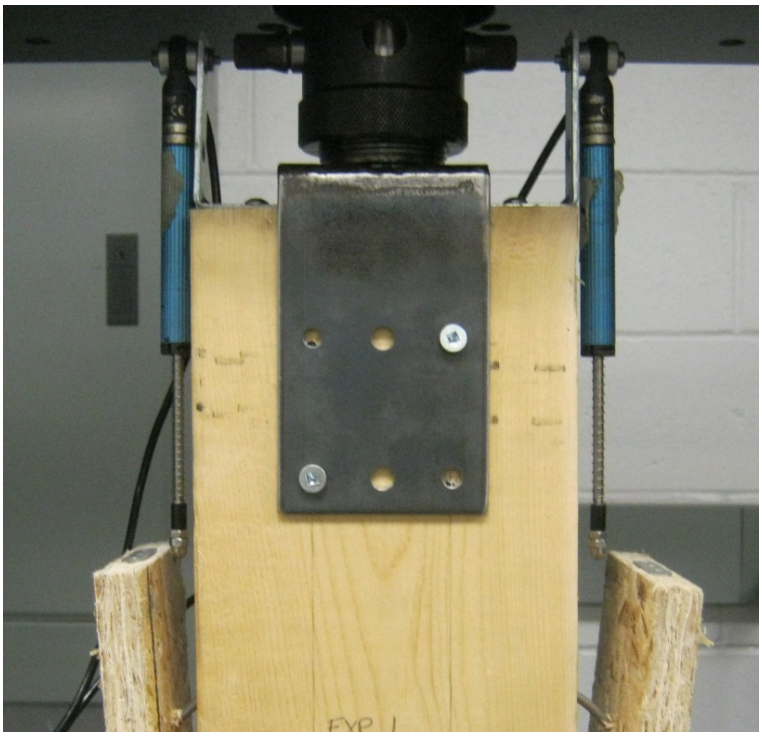

Figure 3.9: Pilot test using LVDT displacement measurement after failure

An alternative method involving string potentiometers was used in this study, which provided a more secure means of attachment and greater displacement range. String potentiometers were suitable as they could measure displacement to any location, whereas LVDTs are limited to recording displacement at a point in line with the LVDT's housing. This arrangement was selected because restricting outward movement would not be representative of nailed connections subjected to lateral load and it would have been very difficult to completely restrict the outward movement of the sheathing panels given the apparatus that was available. Nail pull out is a phenomenon that is likely to occur in the nailed connections in light frame shear walls, and must be accounted for. String potentiometers were the best means of recording displacement given an anchor point that displaces both downward and outward (away from the stud) relative to the mounting point.

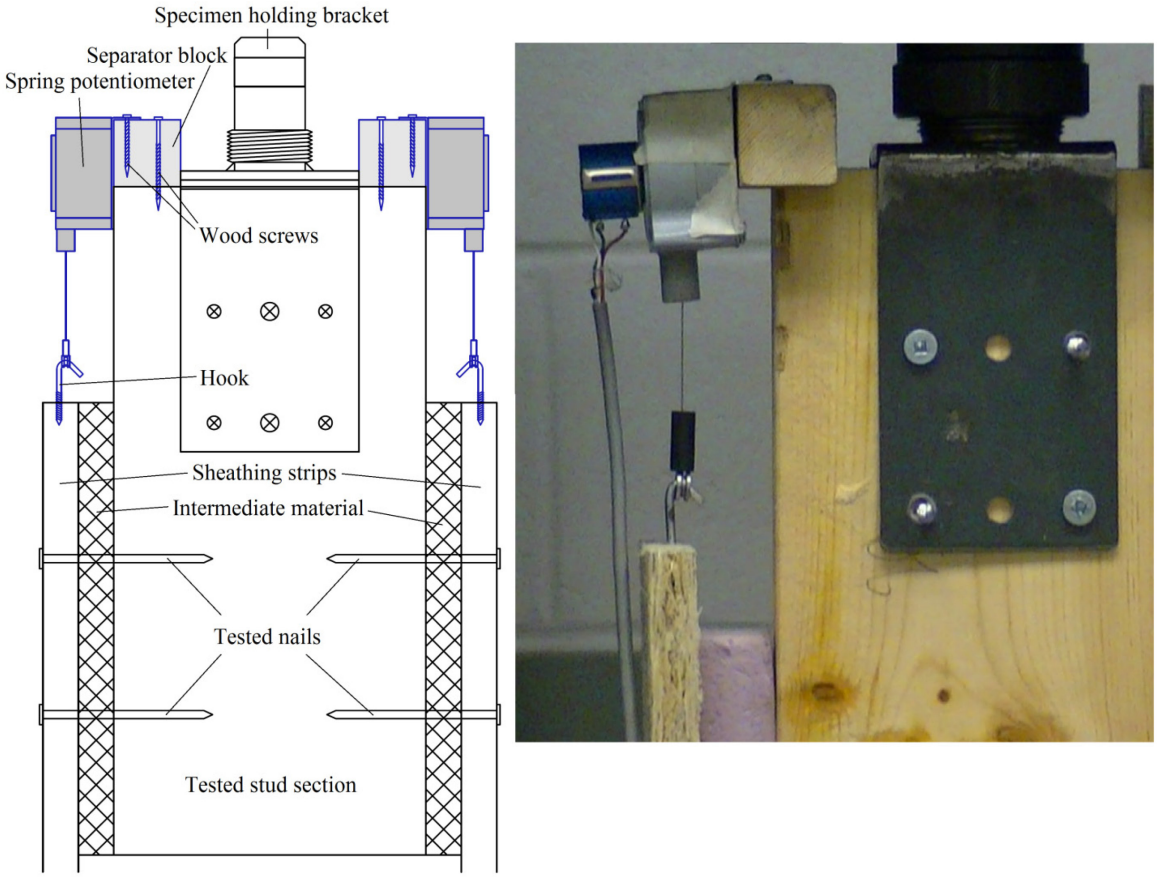

Note: location of hook and size of separator blocks depends on intermediate material thickness

Figure 3.10: Displacement measurement mechanism schematic and photo

A schematic of the mounting arrangement used, with photo, can be seen in Figure 3.10: a pair of string potentiometers were mounted on either side of the tested stud by means of separator blocks (which were adjusted in size as necessary to accommodate the intermediate material thicknesses) with the ends of the cables fastened to the ends of the sheathing using a pair of hooks. The string potentiometers were calibrated prior to testing.

During tests, as the nails begin to deform under loading, the sheathing displaces downwards relative to the stud, thus pulling on the hooks and potentiometer cable. It was

assumed that the deformation of the sheathing between the hook and the nails was negligible compared to the overall shear deformation of the interface. In this manner, each string potentiometer effectively recorded the shear deformation of the nailed interface, localized to the nailed connection on one side of a tested stud. Following testing, the mean displacement value between the two potentiometers was calculated, and the recorded load on the system was divided by 4 (for 4 nails), to produce load-deformation response curves on a per-nail basis (as will be discussed in Chapter 4).

The Standard Test Methods for Mechanical Fasteners in Wood (ASTM, 2012) requires that the displacement rate for tests of nailed connections subjected to lateral loading be 0.10" (2.54 mm) / min ±25%. The load frame was set to apply displacement at a rate of 2.50 mm/min. The applied displacement rate is an important parameter to consider because the strength of a nailed connection is affected by loading rate. The load frame used in this study was an Instron 5582, capable of applying rates of displacement between 0.001 and 500 mm/min to an accuracy of 0.1% (Instron, 2005). The mean recorded displacement rate at the level of the nailed connections was 2.44 mm/min, which is within the acceptable range as defined by the standard.

3.5 Force Measurement and Data Collection

All experimental testing was performed in an Instron 5582 load frame, made by Instron Engineering Corporation. The built-in load cell is capable of recording applied loads between 2N and 100kN. Measurement accuracy varies depending on the applied load, being slightly more accurate at higher loads. For loads close to those tested in this study, the accuracy of load measurement was 0.4%, according to the Instron Series 5500

Load Frames Reference Manual (Instron, 2005). Data acquisition was managed by a nearby computer terminal, which can be seen in Figure 3.11.

Displacement measurement was recorded on a separate computer terminal. For both sets of data, recordings were taken at intervals of 100 ms, or one every roughly 0.004 mm of nail displacement. Each set of data had an associated time stamp accurate to 100 ms, so that load and displacement data could later be combined properly. The results from all tests are presented and discussed in Chapter 4.

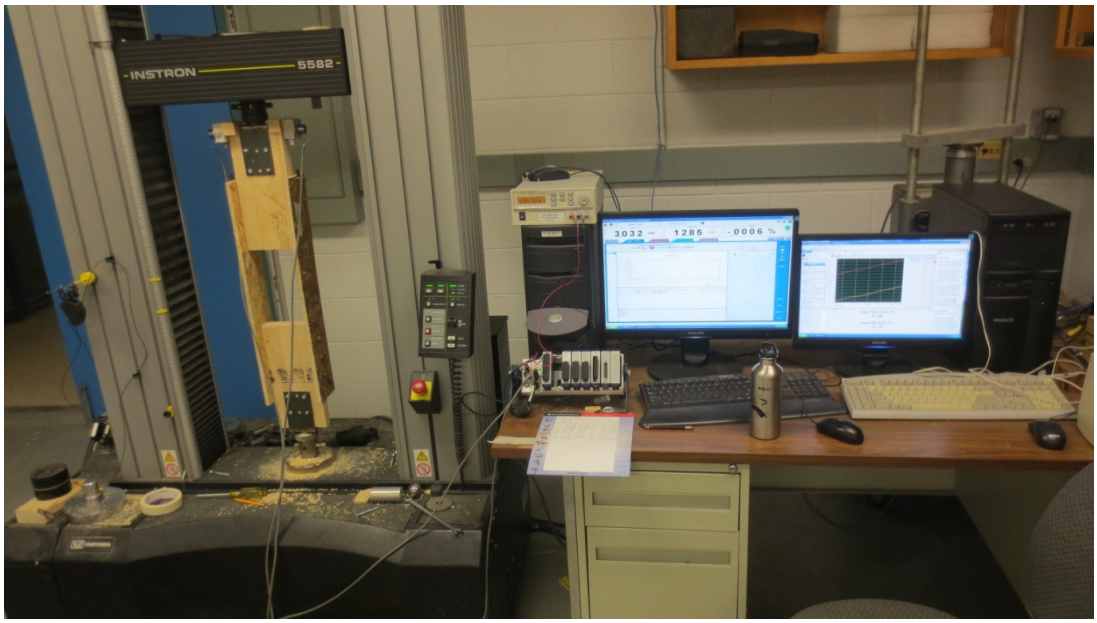

Figure 3.11: Load frame and experimental setup with specimen ready for testing

3.6 Testing Matrix

This section will describe the selection of appropriate combinations of intermediate material thickness, sheathing thickness and nail size used in this study. For tests with gypsum wallboard (GWB) as the intermediate material, selections were made

from Table 9.5.1A from the standard for Engineering Design in Wood (CSA, 2010) (Figure 2.4). For each combination, six copies were constructed for testing.

3.6.1 Tests involving GWB as the intermediate material

In the case of testing GWB as the intermediate material, the following considerations were made in the selection of the combinations of nail size, sheathing thickness and gypsum wallboard thickness that were tested:

- As specified in note 4 to Table 9.5.1A (CSA, 2010), a panel of gypsum wallboard of thickness 12.7 mm or 15.9 mm may be used provided that minimum nail penetration is satisfied. Therefore, three cases were considered: (1) no gypsum wall board, (2) 1/2" thick gypsum wallboard (12.8 mm), and (3) 5/8" thick gypsum wallboard (15.9 mm).
- With regards to nail size, Table 9.5.1A (CSA, 2010) lists 3 distinct common nail sizes for use in light frame shear walls. All 3 were readily available, therefore cases with 6d, 8d and 10d sized nails were considered. Three nail sizes combined with three possible gypsum wallboard thicknesses resulted in 9 combinations for testing, as listed in Table 3.3.
- For combinations involving size 10d nails, Table 9.5.1A allows the use of either 1/2" or 5/8" panels. 5/8" thick sheathing panels were selected, because they represented an "upper bound", theoretically resulting in the highest capacity available. This thickness and also presented a greater contrast to the 7/16" sheathing thickness selected for smaller nail sizes.

- For combinations involving size 8d nails, 7/16" panels were selected. This sheathing thickness allows the investigation of the effect of satisfying the minimum nail penetration on the strength and stiffness of the connection. In the case of 1/2" and 5/8" GWB, nail penetration is 1.7 mm more than the limit and 1.1 mm less than the limit, respectively.
- For combinations involving 6d size nails, sheathing thinner than 7/16" was not readily available, thus 7/16" sheathing panels were used. It should be noted that there are no valid combinations of 2.84 mm diameter nails (6d size nails, with a length of 2" or 50.4 mm), with a layer of GWB of the thicknesses considered and a layer of sheathing of any allowed thickness which satisfy the minimum penetration limit.

Although Table 2.4 does not list nail length, according to nail sizing guidelines within the Standard Specification for Driven Fasteners: Nails, Spikes and Staples (ASTM, 2011), there exists only one standard common nail length for each nail diameter. Nail sizes, diameters and lengths as listed in F1667 (ASTM, 2011) (Table 2.3) are those most commonly available and, it is assumed, the most commonly used in shear wall construction. Only standard nail sizes were considered in this study. All of the tested combinations for specimens with GWB as the intermediate material are listed in Table 3.3.

Table 3.3: Testing matrix for gypsum wallboard

GWB Thickness	Sheathing Thickness	Nail			Penetration (mm)	
		Size	Dia.(mm)	Length	Min.*	Actual
0mm (0")	11.1mm (7/16")	6d	2.84	50.8mm (2.0")	31.0	39.7
0mm (0")	11.1mm (7/16")	8d	3.25	63.5mm (2.5")	38.0	52.4
0mm (0")	15.9mm (5/8")	10d	3.66	76.2mm (3.0")	41.0	60.3
12.7mm (1/2")	11.1mm (7/16")	6d	2.84	50.8mm (2.0")	31.0	27.0**
12.7mm (1/2")	11.1mm (7/16")	8d	3.25	63.5mm (2.5")	38.0	39.7
12.7mm (1/2")	15.9mm (5/8")	10d	3.66	76.2mm (3.0")	41.0	47.6
15.9mm (5/8")	11.1mm (7/16")	6d	2.84	50.8mm (2.0")	31.0	24.2**
15.9mm (5/8")	11.1mm (7/16")	8d	3.25	63.5mm (2.5")	38.0	36.9**
15.9mm (5/8")	15.9mm (5/8")	10d	3.66	76.2mm (3.0")	41.0	44.8

Notes: *minimum as defined by table 9.5.1A, ** does not meet minimum

3.6.2 Tests involving rigid insulation as the intermediate material

The second part of the experimental portion of this study dealt with the effects of rigid insulation as an intermediate material between sheathing and framing. The key parameter tested here was the thickness of the intermediate material, without varying the sheathing thickness and nail size. Insulation is only effective when used in thicknesses relatively large in comparison with the thicknesses of GWB used in the previous experiment (described above). In addition, the maximum thickness of any intermediate material while satisfying minimum nail penetration (described above), is relatively small, therefore only the largest (and consequently longest) usable nail sizes were considered.

The largest nail size referred to in Table 2.4 is 10d, with a length of 3" (76.2 mm). This nail size was considered in combination with a sheathing panel thickness of 5/8" and 7 different insulation thicknesses ranging from 1/8" (3.2 mm) to 1" (25.4 mm)

incremented by 1/8". The base case of no intermediate insulation was identical to the base case used in the above GWB testing. The limit on penetration distance was satisfied for all combinations except for the case of the greatest insulation thickness of 1" (25.4 mm), where the penetration is 6.1 mm less than the limit.

Table 3.4: Testing matrix for rigid insulation

Insulation Thickness	Sheathing Thickness	Nail			Penetration (mm)	
		size	dia.(mm)	length	Min.*	actual
3.2mm (1/8")	15.9mm (5/8")	10d	3.66	76.2mm (3.0")	41.0	57.2
6.4mm (1/4")	15.9mm (5/8")	10d	3.66	76.2mm (3.0")	41.0	54.0
9.5mm (3/8")	15.9mm (5/8")	10d	3.66	76.2mm (3.0")	41.0	50.8
12.7mm (1/2")	15.9mm (5/8")	10d	3.66	76.2mm (3.0")	41.0	47.6
15.9mm (5/8")	15.9mm (5/8")	10d	3.66	76.2mm (3.0")	41.0	44.5
19.1mm (3/4")	15.9mm (5/8")	10d	3.66	76.2mm (3.0")	41.0	41.3
25.4mm (1")	15.9mm (5/8")	10d	3.66	76.2mm (3.0")	41.0	34.9**
0mm (0")	15.9mm (5/8")	16d	4.06	88.9mm (3.5")	-	73.0
6.4mm (1/4")	15.9mm (5/8")	16d	4.06	88.9mm (3.5")	-	66.7
12.7mm (1/2")	15.9mm (5/8")	16d	4.06	88.9mm (3.5")	-	60.3
19.1mm (3/4")	15.9mm (5/8")	16d	4.06	88.9mm (3.5")	-	54.0
25.4mm (1")	15.9mm (5/8")	16d	4.06	88.9mm (3.5")	-	47.6
38.1mm (1.5")	15.9mm (5/8")	16d	4.06	88.9mm (3.5")	-	34.9

Note: *minimum as defined by Table 9.5.1A, ** does not meet minimum

To provide a second set of data for a different nail size, it was decided to also run tests with specimens using an even larger 16d nail (diameter of 4.06 mm, length of 3.5" or 88.9 mm). This nail size is not listed in Table 9.5.1A (Table 2.4), therefore it is likely too large to be used in shear wall construction under current code requirements, however

it does satisfy the limit on edge distance to prevent splitting in the cases of sections of SPF or northern species (CSA, 2010), Table 10.9.2.1. 6 combinations with 16d nails, 5/8" sheathing and insulation thicknesses from 0" (0 mm) to 1.5" (38.1 mm), incremented at 1/4" (6.4 mm), were tested. All of the tested combinations for specimens with insulation as the intermediate material are listed in Table 3.4.

4. EXPERIMENTAL RESULTS

This chapter presents the results from all experimental testing done in this study. In addition to the testing of nailed connection specimens, tests on individual materials were conducted to determine material behavior for input parameters in a finite element model of the nailed connection (which will be described in Chapter 5). These tests were also used to verify the material properties for confirmation of adherence to ASTM standards. These tests included:

- Nail center point bending tests
- Nail bearing tests on samples of framing and sheathing
- Compression tests on samples of intermediate materials
- Nail pullout tests from framing

Detailed results of all of these supplementary tests are provided in Appendix B.

All experimental tests on nailed connection specimens were conducted in accordance with the methods that were described previously in Chapter 3. For clarity, the results in this chapter will be split between those nailed connection specimens using gypsum wallboard (GWB) as the intermediate material between the sheathing (OSB) and framing (SPF) and those using insulation (extruded polystyrene) as the intermediate material. This chapter will compare connection capacity, calculate the yield point using various commonly used methods, apply curve fitting methods to load-displacement behavior and compare the overall drop in connection capacity and stiffness with intermediate material thickness and type.

4.1 Results of Testing Individual Shear Wall Components

This section will describe the method and results from conducting supplementary tests on all materials involved in this study. The purpose of these tests was to provide material input values for the finite element model (as will be discussed in detail in Chapter 5), and to confirm that all materials adhered to advertised properties in accordance with relevant standards. Complete results from all supplementary tests are provided in Appendix B.

4.1.1 Center point nail bending test

The specific bending yield strength of common nails of the sizes used in this study was determined via center point bending tests as required by the Standard Test Method for Determining Bending Yield Moment of Nails (ASTM, 2008). The center-point bending test involves simply supporting each nail and applying a point load half way between the supports. The standard also describes the means by which the bending yield strength may be calculated based on the response generated by this test. 5 identical nail bending tests were conducted for nail sizes of 6d, 8d and 10d. Figure 4.1 shows the setup used for nail bending tests. The load frame (described in Section 3.5), applied load a displacement rate 2.54 mm/min (0.1"/min). The loading rate for this test was significantly less than the maximum stated by the standard of 0.25"/min. Measurements were taken to ensure that the point of applied load was equidistant from the supports.

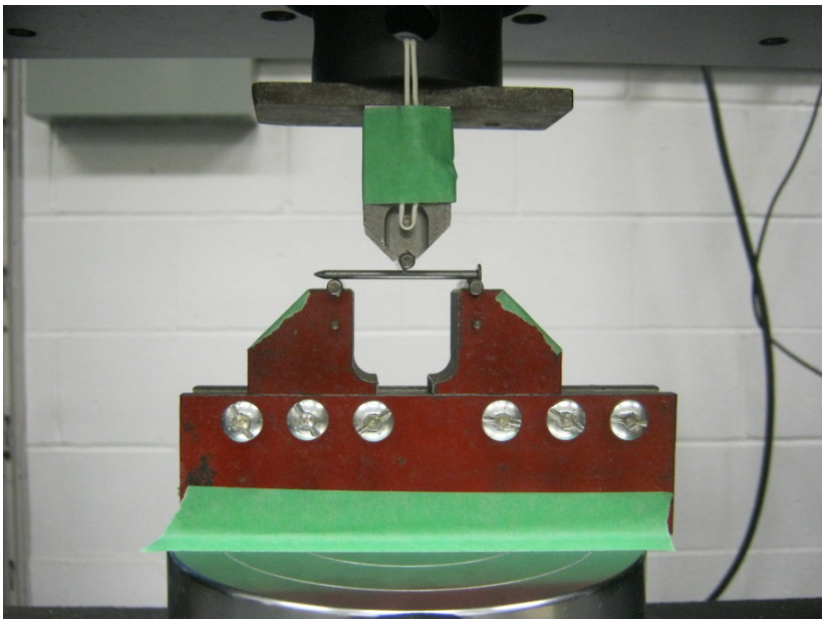

Figure 4.1: Center-point bending test performed on 6d, 8d, and 10d nails

Response curves from all nail bending tests can be found in Appendix B. To ensure greater accuracy, the diameter of each nail was recorded at 5 locations with digital calipers accurate to 0.01 mm. The standard specification for Driven Fasteners: Nails, Spikes, and Staples (ASTM, 2013) lists required values for common wire nails, as does CSA-O86 clause A.9.5.1.1 (CSA, 2010). As can be seen in Table 4.1, the bending test provided very consistent results, which indicate that, in bending, the selected nails perform at an acceptable level.

Table 4.1: Result from center-point bending tests

Nail Size	Mean Nail Diameter (mm)	Bending yield strength (MPa)	Coefficient of Variation[1]	ASTM F1667 Strength		CSA-O86 min. strength (MPa)
				psi	MPa	
6d	2.836	705.7	0.036	100,000	689.5	635
8d	3.247	639.5	0.053	100,000	689.5	635
10d	3.730	611.9	0.165	90,000	620.5	615

[1]COV of peak bending yield strengths

4.1.2 Nail bearing test

Nail bearing tests were performed on specimens of SPF and OSB, in accordance with the Standard Test Method for Evaluating Dowel-Bearing Strength of Wood and Wood-Based Products (ASTM, 2005), in order to determine the embedment properties of the framing (SPF) and sheathing (OSB) materials used in this study. Five identical tests were performed on each combination of specimens of SPF and OSB and all nail sizes (6d, 8d, 10d, and 16d). This resulted in a total of 40 bearing tests performed. Figure 4.2 shows nail bearing tests being performed on specimens of SPF and OSB with 10d nails. Details on all materials were provided previously in Chapter 3. The direction of loading on all specimens was parallel to grain, simulating the effect of a nail in tearout. Figure 4.3 shows sample results from the nail bearing tests done on specimens of OSB with 6d nails. From these results, the yield point, stiffness and embedment strength were calculated, as will be discussed in Section 5.3.

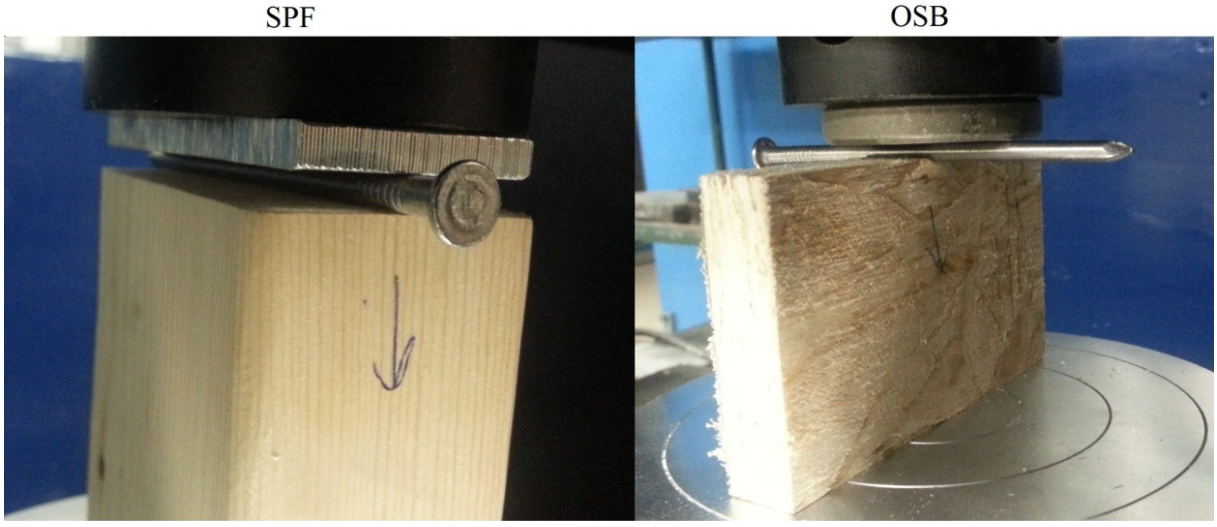

Figure 4.2: Nail bearing tests

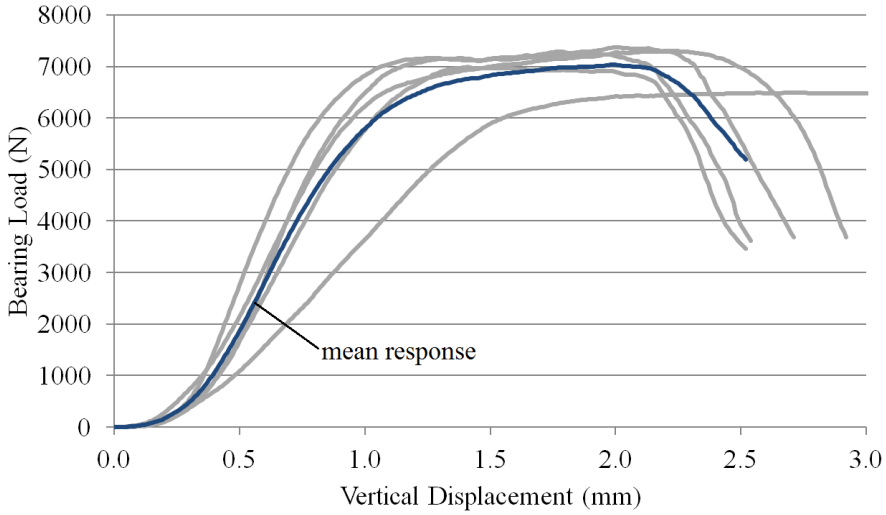

Figure 4.3: Nail bearing test sample data on 6d nails in SPF

4.1.3 Compression tests

Compression tests were conducted on both intermediate materials: extruded polystyrene insulation (XPS), and gypsum wallboard (GWB) to determine embedment properties. Compression tests were done as opposed to bearing tests because the standard for bearing tests does not apply to these materials.

Extruded Polystyrene Insulation

6 specimens of insulation were cut from the 1" (25.4mm) thick sheet used in this study, into cubes with a bearing area of 1 square inch (25.4 x 25.4mm) and compressed. The Standard Specification for Rigid, Cellular Polystyrene Thermal Insulation (ASTM, 2012) lists compressive resistance of polystyrene insulation based on type, which varies from 35 kPa to 690 kPa. The specific type of polystyrene insulation used in this study was identified as type 4. Figure 4.4 presents the results from all tests on insulation, which shows compressive yielding at approximately 120 kPa.

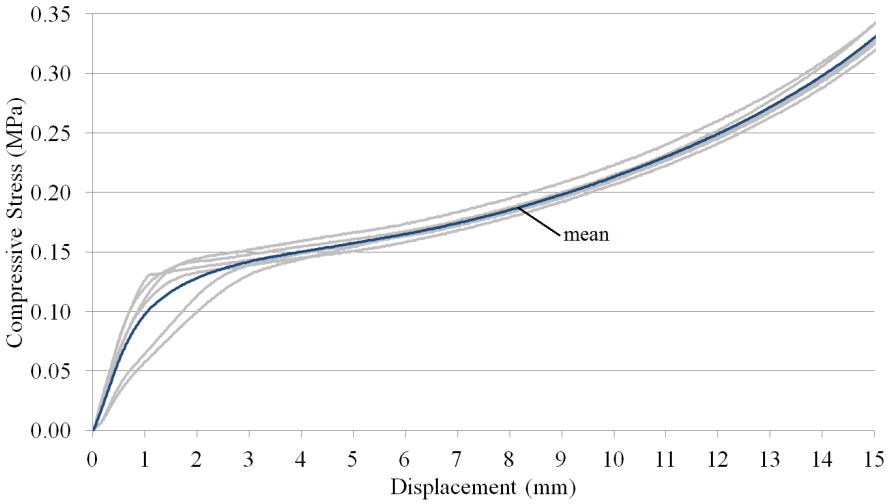

Figure 4.4 Results from compression test on insulation specimens

Gypsum Wallboard

Six specimens of GWB were split into sizes of approximately 2" x 2" (50x50mm) from a sheet of 5/8" (15.88mm) thick insulation used in the main portion of this study. Prior to testing, specimens were covered with a single layer of tape on exposed edges, as the material is highly brittle. The Standard Specification for Gypsum Board (ASTM, 2013) lists physical and structural requirements for GWB, however there is no requirement for compressive strength in the direction parallel to planar, as was considered in this study, nor is there a standard for its measurement. Figure 4.5 presents the results of compression tests on GWB, which indicate that the material begins to crush at approximately 2.3 MPa. GWB has brittle failure in a highly irregular and unpredictable fashion.

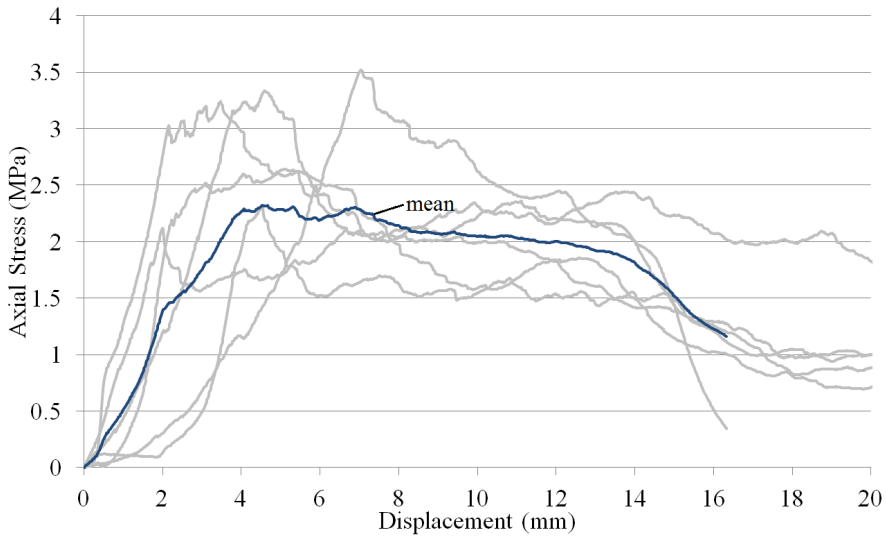

Figure 4.5: Results from compression test on gypsum wallboard specimens

4.1.4 Nail pull-out tests

5 nail pullout or withdrawal tests were conducted on size 10d nails. The Standard Test Methods for Mechanical Fasteners in Wood (ASTM, 2012) specify requirements for nail withdrawal tests such as rate of withdrawal, wood block size, edge distances, and nail sizes. These requirements were followed for this test. Of the 5 tests, the load vs. nail withdrawal curves for 4 are presented in Figure 4.6, with the mean response highlighted. The resistance of a nail to withdrawal is almost entirely dependent on friction between the nail and wood grain. The response of a nail shows a high initial stiffness (approximately 1 kN/mm) until the static friction slip load is exceeded. Once this occurs, load in the nail drops abruptly by about 10%, after which it drops more gradually in an approximately linear fashion. Of the withdrawal tests performed in this study, the post-peak force in the nail dropped roughly in proportion to the length of the nail remaining embedded in the wood block.

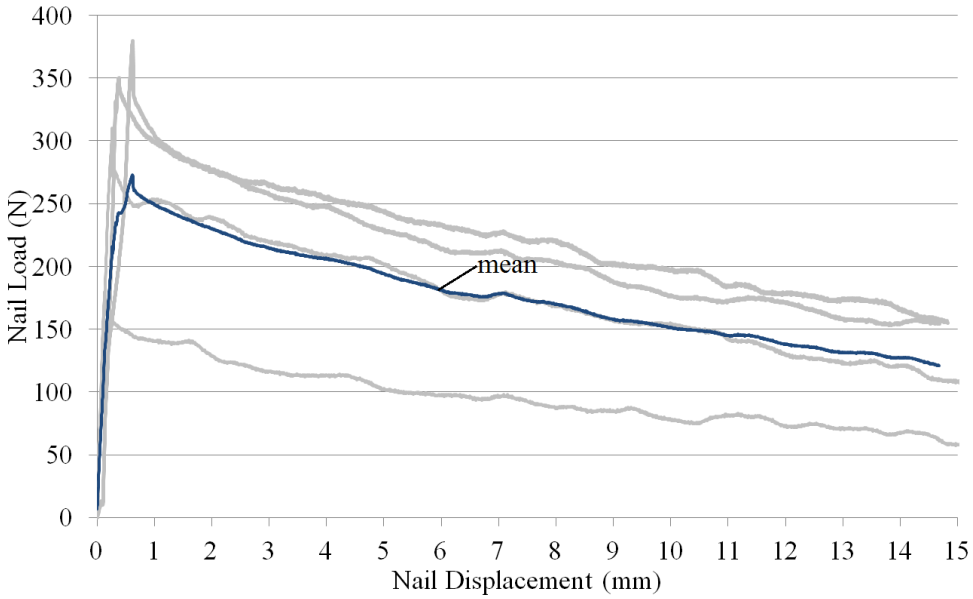

Figure 4.6 Results from 10d nail pull out test on SPF lumber specimens

4.2 Results for Nailed Connection Specimens with Gypsum Wallboard

Figure 4.7 shows the unmodified load-deformation response of an individual nailed joint specimen connecting an OSB sheathing panel to a lumber stud, with gypsum wallboard (GWB) located between the sheathing and stud. The example shown in the figure is from a connection with 6d nails and a 1/2" (12.7 mm) thick intermediate GWB layer.

This data shows the response recorded by the load frame on the entire specimen, which contains 4 nails tested simultaneously. To facilitate comparison with other test results, the load values were divided by 4 to determine the response on a per-nail basis. Since there were six individual tests for each type of test specimen, the mean of the load and displacement values from the six tests (with the same nail size, gap size and gap material) were then calculated to construct the mean response curves.

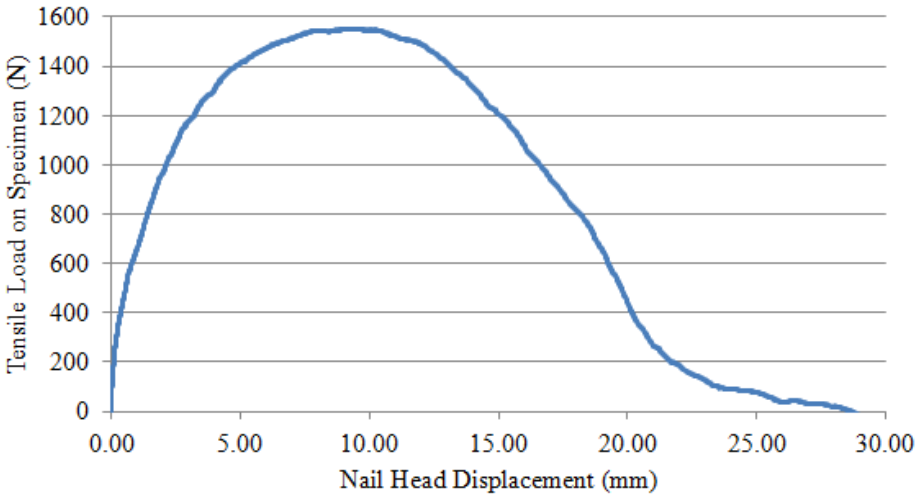

Figure 4.7: Sample experimental response data

Figures 4.8, 4.9, and 4.10 show the mean responses of each set of six identical tests for 6d, 8d and 10d size nails respectively. In each figure, the baseline case using no gypsum wallboard, as well as GWB thicknesses of 1/2" (12.70 mm) and 5/8" (15.88 mm) are shown. These initial observations show that there is a significant drop in both capacity and stiffness when gypsum wallboard is added to the assembly, regardless of the nail size. The magnitude of this drop is quantified later in this chapter and is most severe in the case of the smallest 6d nails, likely due to the fact that the addition of a gap would leave the nail with much less penetration relative to its length. Note that some of these tests were designed to purposely not satisfy the minimum penetration as listed in Table 2.1, as was discussed previously in Section 3.6.

Specimens with 6d and 8d nails used an OSB sheathing of thickness 7/16" (11.1 mm), whereas the other tests, including those with insulation, used a sheathing thickness of 5/8" (15.9 mm). This combination of nail sizes and sheathing thicknesses is based on Table 2.1, and was also discussed previously in Section 3.6.

Note that all specimens with GWB and 6d nails, and specimens with 5/8" GWB and 8d nails did not meet the minimum nail penetration as defined by the standard (CSA, 2010), as was mentioned previously in Section 3.6. The fact that specimens which satisfy the minimum nail penetration (those with 10d nails, and that with 8d nails and 1/2" thick GWB) consistently underperform baseline cases with no GWB, contradicts note 4 to Table 9.5.1A, which states that GWB can be used as an intermediate material so long as minimum penetration distance is met.

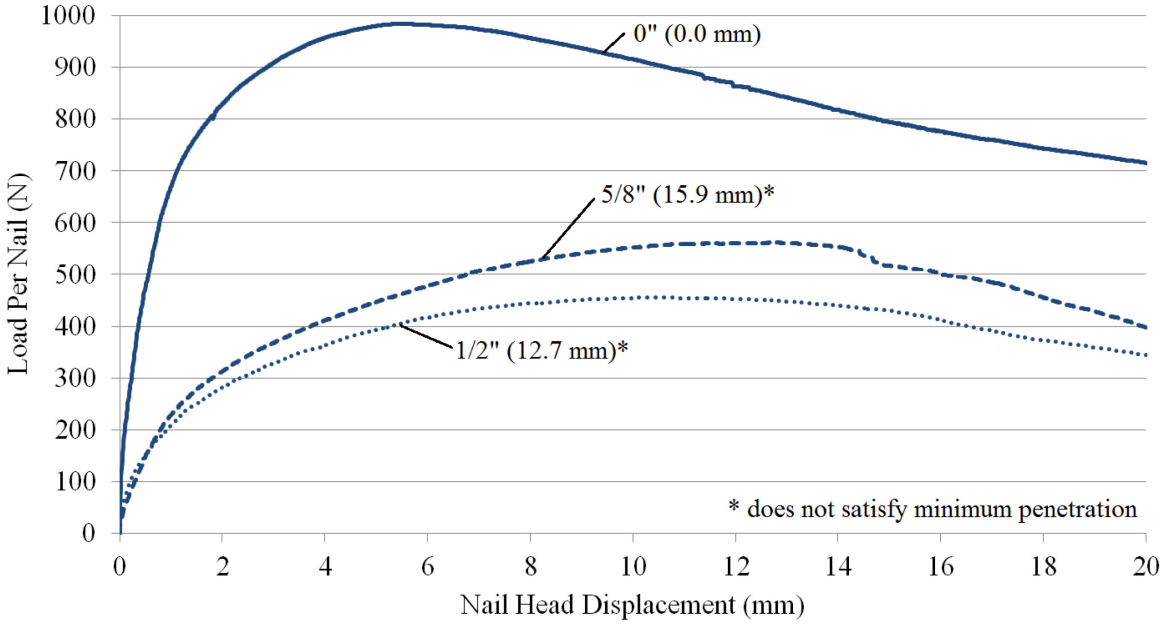

Figure 4.8: Mean responses using gypsum wallboard (GWB) and 6d nails

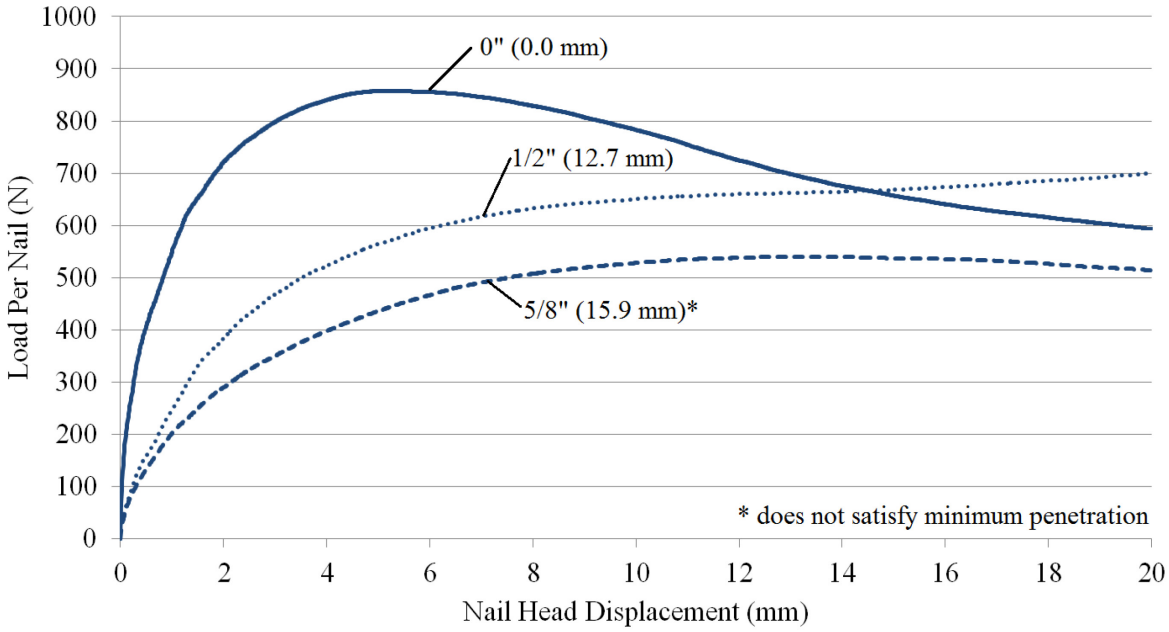

Figure 4.9: Mean responses using gypsum wallboard (GWB) and 8d nails

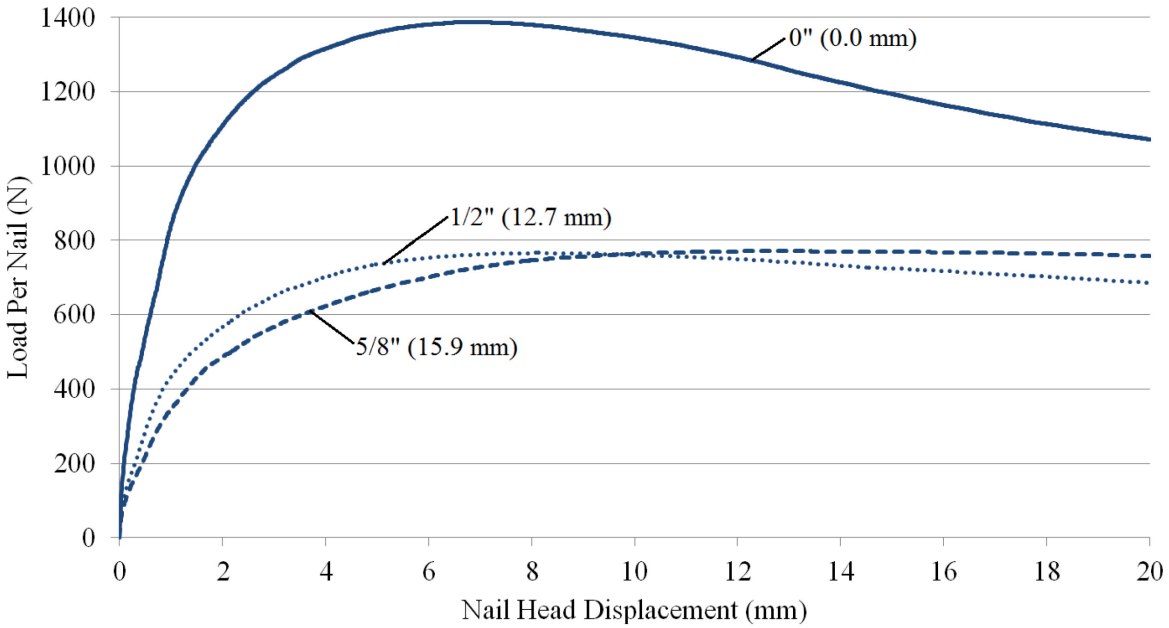

Figure 4.10: Mean responses using gypsum wallboard (GWB) and 10d nails

Response curves from each of the 54 tests conducted on specimens with intermediate GWB are provided in Appendix C. The coefficient of variation (defined as the standard deviation divided by the mean) of the peak load of each test was calculated for each gap and nail size combination and is indicative of the relative amount of spread between identical tests. Table 4.2 presents the mean value of the peak load per nail, the associated coefficient of variation (COV), and the capacity as a percentage of the base case (with no GWB) for all specimens involving GWB as an intermediate material between sheathing and studs. The COV for all tests involving intermediate GWB was 0.206. Figures 4.11 and 4.12 show the response curves for the tests that used 10d nails with 5/8" of GWB and 8d nails with no GWB, respectively, representing those cases with the least and most variation, respectively. The amount of variation in experimental testing can explain the small difference in behavior between tests with 1/2" and 5/8" intermediate GWB.

As was introduced in Section 2.3, the part of the standard for timber design in the United States that deals with the design of lateral load resisting systems, Special Design Provisions for Wind and Seismic (SDPWS) requires increasing the nail size to compensate for the effect of an intermediate layer of GWB (AWC, 2012). From Table 4.2, it can be seen that this would not be enough to overcome the observed losses. For example, the capacity of a nailed connection with an 8d nail and no GWB is 863.4 N. Introducing a 1/2" or 5/8" layer of GWB and a larger 10d nail will not restore the capacity of the connection completely.

Table 4.2: Comparison of maximum capacity for specimens with intermediate GWB

Gypsum Wallboard Thickness	6d Nail			8d Nail			10d Nail		
	Mean	COV	% base capacity	Mean	COV	% base capacity	Mean	COV	% base capacity
0" (0.00mm)	985.6	0.193	100.0	863.4	0.317	100.0	1389.6	0.245	100.0
1/2" (12.7mm)	488.6	0.289	49.6	702.6	0.209	81.4	768.5	0.117	55.3
5/8" (15.9mm)	582.7	0.204	59.1	556.7	0.175	64.5	779.2	0.104	56.1

Note: mean capacity values in Newtons

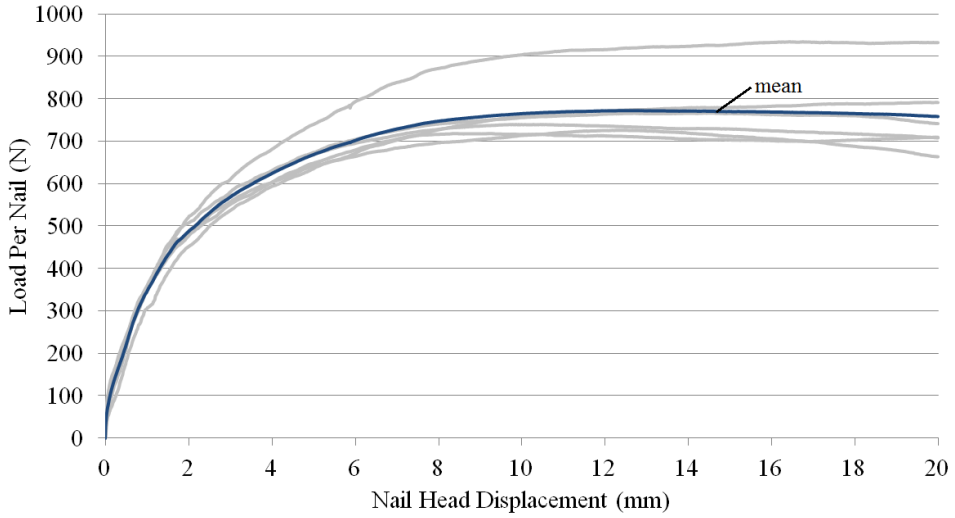

Figure 4.11: Individual tests for the case of 10d nails with 5/8" GWB (least variation)

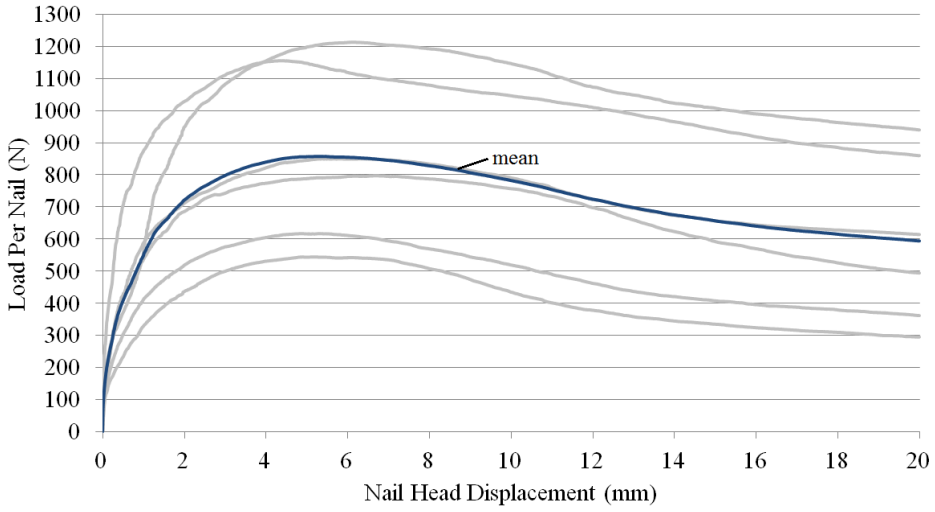

Figure 4.12: Individual tests for the case of 8d nails with no GWB (most variation)

Figure 4.13 groups together mean response values of tests with identical GWB thickness to show the effect of increasing nail size and sheathing thickness. Every combination of nail size and GWB thickness consistently underperforms every base case with no GWB in both connection capacity and connection stiffness. This suggests that increasing the nail size to the maximum of 10d and sheathing thickness to 5/8" is not enough to overcome the observed losses from introducing GWB as an intermediate material in any of the permitted cases.

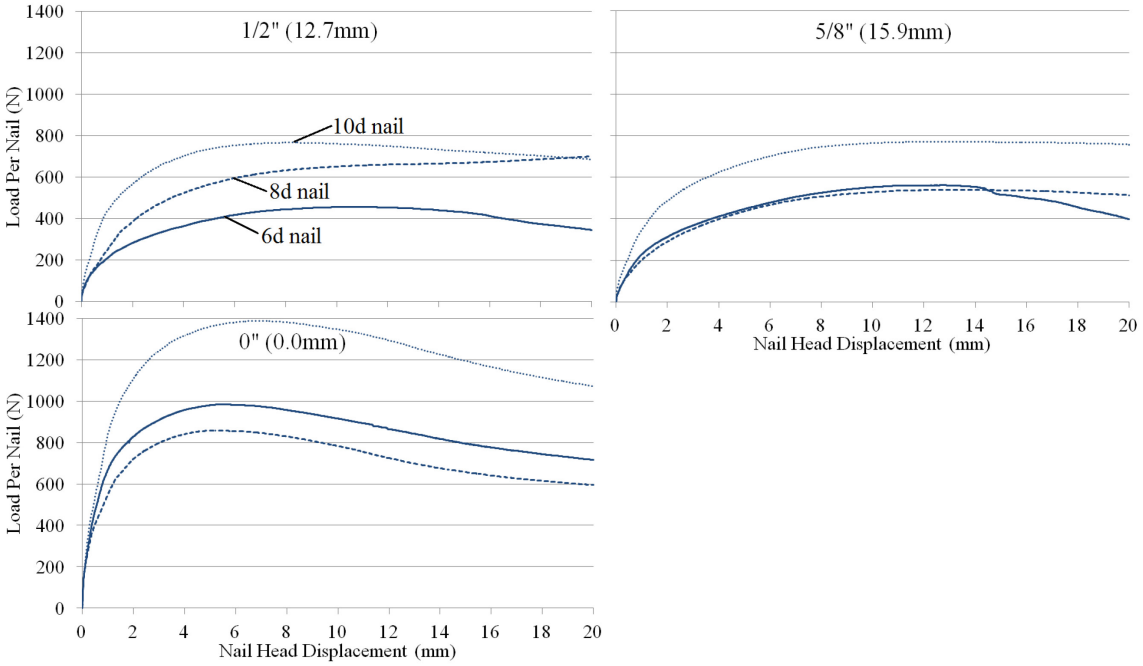

Figure 4.13: Comparison of nail sizes with gypsum wallboard as intermediate material

4.3 Results for Specimens with Rigid Insulation

Tests of nailed connections with insulation located between the sheathing and studs were conducted and analyzed in a manner similar to those with GWB. Load values from each test were divided by 4 to get the load per nail. Figures 4.14 and 4.15 show mean load-deformation curves for size 10d and 16d nails, respectively. Similarly to the tests with gypsum wallboard, each line is the mean result from 6 identical tests. Both

figures have been labeled with the thickness of the insulation. Initial observation shows that for the standard 10d nails, there is an immediate and significant loss in capacity when an intermediate space of any size is introduced, which continues to reduce with the use of larger insulation thicknesses. For the larger 16d nails, the initial drop in capacity occurs to a much lesser degree, along with a greater decrease in stiffness. The magnitude of this loss will be discussed and quantified in Sections 4.4 to 4.6 through the identification of the yield point and curve fitting. As the insulation thickness increases, the displacement corresponding to peak load increases as well.

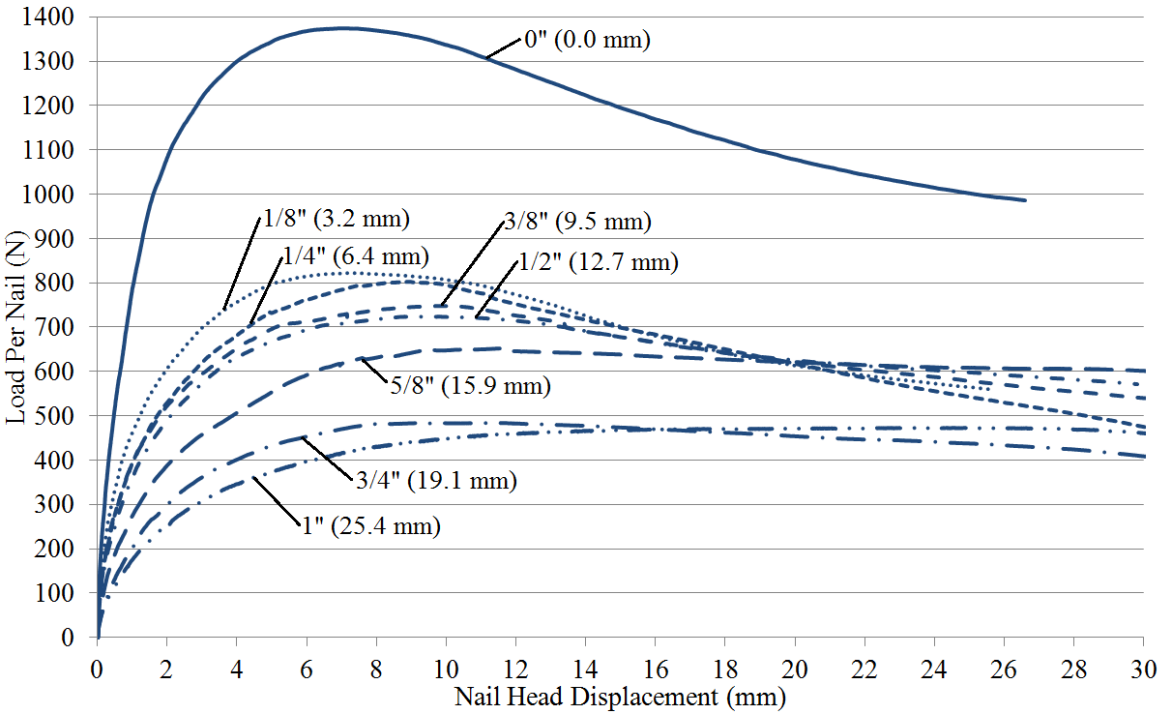

Figure 4.14: Mean responses using rigid insulation and 10d nails

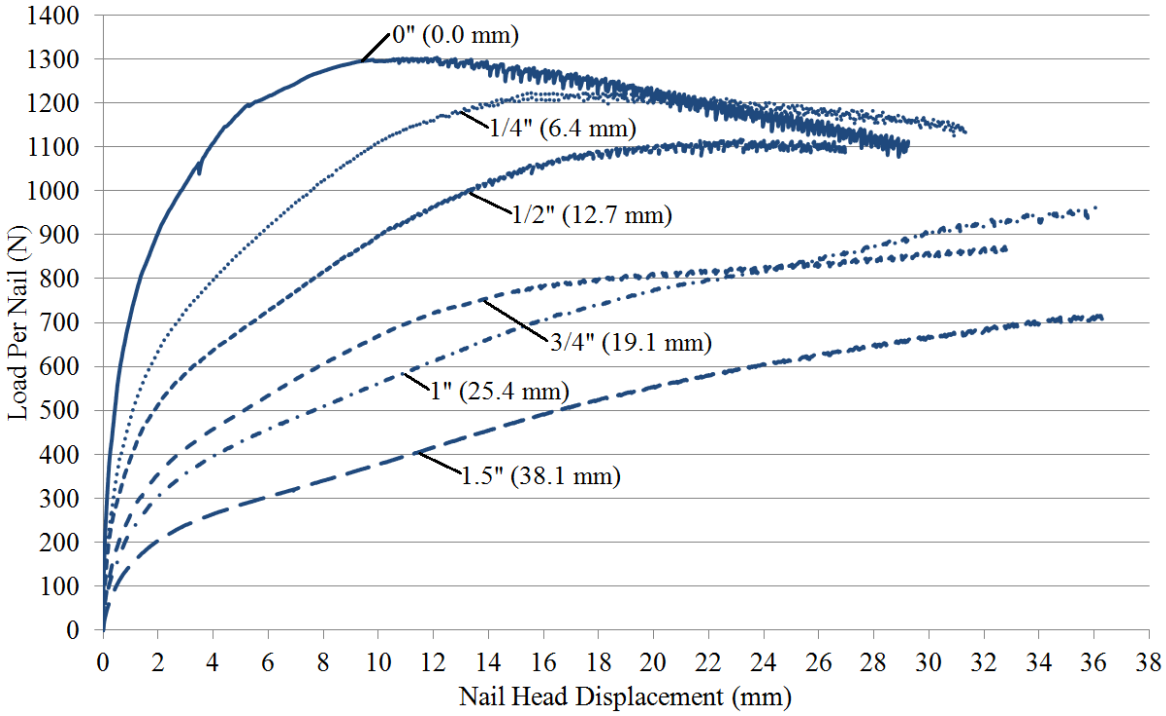

Figure 4.15: Mean responses using rigid insulation and 16d nails

Post peak behavior flattens with increasing insulation thickness. Both of these trends result in a change in overall behavior from one in which load increases to a maximum and then drops, to one where load keeps increasing for the entire duration of the test. This can be observed clearly in the tests done on 16d size nails, where those tests with an intermediate layer of insulation 1/2" (12.7 mm) and thinner have a clear maximum, and those tests with a thicker layer of insulation do not. A likely cause of this behavior is that as insulation thickness increases, the nail gradually changes from predominantly two-way bending to one-way bending. Note that all tests were concluded at a lateral nail deformation of approximately 37.5 mm.

Just as with gypsum wallboard, Table 4.3 presents the mean value of the peak load per nail, the associated coefficient of variation (COV), and the capacity as a percentage of the base case for tests involving insulation.

Table 4.3: Comparison of maximum capacity for specimens with intermediate insulation

10d Nails				**16d Nails**			
Insulation Thickness	Mean	COV	% base capacity	Insulation Thickness	Mean	COV	% base capacity
0" (0.0 mm)	1389.6	0.245	100.0	0" (0.0 mm)	1317.7	0.185	100.0
1/8" (3.2 mm)	829.2	0.098	59.6	1/4" (6.4mm)	1252.4	0.138	95.0
1/4" (6.4 mm)	818.1	0.237	58.9	1/2" (12.7 mm)	1125.5	0.186	85.4
3/8" (9.5 mm)	756.1	0.069	54.4	3/4" (19.1 mm)	819.0	0.188	62.2
1/2" (12.7 mm)	731.4	0.124	52.6	1" (25.4 mm)	776.8	0.148	59.0
5/8" (15.9 mm)	689.5	0.196	49.6	1.5" (38.1 mm)	555.9	0.140	42.2
3/4" (19.1 mm)	490.4	0.167	35.3				
1" (25.4 mm)	474.2	0.262	34.1				

Note: mean capacity values in Newtons

The coefficient of variation for all tests with intermediate insulation was 0.170, which is slightly less variation than for those tests with GWB. The drop in mean connection capacity is visualized in Figure 4.16. Raw load-deformation data for each of the 78 tests with insulation is provided in Appendix D.

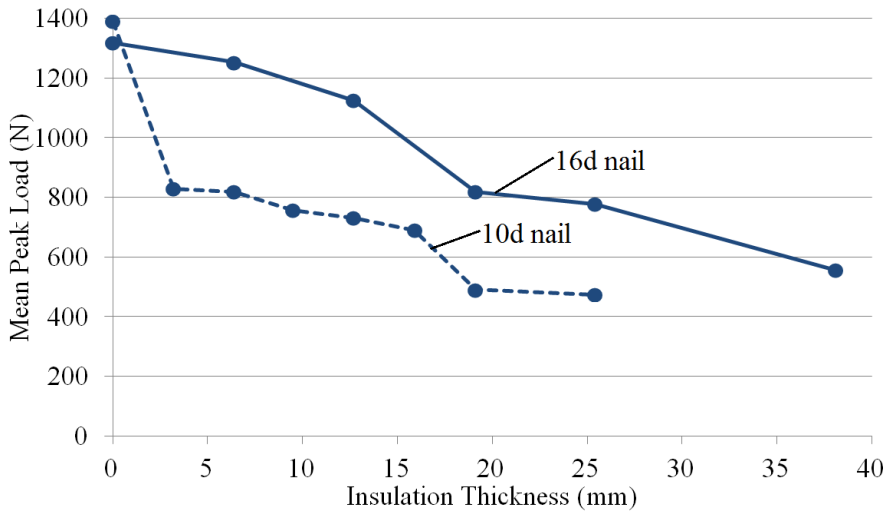

Figure 4.16: Maximum capacity for specimens with intermediate insulation

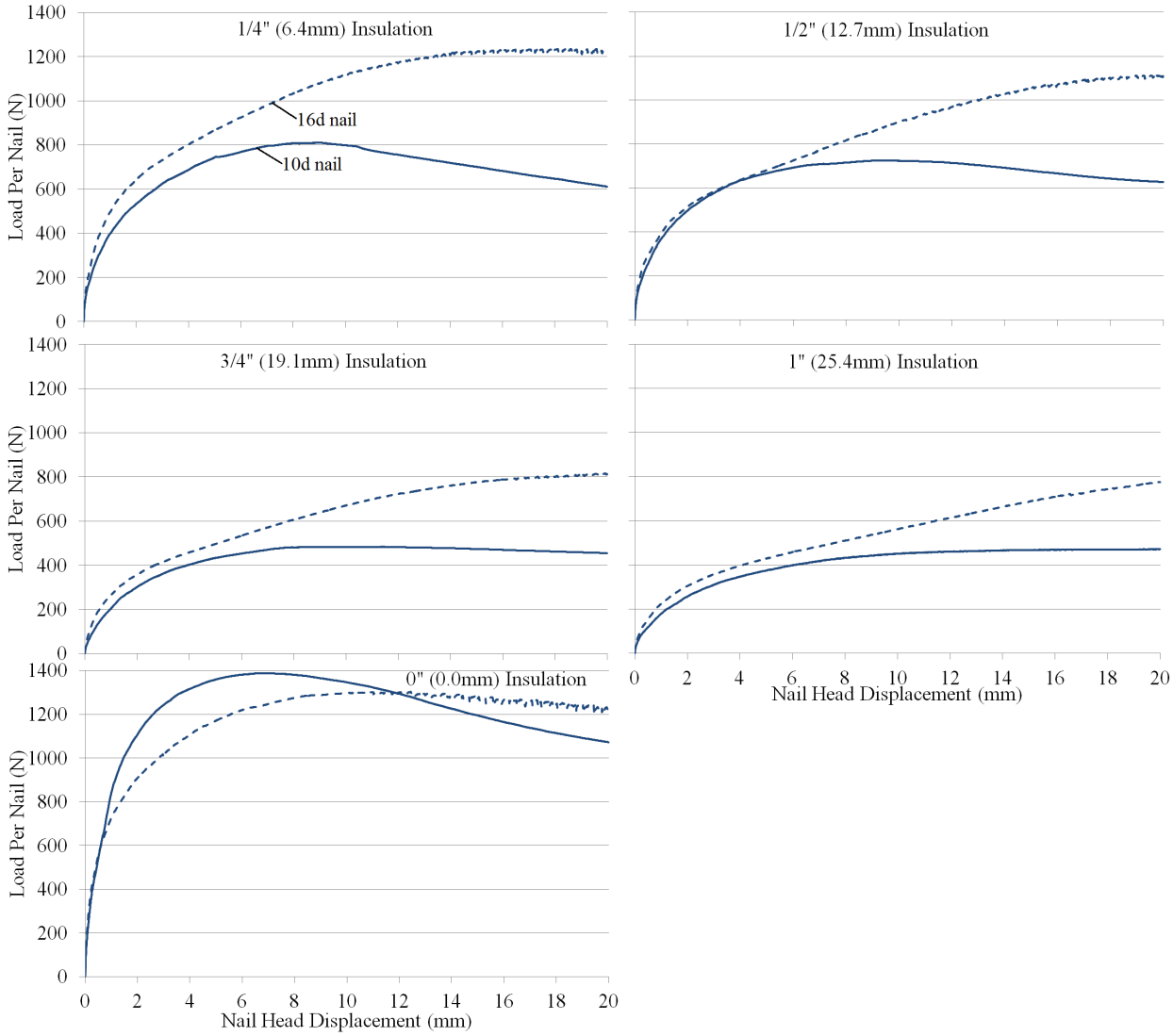

Figure 4.17: Comparison of nail sizes with rigid insulation as intermediate material

Figure 4.17 compares the responses of specimens with 10d and 16d nails in the five cases of identical insulation thickness (0", 1/4", 1/2", 3/4" and 1"). For the base case of no insulation, specimens with 10d nails resulted in a higher load at low displacement (nail slip) than those with the larger 16d nail, as the 16d nail specimens took longer to develop their maximum strength. This is likely due to a later development of plastic moment capacity, although it may be an artifact resulting from variability in the data. The observed difference is small enough that it falls within the load-deformation variability between identical base case tests.

In the case of any non-zero insulation thickness, the specimens with the larger 16d nail consistently resulted in a higher strength than those with the 10d nail; this was as expected. It is important to note that nail size has a large impact on connection capacity and stiffness. This has been an established principle since the introduction of the European Yield Model (EYM), and is assumed in this study. Consequently, the fact that connections with intermediate insulation retained a greater proportion of strength properties than did connections with intermediate GWB was a result of the use of larger nails in the case of intermediate insulation, and is not a product of the properties of the intermediate materials themselves.

4.4 Estimation of the Yield Point

This section deals with the determination of the yield point of the experimental data using various methods. Finding the yield point is essential to determining connection stiffness and strength for the purpose of comparing various intermediate material thicknesses. As was seen in Sections 4.2 and 4.3, introduction of any intermediate

material between the stud and the sheathing in a nailed shear wall interface changes the overall shape of the connection response significantly, therefore several different methods were considered. Muñoz et al. (2008) have provided a review of six of the most common and accepted methods in use in North America, Europe, Japan and Australia for determining the yield point of timber assemblies, and are summarized as follows. The use of each of these methods on sample test data is shown in Figure 4.18 (reproduced from Williams at al.)

K&C (Karacabeyli & Ceccotti, 1996)

The yield point is considered the location on the load-deformation curve corresponding to 50% maximum capacity.

CEN - European Committee for Standardization (Ceccotti, 1995)

A secant line, K_α, is drawn from a point at 10% maximum capacity to a point at 40% maximum capacity. The slope of this line, angle α, is then calculated. A line K_β, is drawn with slope β tangent to the load-distribution curve, such that:

$$\tan\beta = \frac{\tan\alpha}{6}$$

The intersection of K_α and K_β is the yield point

CSIRO (Commonwealth Scientific and Industrial Research Organization, 1996)

The displacement of a point on the load-deformation curve at 40% peak load is calculated. This displacement is multiplied by a factor of 1.25.The yield point is the point of the load-deformation curve corresponding to this new displacement

EEEP - Equivalent Energy Elastic-Plastic Curve from the Standard Test Method for Cyclic (Reversed) Load Test for Shear Resistance of Walls for Buildings (ASTM, 2005)

The initial stiffness (K) from 0% to 40% load is calculated, along with the failure location which is defined as the point when the strength drops from maximum to 80% peak load. Then the yield load is calculated using the following expression:

$$P_y = \left[\Delta_{failure} - \sqrt{\Delta_{failure}^2 - \frac{2w_{failure}}{K}}\right] * K$$

where: P_y - yield load, $\Delta_{failure}$ - deformation at failure, $w_{failure}$- energy dissipated until failure (area under load-deformation curve)

The yield point is the location where the secant to 40% stiffness found initially reaches the yield load, P_y.

Y&K (Yasumura & Kawai, 1998)

Two secant lines are drawn: one from a point at 10% maximum capacity to a point at 40% maximum capacity ($K_{10\text{-}40}$), and one from a point 40% maximum capacity to a point at 90% maximum capacity ($K_{40\text{-}90}$). A tangent line is drawn to the load displacement curve, parallel to $K_{40\text{-}90}$, $K_{//40\text{-}90}$. The location of the intersection between $K_{10\text{-}40}$ and $K_{//40\text{-}90}$ is determined. This point is projected in the direction of the deformation axis on the load-deformation curve, which becomes the yield point.

5% of diameter from the Standard Test Method for Evaluating Dowel-Bearing Strength of Wood and Wood-Based Products (ASTM, 2005)

A secant line is drawn from 0% capacity (origin) to 40% maximum capacity. A line parallel to this is drawn, offset by a distance equal to 5% of the diameter of the connector. The location where this new line intersects with the load-deformation curve is the yield point.

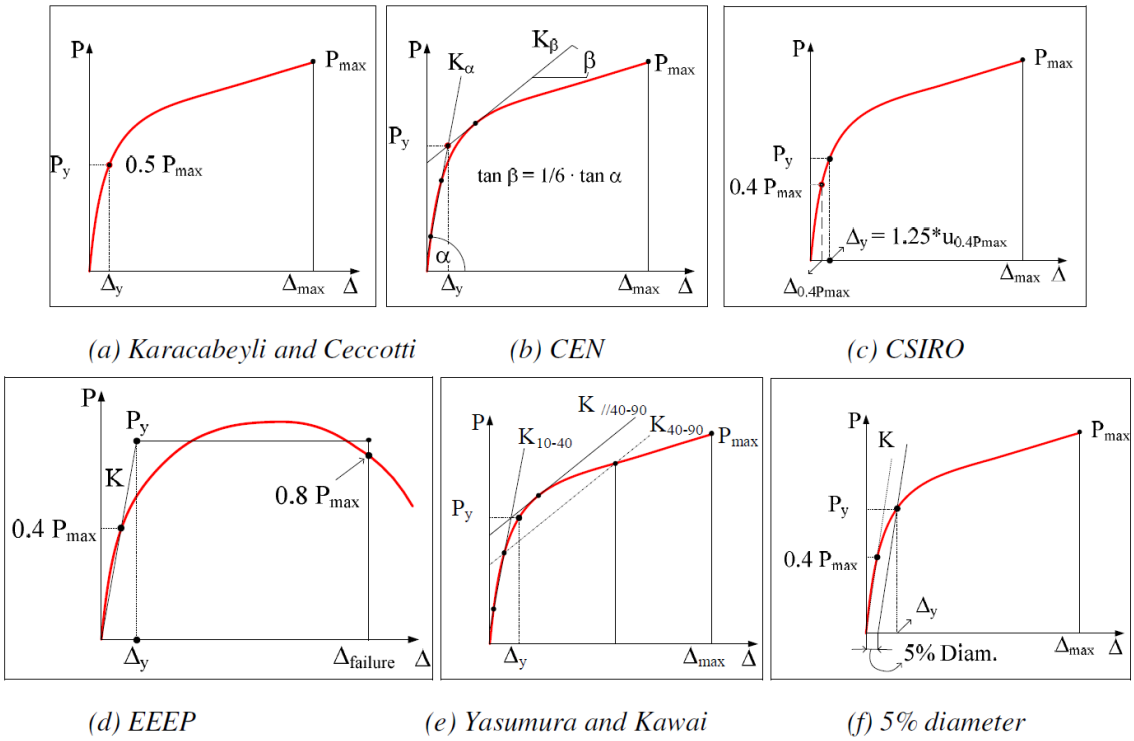

(a) Karacabeyli and Ceccotti *(b) CEN* *(c) CSIRO*

(d) EEEP *(e) Yasumura and Kawai* *(f) 5% diameter*

Figure 4.18: Methods of determining yield point for timber connections (Muñoz et al, 2008)

All of these methods require knowledge of the maximum capacity as an input. It is important to note that for several experimental tests, the load never reached an ultimate maximum value (defined as a point beyond which the load values decrease). This tends to occur with an intermediate material thickness greater than 1/4" (6.4 mm) with 16d nails and is clearly observed in the test summary Figures 4.14 and 4.15. Despite not reaching a

maximum for some tests, all tests were pushed far beyond the yield point of their respective connections.

Although these yield point calculation methods are intended for timber connections, their development likely did not consider the specific type of connection discussed in this study. These are, however, the most common methods used to determine the yield point of a timber assembly, and short of developing a new method, are the best options available in the literature. As was mentioned in Section 3.4, all experimental tests were stopped at an imposed lateral nail displacement of approximately 37.5 mm, which was the limit of the instrumentation. Nevertheless, it is clear that applying an even greater displacement would have increased the load further, to some small degree. The maximum load recorded at the end of such tests will therefore be used when needed, although it is also clear that in such cases, the maximum capacity is actually slightly higher than stated. The yield point was calculated using all but one of these methods. The EEEP method was not used since it requires a response curve that eventually reduces to 80% of peak load, which occurred in very few non-zero gap situations.

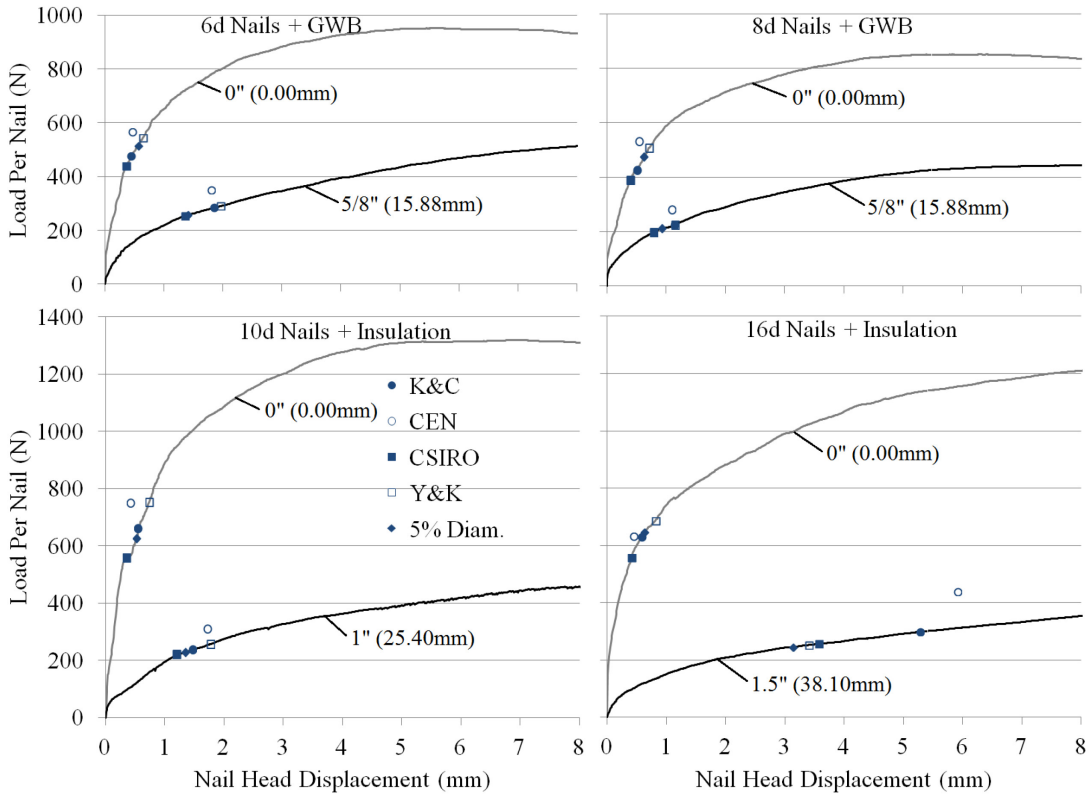

Figure 4.19: Comparison of methods of determining yield point

As a point of reference to visually gauge the validity of each of these methods, Figure 4.19 shows the location of the yield point calculated using each method on sample specimens of each nail size for cases of minimum (zero) and maximum intermediate material thickness.

The yield point as calculated by all methods with the exception of CEN, lie on the load deformation curve. As shown by Figure 4.19, for base cases with no intermediate material, these methods are fairly accurate in capturing the initial slope (secant stiffness) as well as the approximate load at which this slope begins to change significantly (yield strength). For those cases with large intermediate material thickness, these methods are noticeably less accurate in locating the yield point, as the slope of the load deformation curve does not appear to be changing significantly.

Figure 4.20 shows the yield strength and secant stiffness of all tests with GWB as an intermediate material, compared with the length of the embedded nail in the SPF stud as a percentage of the minimum as defined by Table 9.5.1 (Table 2.1). The error bars shown represent one standard deviation between the six identical tests. Three cases with GWB fall below the minimum required penetration (<100%), three satisfy the required penetration (>100%) and the remaining three are base cases with no GWB (which also satisfy the required penetration). As can be seen by the size of the error bars, base cases with no GWB exhibited proportionally more variation than those with GWB. The likely explanation for this is that since the variability in the yield strength of a nail is lower than that of wood materials, and that tests with no GWB are more dependent on the strength of the wood materials, this results in more variability in the strength of the connection as a whole. Nevertheless, regardless of the method used, tests with intermediate GWB consistently resulted in lower yield strength and significantly lower secant stiffness. There does not appear to be a significant change in strength or stiffness occurring exactly at the nail embedment limit (100%), rather the determining factor to either parameter seems to be simply whether or not GWB is included in the connection. Although strength and stiffness values vary between the five methods used, the trends observed are consistent.

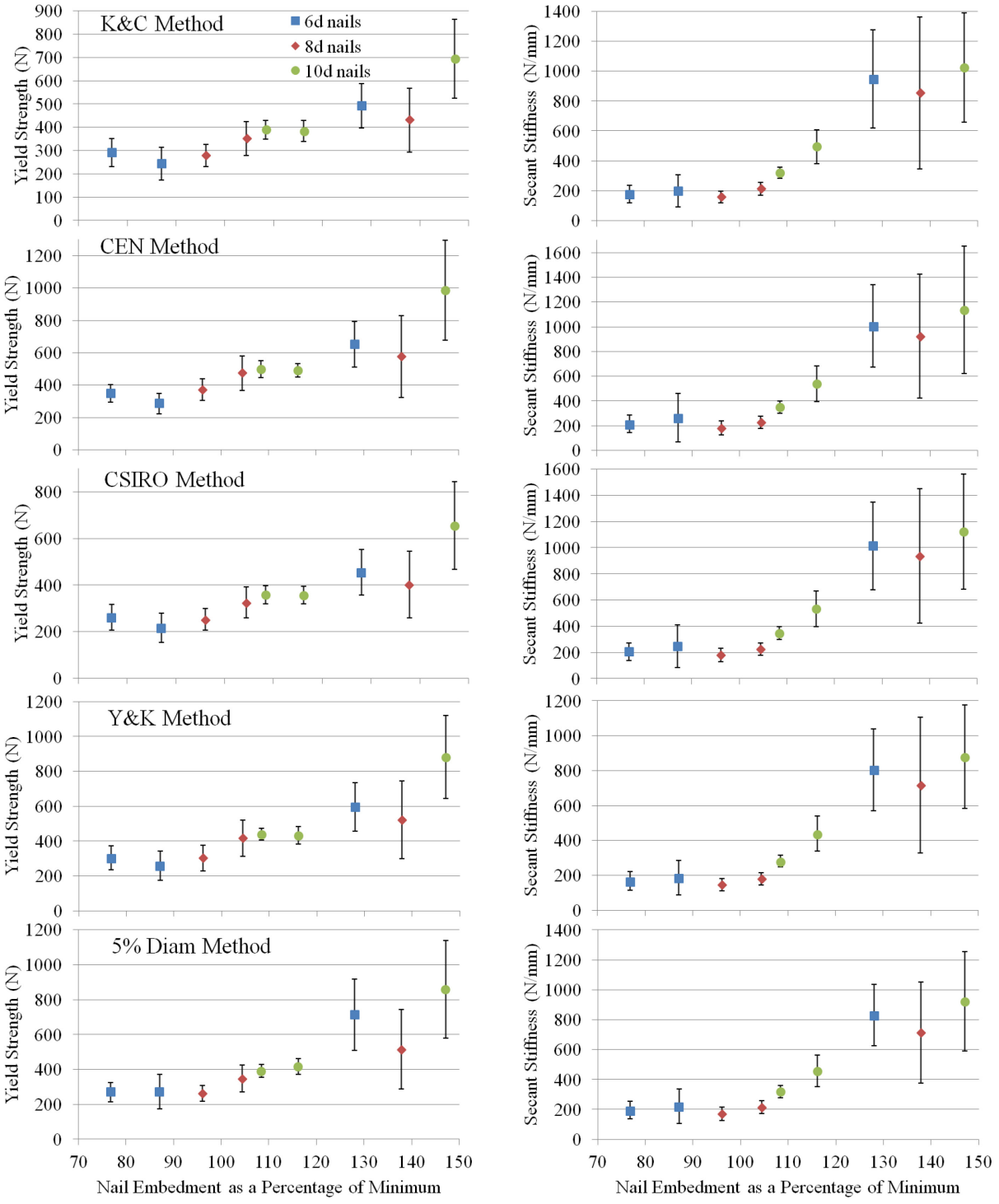

Figure 4.20 Yield point methods for tests with gypsum wallboard

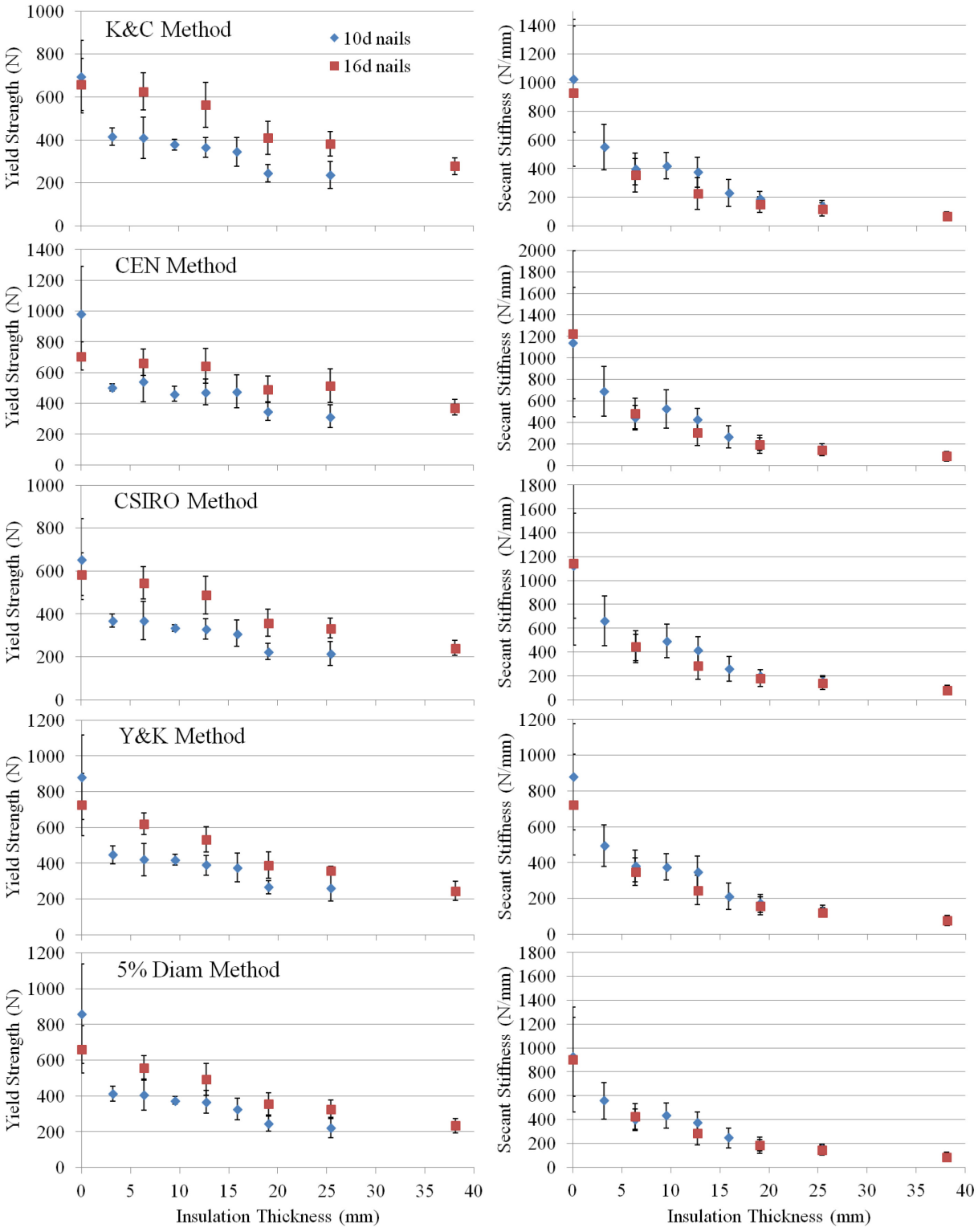

Figure 4.21: Yield point methods for tests with rigid insulation

Figure 4.21 shows the yield strength and secant stiffness of all tests with insulation as an intermediate material versus the insulation thickness. Once again, error bars show one standard deviation between identical tests and base cases with no insulation consistently exhibit more variation than those with insulation. There is a declining trend in yield strength, regardless of the method used, with specimens with 10d nails consistently losing more yield strength than those with 16d nails. Just as with specimens with GWB, there is a more significant drop in secant stiffness with any thickness of insulation. Larger insulation thicknesses result in very little secant stiffness, regardless of nail size or calculation method.

Figure 4.22 compares the mean values of yield strength and secant stiffness as calculated using each method for those tests with insulation as the intermediate material. Here, the five methods are compared with each other. Overall use shows that they are relatively consistent in predicting yield load and secant stiffness, although there is some spread between methods. In the case of yield strength, the lowest losses with increasing intermediate material thickness are seen with the K&C method (which will be considered the most optimistic), while the greatest losses are seen with the 5% diameter method (the most pessimistic). Similarly for secant stiffness, the 5% diameter and K&C methods result in the lowest and greatest relative drop, respectively.

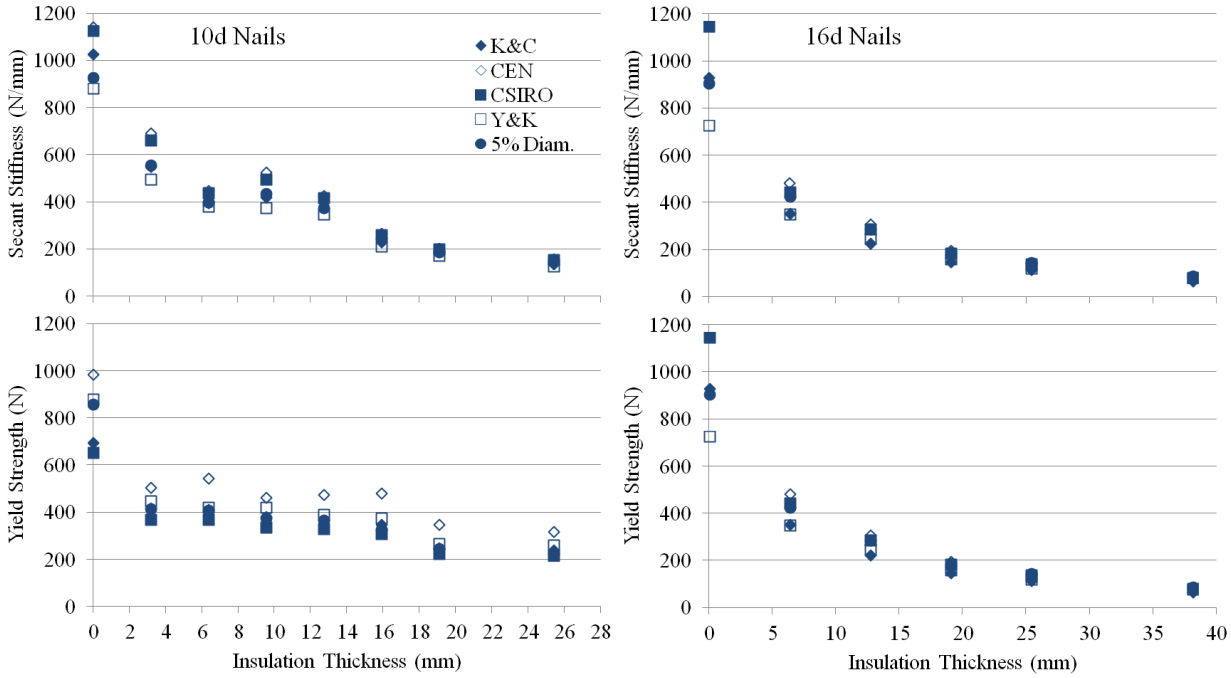

Figure 4.22: Summary of yield point methods for tests with rigid insulation

4.5 Estimation of the Stiffness Using Curve Fitting and Elasticity

Another means of determining connection stiffness is through curve fitting. Curve fitting involves the application of an empirical model to the test data through the determination of that model's parameters which will create the lowest square error (R-square). There are two common methods: the 3-parameter exponential model, introduced by Foschi (1974), and the Asymptotic Model (McLain, 1975). The following describes each empirical model, with Figure 4.23 showing how the 3-Parameter Exponential model is applied:

3-Parameter Exponential:

$$y = [p_1 - k_1 x]\left[1 - e^{\frac{-k_o x}{p_1}}\right]$$

where: x: nail slip (mm) , y: applied lateral load per nail (N), k_1: initial tangent stiffness (N/mm), k0: final tangent stiffness (N/mm), p_1: intercept of final tangent on load axis (N)

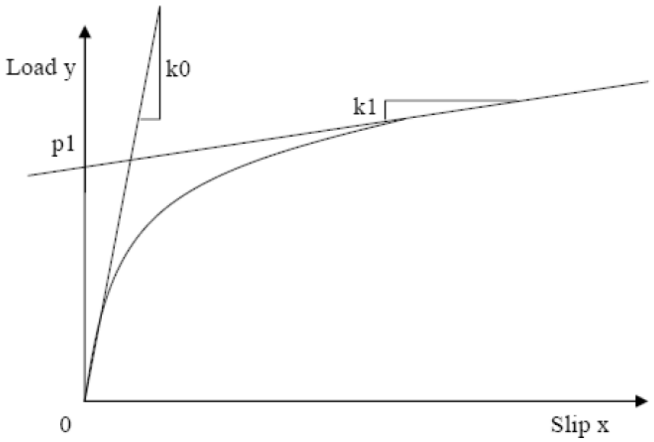

Figure 4.23: 3-Parameter exponential model (Foschi, 1974)

Asymptotic:

$$y = a - bc^x$$

where: x: nail slip (mm), y: applied lateral load per nail (N), and a, b, and c are model parameters

The validity of both methods is up to the maximum load value, therefore the previously discussed issue of the location of this maximum load reemerges, as maximum load was not reached in many of the tests. For those cases in which the load keeps increasing up to the end of the test, the maximum load is taken as the load at the end of the test, and thus the curve fitting method is applied to the entire range of test data. The statistical analysis software Origin (Pro v.8) was used to perform the multi-parameter fit. Figure 4.24 shows sample curve fitting data for all nail sizes for sample tests in the cases of no intermediate material (base case) and maximum intermediate material thickness. For large thicknesses, the 3-parameter exponential model is better at capturing the initial tangent stiffness, whereas the asymptotic model is fairly poor, and better suited to capturing the behavior near peak load.

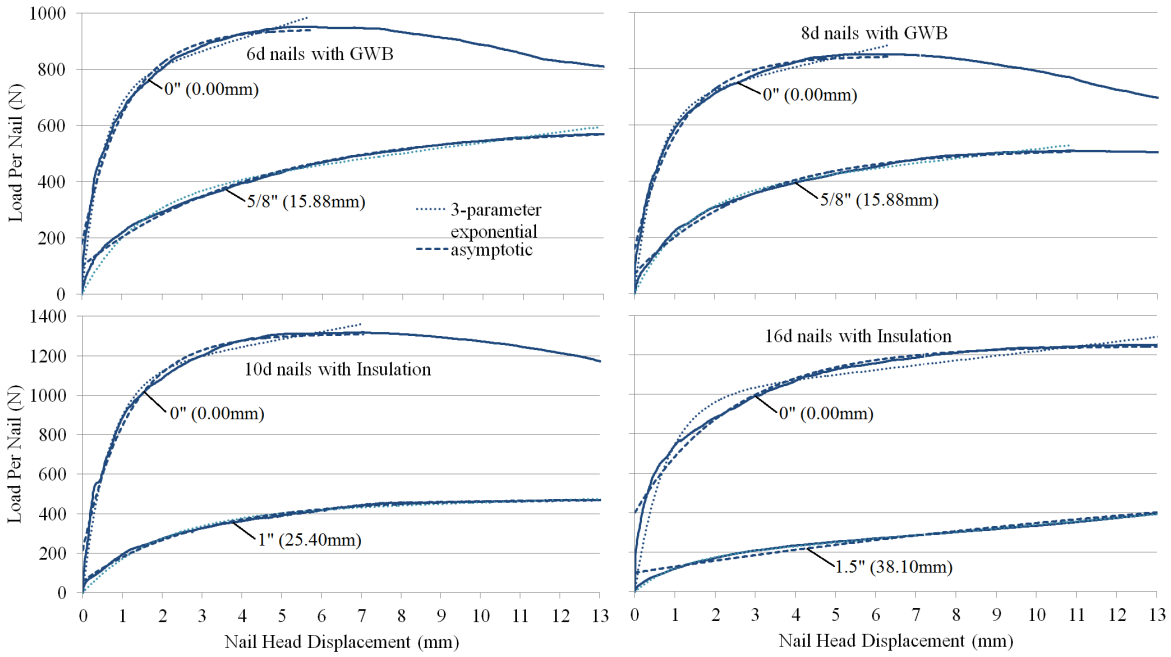

Figure 4.24: Sample curve fitting data

Tables 4.4 and 4.5 summarize parameters from both models for each load case for GWB tests and rigid insulation tests respectively. The values presented are the mean values from curve fits for all six identical tests. Values of all parameters for individual tests, along with the standard deviations and COVs, can be found in Appendices C and D for tests with GWB and insulation, respectively. The two curve fitting methods perform fairly well, achieving an R-square value greater than 0.90 for any individual test, and values of at least 0.96 for the mean of any six identical tests. Most curve fits on individual tests performed better than 0.99.

The parameter k_0 from the 3-Parameter exponential model represents an estimate of the initial stiffness of the connection. Parameters a from the asymptotic model and p_1 from the 3-parameter exponential model can be considered means of calculating the peak load. The accuracy of parameter a, however, is limited to cases when a maximum load is reached, as it can be seen from Table 4.5 that in most cases of 16d nails, parameter a

significantly overestimates peak load determined experimentally. Parameters p_1, k_0 and a (from both models) are reused in Section 4.6 as a means to calculate the relative drop in strength and stiffness.

Table 4.4: Mean values of curve-fitting empirical model parameters on tests with GWB

Case		3-Parameter Exponential				Asymptotic			
Nail	**Int. layer thickness**	**k_1 (N/mm)**	**k_0 (N/mm)**	**p_1 (N)**	**R^2**	**a (N)**	**b**	**c**	**R^2**
6d	**0"**	-40.62	1399.4	783.3	0.990	976.3	835.6	0.397	0.991
6d	**1/2"**	-16.18	332.3	318.0	0.981	498.0	398.1	0.743	0.989
6d	**5/8"**	-18.30	296.2	372.3	0.991	595.7	505.1	0.764	0.990
8d	**0"**	-33.78	1258.1	717.0	0.984	866.7	727.3	0.429	0.992
8d	**1/2"**	-5.72	306.9	597.7	0.995	684.6	614.9	0.711	0.991
8d	**5/8"**	-8.98	234.7	444.2	0.989	561.4	493.9	0.744	0.995
10d	**0"**	-14.50	1486.0	1332.4	0.992	1388.7	1264.6	0.445	0.992
10d	**1/2"**	-19.05	682.9	631.7	0.989	766.9	672.9	0.533	0.993
10d	**5/8"**	-14.86	461.0	628.1	0.990	776.9	669.4	0.671	0.993

Table 4.5: Mean values of curve-fitting empirical model parameters on tests with insulation

Case		3-Parameter Exponential				Asymptotic			
Nail	**Int. layer thickness**	**k_1 (N/mm)**	**k_0 (N/mm)**	**p_1 (N)**	**R^2**	**a (N)**	**b**	**c**	**R^2**
10d	**0"**	-14.54	1486.6	1332.1	0.992	1388.6	1264.5	0.445	0.992
10d	**1/8"**	-27.11	819.2	654.5	0.981	834.1	688.9	0.557	0.993
10d	**1/4"**	-32.78	624.7	564.4	0.984	856.2	727.9	0.638	0.995
10d	**3/8"**	-29.60	676.1	534.7	0.985	761.4	623.1	0.621	0.988
10d	**1/2"**	-30.66	602.0	507.6	0.989	751.1	638.0	0.623	0.994
10d	**5/8"**	-30.25	396.0	420.7	0.990	724.0	627.0	0.722	0.993
10d	**3/4"**	-5.52	256.1	439.1	0.992	494.9	452.5	0.651	0.997
10d	**1"**	-5.99	204.6	386.4	0.989	475.9	413.6	0.732	0.995
16d	**0"**	-31.42	1277.5	1016.6	0.967	1308.8	989.9	0.639	0.986
16d	**1/4"**	-35.36	684.0	734.3	0.979	1306.4	1021.5	0.823	0.987
16d	**1/2"**	-35.16	695.0	530.9	0.986	1610.1	1333.8	0.893	0.985
16d	**3/4"**	-22.25	345.8	431.9	0.984	920.4	755.0	0.878	0.989
16d	**1"**	-23.83	333.4	320.6	0.995	1078.6	922.8	0.902	0.988
16d	**1.5"**	-18.48	246.1	193.2	0.999	808.4	692.2	0.945	0.982

Parameter k_0 results in a consistently higher estimation of connection stiffness than the secant stiffness found through any of the 5 yield point calculation methods. It was found that the CEN method was closest to the 3-parameter exponential curve fitting method in predicting connection stiffness.

4.6 Capacity and Stiffness Reduction Analysis

At this point, the strength, stiffness and yield point of each set of experimental tests has been estimated using the methods described above. It is clear that there is a substantial decrease in both capacity and stiffness as a gap of any size is introduced, regardless of the intermediate material, even for the majority of cases where the nails retain the minimum required penetration. Figure 4.25 compares the relative drop in

capacity, as a fraction of the capacity of the base case with no intermediate material, using the following methods:

- Recorded Maximum: mean peak load
- Yield point K&C Method: (optimistic) the yield point method resulting in the lowest overall loss of strength
- Yield point 5% Diameter Method: (pessimistic) the yield point method resulting in the greatest overall loss of strength
- Parameter p_1: calculated from the 3-parameter exponential curve-fitting model
- Parameter a: calculated from the asymptotic curve-fitting model

In the cases of insulation as the intermediate material, for both nail sizes, declining, roughly linear trends can be observed when comparing the capacity as a fraction of the base case. On the introduction of a layer of any thickness, connections with standard 10d nails immediately lose between 40-46% of their capacity, regardless of how this is calculated, and continue declining as thicker material is used. The rate of this decline is roughly another 30% loss per inch or 12% per 10 mm of insulation. In the case of connections with 16d nails, there is a negligible loss in capacity initially (from 0" to 1/8" of insulation), and therefore the connection retains most of it as thicker insulation is used, although the rate of decline is greater (approximately 50-55% per inch or 20% per 10 mm of insulation) than for connections with 10d nails.

In the cases of gypsum wall board as the intermediate material, there is a consistent loss of capacity of 40-50% regardless of nail size, gypsum wall board thickness, or method of calculation. This is comparable to the loss of capacity for

insulation and 10d nails. It does not appear that the connection capacity gains anything from the use of GWB over insulation.

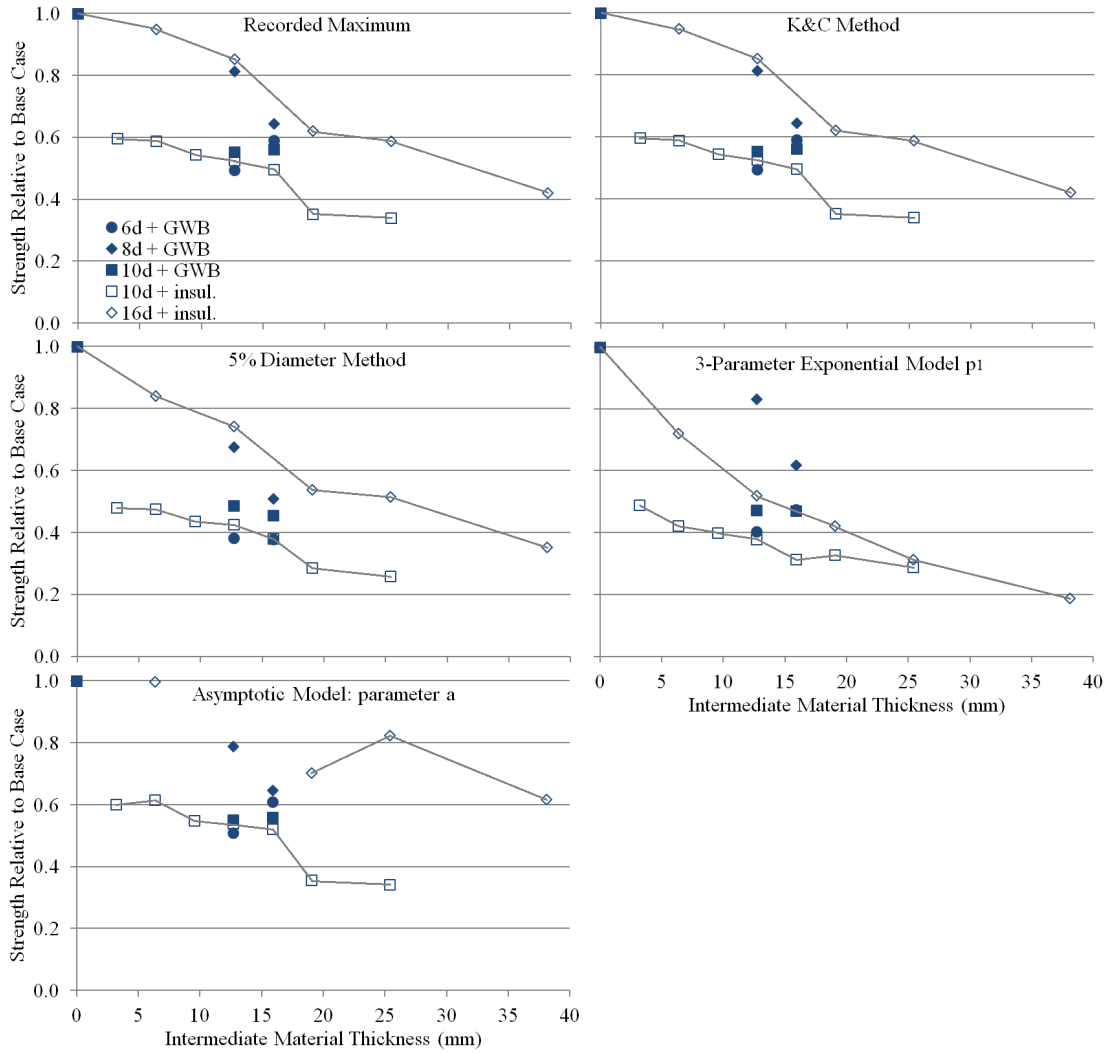

Figure 4.25: Comparison of relative drop in capacity from base case

Figure 4.26 compares the relative drop in stiffness (secant stiffness or yield stiffness in some cases), as a fraction of the stiffness of the base case with no intermediate material, using the following methods:

- Secant stiffness based on the yield point from the 5% Diameter Method: (optimistic) the yield point method resulting in the lowest overall loss of stiffness
- Secant stiffness based on the yield point from the K&C Method: (pessimistic) the yield point method resulting the greatest overall loss of stiffness
- Parameter K_0: calculated from the 3-parameter exponential curve-fitting model

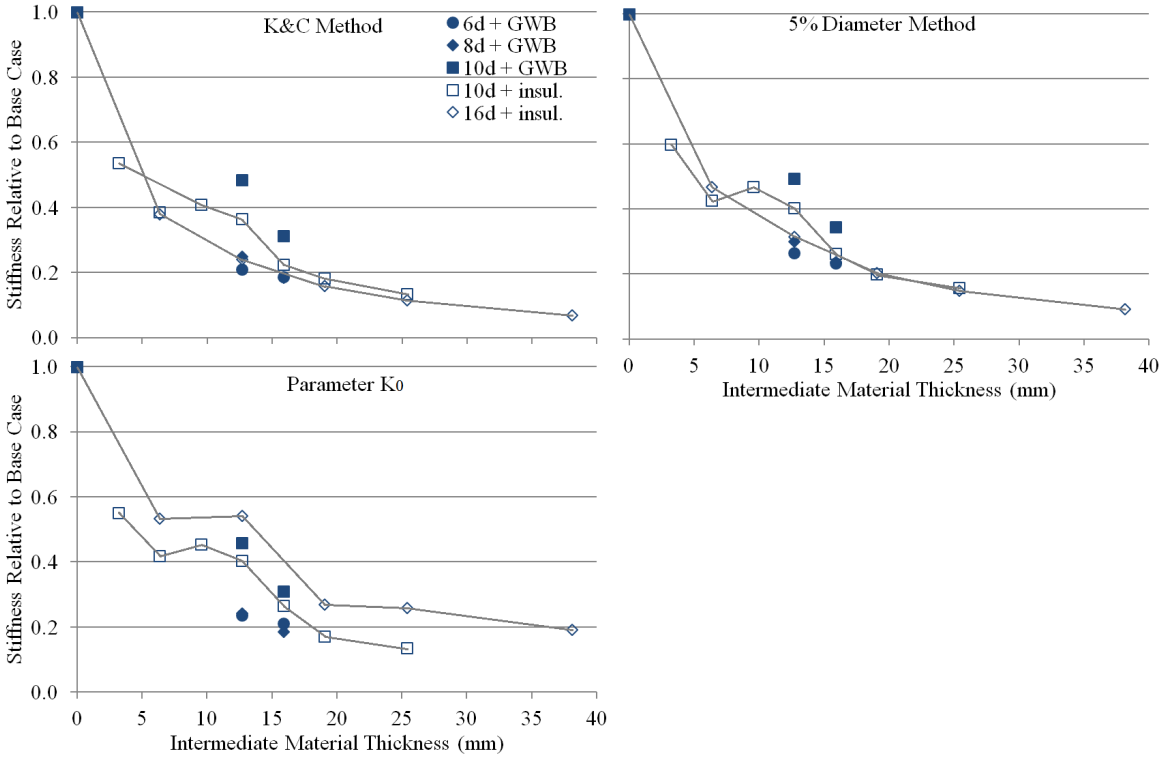

Figure 4.26: Comparison of relative drop in stiffness from base case

Regardless of intermediate material, nail size or calculation method, there is a significant, exponentially decaying drop in stiffness with increasing intermediate material thickness. Considering any nail size, half an inch (12.7 mm) of any intermediate material results in a loss of 45-80% of the connection stiffness. 1 inch (25.4 mm) of insulation results in a loss of 75-90% of the connection stiffness.

The proposed explanation for the trends in Figures 4.25 and 4.26, and consequently this study, are as follows:

It was observed in nail pull-out tests (which were discussed previously in Section 4.1), that the initial pull-out stiffness of a nail is very high. Once the maximum pull out strength is reached, pull-out resistance drops slowly and roughly proportionally to the length of nail that remains embedded. This, combined with visual observations of specimens during testing suggests that well before the maximum capacity of the connection is reached, and well before any significant nail pull-out occurs, the applied lateral load causes the nail to bend inward, toward the stud. Mainly by means of the nail head, this would have the effect of increasing the normal force between the connected members, and therefore increasing or at least maintaining friction. This friction seems to contribute significantly to the maximum lateral capacity of the connection. Of course, this effect would be significantly reduced if a softer intermediate material of any kind is introduced, which could explain the loss of stiffness and capacity observed in such cases during the testing program.

It is well known that frictional forces contribute significantly to the strength of a nailed connection. Several past studies have sought to eliminate friction by providing a thin material between the wooden surfaces such as that by Asiz et al. (2010). In this study, an intermediate material of any thickness creates this effect. In the case of 6d, 8d and 10d size nails, a large drop in capacity and stiffness is observed, due to the lack of friction. The remaining strength of the connection comes from the bending resistance of the nail itself. The larger the nail diameter, the greater the section modulus, and therefore

the greater the force that can be resisted through bending. For this reason, a much smaller initial loss in capacity was observed with the larger 16d size nails. With increasing gap sizes, the nail begins to act as a simple cantilever of increasing length.

The upper limit on wall drift for seismic design in Canada is 2.5% (NBCC, 2010). An individual nailed connection that is part of a shear wall of any design will experience at most 10 mm of deflection at this level of wall drift, according to the deflection calculation that was previously discussed in Section 2.2. Nailed connections with thick intermediate materials subjected to deformations exceeding this resulted in extremely low levels of stiffness and ductility. This is very undesirable for shear walls as it would compromise the wall's ability to effectively dissipate energy.

As note 4 from Table 9.5.1A allows the use of GWB as an intermediate material provided that minimum nail penetration is satisfied, and that GWB alone is sometimes used in place of a sheathing material in shear walls, it was expected that the experimental tests conducted in this study would result in connection capacities and stiffnesses on par with or exceeding base cases with no intermediate GWB. The results presented in this study *contradict* this, and suggest that a nailed connection is significantly weakened by the introduction of an intermediate material of any kind and of any thickness.

5. CONNECTION MODELING

In order to provide further explanation for the observed experimental behavior quantified in the previous chapter, predict connection responses for untested scenarios and better establish a relationship between connection strength and intermediate material thickness, a finite element model and an analytical model of the nailed connection was created. This Chapter will discuss their development and use.

The finite element (FE) model is a mathematical approximation of the connection which consists of nodes that are connected to each other with elements which approximate the behavior of the materials involved: nail steel, spruce-pine-fir lumber (SPF), Oriented strand board (OSB) and intermediate materials. The intermediate materials are gypsum wallboard (GWB) and extruded polystyrene insulation. The model is subjected to imposed displacements which simulate the connection being loaded laterally, and the response is evaluated numerically, at progressively increasing displacement steps by a software tool. A FE model of a nailed connection has been created to simulate the behavior of the nailed connection considered in this study, which includes an intermediate material of variable thickness and strength. Nail bending and material bearing tests (discussed previously in Chapter 4) were performed to determine model input parameters. This Chapter will also describe the model's assumptions, predictive capability and limitations.

The final part of this chapter will compare experimental results and the output from the FE model with an analytical model that will be derived from yield equations first introduced by Johansen (Johansen, 1949).

5.1 Model Development

The finite element modeling software OpenSees version 2.4.2 (revision 5540) was used to create and run all finite element models discussed in this Chapter (McKenna et. al, 2000). OpenSees is a versatile FE analysis program that is primarily used in structural engineering applications. Prior to creating and testing full connection models in OpenSees, the software was used to simulate the center-point nail bending test that was discussed previously in Section 4.1. The purpose of this initial model was to calibrate the nail material behavior for the full connection models. Figure 5.1 shows the center-point nail bending problem considered in this preliminary model with 6 beam column elements and 7 nodes.

Nodes 1 and 7 represent the support conditions in the nail, while node 4 represents the location where displacement was applied by the load frame. The remaining nodes are free to displace in any direction. All nail elements are modeled using a nonlinear beam-column element with multiple integration points. At each integration point, the moment curvature behavior of the nail was modeled using a fiber section. Through repeated testing, it was determined that 5 integration points for each of 7 elements were ideal, because tests with more integration points or more elements increased computation time with no visible difference in response.

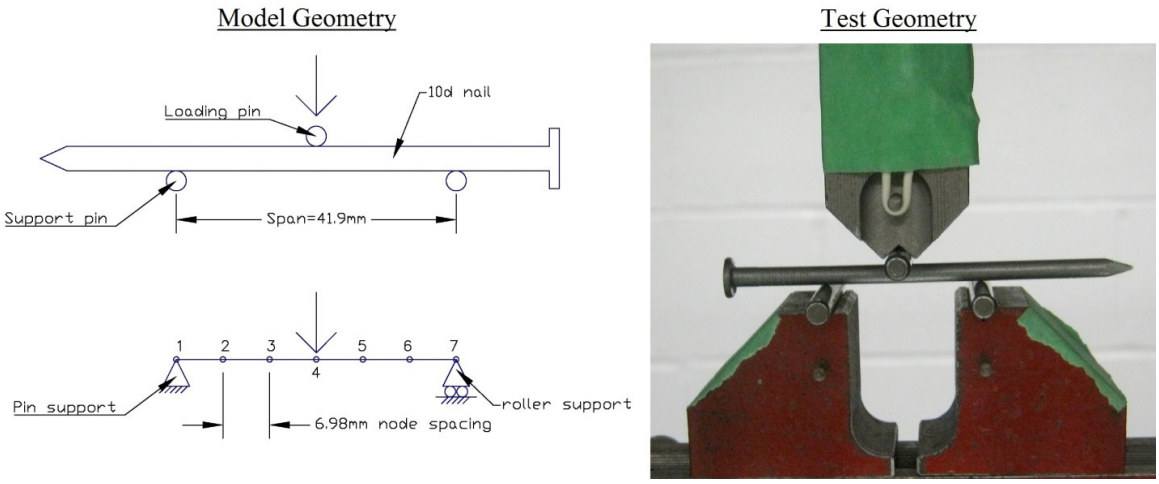

Figure 5.1: Center point nail bending FE model

Figure 5.2A shows a representation of the fiber sections for all nail sizes considered in this study. For each fiber section, the circular cross section of a common nail is approximated by 16 lumped fibers along the height of the section. Each fiber represents the cross sectional area of steel, located at evenly spaced intervals from the neutral axis and is subjected to a uniform strain. The steel-02 material within OpenSees (Giuffre-Menegotto-Pinto model with isotropic strain hardening) was applied to each fiber (Filippou et al., 1983).

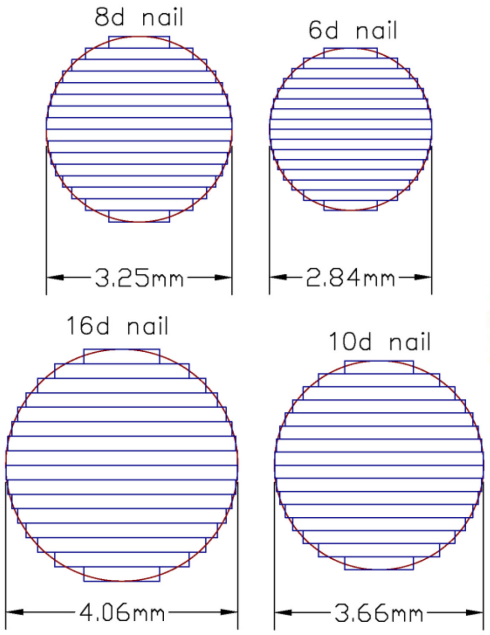

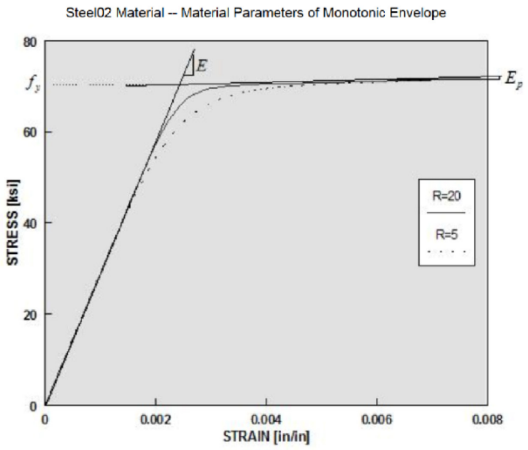

Figure 5.2A: Fiber section for steel Figure 5.2B:Steel 2 material (Berkeley, 2012)

The shape of the stress strain curve of the Steel-02 material is defined by a specified modulus of elasticity E, yield stress F_y, post yield stiffness factor b and three specific material parameters R_0, cR_1, cR_2 . Figure 5.2B shows the stress-strain behavior of the Steel-02 material, as well as the effect of changing the R_0 variable (shown as R in the figure). The effect of all of these inputs was tested by comparing the load deformation response output of the FE model with experimental tests. The FE model was displacement controlled, meaning that a new model solution was recalculated for increasing values of displacement at node 4. The following values were determined to result in the most accurate load deformation response when compared to the experimental response:

- Modulus of elasticity, E = 200 GPa
- Yield stress, F_y = 707 MPa
- Post-yield stiffness factor, b = 0.02 (Post-yield stiffness = 4 GPa)

- Material parameter $R_0 = 15$
- Material parameter $cR_1 = 0.925$ (default value)
- Material parameter $cR_2 = 0.15$ (default value)

The material parameter R_0 defines the sharpness of the curve that transitions between initial stiffness into post yield stiffness. The parameters cR_1 and cR_2 affect the stress-strain relationship when considering cyclic behavior. The chosen values for these are default values that do not have an effect on the monotonic loading response considered here. The yield stress of 707 MPa is slightly above that required by the Standard Specification for Driven Fasteners: Nails, Spikes and Staples (ASTM, 2013), and the standard for Engineering Design in Wood (CSA, 2010), clause A9.5.1.1.

Five experimental tests were conducted on a size 10d nail, as previously mentioned in Section 4.1, and compared with the FE model. Figure 5.3 shows a sample load-deformation response generated by this model in comparison with the mean experimental response. The generated response from the FE model closely matches that of the response from experimental testing, and therefore it was concluded that the selected means of modeling a nail in bending were suitable.

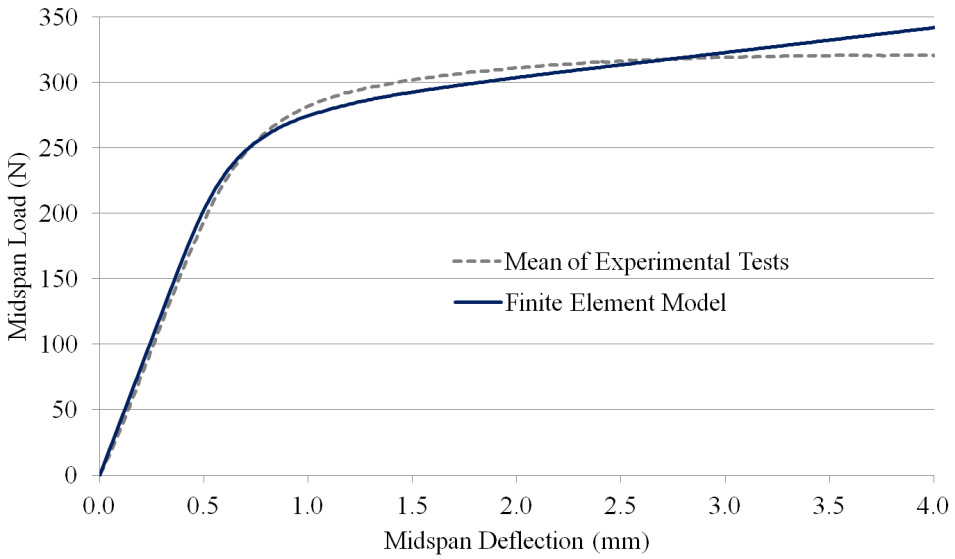

Figure 5.3: Center point nail bending test FE model output

5.2 Model Structure

During the development of the FE model of the entire nailed connection, several revisions to improve accuracy were considered. These were tested and compared with experimental response data, in an attempt to determine the best representation of the reality of the actual connection when loaded. As far as it is known, some of these ideas are new to the FE modeling of nailed connections, and will be discussed in this section.

The final version of finite element model, which simulates an individual nailed connection with an intermediate material subjected to lateral loading, is shown in Figure 5.4. The model exists in 2 dimensions, with 3 degrees of freedom (displacement in x, y and rotation).

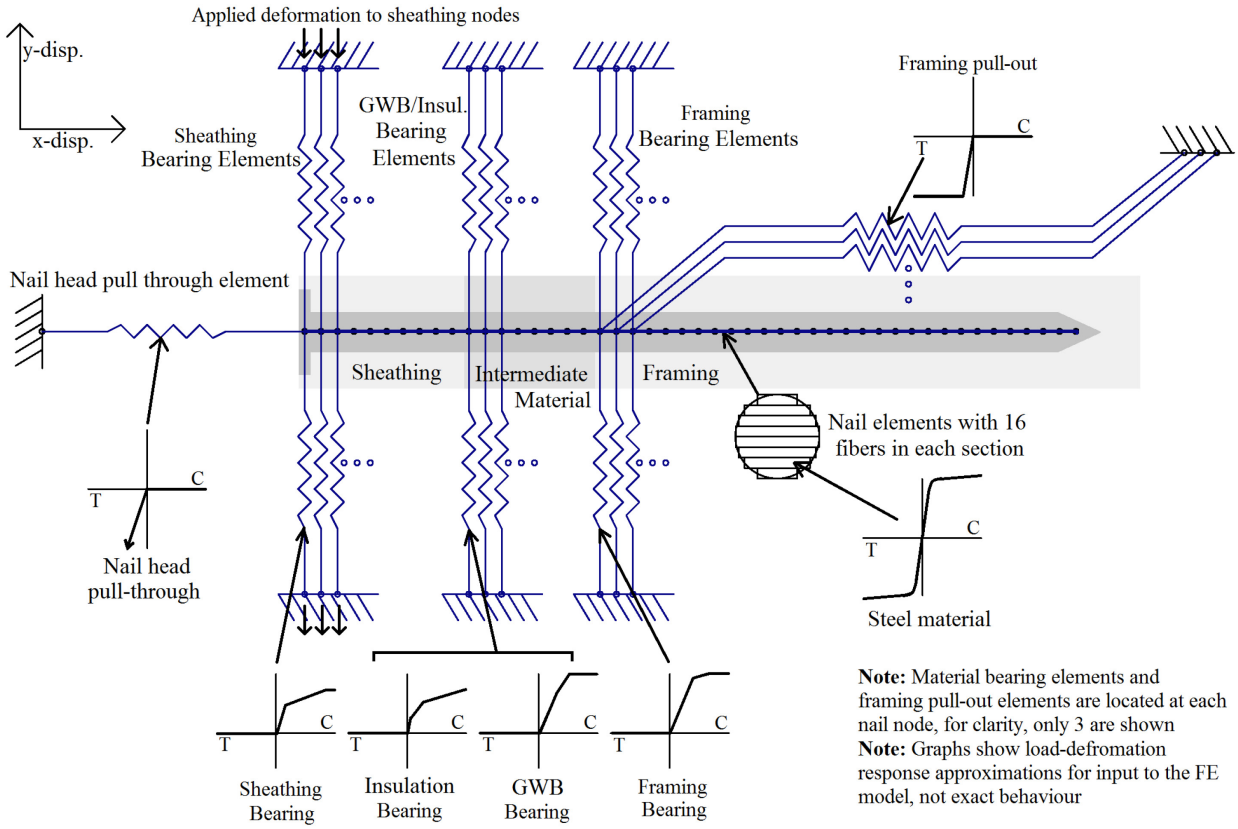

Figure 5.4: Finite element model diagram

The model includes the following components:

Beam-Column nail elements: Beam-column elements are used to approximate the behavior of the nail. The response of the preliminary nail bending model discussed in Section 5.1 has shown that beam-column elements with multiple fiber sections along the length model the nail behavior well. Nail node spacing was selected as 1/16" (1.5875 mm) to provide sufficient sensitivity and accommodate material thicknesses in multiples of 1/16". The steel-02 material used with the parameter inputs as discussed previously and was applied to all Beam-Column nail elements.

Truss elements for bearing in embedment materials: Connected to each nail node, oriented perpendicular to the direction of the nail and parallel to the direction of applied displacement, are two truss elements, which simulate the effect of the nail bearing on a material. Four different potential behaviors are used to simulate each of the embedment materials: SPF, OSB, and the two intermediate materials (GWB and insulation). Within OpenSees, a three point uniaxial hysteretic material stress-strain relationship may be defined. Using this, a bilinear relationship was used to approximate the bearing behavior of each material. The specific behavior of each material model is discussed in Section 5.3.

There are two sets of identical truss elements located above and below each nail node. All such elements were set to produce a response in compression only to model elongation of the holes due to bearing.

Truss elements for nail pull-out: Connected to each nail node within the framing member (SPF), is an additional truss element, oriented parallel to the nail, which simulates the resistance of the nail to pull-out. Resistance to pull-out is a result of friction generated between the framing member and nail in the nail's longitudinal direction. Since resistance to pull out was significant only in the SPF, it was deemed unnecessary and not modeled for the OSB and intermediate materials.

Similar to the truss elements for bearing, those for pull-out are modeled with a uniaxial hysteretic material. This material generates a response only in tension and approximates the load-deformation response generated by nail pull out tests.

Truss element for nail head: An additional truss element was added, connected to the nail head, parallel to the longitudinal axis of the nail but directed away from the connection. This element was intended to simulate the resistance of the nail head to pulling through the sheathing. A uniaxial elastic material was applied to this element. The element has a linear elastic response in tension, with no response in compression. The response in tension was scaled to the size of the bearing area of the nail head against the OSB sheathing, with an elasticity of 3 GPa. This value was not obtained from any compression test done in this study, and is a typical value for elasticity of OSB (FPL, 2010).

5.2.1 Boundary conditions

All truss elements are 100mm long, connected to their respective nail nodes on one end, and fixed in all degrees of freedom at the other end. The modeled connection is loaded laterally by means of displacement control of the fixed OSB reaction nodes, while the SPF reaction nodes remain in place. This is achieved within OpenSees by means of an imposed motion, where fixed nodes may be displaced in the model.

It was decided that a bearing test on embedment materials (SPF, OSB, GWB, and insulation) was insufficient to fully capture their behavior when part of a nailed connection, because there is some degree of deformation that occurs in the material, localized around a nail, when the nail is driven. In an attempt to simulate this, it was decided to model some degree of pre-compression in the materials to account for local deformation around the nails. As there was only one spring at each node to simulate feedback, the amount of pre-compression was determined such that the area of compressed wood was equal to half of the cross section of the nail. This is illustrated in

Figure 5.5, where the pre-compression distance multiplied by the nail diameter is equal to half of the nail cross section.

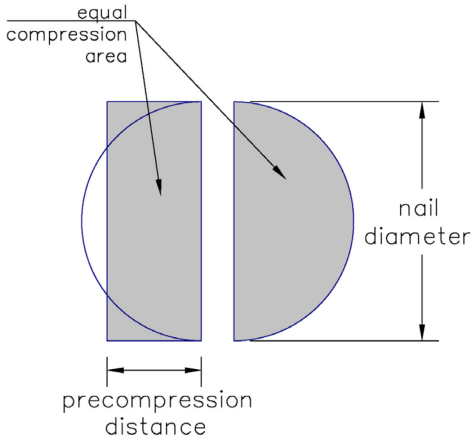

Figure 5.5: Nail pre-compression in FE model

The pre-compressed distance is therefore equivalent to:

$$P = \frac{\pi D}{8} \qquad (\mathbf{5.1})$$

where D is the nail diameter. P was set to 1.12, 1.28, 1.44, and 1.59 mm for nail sizes 6d, 8d, 10d, and 16d, respectively. Pre-compression was added using an imposed deformation, in a similar fashion to how overall lateral displacement was modeled. Pre-compression simulates the reaction of the wood on both sides of the nail: as the connection is loaded laterally, wood on the bearing face of the nail is compressed more, while simultaneously wood on the opposite face is decompressed, but still exerts some force. It was later determined after running the FE model in every experimentally tested scenario that including nail pre-compression had a minimal effect on the load-deformation behavior of the entire nailed connection.

The way that both pre-compression and overall imposed displacement were implemented is illustrated in Figure 5.6, which shows the imposed displacement on 4

groups of fixed nodes: top OSB reaction nodes, bottom OSB reaction nodes, top SPF reaction nodes, and bottom SPF reaction nodes (refer to Figure 5.4 for the locations of these nodes). The imposed displacements on fixed nodes for the intermediate materials were tied to those of the SPF nodes. In the initial 400 displacement steps, pre-compression is established by moving the bottom nodes up by *P* and the top nodes down by *P*. At displacement step 600, displacement begins to be applied by means of moving both top and bottom sets of OSB nodes downward, while holding the other nodes in place. The program was set to finish after 4600 displacement-steps, at an imposed displacement of 20 mm.

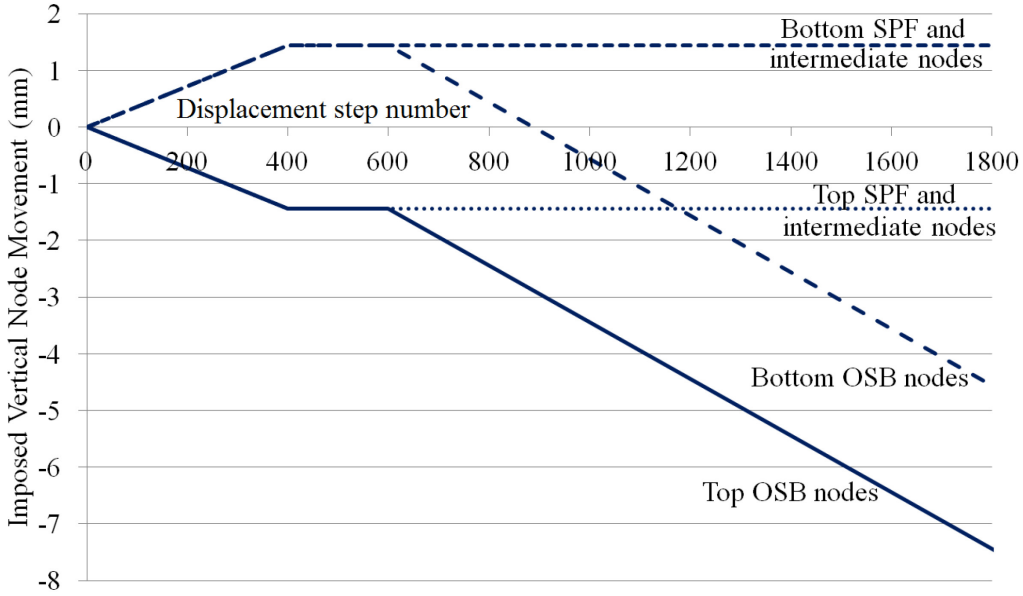

Figure 5.6: Behavior of boundary conditions during tests with 10d nails

5.3 Nail Bearing and Pullout Tests

This section will describe how material property input values for the FE model were determined based on experimental bearing and pull out tests (as were previously described in Section 4.1).

Bearing tests were performed in accordance with the Standard Test Method for Evaluating Dowel-Bearing Strength of Wood and Wood-Based Products (ASTM, 2005). A total of 40 bearing tests were performed: 5 identical tests for each combination of 4 different nail sizes, and 2 different embedment materials (SPF and OSB). The standard also describes the means by which the yield strength in bearing must be calculated from the load-deformation response of a bearing test (ASTM, 2005). A sample case is presented in Figure 5.7, which shows a typical load-deformation response for a 10d nail embedded in a block of SPF.

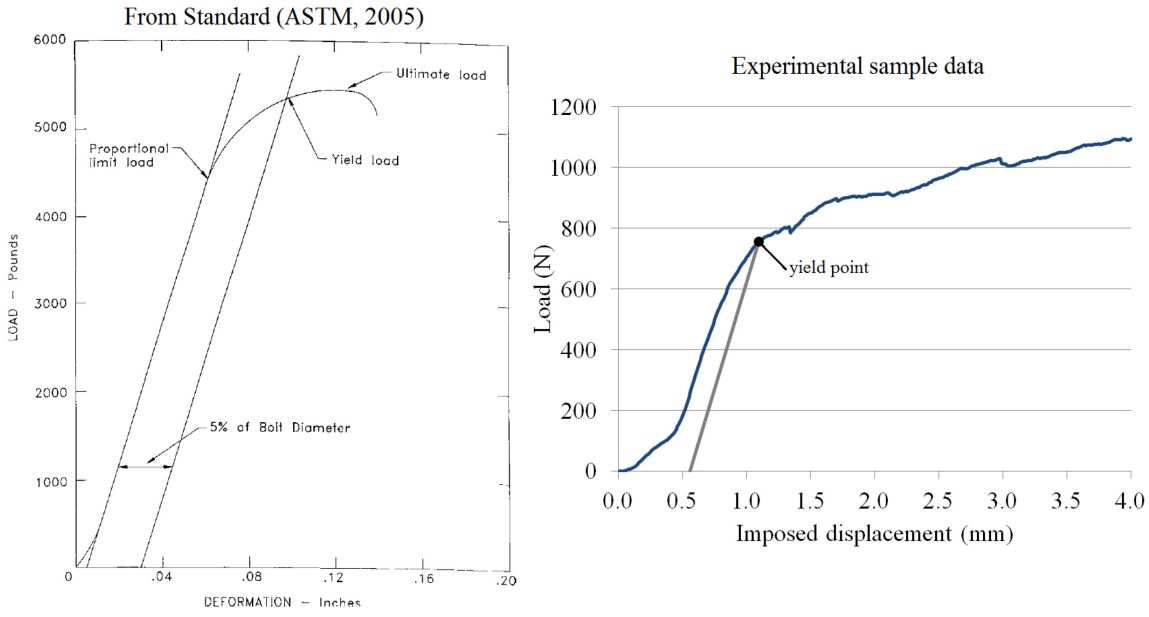

Figure 5.7: Sample yield point calculation for bearing test on 10d nail in SPF

The yield point is calculated using the method described in the standard. The linear portion of the load-deformation response is found and extended down to an intercept on the x-axis. The standard does not describe how to find the initial linear portion, so the linear portion was determined by calculating the mean slope (stiffness) between 1/4 and 1/2 of peak recorded load. The initial portion of the graph is ignored, as this region reflects the nail not yet fully bearing against the tested material. A new line, parallel to the first is drawn, offset by a distance equal to 5% of the nail diameter. The yield point is the location where this new line intersects with the load-deformation response curve.

Table 5.1 and Figure 5.8 compare the yield strength calculated from bearing tests performed in this study with the embedment strength as defined by the standard for Engineering Design in Wood (CSA, 2010), for each set of identical tests. The load values are presented in terms of load per mm of nail bearing length, because the bearing length varied depending on the length of the nail and size of the wood block being tested

Table 5.1: Bearing test results: yield strength

Material:	Oriented Strand Board (OSB)				Lumber (SPF)			
Nail size	Yield Load (N/mm)	Yield Strength (MPa)	COV Yield Strength	Design strength* (MPa)	Yield Load (N/mm)	Yield Strength (MPa)	COV Yield Strength	Design strength* (MPa)
6d	66.7	23.49	0.097	31.3	130.5	45.95	0.043	20.4
8d	82.0	25.23	0.185	29.5	145.3	44.71	0.248	20.3
10d	59.5	16.26	0.348	27.7	194.9	53.25	0.206	20.2
16d	52.9	13.03	0.101	25.9	199.9	49.24	0.088	20.1

Notes: *as calculated by the standard for Engineering Design in Wood (CSA, 2010)

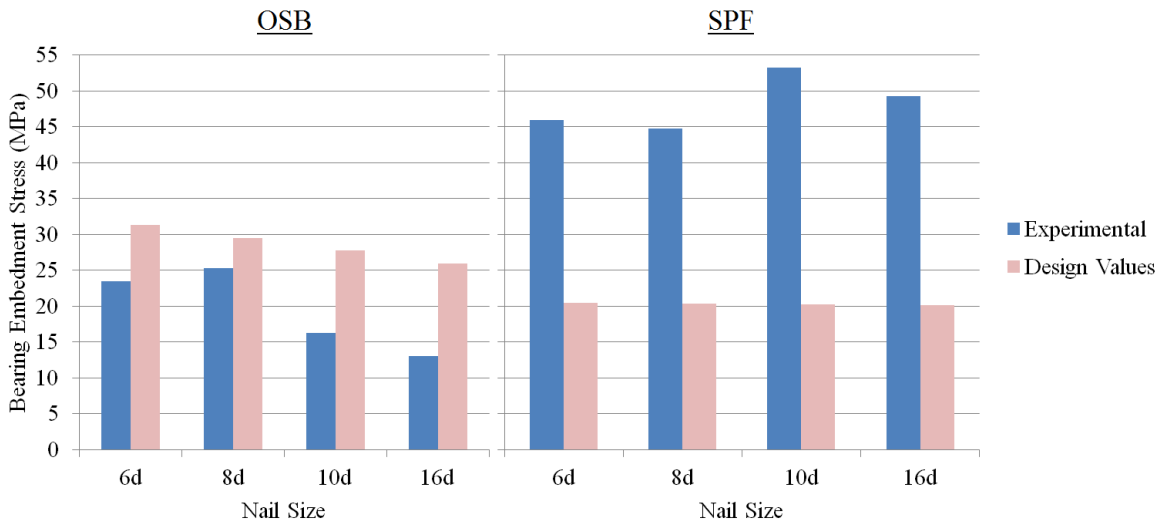

Figure 5.8: Bearing and embedment strength comparison for OSB and SPF

In the case of the bearing strength of OSB, experimental values were considerably lower than the design embedment strength. This is likely due to the fact that design equations were not developed for this specific type of test, and that the embedment strength of OSB is considerably higher than its bearing strength. The Standard for Engineering Design in Wood (CSA, 2010), specifies the design embedding strength of OSB with the following expression:

$$f_1 = 104G(1 - 0.1d_f) \qquad (\mathbf{5.2})$$

Where G = 0.42 is the assumed value from the standard for OSB and d_f is the nail diameter in mm. This expression results in decreasing embedment strength with increasing nail size. A similar decreasing trend is observed in the experimental results, however this trend is much more pronounced in the test results than in the design standard expression, resulting in much lower bearing strength, and results in no discernible increase in total yield load with increasing nail size. This inconsistency may be explained by the differences between bearing and embedment testing and by variation in experimental results. In order to provide the FE model with data that most closely

resembles the actual materials tested, however, it was decided to use a single load-deformation relationship to represent the response of the OSB for all nail sizes. Figure 5.9 shows the selected relationship used within the FE model, along with the distribution of responses from all 20 OSB bearing tests. Since the uniaxial hysteretic material available within OpenSees allowed up to 3 points to define a stress-strain relationship, and the result from all bearing tests showed significant post-yield stiffness, a post-yield stiffness up to ultimate bearing strength was calculated from the experimental response data.

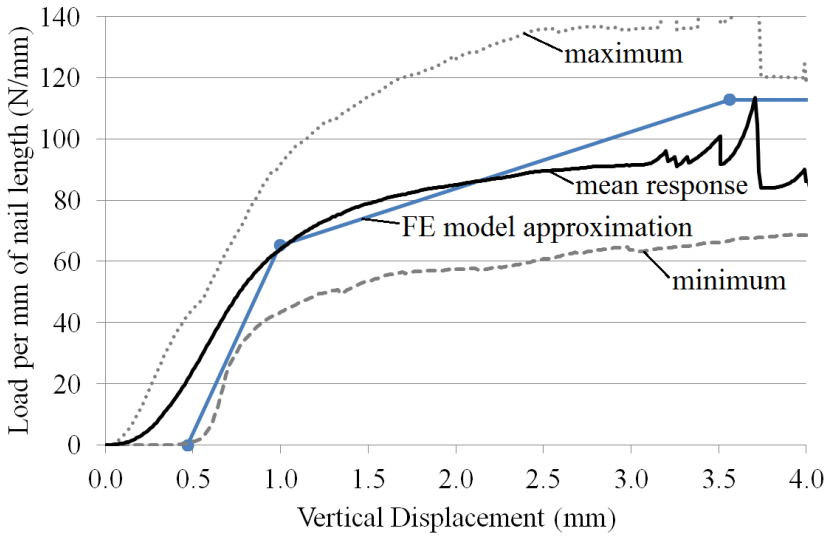

Note: FE model response is shown roughly co-linear with the mean experimental response.
The actual FE model response begins at a deformation of zero.
Mean response beyond 3.0 mm was affected by the failure of smaller sized nails

Figure 5.9: OSB Bearing strength results and FE model approximation

In contrast to OSB bearing results, there was a strong relationship between nail size and bearing strength in SPF stud specimens. Larger nail sizes resulted in greater bearing load. The standard for Engineering Design in Wood (CSA, 2010) specifies the embedment strength of SPF with the following expression:

$$f_2 = 50G\left(1 - 0.01d_f\right) \qquad (\mathbf{5.3})$$

Where $G = 0.42$ is the assumed value from the design standard for SPF and d_f is the nail diameter in mm. This expression also results in decreasing embedment strength with increasing nail size, but it is much less pronounced than that for OSB. This results in an increasing load with nail diameter when considering member thickness.

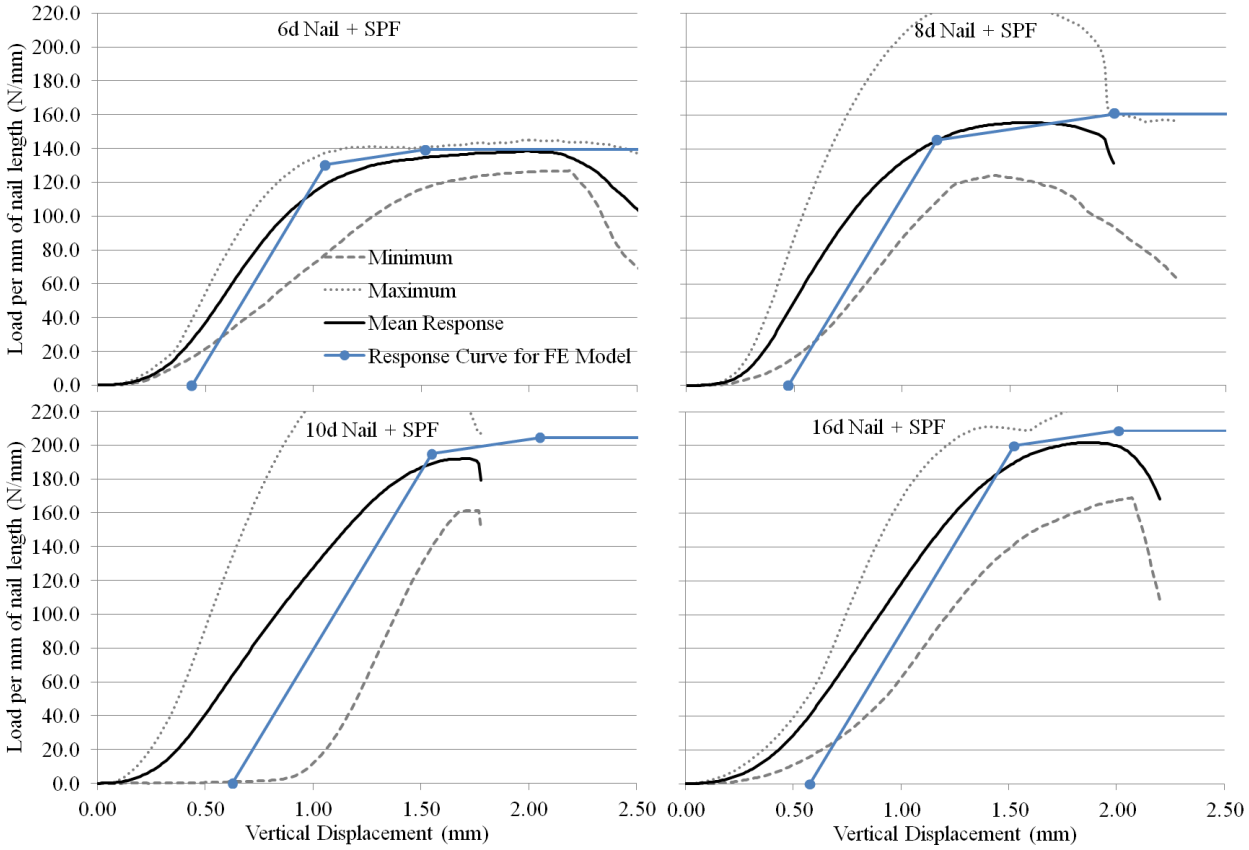

Note: FE model response is shown roughly co-linear with the mean experimental response. The actual FE model response begins at a deformation of zero.

Figure 5.10: SPF Bearing strength results and FE model approximation

Experimental data shows that the overall strength (in N per mm of bearing length) increases with increasing nail size, therefore, a stress-strain relationship was calculated to approximate the embedment response in SPF for each nail size separately. Figure 5.10 shows the selected relationships for bearing on SPF, used within the FE model, for each

nail size. Just as with the relationship for bearing of OSB, a post-yield stiffness up to an ultimate bearing strength was calculated for each nail size.

In addition to the embedment tests, a series of 5 nail pull out tests were performed on a size 10d nail embedded within SPF. The method of these tests was discussed previously in Section 4.1. Figure 5.11 shows the mean load-deformation response of a size 10d nail embedded in SPF subjected to pull out, as well as the FE model's approximation of this behavior. The response for other nail sizes was scaled to be proportional to the contact area between the nail and SPF.

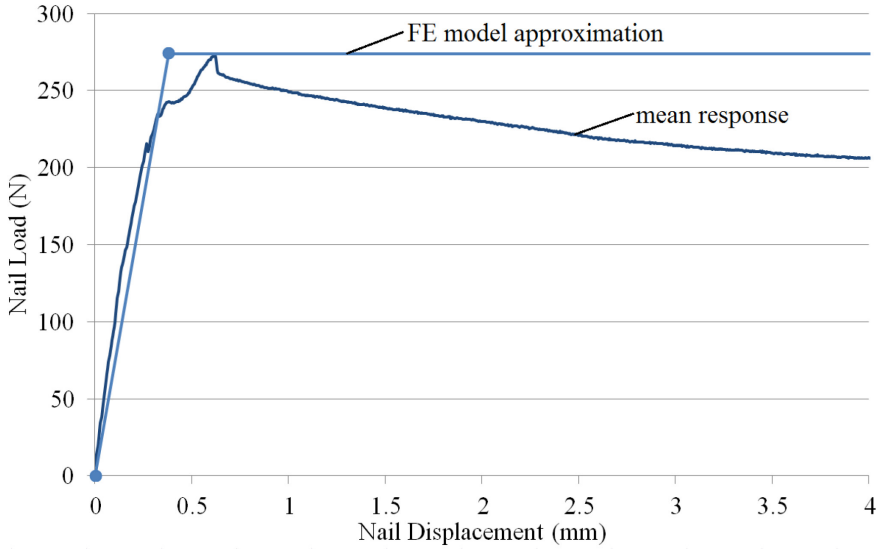

Figure 5.11 SPF with 10d nail pull-out experimental response and FE model approximation

The load-deformation response has a very high initial stiffness reflecting the static friction between the nail and SPF, up to a failure point. After failure, load sharply drops, reflecting the change from static to kinetic friction. Beyond this, load continues to drop in an approximately linear fashion, and roughly proportional to the length of nail remaining embedded in the SPF. The layout of the finite element model (Figure 5.4) would suggest that as soon as a nail node moved outside of the SPF, the response from the pull-out

element for that node should drop to zero. It was not possible to model this behavior; however, since the FE model exhibited only approximately 2 mm of pull out at peak lateral load, the effect of nail withdrawal from SPF resulting in a reduced pull-out load was as assumed to be minimal.

Pull out tests for nails embedded in OSB or intermediate materials (GWB and insulation) were not done because it was assumed these materials exhibited negligible pull out resistance acting on the nail shank on their own. Note that pull out resistance due to the effect of the nail head was accounted for separately by a nail head pull through element (discussed in Section 5.2).

Bearing strength of the intermediate materials GWB and insulation was modeled based on the compression tests discussed in Section 4.1. Figures 5.12 and 5.13 show the mean load-deformation response and FE model approximation of GWB and rigid insulation, respectively.

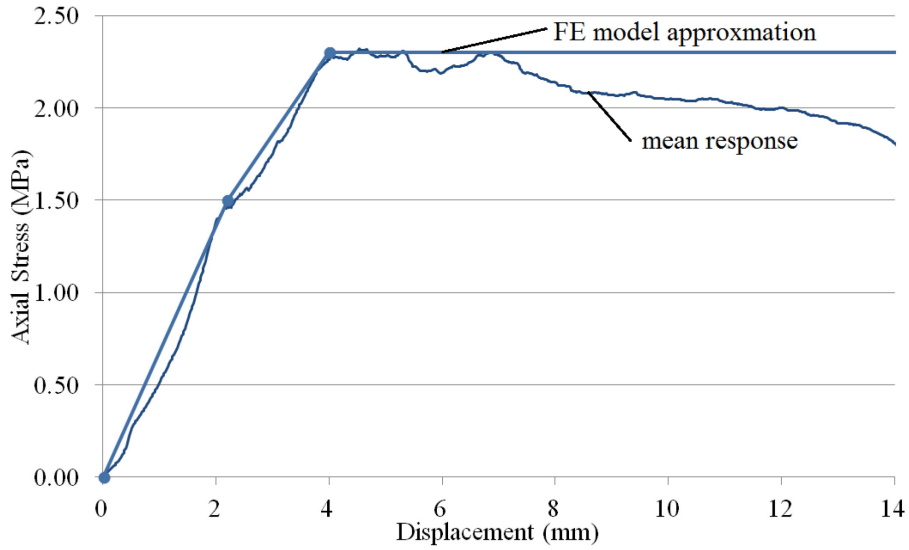

Figure 5.12: GWB compression strength results and FE model approximation

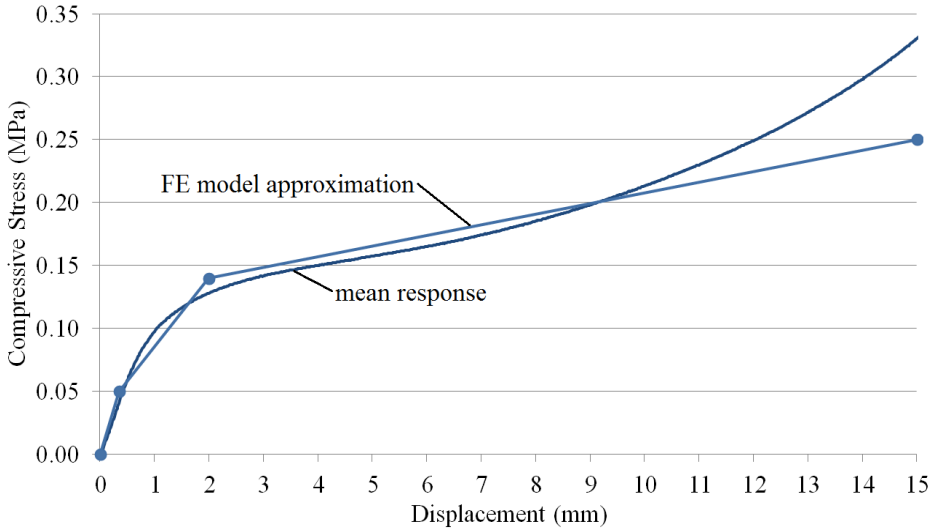

Figure 5.13: Insulation compression strength results and FE model approximation

5.4 Results and Analysis

The FE model was run with every nail size and both intermediate material types that were tested experimentally. Thicknesses were incremented in steps of 1/16" (or 1 node), up to a thickness of 12 nodes or 3/4" (19.05 mm), beyond which thickness was incremented in steps of 1/8" (2 nodes), up to a thickness of 24 nodes or 1.5" (38.1 mm), beyond which thickness was incremented in steps of 1/4" (4 nodes), up to a thickness of 32 nodes or 2" (50.8 mm). Figure 5.14 shows a sample run of the model for a connection with a 10d nail with a 1/4" layer of insulation, compared with experimental results. Load-deformation response curves for all tests can be found in Appendix E.

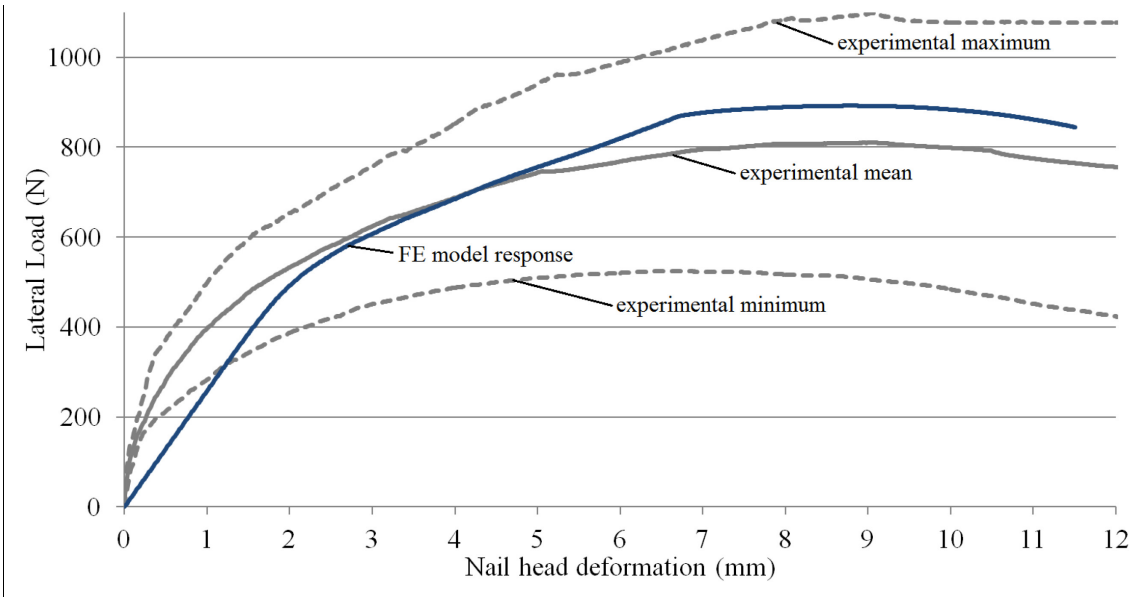

Figure 5.14: FE model sample output in the case of 10d nail with 6.35mm (1/4") of insulation

Overall, the model performed well in capturing the magnitude of the peak load as well as the nail head deformation (slip) occurring at peak load for all nail size and material thickness combinations. All responses from the FE model fell between minimum and maximum experimental tests, with the exception of the initial stiffness, which was not possible to replicate in any test, and will be discussed in Section 5.6. Given the variability in the experimental data, it can be said that the FE model performed well in capturing the overall behavior of this type of connection.

All combinations considered by the FE model showed similar behavior, as is illustrated by Figure 5.15, which shows FE model output for all thicknesses of insulation tested with a 10d nail. Increasing intermediate material thickness results in a load-deformation response which consistently decreases in load and increases in displacement. The load-deformation behavior can be described as follows (with reference to the stage numbers shown in Figure 5.15):

1. Initial stiffness during which none of the member materials have begun to crush and the steel in the nail is within the elastic region, thus load increases linearly with deformation.
2. The approximate location of the overall connection yield point as calculated by the methods discussed in Chapter 4. In this region, the steel in the nail begins to yield, and then enters post-yield stiffness.
3. Post-yield region in which the nail is yielding in bending at one location, SPF and OSB materials have begun to crush at the outermost edges.
4. A sharp change in stiffness indicating that the nail has overcome static friction and has begun to pull out.
5. All member materials have begun to crush in this region. The nail continues to pull out of the SPF, this results in less area for load to be applied, thus a maximum is reached beyond which the load decreases slightly
6. Eventually, the model fails to converge on a solution due to numerical instability

Note that there is no specific location indicating crushing of the OSB, SPF or intermediate materials. Over the course of a test, the onset of crushing in the OSB and SPF is gradual, occurring at one node at a time.

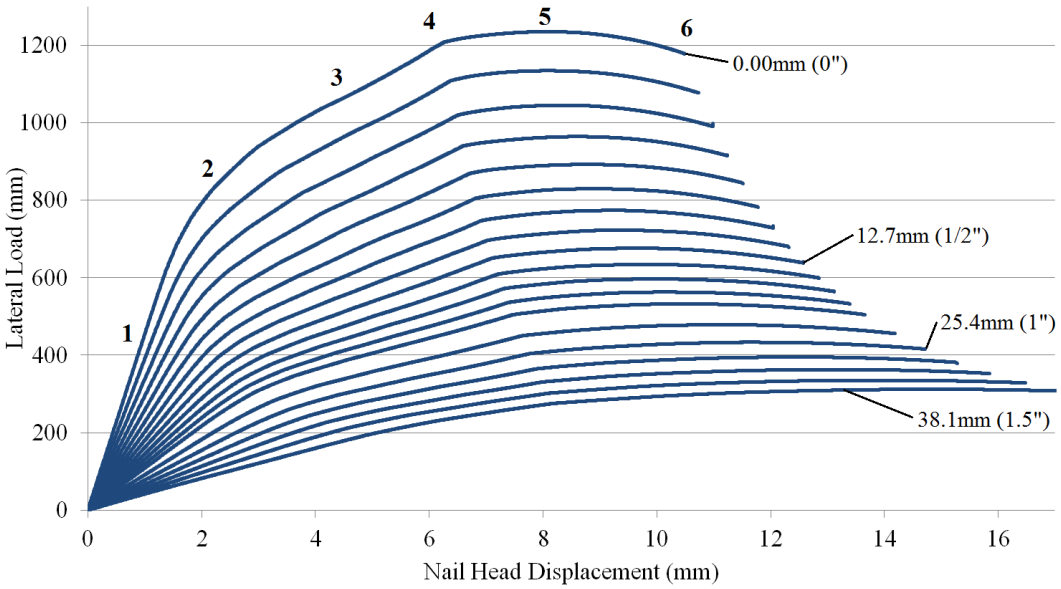

Figure 5.15: FE model result for 10d nails with insulation of multiple thicknesses

Overall, it is thought that the FE model captures the behavior of a nailed connection well, and that material crushing/yielding occurs in the same order.

The effect of using GWB as an intermediate material as opposed to insulation can be compared in tests involving 10d nails. Tests with GWB resulted in a slightly higher load and stiffness than tests with an equivalent thickness of insulation. Table 5.2 compares peak load from experimental tests with peak load from the output of the FE model. The model behaves fairly well in capturing this peak, with results on average 12% less than experimental.

Table 5.2: Peak load: comparison between experimental testing and FE model

Tests with gypsum wallboard

Nail Size	GWB thickness (mm)	Peak load (N)		Percentage Difference
		Experimental mean	FE model result	
10d	0.00 (0")	1389.6	1234.5	11.8
10d	12.70 (1/2")	768.5	710.1	7.9
10d	15.88 (5/8")	779.2	640.6	19.5
8d	0.00 (0")	863.4	1033.3	17.9
8d	12.70 (1/2")	702.6	534.8	27.1
8d	15.88 (5/8")	556.7	475.9	15.7
6d	0.00 (0")	985.6	860.4	13.6
6d	12.70 (1/2")	488.6	427.8	13.3
6d	15.88 (5/8")	582.7	380.7	41.9

Tests with insulation

Nail Size	Insulation thickness (mm)	Peak load (N)		Percentage Difference
		Experimental mean	FE model result	
16d	0.00 (0")	1317.7	1437.1	8.7
16d	6.35 (1/4")	1252.4	1065.9	16.1
16d	12.70 (1/2")	1125.5	819.6	31.4
16d	19.05 (3/4")	819	652.8	22.6
16d	25.40 (1")	776.8	531.2	37.6
16d	38.10 (1.5")	555.9	371.0	39.9
10d	0.00 (0")	1389.6	1234.5	11.8
10d	3.18 (1/8")	829.2	1044.6	23.0
10d	6.35 (1/4")	818.1	892.0	8.6
10d	9.53 (3/8")	756.1	773.5	2.3
10d	12.70 (1/2")	731.4	675.8	7.9
10d	15.88 (5/8")	689.5	596.3	14.5
10d	19.05 (3/4")	490.4	532.4	8.2
10d	25.40 (1")	474.2	433.2	9.0

Variation between the experimental mean capacity and the capacity predicted by the FE model can be attributed to scatter in experimental response data.

Figure 5.16 compares the peak load from all experimental tests with the peak load from the output of all tests using the FE model. Since increments of 1/16" (1.5875mm) were used, a smooth, load decay curve is observed. The observed trend with increasing intermediate material thickness appears to be an exponential decay.

Variation in experimental data contributes to some amount of error, however the model presented here shows good correlation with experimental data when using this metric of comparison, despite not considering initial interface friction. Both intermediate material types show good correlation, with generally a slight underestimation in FE model output peak load.

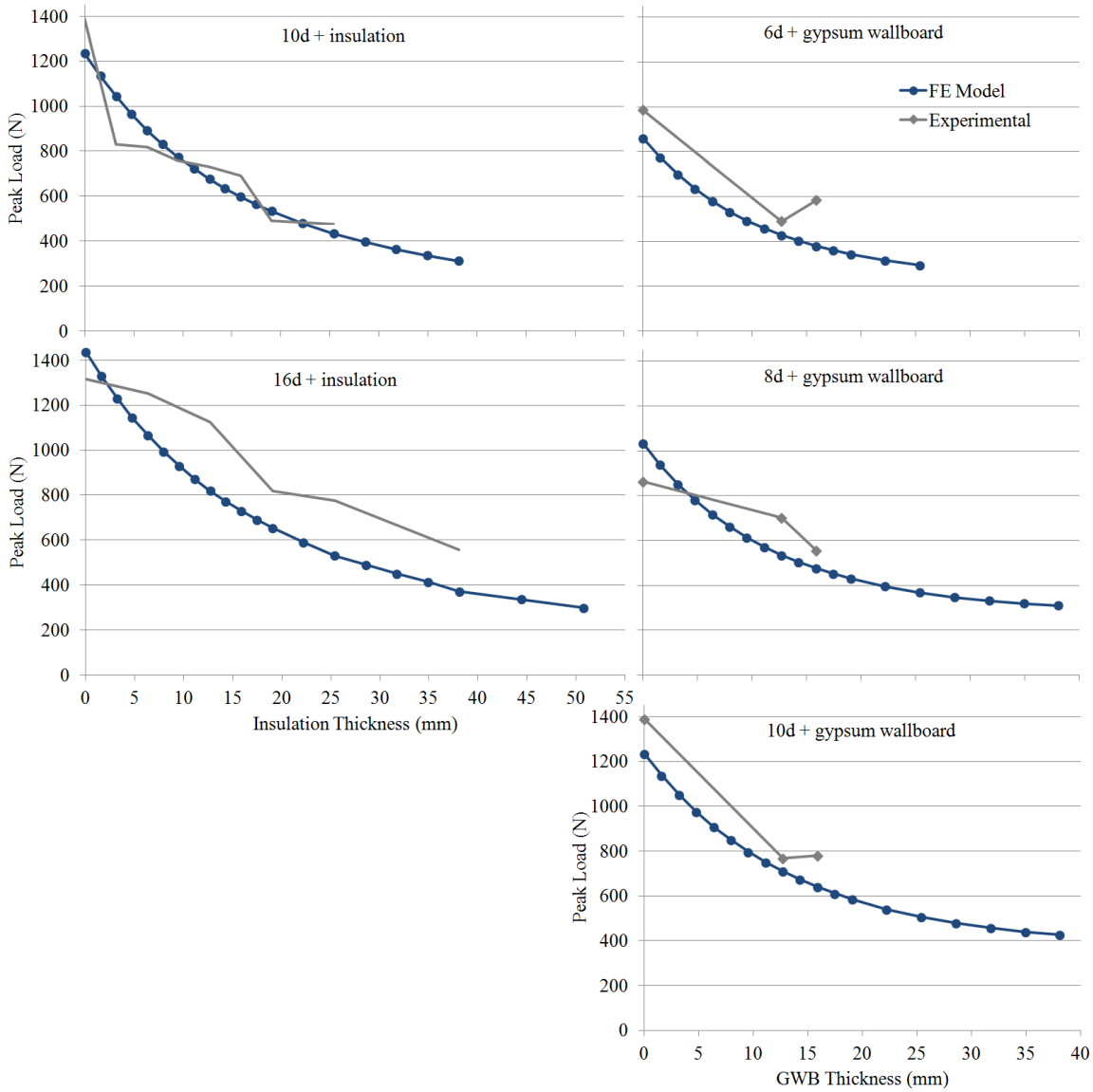

Figure 5.16: Comparison in peak load between the FE model and experimental results

5.4.1 Yield point comparison

The yield point of all FE model output was determined using all five yield point calculation point methods discussed previously in Chapter 4. Figure 5.17 shows the result of using these methods on a sample data set using a 10d nail with 6.36 mm (1/4") of insulation. All yield point methods with the exception of the CEN method lie fairly close together on the load-deformation response curve.

In Chapter 4, the 5% diameter and K&C methods were compared, as they were the most and least optimistic means of calculating the yield point, respectively. Figures 5.18 and 5.19 compare the yield load calculated from the FE model response with that calculated from the experimental response, using the K&C Method and 5% diameter method, respectively.

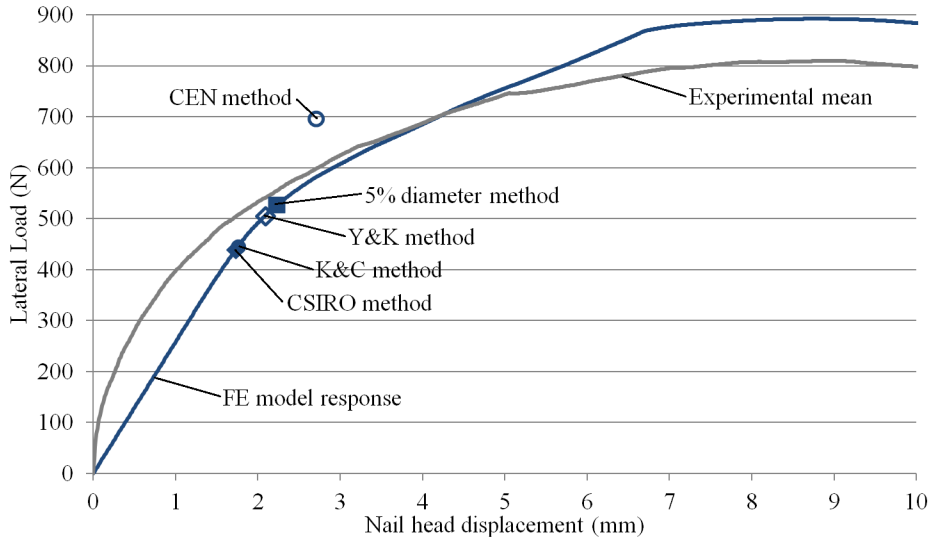

Figure 5.17 Sample result for yield point calculation on FE model output on tests with 10d nails and 1/4" of insulation

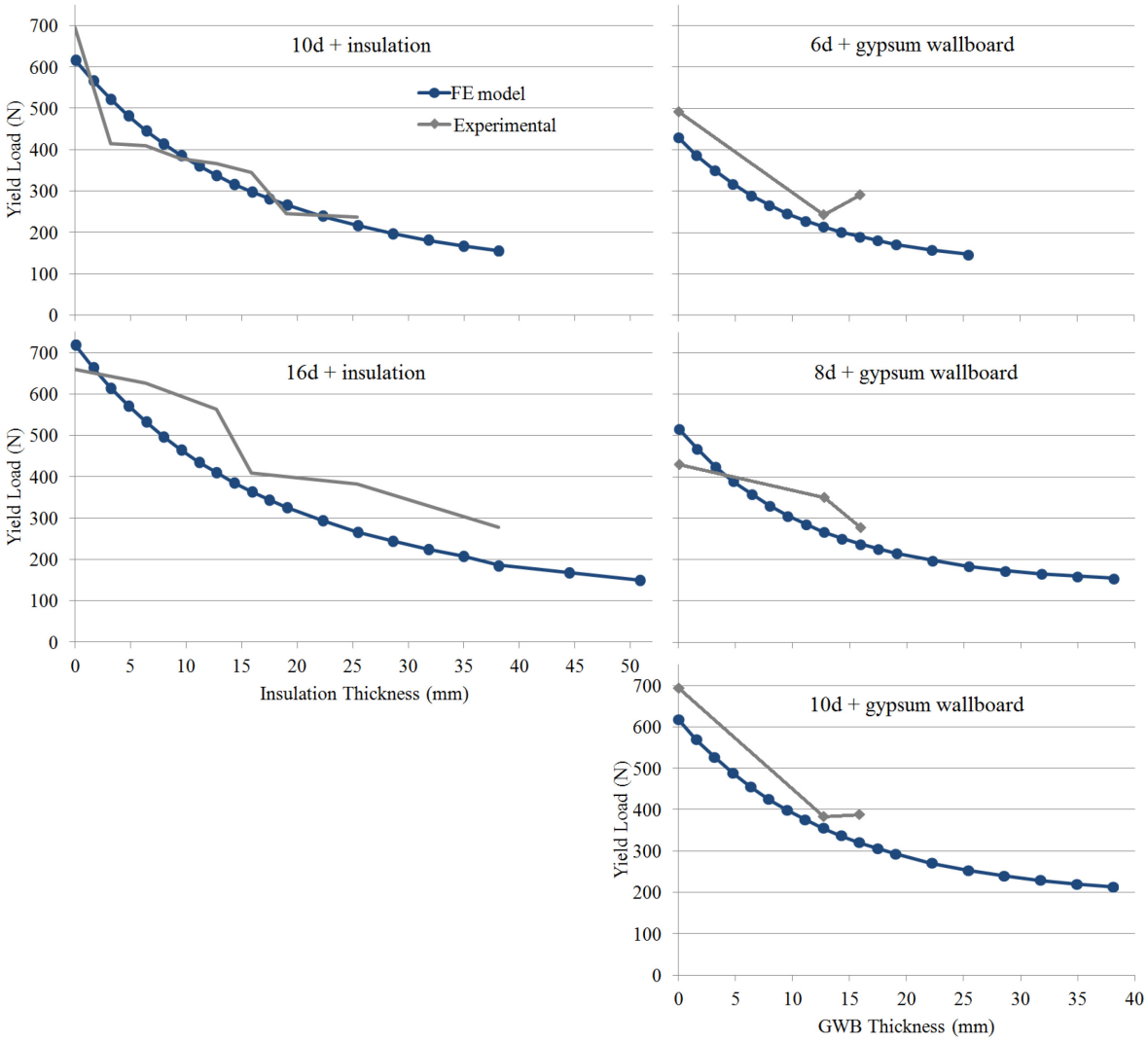

Figure 5.18: Yield load comparison using the K&C method

Both methods show a fairly good correlation between FE model yield load and experimentally determined yield load. The FE model does not consistently over-estimate or under-estimate the experimental response using either method. Use of either of these methods seems to be a practical way to predict the yield point of wood connections with intermediate materials. Complete results, comparing the magnitude the yield load and corresponding secant stiffness, using all 5 calculation methods are listed in Appendix E.

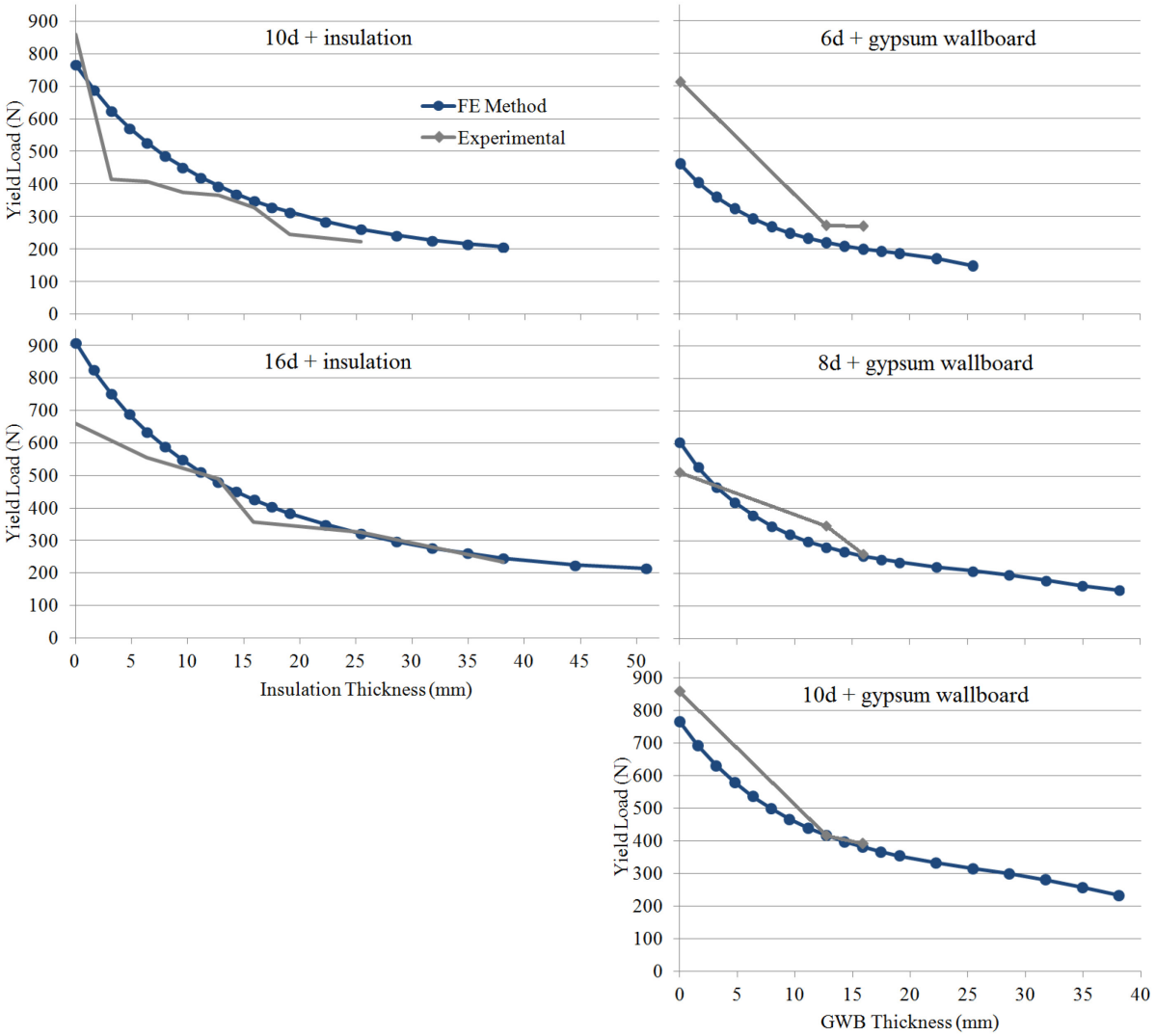

Figure 5.19: Yield load comparison using the 5% diameter method

5.4.2 Curve fitting

The curve fitting methods discussed in Chapter 4 (asymptotic and 3-parameter exponential), were applied to all output from the FE model. Figure 5.20 shows the result of using these methods on a sample data set, using a 10d nail with 6.35 mm (1/4") of insulation. Both curve fitting methods result in a very similar approximation of the load-deformation relationship. All curve fitting operations on output data from the FE model

resulted excellent correlation. The R-square for curve fits on all tests was 0.985 and higher, with a majority fits at 0.995 or higher.

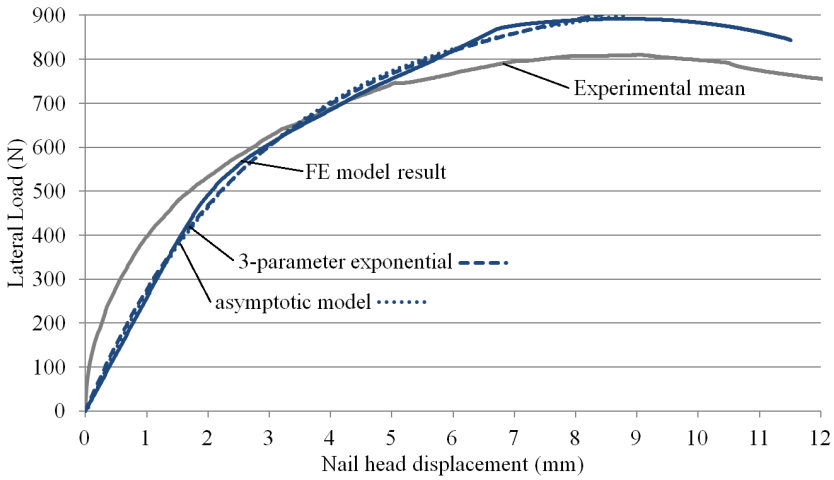

Figure 5.20: Curve fitting sample response on tests with 10d nail and 1/4" of insulation

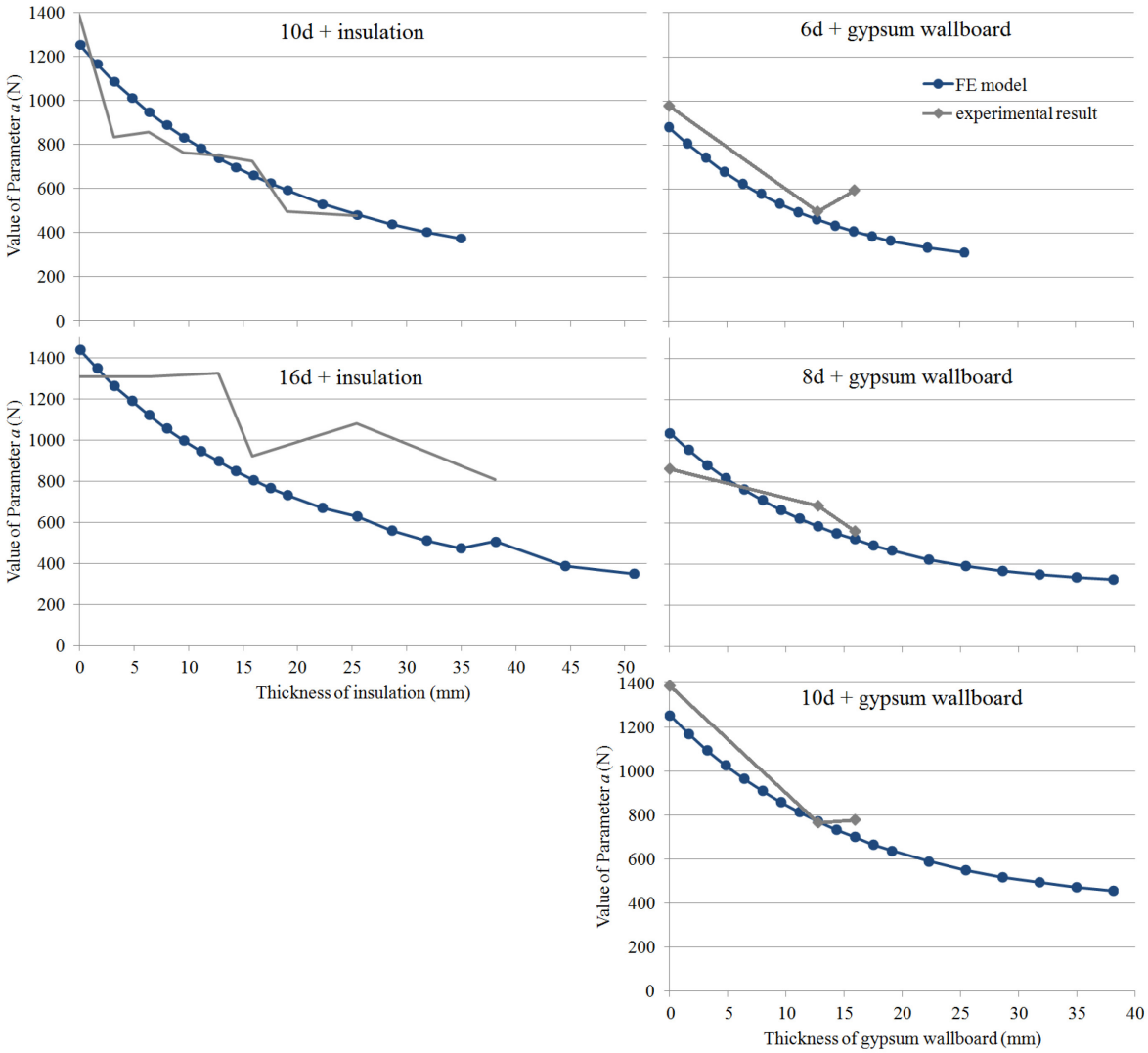

Figure 5.21: Comparison of parameter *a* from the asymptotic curve-fitting method

Figure 5.21 compares the value of parameter *a* from the asymptotic model as calculated from the FE model output and experimental results. Parameter *a* can be considered an alternate means of calculating the peak load of the connection in cases when a peak load is not reached. The FE model captures the value and decay of this parameter fairly well.

Figure 5.22 compares the value of parameter k_0 from the 3-parameter exponential model. Parameter k_0 can be considered a means of calculating the initial tangent stiffness. The FE model consistently and significantly underestimates this value.

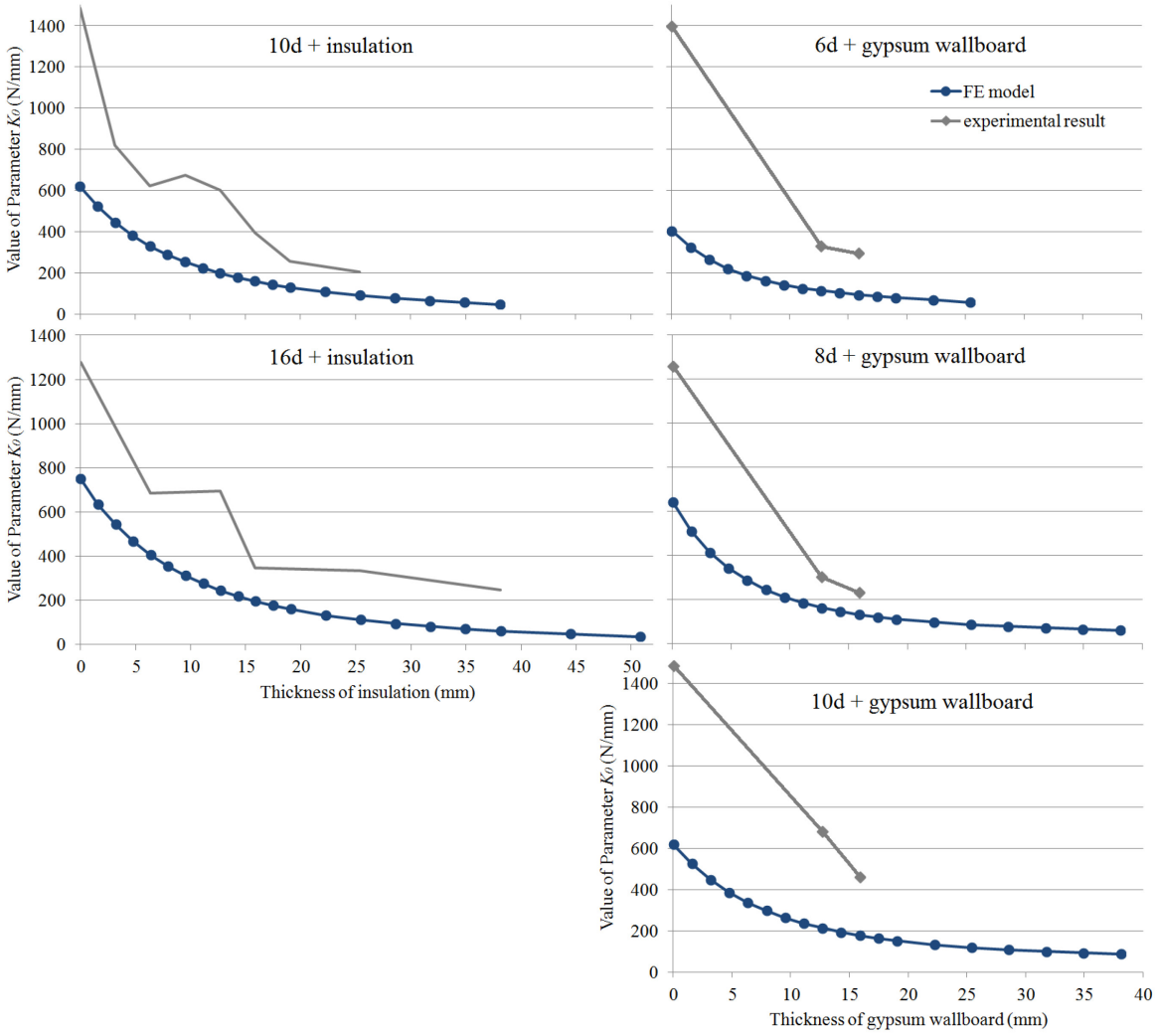

Figure 5.22: Comparison of parameter k_0 from the 3-parameter exponential curve-fitting method

5.4.3 Initial stiffness estimation

A more direct means of calculating connection stiffness is to consider the stiffness occurring between 10% and 40% of maximum load directly from the load-deformation relationship. The initial 10% is neglected in an attempt to eliminate the initial stiffness

due to interface fiction. Figure 5.23 compares the stiffness of the FE model with experimental data calculated using this method.

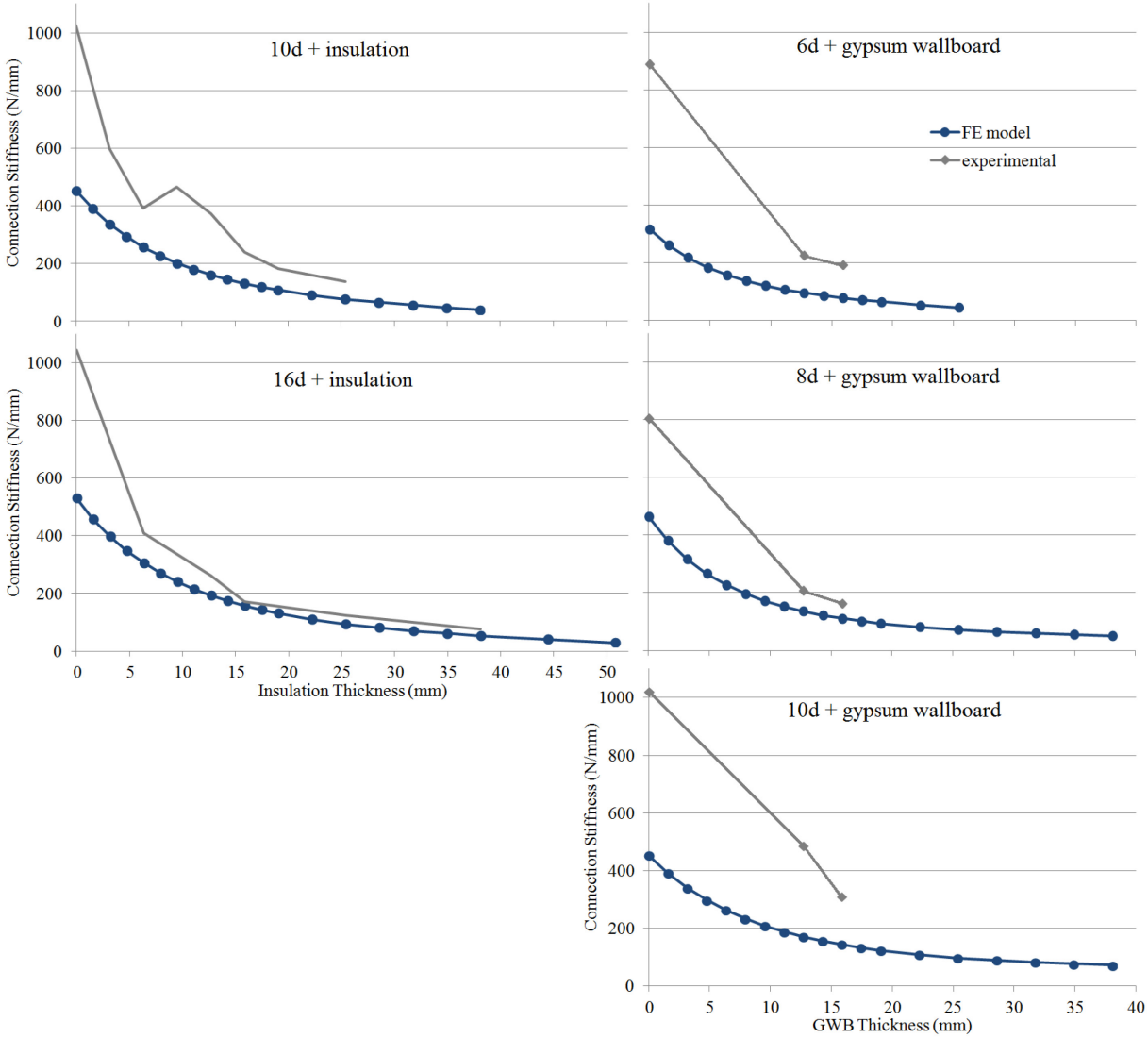

Figure 5.23: 10-40 stiffness comparison

This approach consistently shows a significant underestimation of stiffness in the FE model as well, however it is slightly more accurate than use of parameter k_0 from the 3-parameter exponential curve fitting method. Tests with GWB as the intermediate material resulted in slightly higher stiffness than those with insulation. This improvement is due to a small contribution from the bearing resistance of GWB in the model.

All methods of measuring initial or tangential stiffness have resulted in a significant underestimation in the model, when compared to experimental results. The degree of this underestimation of stiffness is approximately half in cases when there is no intermediate material and improves (less underestimation) when an intermediate material is added.

The most likely explanation for this is that the FE model does not consider interface friction (friction between any two material surfaces). The amount of interface friction is a product of the normal force acting on material surfaces and the coefficient of friction between adjacent surfaces. Both parameters can be difficult to estimate. Experimentation has shown that the coefficient of static friction between Lumber and OSB can vary between 0.25 and 0.32, depending on the orientation and specific gravity of both surfaces (Meng et al., 2008).

The normal force between two adjacent surfaces is difficult to measure. It is speculated that the total normal force is a sum of any residual force in the nail from driving and any additional normal force induced from nail deformation (prior to nail pull-out, adjacent material surfaces are pressed together).

As was mentioned in Section 2.4, a relationship between joint stiffness, *K (N/mm)*, and intermediate material thickness, *g (mm)*, was proposed in the thesis *Interlayer Gap Effect on Nailed Joint Stiffness* (Antonides et. al., 1979):

$$\log K = C_a - C_b g \qquad (\mathbf{5.4})$$

Where C_a and C_b are constants.

Curve fitting was performed on the results from calculating connection stiffness using the 10-40 stiffness method, the results of which are shown in Figure 5.24, with the corresponding values of the constants C_a and C_b shown in Table 5.3.

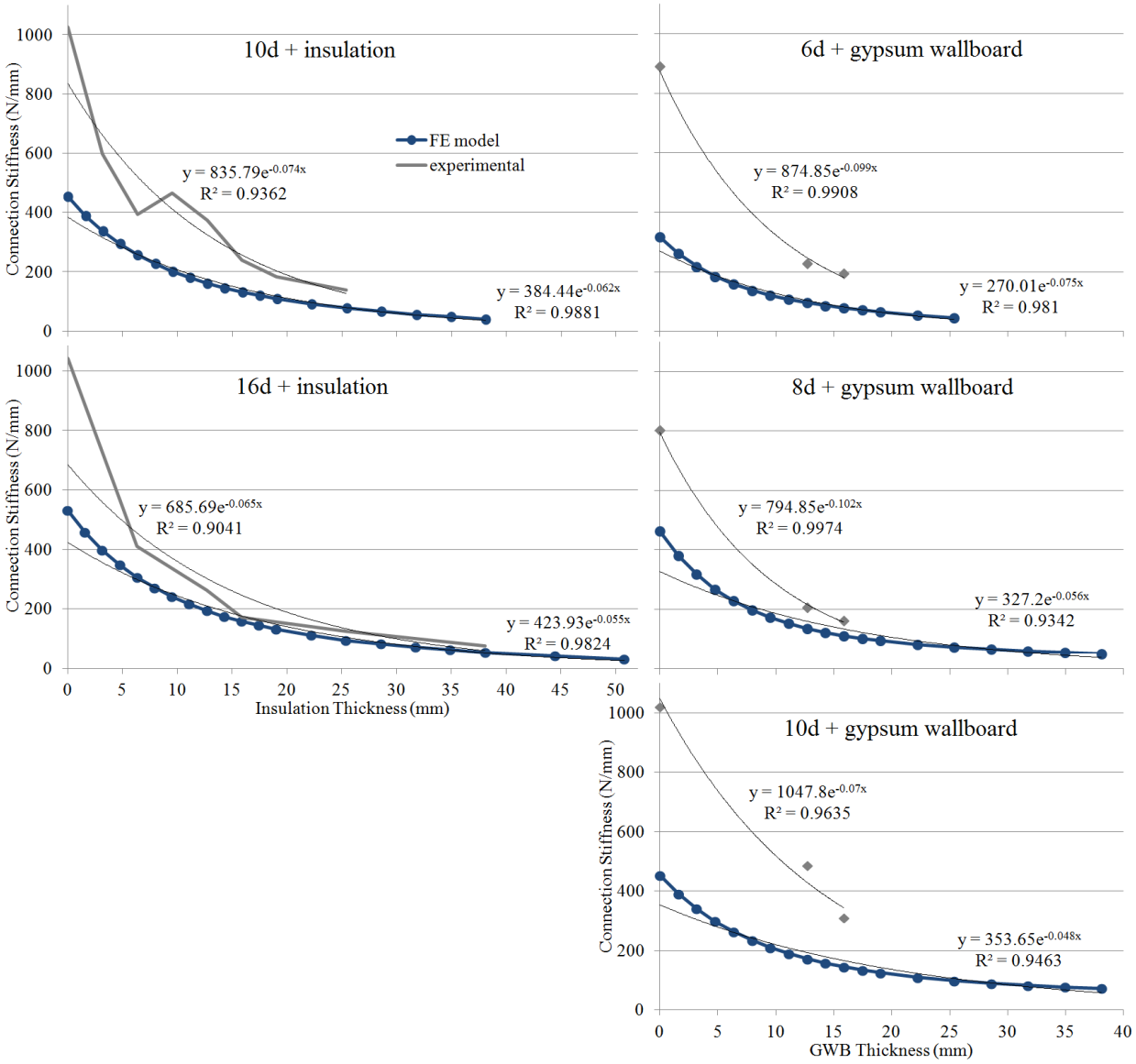

Figure 5.24: Stiffness relation curve fitting on all experimental data

Table 5.3: Stiffness relationship parameters

Connection case	FE model			Experimental Results		
	C_a	C_b	R-square	C_a	C_b	R-square
6d with GWB	270.0	0.075	0.9810	874.9	0.099	0.9908
8d with GWB	327.2	0.056	0.9342	794.9	0.102	0.9974
10d with GWB	353.7	0.048	0.9463	1047.8	0.070	0.9635
10d with insulation	384.4	0.062	0.9881	835.8	0.074	0.9362
16d with insulation	423.9	0.055	0.9824	685.7	0.065	0.9041

It is difficult to determine if these results confirm or deny the proposed stiffness relationship. When the relationship is applied to experimental results alone, the decay in connection stiffness is captured fairly well, considering the variation in experimental data. Various curve fitting methods were applied to FE model output data, and it was determined that a 4th or 5th order polynomial expression can fit the data better than the exponential relationship proposed by Antonides et. al. Since this study considered only one type of sheathing material, one type of embedment material, it is impossible to confirm or deny the validity of the proposed stiffness relationship, nor is it possible to conclude any relationship for constants C_a and C_b.

5.5 Derivation of Yield Equations for Cases with Intermediate Materials

This section describes a new analytical model for nailed light-frame connections that include an intermediate material, and compare the resulting peak load estimates with both experimental results and those generated by the FE model. The yield equations previously discussed in Chapter 2, first developed by Johansen, where later adapted to fit

a wide variety of lateral loading cases. The following loading situations were considered on individual nailed connections (Aune and Patton-Mallory, 1986):

- Two members with equal embedding strength
- Two members with unequal embedding strength
- Two members with head side member replaced with a steel plate
- Three members with equal embedding strength
- Three members with unequal embedding strength
- Three members with unequal embedding strength, with steel side plates or steel central plate
- Two members with an intermediate layer of insulation, with equal embedding strength

Aune and Patton-Mallory did not consider the connection case that has been the focus of this study: two members with unequal embedding strength with an intermediate layer of insulation. New yield equations for this loading case will be derived in this section. There are two relevant failure modes considered: #1; the nail yields at two locations; in the sheathing and stud, and #2; nail yields only in stud. The governing case is assumed to be the one which results in a lower yield load. The following assumptions are made in the derivation:

- A constant value for bending moment in nail
- A constant value for load in head-side and point-side materials
- No friction between adjacent surfaces
- Trigonometric approximation of bend angle in nail: $\tan(\theta) = \theta$

- The volume of compressed wood in a member surface is proportional to the work done by the nail on that surface

This analytical model was considered in the case of insulation as an intermediate material, as it was assumed that insulation would have a negligible contribution to connection strength (zero embedment strength). Experimentally, and through the FE model, it has been shown that use of GWB increases connection strength (peak load and yield load) by a small amount, therefore, a more accurate analytical model of such a connection might be based on one with 3-members with unequal bearing strength.

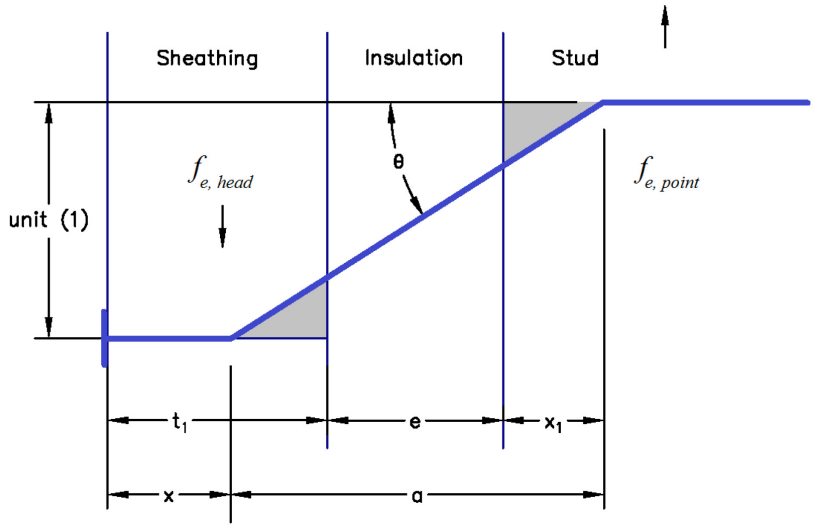

Note: Nail is shown in blue

t_1 = head-side member thickness (thickness of sheathing panel) (mm)
e = thickness of intermediate material (insulation) (mm)
$f_{e,head}$ = embedding strength of head side member (sheathing panel) (N/mm)
$f_{e,point}$ = embedding strength of point side member (stud) (N/mm)
a = thickness of cleat under nail head (mm)

Figure 5.25: Analytical nail model with 2-way yielding

Failure Mode #1:

The first failure mode is shown in Figure 5.25. Yielding in bending is occurring in the nail (represented by the thick line) at two locations: within the sheathing and within

the stud. The shaded region represents the area of wood compressed by the nail as it deforms. A unit displacement is assumed between the layer of sheathing and the stud.

The following parameters are defined, based on Figure 5.25:

$$\beta = \frac{f_{e,point}}{f_{e,head}} \quad \gamma = \frac{M_y}{f_e} \qquad (\mathbf{5.5})$$

where:

β is the ratio of the embedding strength if the stud and the head

M_y = nail yield moment (in bending) (Nmm)

The yield load (F_y) for the 2-way yielding failure mode can be derived using the virtual displacement method:

$$W = f_e \int \eta d\xi + \sum M_y \theta \qquad (\mathbf{5.6})$$

where:

θ = angular rotation of the yielded nail

η, ξ = integration variables for area of wood experiencing deformation

W = work done by the whole joint

Approximation for a small angle of nail bending is assumed:

$$\tan(\theta) \doteq \theta = \frac{1}{a}$$

Thus (5.6) can be rewritten as follows:

$$W = \sum f_e A + M_y \frac{1}{a} \qquad (\mathbf{5.7})$$

where:

A = wood crushed by nail bearing (shaded area in Figure 5.25).

It follows from geometry that:

$$a = x_1 + e + t_1 - x \qquad (\mathbf{5.8})$$

where x is the distance from the nail head to the location of the first yield point in the nail.

Assuming a proportional area for embedment on either side of the nail:

$$f_e(t_1 - x) = \beta f_e x_1$$

Re-arranged:

$$x_1 = \frac{t_1 - x}{\beta} \qquad (\mathbf{5.9})$$

Re-arrange (5.5) for γ:

$$M_y = \gamma f_e \qquad (\mathbf{5.10})$$

Create an expression for the size of deformed areas (shaded region in Figure 5.25):

$$\sum f_e A = f_e \left[\frac{1}{2}(t_1 - x)\frac{(t_1 - x)}{a}\right] + f_e \beta \left[\frac{1}{2}(x_1)\frac{(x_1)}{a}\right] \qquad (\mathbf{5.11})$$

Assuming a unit displacement (d), results in:

$$W = dF = 1 * F \qquad (\mathbf{5.12})$$

Substitute (5.8), (5.9), (5.10), (5.11), (5.12) into (5.7):

$$F = \frac{f_e(\beta t_1^2 - 2\beta t_1 x + \beta x^2 + t_1^2 - 2t_1 x + x^2 + 2\gamma\beta)}{2(t_1 - x + e\beta + t_1\beta - x\beta)} \qquad (\mathbf{5.13})$$

Differentiate (5.13) with respect to *x*:

$$\frac{dF}{dx} = \frac{1}{2}\frac{f_e(\beta t_1^2 - 2\beta t_1 x + \beta x^2 + t_1^2 - 2t_1 x + x^2 + 2\gamma\beta)(1+\beta)}{(x - t_1 - e\beta - t_1\beta + x\beta)^2}$$

$$- \frac{f_e(x\beta - t_1 + x - t_1\beta)}{(x - t_1 - e\beta - t_1\beta + x\beta)}$$

Equate the derivative to zero, to find the minimum, and obtain solutions for *x*:

$$x = \frac{e\beta + t_1\beta + t_1 \pm \sqrt{e^2\beta^2 + 2\gamma\beta + 2\gamma\beta^2}}{1+\beta} \qquad (\mathbf{5.14})$$

All terms in the expression for *x* are positive and *x* must be located within the sheathing layer from the assumed geometry, thus x must be less than t_1 (the thickness of sheathing), thus the root must be subtracted. The positive sign is discarded in (5.14). Substitute (5.14) into (5.13), creating an expression for lateral load at a minimum:

$$F_y = \frac{\beta f_e\left[e^2\beta + 2\gamma\beta + 2\gamma - e\sqrt{\beta(e^2\beta + 2\gamma + 2\gamma\beta)}\right]}{\sqrt{\beta(e^2\beta + 2\gamma + 2\gamma\beta)}(1+\beta)} \qquad (\mathbf{5.15})$$

Failure Mode #2:

The second failure mode is shown in Figure 5.26. Yielding is occurring at one location within the nail; at some distance x_1 within the stud. As before, the shaded region represents the area of wood compressed by the nail as it deforms.

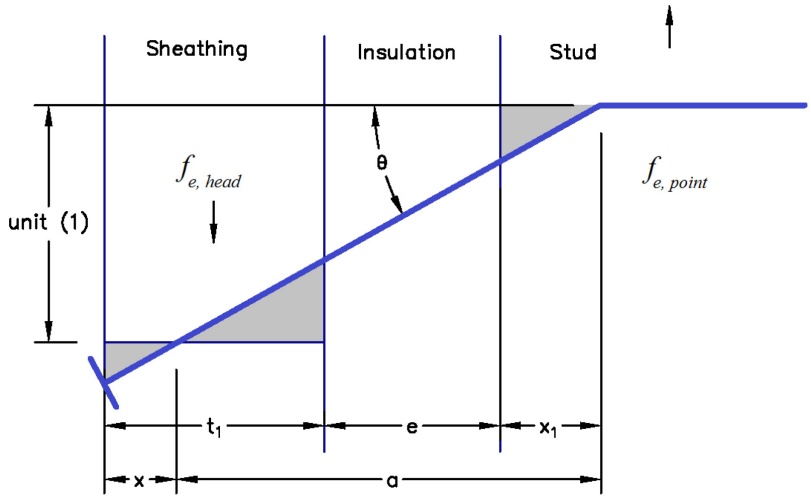

Note: Nail is shown in blue

Figure 5.26: Analytical nail model with 1-way yielding

Relationships which apply from the previous failure mode:

$$\tan(\theta) \doteq \theta = \frac{1}{a} \qquad W = \sum f_e A + M_y \frac{1}{a} \qquad M_y = \gamma f_e \qquad \beta = \frac{f_{e,point}}{f_{e,head}}$$

Similarly, from geometry:

$$a = x_1 + e + t_1 - x$$

An area proportional to embedment strength is assumed on either side of the nail:

$$f_e(t_1 - x) = f_e x + \beta f_e x_1$$

Re-arranged:

$$x_1 = \frac{t_1 - 2x}{\beta}$$

Create expression for deformation areas:

$$\sum f_e A = f_e \left[\frac{1}{2}(t_1 - x)\frac{(t_1 - x)}{a}\right] + f_e \left[\frac{1}{2}(x)\frac{(x)}{a}\right] + f_e \beta \left[\frac{1}{2}(x_1)\frac{(x_1)}{a}\right]$$

$$\sum f_e A = \frac{f_e}{2a}[(t_1 - x)^2 + x^2 + \beta x_1^2]$$

Substitute the above into the expression for virtual displacement:

$$F = \frac{1}{2}\frac{f_2(\beta t_1^2 - 2\beta t_1 x + \beta x^2 + t_1^2 - 4t_1 x + 4x^2 + 2\gamma\beta)}{(t_1 - 2x + e\beta + t_1\beta - x\beta)}$$

Differentiate with respect to *x*:

$$\frac{dF}{dx} = \frac{f_e(2x\beta - t_1\beta - 2t_1 + 4x)}{(t_1\beta - x\beta + e\beta + t_1 - 2x)}$$

$$+ \frac{1}{2}\frac{(\beta t_1^2 - 2\beta t_1 x + 2\beta x^2 + t_1^2 - 4t_1 x + 2\gamma\beta)(\beta + 2)}{(x\beta - t_1\beta - e\beta - t_1 + 2x)^2}$$

Equate derivative to zero, to find the minimum, and obtain solutions for *x*:

$$x = \frac{1}{2} * \frac{2t_1\beta + 2e\beta + 2t_1 \pm \sqrt{2t_1^2\beta^2 + 4t_1\beta^2 e + 2\beta t_1^2 + 4e^2\beta^2 + 4\gamma\beta^2 + 8\gamma\beta}}{\beta + 2}$$

As before, *x* must be located within the sheathing layer, thus discard the positive sign.

Evaluate the expression for lateral load at a minimum, and simplify:

$$F_y = \frac{f_e}{\beta + 2}\left[\sqrt{2\beta(\beta t_1^2 + 2t_1 e\beta + t_1^2 + 2e^2\beta + 2\gamma\beta + 4\gamma)} - t_1\beta - 2e\beta\right] \qquad (\mathbf{5.16})$$

To further validate the use of the derived expressions from Aune and Marcia as a means of predicting joint yield load, base cases with no intermediate material were compared. The following are analytical expressions for the yield load of two-member joints with members with unequal embedding strength (Aune and Marcia, 1986):

Failure mode 1:

$$F_y = \sqrt{\frac{\beta * 4f_e * M_y}{(1 + \beta)}} \qquad (\mathbf{5.17})$$

Failure mode 2:

$$F_y = f_e \left[\sqrt{\frac{2\beta(1+\beta)t_1^2}{(2+\beta)^2} + \frac{4\beta\gamma}{(2+\beta)}} - \frac{\beta t_1}{(2+\beta)} \right] \qquad (\mathbf{5.18})$$

The same parameter definitions and failure mode shapes apply from before. Expressions (5.17) and (5.18) can be formed from (5.15) and (5.16) respectively, by substituting an insulation thickness of $e = 0$.

5.5.1 Results of the analytical model with insulation

Figure 5.27 compares the yield load calculated using the proposed analytical model (the result of equations 5.15 and 5.16, above) with the yield load calculated from the FE model and experimental results, for both intermediate materials considered in this study. The results shown for the FE model and experimental results were found using the K&C method for calculating yield load.

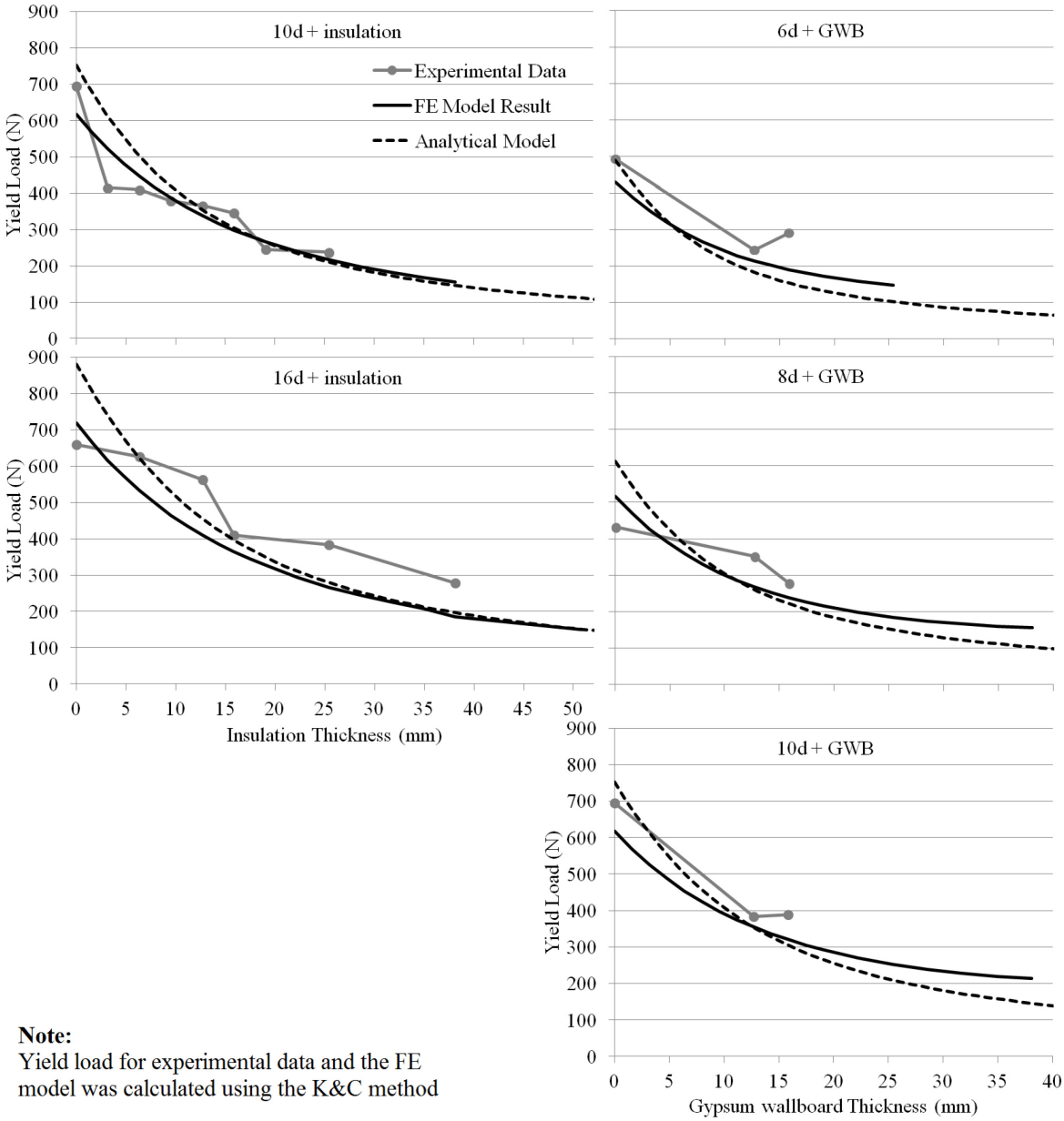

Figure 5.27: Analytical model yield load comparison

The analytical model performs about as well as the FE model in predicting yield load. The two methods deviate from the experimental result by approximately the same amount. The analytical model creates a roughly exponential decay relationship, just as the FE model does. It differs in that its prediction of yield load is higher than the FE model in cases of no or very thin insulation layers, and lower than the FE model in cases of very

thick insulation layers. The cause of this difference is difficult to identify, however, it can be assumed that it is due to the limitations and assumptions of the analytical model. Failure mode 1 (nail yielding at 2 points) governs the analytical model in all tested situations, meaning that the analytical model assumes nail yielding at two points (in the sheathing and in the stud). Given the structure of the model, it is expected that the failure mode is most dependant on the thickness of the sheathing (OSB), and may change to failure mode 2 provided that a sufficiently thin panel of sheathing is used. This is in comparison with the FE model, which yielded in one location (in the stud), and the experimental results, which showed a gradual transition between the two, with increasing intermediate material thickness.

5.6 Limitations and Conclusions

Over the course of the development of the FE model, effort was made to consider and represent all effects that would be likely to have a significant impact on the overall result. The following are known phenomena that were not accounted for:

- Friction in the interface between any two embedment materials
- Interaction between shear and axial strength in the steel of the nail. This effect was also neglected in other studies (e.g. Chui and Li, 2005; Ni, 1997)
- Resistance to nail head rotation caused by the nail head entering the OSB
- Pull out resistance due to the nail shank in OSB and intermediate materials (was assumed to be negligible)

- Two-way bending in the nail was not observed: At the end of a selected number of tests of the FE model, the final nail shape was examined. The FE model consistently generates a final nail shape with only one point of bending. The most likely explanation for this is that the characteristic two-way bending (S-shaped) occurs beyond the failure point and extent of the FE model, therefore it did not have a chance to manifest.

Further developments in the FE model are certainly possible. It is recommended that subsequent FE models of nailed connections with intermediate materials, subjected to lateral loads consider the effect of interface friction more closely. As was mentioned previously, interface friction was not included in this model as the amount of friction between surfaces is highly variable and is difficult to quantify. This resulted in a significant underestimation of connection stiffness as calculated using commonly used methods. A possible means of accounting for friction in the model or subsequent models may be to treat the relevant coefficients of friction and normal forces imposed on the interface(s) as inputs which can be found via rudimentary experimentation.

Overall results show that the FE model performed fairly well in capturing the load-deformation relationship in experimental data in every type of connection tested. The FE model provides good estimates of both maximum force and yield force for nailed connections with intermediate materials. The model has good predictive capability, and can be used to extrapolate the response of different embedment materials (different framing, sheathing and intermediate materials), as well as different nail sizes. Since the FE model was tested for many different intermediate material thicknesses, the stiffness

relationship proposed by Antonides et al. was quantified (Antonides et al., 1984), however it was impossible to confirm or deny this relationship, given a lack of data points.

In order to create and/or validate a relationship between connection strength or stiffness and intermediate material thickness, it is necessary to consider the effect of different framing and sheathing materials (which have different bearing properties). It is possible that the FE model proposed in this study already has this ability, however, since there are no experimental tests on different framing and sheathing materials to compare to (and thus confirm validity), new strength and stiffness relationships are not proposed here.

The analytical model was successful in capturing the decay of yield load with increasing intermediate material thickness. In this regard, it performed with about as much accuracy as the FE model. The analytical model has the advantage of being easier to use, as it is essentially a system of relatively simple expressions. It has the disadvantage of not being able to capture other important connection characteristics, such as stiffness and peak load, and also makes more broad assumptions (See Section 5.5) than the FE model.

6. SUMMARY, CONCLUSIONS AND RECOMMENDATIONS

This Chapter will summarize the findings from every part of this thesis. General conclusions from experimental and modeling work will be discussed, along with the limitations associated with the research. In light of the findings, recommendations to changes to CSA-O86 are provided along with recommendations for future research.

6.1 Summary of Findings

This thesis describes a study of interface gaps within the individual sheathing-to-framing nailed connections in light frame timber shear walls. The study was motivated by the lack of experimental testing to support note 4 to Table 9.5.1A in the standard for Engineering Design in Wood, CSA-O86. Note 4 states that shear walls may be sheathed over top of 1/2" (12.7 mm) or 5/8" (15.9 mm) panels of gypsum wallboard (GWB) as long as minimum nail penetration (listed in Table 9.5.1A) is satisfied. Such a resulting shear wall would have the same capacity as one without an intermediate GWB panel (CSA, 2010). The intention of this study was to experimentally test this using individual nailed connections.

The effect of the thickness of an intermediate layer of insulation (in place of gypsum wallboard) on connection strength properties was also tested. This was motivated by a lack of understanding of the effects of relatively thick (up to 1.5", or 38 mm) layers of intermediate insulation within such shear wall assemblies, as well as the recent development of sheathing technologies incorporating insulation, such the Zip-sheathing system, introduced by Huber Engineered Woods LLC (Huber, 2012).

For both types of intermediate material, finite element (FE) and analytical models were used to simulate the connection and further explain the behavior present. The accuracy of these models was confirmed by the results from experimental testing.

Chapter 2 reviewed the process of designing shear walls and nailed connections according to the Canadian standard CSA-O86, past literature related to nailed connections with interface gaps and intermediate materials, as well as details into how such shear walls are designed in the United States. It was found that previous research in the area of intermediate materials is limited to situations with very small interface gaps. It was seen that connection strength properties decreased sharply with increasing gap size (Figures 2.5, 2.6 and 2.7). The research report on which the standard for light frame shear walls in the United States, Special Design Provisions for Wind and Seismic (SDPWS), was based, suggested that in the case of GWB as an intermediate material, there is some drop in connection properties (Tissel, 1993). These findings alone suggest that note 4 may not be conservative, or at the least that it would result in significantly lower factors of safety for shear walls sheathed over GWB than equivalent shear walls sheathed directly over framing. There exists a significant knowledge gap in the area of intermediate materials of any kind. Review of previous studies which modeled nailed connections found that many FE models of nailed connections and some of corresponding shear walls already exist and are accurate, however FE modeling of the specific case of a nailed connection with an intermediate material was not found.

Chapter 4 analyzed and discussed the results of the experimental portion of this study. From the load-deformation response of each test, the ultimate capacity was identified, the yield point was calculated using five commonly used methods, and the stiffness was calculated using several other common methods. It was found that there is a significant drop in connection capacity and stiffness as the intermediate material thickness increases.

In the case of GWB, the thicknesses specified by note 4 were tested in combination with 6d, 8d and 10d nails. Capacity and stiffness were compared with nail embedment as a percentage of the required minimum embedment. It was found that there did not exist a relationship between this minimum embedment and connection strength properties. Rather, the strength and stiffness were reduced significantly with the addition of a GWB layer regardless of the layer thickness, nail size or sheathing thickness. The addition of an intermediate GWB layer resulted in a mean loss of approximately 40% of connection capacity and 70% of connection stiffness.

In the case of insulation as the intermediate material, 7 different thicknesses were tested with 10d nails and 5 different thicknesses were tested with 16d nails. An exponentially decaying relationship was found for both the capacity and stiffness of such connections with increasing insulation thickness. A connection with an intermediate layer of insulation performed slightly worse than with GWB as the intermediate material. For example, a 1/2" layer of intermediate insulation resulted in a mean loss of connection capacity of 52% and connection stiffness of 61%.

With regard to note 4, these results show that the loss in connection capacity and stiffness is too great to justify the assumption that shear walls sheathed over GWB will

perform as well as those without. If insulation is used as an intermediate material, it seems as though connections with very thin layers may retain enough strength and stiffness that they might be practical in shear walls. For thicknesses greater than 1/2", however, this assumption would not be justified as it would require too many additional nails to restore connection strength properties.

Chapter 5 considered the development and use of two models of a nailed connection with an intermediate material: an FE model based on one previously developed by Ni (1997), and an analytical model, based on yield equations previously derived by Aune and Marcia (1986) and Johansen (1949).

The material property inputs for the FE model were determined by nail bending tests, nail embedment tests on samples of sheathing (OSB) and framing (SPF), nail pull-out tests, and compression tests on samples of GWB and insulation. Load-displacement results show good correlation between the FE model and mean experimental response. The FE model predicted the magnitude and nail-slip of the ultimate load well, however the model consistently underestimated initial stiffness. The likely reason for this was that the model did not take interface friction between the different layers into account. The decay in yield load was compared to experimental data using the same methods used in Chapter 4 and showed good correlation. The developed FE model was shown to be an accurate means of predicting the capacity of nailed connections with intermediate materials.

The results from the nail bending and embedment tests were also used as input values for the analytical model. This model was used to calculate the yield load in two

failure cases: nail yielding within the framing and nail yielding within both the framing and the sheathing. It was found that nail yielding in both the framing and sheathing governed all cases. The decay in yield load with increasing intermediate material thickness was compared with the result from the FE model and with experimental results. All three sets of results showed good correlation, indicating an overall reduction in yield load of approximately 50% in the case of a 1/2" (12.7 mm) layer of either type of intermediate material.

6.2 Limitations

This study addresses note 4 to Table 9.5.1A in CSA-O86 with the experimental testing and modeling of individual nailed connections. The note and table, however, apply to entire shear walls. It is well known that the properties of a shear wall heavily depend on its nailed connections, however this does not mean that the results of the testing of individual nailed connections translate directly to results for corresponding shear walls. To quantify losses in entire shear walls, it is suggested that the reduced properties of individual nailed connections found in this study be applied to existing shear wall models. To prove actual losses in entire shear walls for the purpose of refining design standards, full-scale testing must be conducted.

6.3 Primary Contributions

1. The introduction of a 1/2" (12.7 mm) or 5/8" (15.9 mm) layer of intermediate GWB in a nailed connection, while maintaining minimum nail penetration, will result in a mean loss of approximately 41% and 45% of connection capacity,

respectively, and 67% and 75% of connection stiffness, respectively. In terms of both capacity and stiffness, 5/8" GWB performs slightly worse than 1/2" GWB.

2. Nail penetration up to 7 millimeters above or below the minimum does not create a significant effect on connection capacity or stiffness, as compared to the introduction of a layer of GWB
3. A nailed connection with an intermediate layer of GWB will perform only slightly better in capacity and stiffness than an equivalent connection with insulation. GWB contributes very little to the strength of the connection due to its location and significantly reduced embedment strength when compared with other sheathing materials.
4. Results from the testing of various insulation thicknesses have resulted in an observed exponentially decaying relationship of connection capacity and stiffness regardless of nail size.
5. There appears to be an immediate drop in connection capacity with the introduction of a gap of any size, likely due to the loss of interface friction.
6. The FE model of the nailed connection is accurate in capturing the general shape of the load-deformation relationship, the capacity of the connection, and the decay of this capacity with increasing intermediate material thickness.
7. The analytical model is good at predicting the decay in yield load with intermediate material thickness, showing good correlation with the FE model and experimental results.
8. Given that a light frame shear wall is highly dependent on individual nailed connections between the framing and sheathing, and the losses observed with the

introduction of an intermediate GWB layer, note 4 is not conservative, regardless of the amount of nail penetration, nail size, or sheathing thickness.

9. Using the current CSA-O86 standard to design a shear wall sheathed over a panel of GWB, taking advantage of note 4, will likely result in a significantly reduced factor of safety.

6.4 Recommendations for CSA-O86 and Designers

Based on these preliminary results, it seems prudent for designers to avoid taking advantage of CSA-O86 Table 9.5.1A, note 4, because the addition of an intermediate layer of gypsum between the sheathing and framing in a shear wall will likely result in a significant loss in capacity and stiffness. As discussed previously, these results should also be confirmed using full shear wall tests. It seems evident that note 4 is problematic for the following reasons:

- Individual nailed connections satisfying the conditions of note 4, and using any allowed nail size or sheathing thickness, will have dramatically reduced capacity and stiffness than equivalent connections without intermediate GWB.
- Given the significance of nailed connections in light frame shear walls, this will likely result in reduced capacity in shear walls that are designed to take advantage of note 4.

The above recommendations are based on the experimental data and extensive connection modeling in this study. The magnitude of the loss of shear wall capacity and

stiffness as a result of this is unknown and can only be quantified through full scale shear wall testing, but is assumed to decay in proportion to the loss in capacity and stiffness in the nailed connections.

It is possible that the anticipated reduction in strength and stiffness may be mitigated by the addition of more nails, however, if a greater number of nails are used in the construction of shear walls sheathed over GWB, the problem of insufficient nail spacing may emerge. In the case of both currently allowed GWB thicknesses, one would have to increase the number of nails by a factor of approximately 2 to restore connection capacity, and approximately 4 to restore connection stiffness. This would likely cause the spacing between adjacent nails to fall below the threshold for splitting of the framing.

With regard to intermediate materials of any type and of any thickness, it is clear that further study is needed to determine whether it should be permissible to include them in nailed connections at all. In light of the prescriptive nature of CSA-O86, and developments in sheathing and insulation technologies, it may be advantageous in the future to incorporate intermediate materials, despite the loss in connection properties. In such an event, the author recommends the use of reduction factors to account for this. These reduction factors should be determined based on full-scale shear wall testing.

6.5 Recommendations for Future Research

It is recommended that subsequent research in the area of intermediate materials be performed to test the capacity and stiffness of full-scale light frame shear walls, sheathed over GWB, with various framing and sheathing materials. The results of such a study may allow the safe use of shear walls sheathed over GWB, provided that

appropriate measures such as additional reduction factors are used to account for the reduction in strength properties.

The findings from this study suggest that light frame shear walls sheathed over rigid insulation may perform just as well as those sheathed over GWB. In light of the global trends in environmental sustainability and energy efficiency, the demand for such shear walls may increase in the near future. The future testing of shear walls sheathed over insulation would be necessary to allow or restrict their use in design.

With regard to the use of intermediate materials in nailed connections in general, it is recommended that research be conducted in testing various materials as point-side or head-side members in combination with an intermediate material of various thicknesses. From this it may be possible to develop prescriptive rules and reduction factors to determine their use in design.

REFERENCES

Antonides, C. E., Vanderbilt, M. D., & Goodman, J. R. (1979). "Interlayer gap effects on nail slip modulus". Civil Engineering Department, Colorado State University.

Asiz, A., Zhou, L., & Chui, Y. H. (2010). Characteristics of Lumber to Lumber Framing Connections in light Frame Wood Structures. In *Proc*.

ASTM Standard C473, (2012), "Standard Test Methods for Physical Testing of Gypsum Panel Products," ASTM International, West Conshohocken, PA, 2012, DOI: 10.1520/C0473-12, www.astm.org.

ASTM Standard C578, (2012b), "Standard Specification for Rigid, Cellular Polystyrene Thermal Insulation," ASTM International, West Conshohocken, PA, 2012, DOI: 10.1520/C0578, www.astm.org.

ASTM Standard C1396, (2013), "Standard Specification for Gypsum Board," ASTM International, West Conshohocken, PA, 2013, DOI: 10.1520/C1396_C1396M, www.astm.org.

ASTM Standard D1761, (2012), "Standard Test Methods for Mechanical Fasteners in Wood," ASTM International, West Conshohocken, PA, 2012, DOI: 10.1520/D1761-12, www.astm.org.

ASTM Standard D2395, (2007a), "Standard Test Methods for Density and Specific Gravity (Relative Density) of Wood and Wood-Based Materials," ASTM International, West Conshohocken, PA, 2007, DOI: 10.1520/D2395-14, www.astm.org.

ASTM Standard D4444, (2013), "Standard Test Method for Laboratory Standardization and Calibration of Hand-Held Moisture Meters," ASTM International, West Conshohocken, PA, 2013, DOI: 10.1520/D4444-13, www.astm.org.

ASTM Standard D5764-97a, (2005b), "Standard Test Method for Evaluating Dowel-Bearing Strength of Wood and Wood-Based Products". ASTM International, West Conshohocken, PA, 2012, DOI: 10.1520/D5764-97AR13, www.astm.org.

ASTM Standard E2126-05, (2005a), "Standard Test Method for Cyclic (Reversed) Load Test for Shear Resistance of Walls for Buildings". ASTM International, West Conshohocken, PA, 2012, DOI: 10.1520/E2126-05, www.astm.org.

ASTM Standard F1575, (2008), "Standard Test Method for Determining Bending Yield Moment of Nails," ASTM International, West Conshohocken, PA, 2008, DOI: 10.1520/F1575, www.astm.org.

ASTM Standard F1667, (2013), "Standard Specification for Driven Fasteners: Nails, Spikes, and Staples," ASTM International, West Conshohocken, PA, 2013, DOI: 10.1520/F1667, www.astm.org.

Aune, P., & Patton-Mallory, M. (1986). Lateral Load-Bearing Capacity of Nailed Joints Based on the Yield Theory. *No. FPL-469, Forest Products Laboratory, US Dept. of Agriculture, Washington, DC*.

AWC. (2008). "Special Design Provisions for Wind and Seismic, SDPWS". American Wood Council. Retrieved June 2014, from: http://www.awc.org/pdf/2008WindSeismic.pdf

AWC. (2012). "National design specification for wood construction: ASD/LRFD Manual". American Wood Council. Retrieved: June 2014, from: http://www.awc.org/pdf/2012ASD-LRFD_Manual_WEB.pdf

Berkeley, University of (2012). "Steel02 Material" In OpenSees Wiki. Retrieved October 1, 2013, from http://opensees.berkeley.edu/wiki/index.php/Steel02_Material_--_Giuffr%C3%A9-Menegotto-Pinto_Model_with_Isotropic_Strain_Hardening

Canadian Standards Association. 1 CSA O325-07 (R2012). *Construction Sheathing*.

Canadian Standard Association. (2010). CSA O86-01 Engineering Design in Wood. *Mississauga, Canada*.

Ceccotti, A. (1995). "Timber connections under seismic actions". In: *Timber engineering–STEP 1*. 1st Edition. STEP/EUROFORTECH. The Netherlands, ISBN 90-5645-001-08. Pp. C17/1-C17/10

Chui, Y. H., & Li, Y. (2005). "Modeling timber moment connection under reversed cyclic loading". *Journal of structural engineering*, *131*(11), 1757-1763.

Commonwealth Scientific and Industrial Research Organization (CSIRO). 1996. "Timber evaluation of mechanical joint systems". Part 3, Earthquake loading. CSIRO, Melbourne, Australia.

Filippou, F. C., Popov, E. P., Bertero, V. V. (1983). "Effects of Bond Deterioration on Hysteretic Behavior of Reinforced Concrete Joints". Report EERC 83-19, Earthquake Engineering Research Center, University of California, Berkeley.

Foliente, G. C. (1993). "Stochastic dynamic response of wood structural systems". Ph.D. dissertation, Dept. of Wood Science and Forest Products. Virginia Polytechnic Institute and State Univ., Blacksburg, VA.

Forest Products Laboratory . (2010). "Wood handbook: wood as an engineering material". General Technical Report FPL-GTR-190. Madison, WI: U.S. Department of Agriculture, Forest Service, Forest Products Laboratory. Retrieved April 2014, from: http://www.nhla.com/assets/1603/wood_handbook.pdf

Foschi, R. O. (1974). "Load-slip characteristics of nails." *J Wood Sci* 7 (1974): 69-74.

Hong, J. P., & Barrett, D. (2010). "Three-dimensional finite-element modeling of nailed connections in wood". *Journal of Structural Engineering*, *136*(6), 715-722.

Huber. (2012). "Zip-R Sheathing Overview". Huber Engineered Woods LLC. Retrieved July 30, 2014, from: http://www.huberwood.com/assets/pdfs/ZIP-R-Sheathing-Overview.pdf

ICCES. (2013). "ICC-ES Evaluation Report ESR-3373". Retrieved July 30, 2014, from: http://www.icc-es.org/Evaluation_Reports/

Instron. (2005). "Series 5500 Load Frames Including Series 5540, 5560, 5580". Reference Manual - Equipment. Retrieved February 2014, from: www.instron.com

Johansen, K. W. (1949). "Theory of timber connections". In *International Association of Bridge and Structural Engineering* (Vol. 9, pp. 249-262).

Jones, S. N., & Fonseca, F. S. (2002). "Capacity of oriented strand board shear walls with overdriven sheathing nails". *Journal of Structural Engineering*, *128*(7), 898-907.

Karacabeyli, E., and A. Ceccotti. (1996). "Quasi-static reversed cyclic testing of nailed joints". *Proceedings of International Council for Building and Research Studies and Documentation Working Commission W18 – Timber Structures*. Pap. 29-7-7. Karlsruhe, Germany.

Kesik, T. J., & Lio, M. (2013). "Canadian wood-frame house construction". Central Mortgage and Housing Corporation.

Malhotra, S. K., & Thomas, B. (1985). "Effect of interface gap on load-slip characteristics of timber joints fabricated with multiple nails". *Canadian Journal of Civil Engineering*, *12*(1), 104-113.

McKenna, F., Fenves, G. L., Scott, M. H., & Jeremic, B. (2000). "Open System for Earthquake Engineering Simulation (OpenSees)" [Computer Software]. Pacific Earthquake Engineering Research Center, University of California, Berkeley, CA. Available from: http://opensees.berkeley.edu/

McLain, T. E. (1975). "Curvilinear load-slip relations in laterally-loaded nailed joints" (Doctoral dissertation, Colorado State University).

Meng, Q., Hirai, T., & Koizumi, A. (2008). "Frictional coefficients between timber and some structural sheet materials". *Journal of the Japan Wood Research Society*, *54*.

Muñoz, W., Mohammad, M., Salenikovich, A., & Quenneville, P. (2008). "Determination of yield point and ductility of timber assemblies: in search for a harmonised approach". *Engineered Wood Products Association*.

NBCC. (2010). "National Building Code of Canada". *National Research Council of Canada*.

Ni, C. (1997). "Behaviour of nailed timber joints under reversed cyclic load" (Doctoral dissertation, University of New Brunswick, Faculty of forestry and Environmental Management).

Pellicane, P. J., Stone, J. L., & Daniel Vanderbilt, M. (1991). "Generalized model for lateral load slip of nailed joints". *Journal of Materials in Civil Engineering*, *3*(1), 60-77.

Pellicane, P. J. (1993). "Plywood-solid-wood nailed joints under lateral loading". *Journal of materials in civil engineering*, *5*(2), 226-236.

Tissell, J. R. (1993). "Wood structural panel shear walls". *American Plywood Association (APA)–The Engineered Wood Association, Tacoma, Wash. Report*, *154*.

Wang, Qing. (2009). "Relationship between fastening properties and load-deflection response of wood shear walls". University of New Brunswick (Canada).

Wilkinson, T. L. (1971). "Theoretical lateral resistance of nailed joints". *Journal of the Structural Division*, *97*(5), 1381-1398.

Xu, J., & Dolan, J. D. (2009). "Development of nailed wood joint element in ABAQUS". *Journal of structural engineering*, *135*(8), 968-976.

Yasumura, M., and N. Kawai. (1998). "Estimating seismic performance of wood-framed structures". *Proceedings of 1998 I.W.E.C*. Switzerland. Vol.2. pp. 564-571.

APPENDIX A: Density and Moisture content of wood materials

Density and Moisture Content for SPF Specimens in testing with GWB

Moisture content and density for tests with GWB was calculated from a pool of cut specimens. Each moisture content test corresponds to one nailed connection specimen.

S #	Mass (g)	Dimensions (mm)			Vol. (cm^3)	Moisture Content Measurements				$Density_2$	
		Length	Width	Depth		#1	#2	Mean	$Adj._{-1}$	Actual	Dry
1	79.9	61.42	77.48	38.18	181.7	10.9	10.6	10.8	11.0	440	374
2	88.1	62.54	91.31	38.12	217.7	10.3	9.8	10.0	10.3	405	347
3	56.0	47.86	76.34	39.06	142.7	12.0	11.1	11.6	11.9	392	330
4	88.3	55.23	93.63	38.47	198.9	8.8	7.7	8.3	8.5	444	391
5	72.4	55.29	75.65	38.19	159.7	9.8	9.9	9.8	10.1	453	390
6	94.2	56.13	85.63	39.09	187.9	14.4	16.3	15.3	15.7	501	401
7	70.1	69.64	74.72	38.47	200.1	10.4	10.4	10.4	10.7	350	299
8	67.2	50.73	92.13	38.47	179.8	9.8	10.2	10.0	10.2	374	321
9	54.5	45.64	74.76	38.39	131.0	8.6	8.4	8.5	8.7	416	365
10	66.7	46.70	82.79	38.26	147.9	10.1	9.5	9.8	10.0	451	389
11	52.7	41.42	69.87	38.62	111.7	10.3	12.0	11.1	11.4	472	399
12	115.7	49.25	109.51	38.82	209.4	8.8	8.6	8.7	8.9	553	484
13	56.8	54.11	56.73	38.63	118.6	10.4	8.6	9.5	9.8	479	414
14	68.7	47.97	84.34	37.27	150.8	9.3	9.0	9.1	9.4	456	396
15	86.3	42.77	98.03	38.69	162.2	8.6	6.8	7.7	7.9	532	472
16	60.2	43.69	70.37	38.75	119.1	10.2	9.1	9.7	9.9	505	436
17	80.3	43.98	98.00	38.03	163.9	7.7	8.5	8.1	8.3	490	432
18	66.4	30.42	106.34	38.92	125.9	10.2	14.1	12.1	12.4	527	440
19	89.1	59.45	105.43	38.10	238.8	9.4	9.9	9.7	9.9	373	322
20	108.6	56.94	103.85	39.10	231.2	9.6	11.3	10.5	10.7	470	401
21	75.7	40.77	92.66	38.64	146.0	13.8	9.4	11.6	11.9	519	436
22	53.1	43.01	79.65	37.91	129.9	9.9	10.3	10.1	10.3	409	351
23	96.7	64.57	70.96	38.66	177.1	8.4	7.8	8.1	8.3	546	482
24	108.9	62.34	99.97	38.72	241.3	8.2	8.9	8.5	8.8	451	396

S #	Mass (g)	Dimensions (mm)			Vol. (cm^3)	Moisture Content Measurements				Density$_2$	
		Length	Width	Depth		#1	#2	Mean	Adj.$_1$	Actual	Dry
25	96.5	57.39	104.03	38.27	228.5	9.6	10.2	9.9	10.2	422	363
26	55.8	42.24	82.61	37.83	132.0	10.0	9.9	9.9	10.2	423	363
27	81.6	68.02	76.86	37.99	198.6	8.6	7.9	8.2	8.4	411	362
28	76.0	56.36	88.62	37.65	188.0	9.3	10.1	9.7	9.9	404	349
29	99.2	61.08	102.10	38.02	237.0	9.8	9.3	9.6	9.8	418	362
30	96.6	72.01	74.15	38.10	203.4	8.4	7.9	8.2	8.4	475	419
31	56.1	46.63	84.15	38.34	150.4	7.9	8.8	8.3	8.6	373	328
32	40.5	36.82	70.00	37.30	96.1	9.7	10.8	10.2	10.5	421	361
33	74.4	63.28	64.20	38.11	154.8	11.4	10.3	10.8	11.1	481	408
34	107.1	65.29	72.39	38.99	184.2	8.3	9.3	8.8	9.0	581	508
35	81.1	71.50	68.45	37.66	184.3	12.0	11.8	11.9	12.2	440	368
36	80.4	55.55	90.20	38.08	190.8	11.6	11.7	11.6	11.9	421	354
37	78.3	59.81	81.68	38.47	187.9	8.0	8.1	8.1	8.3	417	368
38	87.2	58.87	77.27	39.06	177.7	8.3	10.9	9.6	9.8	491	424
39	102.0	61.60	80.48	38.55	191.1	10.3	17.5	13.9	14.3	534	434
40	76.3	58.08	64.12	38.95	145.0	13.3	11.9	12.6	12.9	526	436
41	73.9	48.18	96.05	37.89	175.3	9.5	8.7	9.1	9.3	422	386
42	60.8	45.64	94.11	38.25	164.3	9.5	10.1	9.8	10.1	370	336
43	110.9	59.64	112.23	38.63	258.6	11.3	11.5	11.4	11.7	429	384
44	76.1	47.79	118.73	38.17	216.6	9.3	11.8	10.6	10.8	351	317
45	52.2	56.28	68.90	38.24	148.3	8.9	9.7	9.3	9.5	352	321
46	85.6	47.36	118.31	38.19	214.0	9.1	10.8	10.0	10.2	400	363
47	72.4	54.67	91.60	38.57	193.1	9.2	8.8	9.0	9.2	375	343
48	62.1	53.83	67.00	38.36	138.3	8.8	10.8	9.8	10.1	449	408
49	44.2	43.04	69.47	38.48	115.0	9.9	9.4	9.7	9.9	384	350
50	62.1	46.48	70.19	38.45	125.4	10.0	9.9	10.0	10.2	495	449
51	66.9	50.85	80.67	38.39	157.4	11.2	10.7	11.0	11.2	425	382
52	59.0	51.93	86.37	38.18	171.2	8.4	8.5	8.5	8.7	345	317
53	48.9	40.11	80.21	38.06	122.4	12.3	11.7	12.0	12.3	399	356
54	71.6	35.42	117.82	38.28	159.7	8.8	9.3	9.1	9.3	448	410
55	36.8	43.03	63.64	38.25	104.7	8.9	10.7	9.8	10.1	351	319
56	52.3	40.36	89.18	38.32	137.9	7.8	7.6	7.7	7.9	379	351

Note: 1 - Adjusted for species and recording conditions, 2 - in kg/m^3

Density and Moisture Content for SPF Specimens in testing with Insulation

Moisture content and density of specimens with insulation was calculated on a per-test basis

Test #	Mass (g)	Dimensions (mm)			Vol. (cm^3)	Moisture Content Measurements				$Density_2$	
		Length	Width	Depth		#1	#2	Mean	$Adj._1$	Actual	Dry
10d nail + 1/8" Insulation											
Test 1	723.3	306	138.2	38.4	1623.9	11.2	11.4	11.3	12.1	*445*	**397**
Test 2	665.6	303	139.9	37.9	1606.6	10.0	10.6	10.3	11.1	*414*	**373**
Test 3	625.1	305	139.9	38.4	1638.5	9.4	9.3	9.4	10.1	*382*	**347**
Test 4	688.2	306	140.1	38.2	1637.7	9.3	9.6	9.5	10.2	*420*	**381**
Test 5	715.4	303	138.6	38.0	1595.8	10.8	10.8	10.8	11.6	*448*	**402**
Test 6	707.8	303	139.4	37.4	1579.7	10.7	10.6	10.7	11.4	*448*	**402**
10d nail + 1/4" Insulation											
Test 1	902.6	307	139.9	38.3	1645.0	8.8	8.9	8.9	9.5	*549*	**501**
Test 2	680.4	306	137.9	37.1	1565.5	8.9	8.7	8.8	9.5	*435*	**397**
Test 3	659.2	307	137.2	38.1	1604.8	9.3	9.3	9.3	10.0	*411*	**373**
Test 4	878.9	306	139.9	38.2	1635.3	8.8	8.7	8.8	9.4	*537*	**491**
Test 5	699.9	306	137.6	37.4	1574.7	8.7	8.7	8.7	9.4	*444*	**406**
Test 6	903.7	305	139.9	38.1	1625.7	9.5	9.7	9.6	10.3	*556*	**504**
10d nail + 3/8" Insulation											
Test 1	698.9	304	139.3	38.3	1621.9	9.0	8.8	8.9	9.6	*431*	**393**
Test 2	866.0	307	139.4	38.5	1647.6	8.6	8.9	8.8	9.4	*526*	**480**
Test 3	652.5	306	136.8	37.9	1586.5	9.3	9.3	9.3	10.0	*411*	**374**
Test 4	720.9	305	139.1	38.2	1620.7	9.7	9.7	9.7	10.4	*445*	**403**
Test 5	631.7	306	137.7	38.2	1609.6	9.9	9.6	9.8	10.5	*392*	**355**
Test 6	683.6	305	137.6	37.4	1569.6	9.6	9.7	9.7	10.4	*436*	**395**
10d nail + 1/2" Insulation											
Test 1	667.5	304	139.3	37.8	1600.7	10.5	10.2	10.4	11.1	*417*	**375**
Test 2	669.5	306	139.9	38.3	1639.6	9.6	9.3	9.5	10.2	*408*	**371**
Test 3	728.8	304	139.2	38.4	1625.0	10.5	10.6	10.6	11.3	*449*	**403**
Test 4	674.5	306	139.1	37.7	1604.7	9.7	9.9	9.8	10.5	*420*	**380**
Test 5	676.6	306	138.6	38.5	1632.8	9.7	9.6	9.7	10.4	*414*	**375**
Test 6	688.1	306	140.6	38.7	1665.0	8.9	8.9	8.9	9.6	*413*	**377**

Test #	Mass (g)	Dimensions (mm)			Vol. (cm^3)	Moisture Content Measurements				Density$_2$	
		Length	Width	Depth		#1	#2	Mean	Adj.$_1$	Actual	Dry
10d nail + 5/8" Insulation											
Test 1	688.8	306	137.0	37.6	1576.3	10.4	9.5	10.0	10.7	*437*	**395**
Test 2	732.2	304	140.0	38.7	1647.1	8.5	8.6	8.6	9.2	*445*	**407**
Test 3	908.1	306	139.8	38.4	1642.7	9.2	9.4	9.3	10.0	*553*	**503**
Test 4	870.2	306	139.7	38.2	1633.0	8.9	9.2	9.1	9.7	*533*	**486**
Test 5	776.6	305	139.7	37.9	1614.9	8.9	8.7	8.8	9.5	*481*	**439**
Test 6	837.7	304	139.2	38.6	1633.4	9.1	9.6	9.4	10.1	*513*	**466**
10d nail + 3/4" Insulation											
Test 1	735.4	307	135.4	37.7	1567.1	9.0	9.1	9.1	9.7	*469*	**428**
Test 2	618.7	304	138.0	38.0	1594.2	8.9	8.7	8.8	9.5	*388*	**355**
Test 3	794.6	306	139.4	38.3	1633.7	8.5	8.4	8.5	9.1	*486*	**446**
Test 4	587.0	304	138.8	37.6	1586.5	8.7	8.8	8.8	9.4	*370*	**338**
Test 5	788.9	307	139.7	38.1	1634.0	9.1	8.7	8.9	9.6	*483*	**441**
Test 6	774.8	307	139.6	38.8	1662.9	9.2	9.2	9.2	9.9	*466*	**424**
10d nail + 1" Insulation											
Test 1	780.4	306	139.4	38.1	1625.2	9.2	9.1	9.2	9.8	*480*	**437**
Test 2	845.0	307	138.8	38.2	1627.8	9.7	9.7	9.7	10.4	*519*	**470**
Test 3	786.9	305	139.3	38.5	1635.7	8.9	8.9	8.9	9.6	*481*	**439**
Test 4	673.6	305	138.9	37.7	1597.1	9.3	9.4	9.4	10.1	*422*	**383**
Test 5	635.7	306	137.2	38.2	1603.8	8.8	8.9	8.9	9.5	*396*	**362**
Test 6	809.2	306	139.6	37.9	1619.0	8.8	9.1	9.0	9.6	*500*	**456**
16d nail + 0" Insulation											
Test 1	716.3	305	134.4	37.4	1533	9.8	9.7	9.8	10.5	*467*	**423**
Test 2	604.1	303	137.6	35.6	1484	8.9	9.3	9.1	9.8	*407*	**371**
Test 3	907.7	307	140.3	38.3	1650	9.2	8.7	9.0	9.6	*550*	**502**
Test 4	684.1	305	139.6	38.3	1631	10.6	10.2	10.4	11.2	*420*	**377**
Test 5	681.5	303	139.3	38.0	1604	10.6	10.5	10.6	11.3	*425*	**382**
Test 6	695.5	305	139.4	38.0	1616	10.4	10.7	10.6	11.3	*430*	**387**
16d nail + 1/4" Insulation											
Test 1	710.8	304	139.6	38.3	1625	10.0	10.2	10.1	10.9	*437*	**394**
Test 2	607.6	305	139.8	38.5	1642	9.7	9.4	9.6	10.3	*370*	**336**
Test 3	672.1	303	140.0	38.6	1637	9.2	9.3	9.3	9.9	*410*	**373**
Test 4	631.4	304	139.6	37.8	1604	10.2	10.2	10.2	11.0	*394*	**355**
Test 5	661.2	305	139.9	38.5	1643	8.7	9.3	9.0	9.7	*402*	**367**
Test 6	706.9	304	139.4	38.4	1627	10.0	10.3	10.2	10.9	*434*	**392**

Test #	Mass (g)	Dimensions (mm)			Vol. (cm^3)	Moisture Content Measurements				Density$_2$	
		Length	Width	Depth		#1	#2	Mean	Adj.$_1$	Actual	Dry
16d nail + 1/2" Insulation											
Test 1	660.6	305	139.4	38.5	1637	9.8	10.0	9.9	10.6	*404*	**365**
Test 2	676.3	305	139.7	38.4	1636	9.8	9.9	9.9	10.6	*413*	**374**
Test 3	726.0	303	139.7	38.0	1609	9.5	10.0	9.8	10.5	*451*	**409**
Test 4	784.4	303	139.8	38.5	1631	9.2	9.2	9.2	9.9	*481*	**438**
Test 5	710.8	304	138.4	37.8	1590	10.5	10.9	10.7	11.5	*447*	**401**
Test 6	767.4	303	139.9	38.1	1615	9.7	10.2	10.0	10.7	*475*	**429**
16d nail + 3/4" Insulation											
Test 1	582.0	305	140.1	38.4	1641	9.6	9.6	9.6	10.3	*355*	**322**
Test 2	579.1	306	139.9	38.5	1648	9.3	8.7	9.0	9.7	*351*	**320**
Test 3	722.7	304	139.9	38.3	1629	9.9	10.7	10.3	11.1	*444*	**399**
Test 4	719.1	303	138.0	37.9	1585	10.6	10.8	10.7	11.5	*454*	**407**
Test 5	711.6	304	139.8	38.3	1628	10.6	10.4	10.5	11.3	*437*	**393**
Test 6	615.9	304	139.5	38.0	1612	10.3	10.1	10.2	11.0	*382*	**344**
16d nail + 1" Insulation											
Test 1	738.7	303	139.1	38.1	1606	11.8	11.5	11.7	12.5	*460*	**409**
Test 2	634.8	304	139.9	38.5	1637	10.1	9.8	10.0	10.7	*388*	**350**
Test 3	696.5	304	141.0	38.6	1655	9.0	8.4	8.7	9.4	*421*	**385**
Test 4	703.6	304	140.7	38.9	1664	9.2	8.9	9.1	9.7	*423*	**385**
Test 5	727.5	304	139.1	38.5	1628	10.8	11.4	11.1	11.9	*447*	**399**
Test 6	703.1	305	140.8	38.9	1671	8.9	9.1	9.0	9.7	*421*	**384**
16d nail + 1.5" Insulation											
Test 1	714.6	304	139.6	38.4	1630	10.6	10.5	10.6	11.3	*439*	**394**
Test 2	671.8	304	139.5	38.3	1624	10.7	10.0	10.4	11.1	*414*	**372**
Test 3	822.8	304	138.8	38.0	1603	11.4	11.3	11.4	12.2	*513*	**457**
Test 4	646.9	304	139.3	38.0	1609	10.5	10.7	10.6	11.4	*402*	**361**
Test 5	787.1	305	138.1	37.4	1575	11.9	11.9	11.9	12.8	*500*	**443**
Test 6	763.7	303	139.9	38.6	1636	9.7	9.8	9.8	10.5	*467*	**422**

Notes: 1 - adjusted for species and recording conditions, 2 - in kg/m^3

Density of Sheathing (OSB)

In this study, two identical panels of 7/16" and three identical panels of 5/8" OSB sheathing were used. Multiple density tests were conducted on specimens of sheathing, however it was found that there was minimal variation in density between identical panels or within the same panel. The following mean recorded density was found for each panel:

- 7/16" OSB panels: 580 kg/m^3
- 5/8" OSB panels: 624 kg/m^3

APPENDIX B: Supplementary Tests and Measurements

Center Point Nail Bending Test

Load Displacement Data:

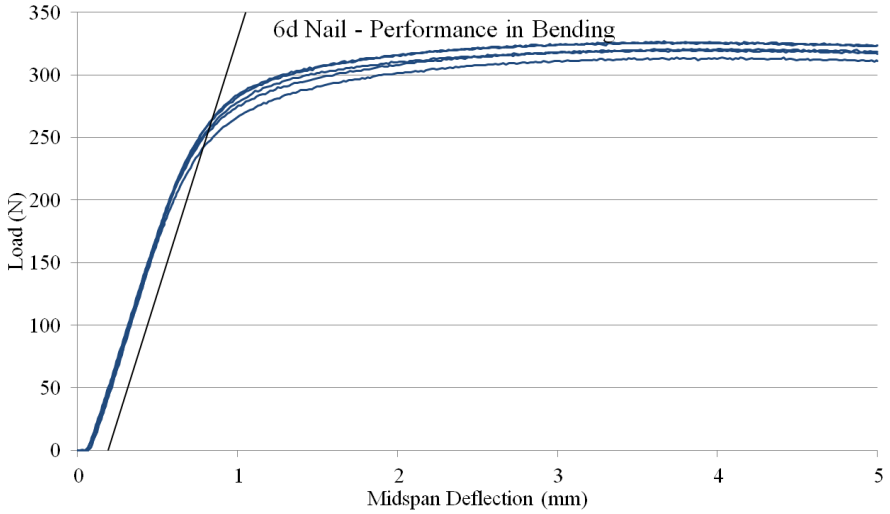

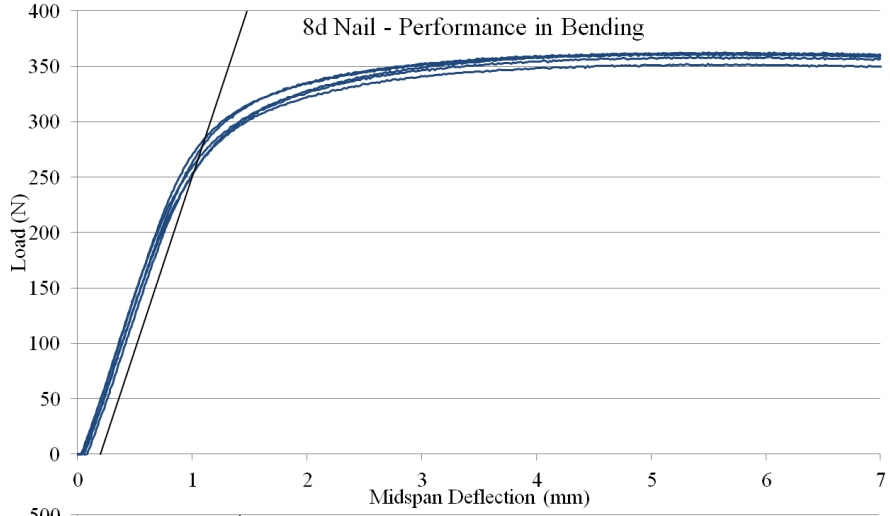

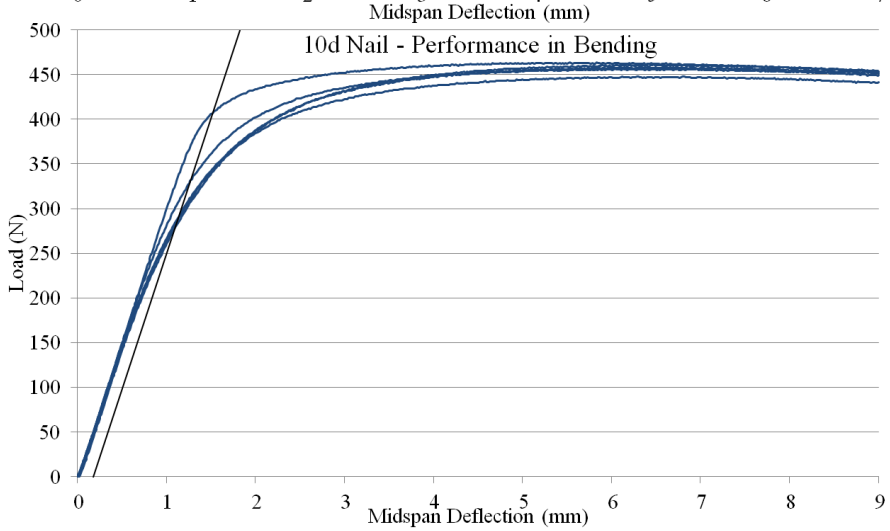

Nail Yield Strength Calculation

Specimen	Yield Load$_1$ (N)	Nail Diameter Measurements (mm)$_2$						Plastic Section Modulus (mm^3)	Moment$_3$ (Nmm)	Yield Strength (MPa)$_4$
		#1	#2	#3	#4	#5	Avg.			
6d Nail										
Nail #1	**254**	2.84	2.84	2.84	2.83	2.83	**2.836**	3.8016	2661	**698**
Nail #2	**264**	2.84	2.84	2.83	2.84	2.83	**2.836**	3.8016	2765	**726**
Nail #3	**242**	2.83	2.84	2.84	2.83	2.83	**2.834**	3.7936	2535	**667**
Nail #4	**258**	2.84	2.84	2.84	2.83	2.83	**2.836**	3.8016	2703	**709**
Nail #5	**265**	2.83	2.84	2.83	2.84	2.84	**2.836**	3.8016	2776	**729**
Mean:	***256.6***						***2.8356***	3.8000	2688	**705.7**
8d Nail										
Nail #1	**254**	3.26	3.22	3.2	3.28	3.24	**3.240**	5.6687	3473	**612**
Nail #2	**284**	3.22	3.26	3.25	3.23	3.25	**3.242**	5.6792	3884	**683**
Nail #3	**266**	3.26	3.22	3.26	3.26	3.23	**3.246**	5.7003	3638	**637**
Nail #4	**254**	3.26	3.24	3.31	3.24	3.23	**3.256**	5.7531	3473	**603**
Nail #5	**278**	3.26	3.25	3.25	3.24	3.26	**3.252**	5.7319	3802	**662**
Mean:	***267.2***						***3.2472***	*5.7066*	*3654*	***639.5***
10d Nail										
Nail #1	**408**	3.74	3.73	3.74	3.71	3.73	**3.730**	8.6492	6763	**781**
Nail #2	**292**	3.74	3.71	3.74	3.72	3.72	**3.726**	8.6214	4840	**561**
Nail #3	**280**	3.75	3.72	3.72	3.74	3.71	**3.728**	8.6353	4641	**537**
Nail #4	**330**	3.72	3.75	3.74	3.74	3.72	**3.734**	8.6770	5470	**630**
Nail #5	**288**	3.74	3.72	3.75	3.74	3.71	**3.732**	8.6631	4774	**551**
Mean:	***319.6***						***3.730***	*8.6492*	*5297*	***611.9***

Notes: 1 - calculated from load-deflection data, using the method described in ASTM - F1575, 2 - evenly spaced measurements along shank length, 3 - maximum moment at mid-span or location of applied load, 4 - bending yield strength

Support spans:

- For 6d nails: 41.9 mm
- For 8d nails: 54.7 mm
- For 10d nails: 66.3 mm

Nail Bearing Tests

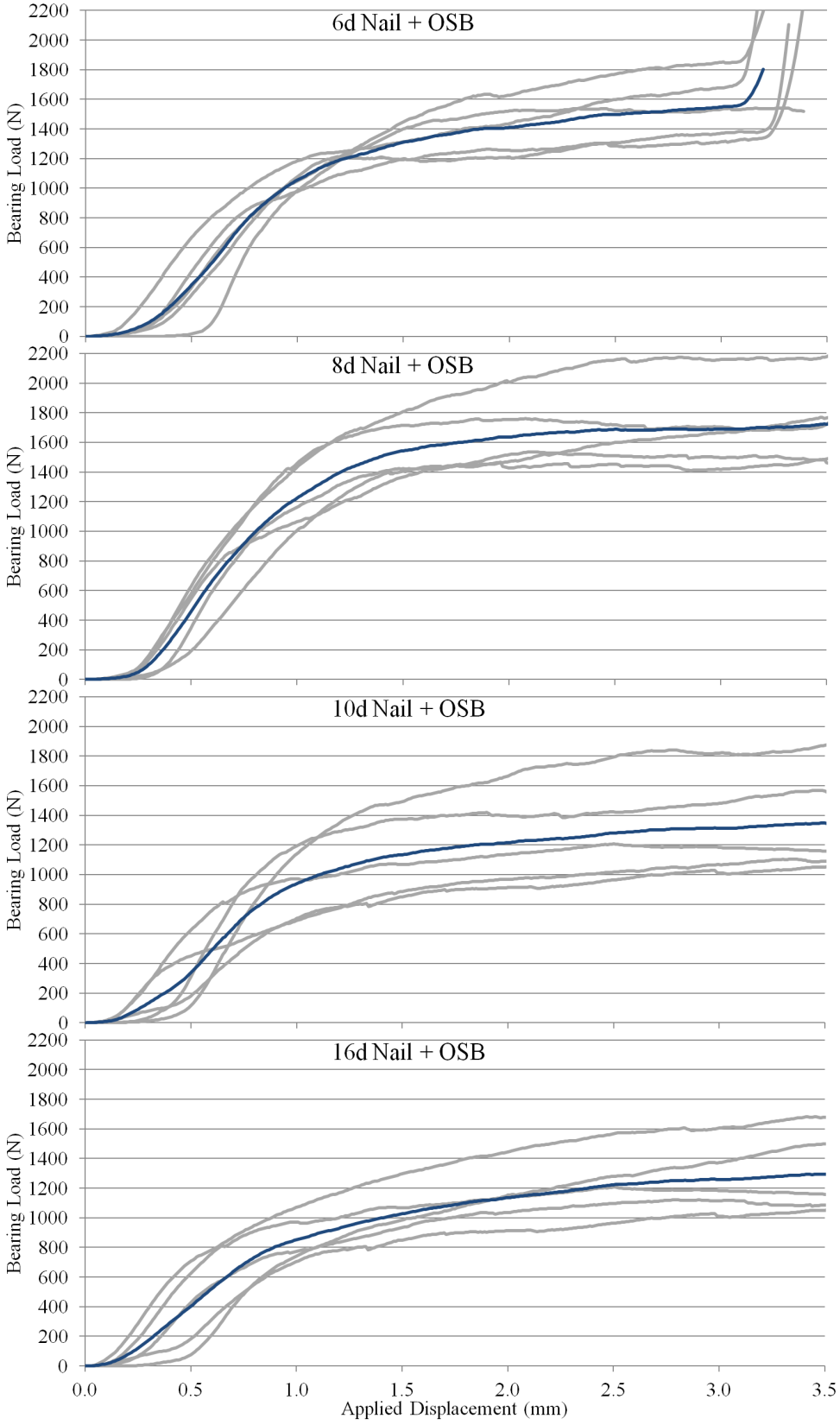

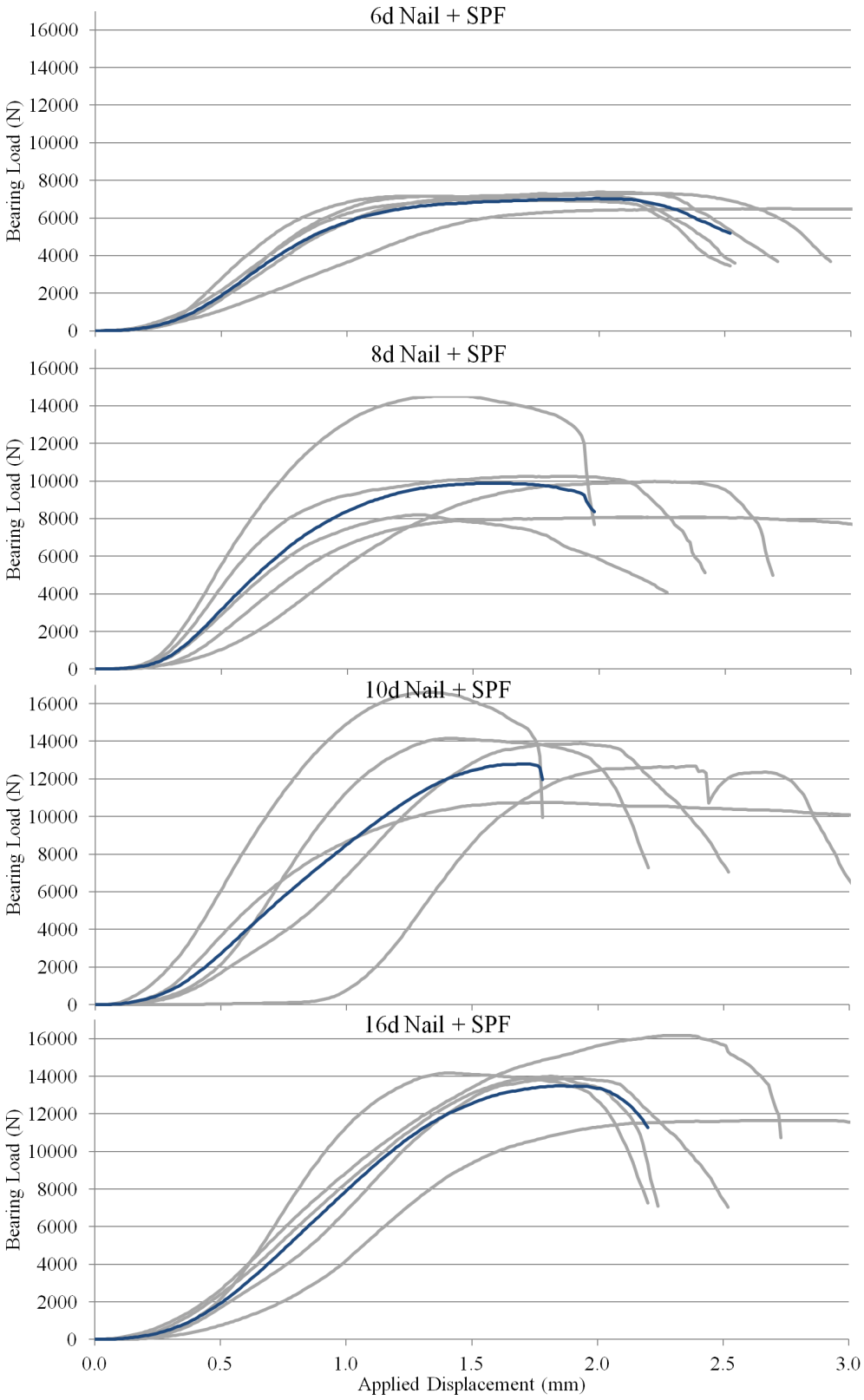

Note: Highlighted lines show mean response

Bearing Yield Strength Calculation:

Parameter	6d nail + OSB					8d nail + OSB				
Test number:	**# 1**	**# 2**	**# 3**	**# 4**	**# 5**	**# 1**	**# 2**	**# 3**	**# 4**	**# 5**
Max. recorded load (N)	1312	1371	1850	1677	1538	2180	1767	1535	1760	1485
Yield Load $(N)_1$	923	1212	1055	1065	1037	1397	1153	987	1617	1359
Stiffness $(N/mm)_2$	2094	1654	1974	2006	3078	2474	2466	2157	1956	1672
Bearing Length $(mm)_3$	15.9	15.9	15.9	15.9	15.9	15.9	15.9	15.9	15.9	15.9
Yield Strength $(MPa)_4$	20.5	26.9	23.4	23.6	23.0	27.2	22.4	19.2	31.4	26.4
Mean Yield Str.(MPa)	23.5					25.3				

Parameter	10d nail + OSB					16d nail + OSB				
Test number:	**# 1**	**# 2**	**# 3**	**# 4**	**# 5**	**# 1**	**# 2**	**# 3**	**# 4**	**# 5**
Max. recorded load (N)	1104	1051	1206	1567	1873	1498	1051	1206	1682	1121
Yield Load $(N)_1$	521	756	912	1203	1330	829	765	924	931	753
Stiffness $(N/mm)_2$	1281	1408	1992	2696	2495	1763	1408	1992	1941	1650
Bearing Length $(mm)_3$	15.9	15.9	15.9	15.9	15.9	15.9	15.9	15.9	15.9	15.9
Yield Strength $(MPa)_4$	9.0	13.0	15.7	20.7	22.9	12.9	11.9	14.3	14.4	11.7
Mean Yield Str.(MPa)	16.2					13.0				

Parameter	6d nail + SPF					8d nail + SPF				
Test number:	**# 1**	**# 2**	**# 3**	**# 4**	**# 5**	**# 1**	**# 2**	**# 3**	**# 4**	**# 5**
Max. recorded (kN)	6.47	7.23	7.30	7.37	6.99	14.51	8.20	8.08	9.97	10.25
Yield Load $(kN)_1$	6.15	6.67	6.68	6.90	6.76	13.07	7.69	7.32	9.15	8.92
Secant Stiff. $(kN/mm)_2$	5.08	12.62	8.60	11.44	8.41	22.99	12.33	11.00	9.68	18.27
Bearing Length $(mm)_3$	50.8	50.8	50.8	50.8	50.8	63.5	63.5	63.5	63.5	63.5
Yield Strength $(MPa)_4$	42.6	46.2	46.3	47.8	46.9	63.3	37.2	35.5	44.3	43.2
Mean Yield Str.	46.0					44.7				

Parameter	10d nail + SPF					16d nail + SPF				
Test number:	**# 1**	**# 2**	**# 3**	**# 4**	**# 5**	**# 1**	**# 2**	**# 3**	**# 4**	**# 5**
Max. recorded (kN)	16.60	13.89	14.17	12.67	10.75	13.99	13.89	14.17	11.65	16.17
Yield Load (kN)$_1$	16.05	13.78	14.06	12.11	8.95	13.83	13.76	14.11	11.38	13.72
Secant Stiff. (kN/mm)$_2$	22.10	9.23	18.56	17.34	14.47	11.84	9.23	18.56	8.56	13.23
Bearing Length (mm)$_3$	66.0	66.7	67.7	66.3	66.6	66.1	66.5	67.1	67.4	67.2
Yield Strength (MPa)$_4$	66.5	56.4	56.7	49.9	36.7	51.5	51.0	51.8	41.6	50.3
Mean Yield Str.	53.3					49.2				

Notes: 1 - yield load as calculated using the method described in Section 5.3, 2 - Stiffness characterized by the linear portion of the load-deformation relationship, or parallel lines defined in ASTM D5764, 3 - contact length between nail and wood surface, 4 - Bearing yield strength

Nail Dimension Measurements

Length Test (20 specimens of each nail size were chosen at random)

Tolerances (ASTM F1667-11a 8.2.1):

- For nails between 1" and 2.5" in length: 1/16" (1.588 mm)
- For nails between 2.5" and 7" in length: 3/32" (2.381 mm)

Nominal lengths:

- For 6d nails: 2" (50.80 mm)
- For 8d nails: 2.5" (63.50 mm)
- For 10d nails: 3" (76.20 mm)

#	6d nails			8d nails			10d nails		
	Recorded Length (mm)	Error (mm)	Pass/ Fail	Recorded Length (mm)	Error (mm)	Pass/ Fail	Recorded Length (mm)	Error (mm)	Pass/ Fail
1	51.90	1.10	Pass	63.48	0.02	Pass	76.43	0.23	Pass
2	51.51	0.71	Pass	63.51	-0.01	Pass	76.59	0.39	Pass
3	51.47	0.67	Pass	63.44	0.06	Pass	77.17	0.97	Pass
4	51.60	0.80	Pass	63.48	0.02	Pass	76.96	0.76	Pass
5	51.51	0.71	Pass	63.34	0.16	Pass	76.91	0.71	Pass
6	51.60	0.80	Pass	63.31	0.19	Pass	76.67	0.47	Pass
7	51.77	0.97	Pass	63.20	0.30	Pass	77.21	1.01	Pass
8	52.06	1.26	Pass	63.54	-0.04	Pass	76.80	0.6	Pass
9	51.67	0.87	Pass	63.45	0.05	Pass	76.84	0.64	Pass
10	51.65	0.85	Pass	63.56	-0.06	Pass	77.28	1.08	Pass
11	51.32	0.52	Pass	63.26	0.24	Pass	77.74	1.54	Pass
12	51.54	0.74	Pass	63.22	0.28	Pass	77.16	0.96	Pass
13	51.78	0.98	Pass	63.38	0.12	Pass	79.59	3.39	*Fail*
14	51.58	0.78	Pass	63.33	0.17	Pass	77.54	1.34	Pass
15	51.51	0.71	Pass	63.40	0.10	Pass	76.76	0.56	Pass
16	51.42	0.62	Pass	63.35	0.15	Pass	76.23	0.03	Pass
17	51.57	0.77	Pass	63.34	0.16	Pass	76.35	0.15	Pass
18	51.50	0.70	Pass	63.41	0.09	Pass	77.12	0.92	Pass
19	51.60	0.80	Pass	63.34	0.16	Pass	77.26	1.06	Pass
20	51.52	0.72	Pass	63.38	0.12	Pass	76.29	0.09	Pass

Shank Diameter Test (10 specimens of each nail size were chosen at random)
Tolerances (ASTM F1667-11a 8.2.1):

- For nails 0.076" in diameter and larger: 0.004" (0.102 mm)

Nominal diameters:

- For 6d nails, diameter: 0.113" (2.87 mm)
- For 8d nails, diameter: 0.131" (3.33 mm)
- For 10d nails, diameter: 0.148" (3.76 mm)

Specimen Number	Shank Diameter Measurements (mm)						Error (mm)	Pass/Fail
	#1	#2	#3	#4	#5	Mean		
6d nails								
1	2.89	2.85	2.85	2.84	2.85	**2.856**	-0.0142	Pass
2	2.83	2.83	2.82	2.85	2.84	**2.834**	-0.0362	Pass
3	2.82	2.83	2.84	2.85	2.84	**2.836**	-0.0342	Pass
4	2.83	2.83	2.83	2.83	2.83	**2.830**	-0.0402	Pass
5	2.84	2.85	2.85	2.84	2.84	**2.844**	-0.0262	Pass
6	2.85	2.84	2.83	2.83	2.84	**2.838**	-0.0322	Pass
7	2.84	2.84	2.84	2.84	2.83	**2.838**	-0.0322	Pass
8	2.85	2.84	2.84	2.85	2.85	**2.846**	-0.0242	Pass
9	2.83	2.84	2.83	2.83	2.84	**2.834**	-0.0362	Pass
10	2.85	2.84	2.83	2.83	2.84	**2.838**	-0.0322	Pass
8d nails								
1	3.21	3.26	3.25	3.25	3.25	**3.244**	-0.0834	Pass
2	3.22	3.26	3.26	3.26	3.26	**3.252**	-0.0754	Pass
3	3.25	3.22	3.22	3.22	3.25	**3.232**	-0.0954	Pass
4	3.25	3.25	3.25	3.24	3.26	**3.250**	-0.0774	Pass
5	3.23	3.26	3.21	3.25	3.23	**3.236**	-0.0914	Pass
6	3.24	3.27	3.25	3.24	3.22	**3.244**	-0.0834	Pass
7	3.27	3.24	3.22	3.28	3.25	**3.252**	-0.0754	Pass
8	3.24	3.25	3.22	3.27	3.26	**3.248**	-0.0794	Pass
9	3.25	3.25	3.26	3.27	3.24	**3.254**	-0.0734	Pass
10	3.25	3.26	3.27	3.22	3.22	**3.244**	-0.0834	Pass
10d nails								
1	3.68	3.70	3.70	3.70	3.72	**3.700**	0.0592	Pass
2	3.72	3.71	3.69	3.69	3.70	**3.702**	0.0572	Pass
3	3.73	3.71	3.70	3.71	3.69	**3.708**	0.0512	Pass
4	3.71	3.71	3.72	3.71	3.72	**3.714**	0.0452	Pass
5	3.70	3.70	3.71	3.70	3.70	**3.702**	0.0572	Pass
6	3.72	3.69	3.72	3.74	3.71	**3.716**	0.0432	Pass
7	3.73	3.73	3.70	3.70	3.70	**3.712**	0.0472	Pass
8	3.70	3.70	3.73	3.73	3.69	**3.710**	0.0492	Pass
9	3.73	3.71	3.70	3.72	3.70	**3.712**	0.0472	Pass
10	3.73	3.70	3.71	3.71	3.71	**3.712**	0.0472	Pass

Head Diameter Test (20 specimens of each nail size were chosen at random)

Tolerances (ASTM F1667-11a 8.2.3.1):

- measured diameter must be within 10% of the nominal head diameter
- of 2 readings, 90 deg. apart, larger reading must be no less than 10% greater than the smaller reading.

Nominal nail head diameters:

- For 6d nails: 0.266" (6.76 mm)
- For 8d nails: 0.281" (7.14 mm)
- For 10d nails: 0.312" (7.92 mm)

For each nail, two measurements were made, 90 deg. apart.

Number	Diameter measurements (mm)		Max. difference between actual diameter and nominal			Difference between min and max diameter measurements		
	# 1	#2	(mm)	(%)	Pass/ Fail	(mm)	(%)	Pass/ Fail
6d nails								
1	6.57	6.42	0.34	4.98	Pass	0.15	2.31	Pass
2	6.40	6.73	0.36	5.27	Pass	0.33	5.03	Pass
3	6.64	6.67	0.12	1.72	Pass	0.03	0.45	Pass
4	6.75	6.65	0.11	1.57	Pass	0.10	1.49	Pass
5	6.77	6.78	0.02	0.35	Pass	0.01	0.15	Pass
6	6.49	6.52	0.27	3.94	Pass	0.03	0.46	Pass
7	6.71	6.45	0.31	4.53	Pass	0.26	3.95	Pass
8	6.40	6.71	0.36	5.27	Pass	0.31	4.73	Pass
9	6.55	6.80	0.21	3.05	Pass	0.25	3.75	Pass
10	6.60	6.71	0.16	2.31	Pass	0.11	1.65	Pass
11	6.71	6.75	0.05	0.69	Pass	0.04	0.59	Pass
12	6.71	6.77	0.05	0.69	Pass	0.06	0.89	Pass
13	6.71	6.81	0.05	0.79	Pass	0.10	1.48	Pass
14	6.69	6.69	0.07	0.98	Pass	0.00	0.00	Pass
15	6.60	6.65	0.16	2.31	Pass	0.05	0.75	Pass
16	6.58	6.64	0.18	2.61	Pass	0.06	0.91	Pass
17	6.83	6.52	0.24	3.50	Pass	0.31	4.64	Pass
18	6.77	6.46	0.30	4.39	Pass	0.31	4.69	Pass
19	6.72	6.50	0.26	3.79	Pass	0.22	3.33	Pass
20	6.63	6.32	0.44	6.46	Pass	0.31	4.79	Pass

Number	Diameter measurements (mm)		Max. difference between actual diameter and nominal			Difference between min and max diameter measurements		
	# 1	#2	(mm)	(%)	Pass/ Fail	(mm)	(%)	Pass/ Fail
8d nails								
1	7.15	7.26	0.12	1.81	Pass	0.11	1.53	Pass
2	7.17	7.22	0.08	1.22	Pass	0.05	0.69	Pass
3	7.14	7.25	0.11	1.67	Pass	0.11	1.53	Pass
4	7.26	7.22	0.12	1.81	Pass	0.04	0.55	Pass
5	7.19	7.11	0.05	0.78	Pass	0.08	1.12	Pass
6	7.15	7.05	0.09	1.29	Pass	0.10	1.41	Pass
7	7.26	7.26	0.12	1.81	Pass	0.00	0.00	Pass
8	7.26	7.10	0.12	1.81	Pass	0.16	2.23	Pass
9	7.12	7.08	0.06	0.85	Pass	0.04	0.56	Pass
10	7.20	7.28	0.14	2.11	Pass	0.08	1.10	Pass
11	7.29	7.34	0.20	3.00	Pass	0.05	0.68	Pass
12	7.17	7.12	0.03	0.48	Pass	0.05	0.70	Pass
13	7.20	7.15	0.06	0.93	Pass	0.05	0.70	Pass
14	7.26	7.18	0.12	1.81	Pass	0.08	1.11	Pass
15	7.23	7.23	0.09	1.37	Pass	0.00	0.00	Pass
16	7.23	7.06	0.09	1.37	Pass	0.17	2.38	Pass
17	7.14	7.19	0.05	0.78	Pass	0.05	0.70	Pass
18	7.15	7.24	0.10	1.52	Pass	0.09	1.25	Pass
19	6.91	7.07	0.23	3.37	Pass	0.16	2.29	Pass
20	7.12	7.09	0.05	0.70	Pass	0.03	0.42	Pass
10d nails								
1	7.81	7.88	0.11	1.70	Pass	0.07	0.89	Pass
2	7.87	7.84	0.08	1.26	Pass	0.03	0.38	Pass
3	7.88	7.93	0.04	0.66	Pass	0.05	0.63	Pass
4	7.82	7.87	0.10	1.55	Pass	0.05	0.64	Pass
5	7.82	7.93	0.10	1.55	Pass	0.11	1.40	Pass
6	7.88	7.96	0.04	0.66	Pass	0.08	1.01	Pass
7	7.93	7.71	0.21	3.18	Pass	0.22	2.81	Pass
8	7.84	7.82	0.10	1.55	Pass	0.02	0.26	Pass
9	7.94	7.72	0.20	3.03	Pass	0.22	2.81	Pass
10	7.84	7.86	0.08	1.26	Pass	0.02	0.25	Pass
11	7.87	7.83	0.09	1.40	Pass	0.04	0.51	Pass
12	7.82	7.84	0.10	1.55	Pass	0.02	0.26	Pass
13	7.84	7.82	0.10	1.55	Pass	0.02	0.26	Pass
14	7.78	7.90	0.14	2.14	Pass	0.12	1.53	Pass
15	7.73	7.95	0.19	2.88	Pass	0.22	2.81	Pass
16	7.76	7.92	0.16	2.44	Pass	0.16	2.04	Pass
17	7.86	7.82	0.10	1.55	Pass	0.04	0.51	Pass
18	7.82	7.78	0.14	2.14	Pass	0.04	0.51	Pass
19	7.76	7.85	0.16	2.44	Pass	0.09	1.15	Pass
20	7.80	7.96	0.12	1.85	Pass	0.16	2.03	Pass

APPENDIX C: Experimental data for specimens with GWB

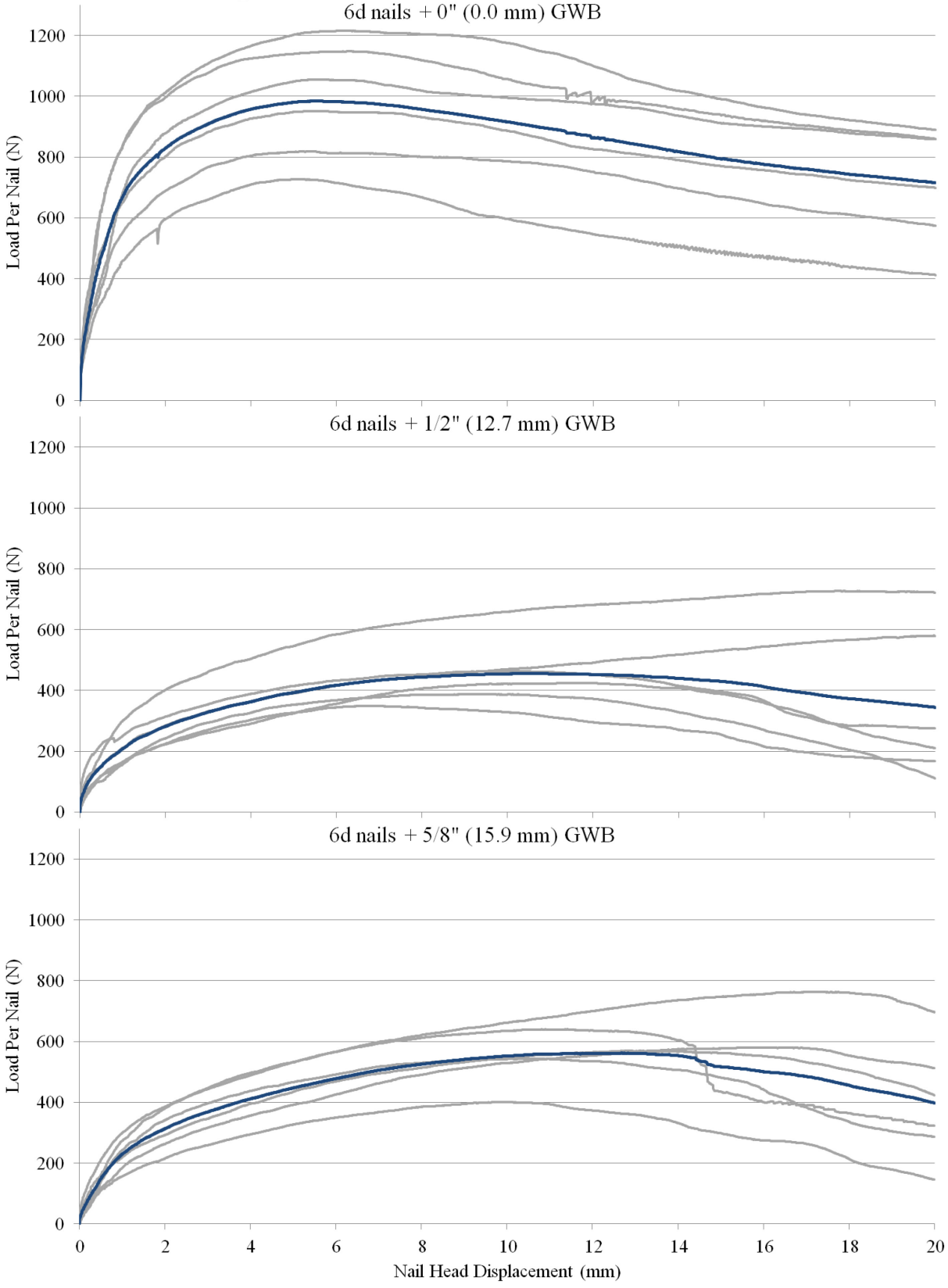

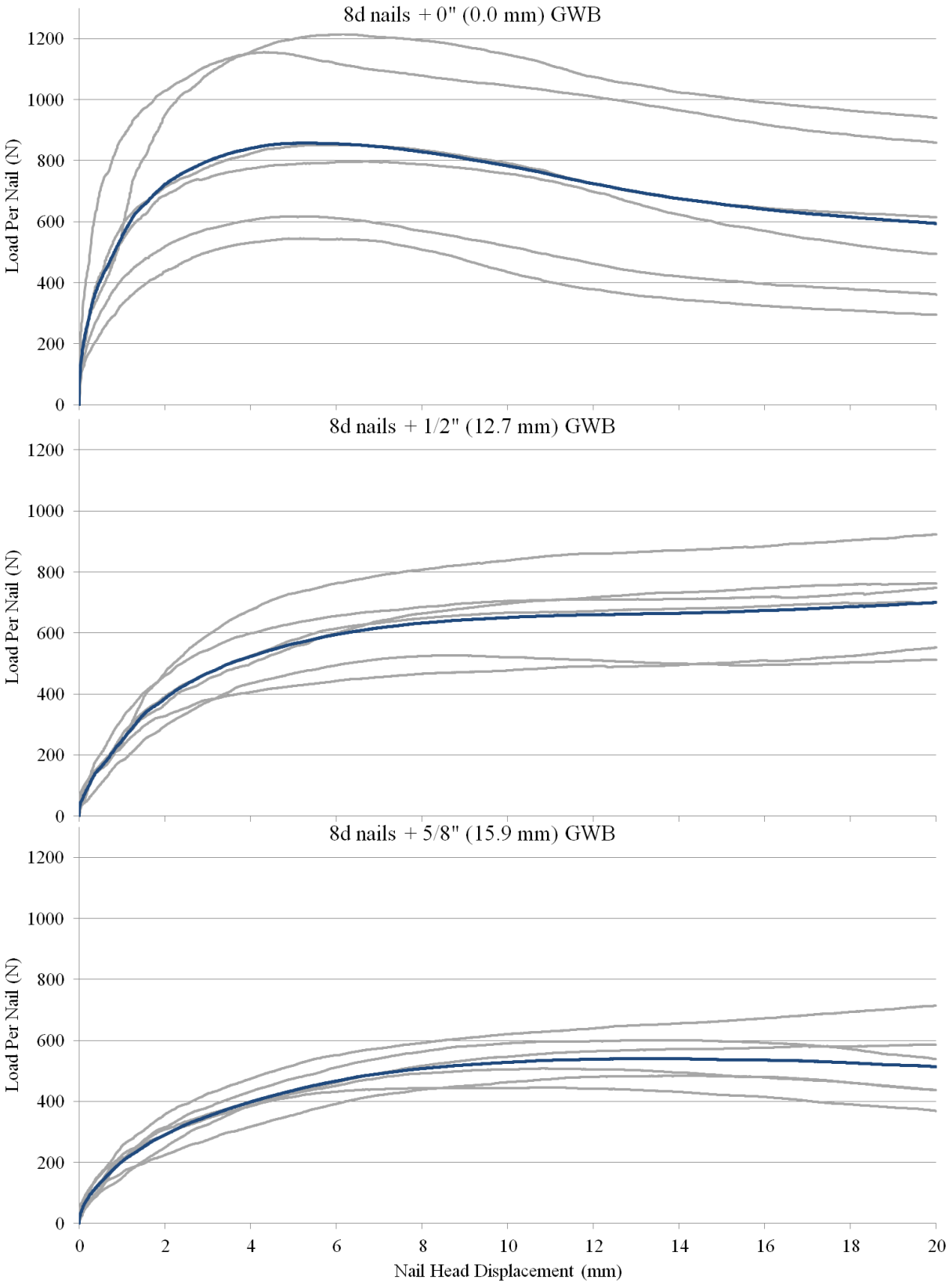
8d nails + 0" (0.0 mm) GWB
8d nails + 1/2" (12.7 mm) GWB
8d nails + 5/8" (15.9 mm) GWB
Load Per Nail (N)
0
200
400
600
800
1000
1200
0
2
4
6
8
10
12
14
16
18
20
Nail Head Displacement (mm)

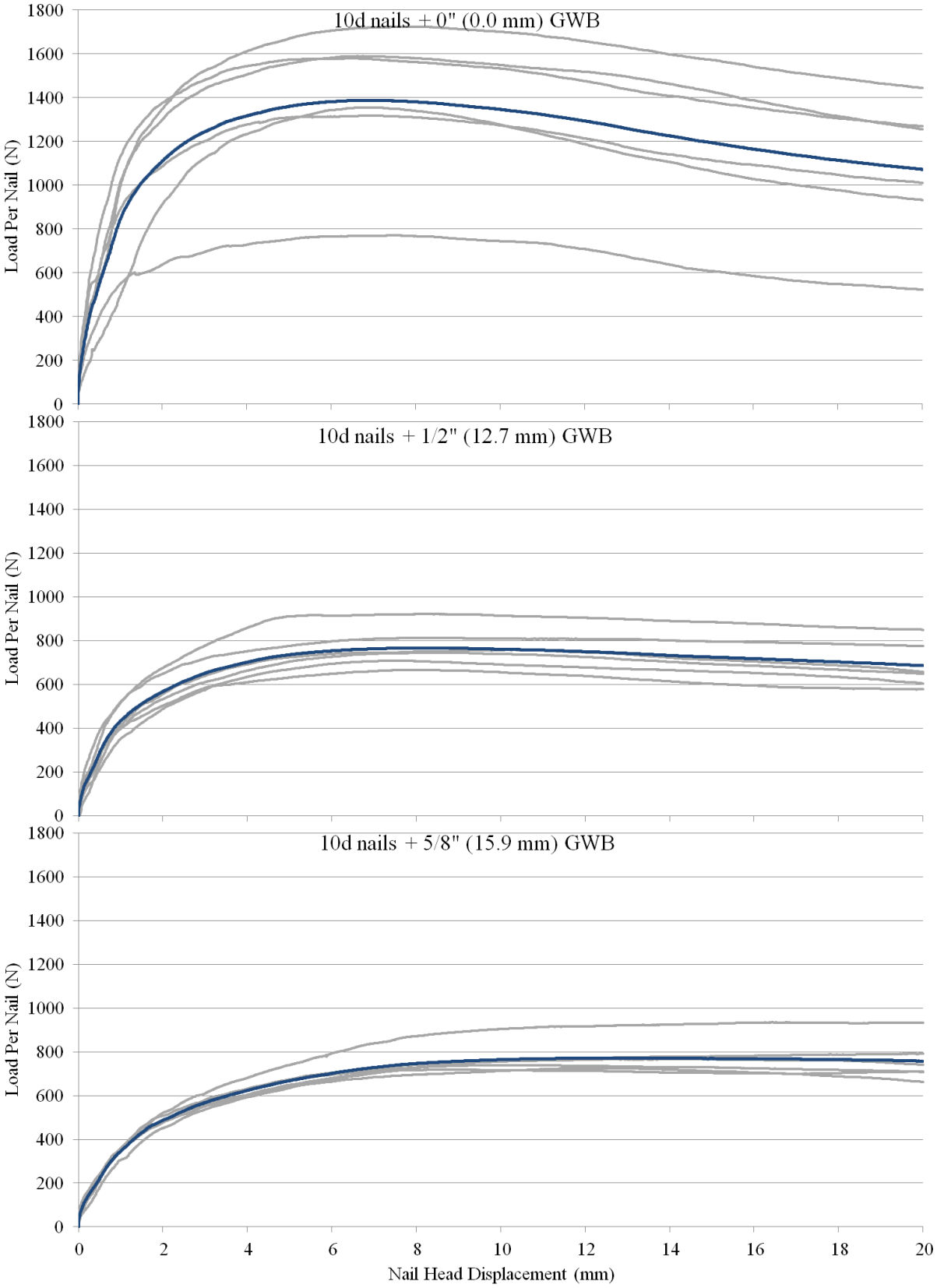

Note: Highlighted lines show mean response

Yield Point Calculation for Tests With GWB

K&C Method

Nail size + GWB thickness	GWB (mm)	Test 1	Test 2	Test 3	Test 4	Test 5	Test 6	Mean	St. Dev.
Yield Strength (N)									
6d + 0	*0.0*	573.8	527.4	607.9	363.2	409.0	475.5	**492.8**	95.0
6d + 1/2"	*12.7*	231.5	212.2	290.0	174.7	193.9	363.4	**244.3**	70.5
6d + 5/8"	*15.9*	319.9	284.6	200.3	290.0	381.8	271.5	**291.3**	59.5
8d + 0	*0.0*	308.6	577.7	425.6	607.2	272.4	398.7	**431.7**	136.9
8d + 1/2"	*12.7*	461.5	276.1	374.0	263.4	351.2	381.6	**351.3**	73.4
8d + 5/8"	*15.9*	242.2	254.1	300.6	222.8	357.2	293.4	**278.4**	48.8
10d + 0	*0.0*	385.3	789.5	677.5	862.3	794.7	659.3	**694.8**	169.9
10d + 0	*12.7*	333.0	378.8	372.6	406.3	354.2	460.7	**384.3**	44.8
10d + 5/8"	*15.9*	383.2	362.7	369.7	359.1	467.3	395.4	**389.6**	40.4
Secant Stiffness (N/mm)									
6d + 0	*0.0*	1309.7	727.4	1306.3	565.7	685.7	1085.9	**946.8**	329.2
6d + 1/2"	*12.7*	406.0	119.4	137.2	156.9	146.2	229.1	**199.1**	108.1
6d + 5/8"	*15.9*	269.5	153.8	118.4	117.0	189.0	214.8	**177.1**	59.5
8d + 0	*0.0*	588.2	1823.0	850.4	573.6	400.2	892.3	**854.6**	509.0
8d + 1/2"	*12.7*	235.9	202.5	281.4	158.2	220.4	180.2	**213.1**	43.5
8d + 5/8"	*15.9*	103.8	185.4	169.7	196.6	178.3	116.9	**158.5**	38.5
10d + 0	*0.0*	804.8	1577.0	489.9	989.9	1089.5	1188.3	**1023.2**	366.5
10d + 0	*12.7*	496.2	443.9	431.1	652.7	348.5	600.0	**495.4**	113.2
10d + 5/8"	*15.9*	335.9	354.7	328.0	355.2	292.8	256.0	**320.4**	39.0

CEN Method

Nail size + GWB thickness	GWB (mm)	Test 1	Test 2	Test 3	Test 4	Test 5	Test 6	Mean	St. Dev.
Yield Strength (N)									
6d + 0	*0.0*	781.8	795.2	749.6	458.4	560.6	564.3	**651.7**	141.7
6d + 1/2"	*12.7*	210.4	284.3	311.9	239.1	277.6	388.6	**285.3**	61.9
6d + 5/8"	*15.9*	354.4	349.6	257.2	377.8	418.1	337.0	**349.0**	53.3
8d + 0	*0.0*	369.5	721.9	532.3	1018.1	363.5	454.4	**576.6**	253.5
8d + 1/2"	*12.7*	659.0	338.6	490.6	407.9	464.4	484.5	**474.2**	107.1
8d + 5/8"	*15.9*	352.1	314.1	410.4	280.2	434.6	440.9	**372.1**	66.8
10d + 0	*0.0*	493.4	1049.7	1129.1	1334.1	1157.9	750.6	**985.8**	307.7
10d + 0	*12.7*	426.2	492.9	467.5	539.5	496.5	531.1	**492.3**	41.8
10d+5/8"	*15.9*	488.8	456.7	503.4	440.2	589.3	510.2	**498.1**	52.2
Secant Stiffness (N/mm)									
6d + 0	*0.0*	1294.5	687.0	1391.3	705.6	727.0	1237.1	**1007.1**	333.1
6d + 1/2"	*12.7*	652.3	139.3	179.3	170.7	161.5	297.3	**266.7**	196.9
6d + 5/8"	*15.9*	328.2	194.4	144.3	141.7	233.7	248.0	**215.1**	70.8
8d + 0	*0.0*	720.3	1803.4	985.7	500.2	447.8	1087.0	**924.1**	500.3
8d + 1/2"	*12.7*	229.5	210.9	307.2	159.6	245.4	214.3	**227.8**	48.4
8d + 5/8"	*15.9*	118.5	215.6	181.3	255.8	205.8	117.3	**182.4**	55.4
10d + 0	*0.0*	926.1	1747.8	453.2	870.4	1077.3	1740.5	**1135.9**	514.6
10d + 0	*12.7*	514.8	497.9	455.0	644.5	357.9	763.4	**538.9**	143.9
10d+5/8"	*15.9*	381.6	388.0	345.1	395.1	322.2	265.1	**349.5**	50.0

CSIRO Method

Nail size + GWB thickness	GWB (mm)	Test 1	Test 2	Test 3	Test 4	Test 5	Test 6	Mean	St. Dev.
Yield Strength (N)									
6d + 0	*0.0*	537.0	495.0	570.8	316.3	375.4	437.0	**455.2**	97.6
6d + 1/2"	*12.7*	194.2	196.1	255.6	158.0	172.3	322.4	**216.4**	61.7
6d + 5/8"	*15.9*	286.5	252.5	179.0	259.1	345.6	246.8	**261.6**	54.4
8d + 0	*0.0*	274.4	540.3	388.4	604.9	244.7	362.6	**402.6**	143.6
8d + 1/2"	*12.7*	436.5	258.3	344.2	255.1	321.4	338.0	**325.6**	66.8
8d + 5/8"	*15.9*	214.3	234.7	278.1	196.9	318.7	275.7	**253.1**	45.7
10d + 0	*0.0*	340.3	705.1	678.0	888.8	762.8	556.7	**655.3**	188.7
10d + 0	*12.7*	306.3	345.6	357.4	388.1	330.9	408.4	**356.1**	37.4
10d + 5/8"	*15.9*	340.3	330.1	343.0	331.4	428.6	375.8	**358.2**	38.3
Secant Stiffness (N/mm)									
6d + 0	*0.0*	1333.6	724.5	1383.8	671.3	736.4	1232.0	**1013.6**	336.1
6d + 1/2"	*12.7*	566.7	139.5	169.8	168.6	158.8	273.3	**246.1**	163.9
6d + 5/8"	*15.9*	314.5	186.1	135.7	134.5	217.5	235.4	**204.0**	68.1
8d + 0	*0.0*	685.2	1867.5	995.7	572.5	448.5	1045.8	**935.9**	513.0
8d + 1/2"	*12.7*	240.8	213.7	303.6	163.3	237.7	200.4	**226.6**	47.2
8d + 5/8"	*15.9*	118.5	213.4	178.0	249.6	195.0	119.6	**179.0**	52.2
10d + 0	*0.0*	893.6	1683.3	490.1	996.4	1132.1	1545.7	**1123.5**	438.6
10d + 0	*12.7*	528.2	483.4	440.4	659.0	363.3	722.6	**532.8**	135.4
10d + 5/8"	*15.9*	372.1	388.9	354.7	388.9	312.9	264.7	**347.0**	49.3

Y&K Method

Nail size + GWB thickness	GWB (mm)	Test 1	Test 2	Test 3	Test 4	Test 5	Test 6	Mean	St. Dev.
Yield Strength (N)									
6d + 0	*0.0*	713.7	714.8	721.9	397.5	493.7	542.0	**597.3**	139.0
6d + 1/2"	*12.7*	236.0	202.9	323.5	179.5	211.7	396.9	**258.4**	84.1
6d + 5/8"	*15.9*	330.7	290.3	201.1	281.7	413.5	302.9	**303.4**	69.2
8d + 0	*0.0*	339.2	691.2	507.6	873.9	291.1	426.5	**521.6**	223.0
8d + 1/2"	*12.7*	597.4	360.7	456.1	299.9	381.4	404.9	**416.7**	102.3
8d + 5/8"	*15.9*	238.8	275.2	315.3	225.3	427.5	331.3	**302.2**	74.0
10d + 0	*0.0*	486.0	955.2	901.4	1173.9	1017.9	751.5	**881.0**	238.0
10d + 0	*12.7*	372.5	428.2	423.4	497.3	389.0	487.1	**432.9**	50.5
10d+5/8"	*15.9*	440.7	421.0	411.7	410.8	501.0	457.2	**440.4**	34.7
Secant Stiffness (N/mm)									
6d + 0	*0.0*	1101.1	657.5	1054.3	524.9	653.4	843.3	**805.7**	234.3
6d + 1/2"	*12.7*	376.4	128.0	114.4	153.0	136.4	204.9	**185.5**	98.6
6d + 5/8"	*15.9*	257.3	147.6	117.7	121.2	168.2	193.1	**167.5**	52.4
8d + 0	*0.0*	517.7	1452.5	712.8	504.2	359.7	758.3	**717.6**	388.7
8d + 1/2"	*12.7*	195.9	138.0	231.6	146.4	199.5	173.1	**180.8**	35.3
8d + 5/8"	*15.9*	105.0	174.6	157.5	195.0	140.1	106.5	**146.5**	36.4
10d + 0	*0.0*	646.8	1290.4	457.7	860.4	1001.7	1021.5	**879.7**	295.4
10d + 0	*12.7*	460.3	396.5	369.7	538.5	303.5	563.5	**438.7**	100.8
10d+5/8"	*15.9*	304.0	298.1	291.9	307.1	269.9	218.9	**281.6**	33.5

5% Diameter Method

Nail size + GWB thickness	GWB (mm)	Test 1	Test 2	Test 3	Test 4	Test 5	Test 6	Mean	St. Dev.
Yield Strength (N)									
6d + 0	*0.0*	736.9	733.4	717.3	1067.4	513.7	512.1	**713.5**	203.3
6d + 1/2"	*12.7*	224.1	199.7	255.9	441.1	181.4	334.0	**272.7**	98.4
6d + 5/8"	*15.9*	303.8	256.9	184.0	257.4	348.6	269.4	**270.0**	54.9
8d + 0	*0.0*	325.5	726.2	473.6	853.7	284.9	423.8	**514.6**	227.3
8d + 1/2"	*12.7*	484.7	283.4	370.9	275.5	338.4	336.8	**348.3**	76.0
8d + 5/8"	*15.9*	213.2	244.8	295.1	211.1	320.8	285.6	**261.7**	45.6
10d + 0	*0.0*	441.0	909.0	934.5	1205.3	1045.1	620.6	**859.2**	280.8
10d + 0	*12.7*	381.1	402.0	408.9	487.0	371.0	453.8	**417.3**	44.6
10d+5/8"	*15.9*	364.7	366.6	375.4	367.1	458.8	416.7	**391.5**	38.4
Secant Stiffness (N/mm)									
6d + 0	*0.0*	1052.6	647.6	1072.3	681.0	624.2	907.4	**830.8**	205.9
6d + 1/2"	*12.7*	435.2	132.5	169.2	173.1	151.4	263.6	**220.8**	114.3
6d + 5/8"	*15.9*	290.1	182.5	132.0	136.0	213.4	220.2	**195.7**	59.4
8d + 0	*0.0*	537.1	1329.8	767.5	511.6	378.0	767.9	**715.3**	337.7
8d + 1/2"	*12.7*	232.4	199.1	283.8	151.6	227.8	201.4	**216.0**	43.9
8d + 5/8"	*15.9*	120.1	196.9	171.9	226.9	194.3	117.7	**171.3**	44.2
10d + 0	*0.0*	713.7	1364.3	446.6	843.4	977.4	1189.9	**922.6**	330.5
10d + 0	*12.7*	450.3	427.0	380.8	548.3	326.3	612.9	**457.6**	106.3
10d+5/8"	*15.9*	346.0	352.1	322.0	348.5	300.3	248.2	**319.5**	40.2

Curve Fitting Parameters for Tests With GWB

3-Parameter Exponential Model

Nail size + GWB Thickness	Parameter	Test 1	Test 2	Test 3	Test 4	Test 5	Test 6	Mean
6d Nail 0" (0.00mm)	k_1	-32.3	-32.4	-48.5	-48.4	-37.5	-44.6	**-40.6**
	k_0	1864	1152	1827	937	1103	1513	**1399**
	p_1	974	886	954	510	644	732	**783**
	R-square	*0.990*	*0.994*	*0.995*	*0.988*	*0.990*	*0.986*	***0.990***
6d Nail 1/2" (12.70mm)	k_1	-19.6	-17.9	-12.9	-24.3	-9.3	-13.1	**-16.2**
	k_0	657	200	286	274	222	355	**332**
	p_1	298	246	337	201	312	515	**318**
	R-square	*0.945*	*0.984*	*0.990*	*0.991*	*0.990*	*0.988*	***0.981***
6d Nail 5/8" (15.88mm)	k_1	-25.2	-18.9	-18.2	-13.6	-18.9	-15.1	**-18.3**
	k_0	462	272	207	185	332	318	**296**
	p_1	398	351	234	384	465	401	**372**
	R-square	*0.985*	*0.984*	*0.993*	*0.989*	*0.996*	*0.996*	***0.991***
8d Nail 0" (0.00mm)	k_1	-40.0	-78.0	-33.5	4.8	-34.3	-21.6	**-33.8**
	k_0	939	2717	1275	852	641	1125	**1258**
	p_1	444	859	672	1264	388	675	**717**
	R-square	*0.987*	*0.984*	*0.987*	*0.990*	*0.980*	*0.977*	***0.984***
8d Nail 1/2" (12.70mm)	k_1	-6.9	-6.9	-4.6	-3.8	-4.2	-7.8	**-5.7**
	k_0	347	328	398	218	297	253	**307**
	p_1	778	403	648	512	622	622	**598**
	R-square	*0.998*	*0.993*	*0.995*	*0.999*	*0.995*	*0.993*	***0.995***
8d Nail 5/8" (15.88mm)	k_1	-9.7	-16.4	-10.7	-5.8	-10.2	-1.1	**-9.0**
	k_0	162	296	232	276	281	161	**235**
	p_1	364	350	479	393	513	566	**444**
	R-square	*0.98*	*0.992*	*0.994*	*0.974*	*0.994*	*0.998*	***0.989***
10d Nail 0" (0.00mm)	k_1	-23.3	-36.8	69.9	-25.0	-34.3	-37.4	**-14.5**
	k_0	1206	2235	654	1468	1637	1715	**1486**
	p_1	623	1376	1969	1550	1380	1097	**1332**
	R-square	*0.985*	*0.993*	*0.997*	*0.996*	*0.998*	*0.985*	***0.992***
10d Nail 1/2" (12.70mm)	k_1	-22.1	-8.9	-19.5	-17.2	-22.0	-24.6	**-19.0**
	k_0	726	595	572	893	486	825	**683**
	p_1	513	678	600	683	562	754	**632**
	R-square	*0.98*	*0.994*	*0.996*	*0.996*	*0.996*	*0.974*	***0.989***
10d Nail 5/8" (15.88mm)	k_1	-8.8	-13.5	-18.4	-32.8	-9.9	-5.7	**-14.9**
	k_0	464	512	478	587	387	338	**461**
	p_1	658	576	579	472	791	692	**628**
	R-square	*0.990*	*0.989*	*0.990*	*0.993*	*0.990*	*0.992*	***0.990***

Asymptotic Model

Nail size + GWB Thickness	Parameter	Test 1	Test 2	Test 3	Test 4	Test 5	Test 6	Mean
6d Nail 0" (0.00mm)	*a*	1131	1045	1189	734	817	942	**976**
	b	956	959	1017	618	701	763	**836**
	c	0.325	0.411	0.374	0.468	0.405	0.399	**0.397**
	R-square	*0.990*	*0.994*	*0.984*	*0.995*	*0.994*	*0.989*	***0.991***
6d Nail 1/2" (12.70mm)	*a*	472	460	577	370	397	711	**498**
	b	321	396	427	319	351	575	**398**
	c	0.705	0.793	0.857	0.670	0.663	0.770	**0.743**
	R-square	*0.988*	*0.991*	*0.977*	*0.995*	*0.999*	*0.985*	***0.989***
6d Nail 5/8" (15.88mm)	*a*	652	591	421	607	760	544	**596**
	b	521	491	368	531	630	489	**505**
	c	0.732	0.790	0.755	0.827	0.814	0.665	**0.764**
	R-square	*0.988*	*0.994*	*0.993*	*0.994*	*0.980*	*0.991*	***0.990***
8d Nail 0" (0.00mm)	*a*	616	1135	844	1252	560	792	**867**
	b	508	880	685	1181	466	644	**727**
	c	0.420	0.303	0.412	0.531	0.508	0.398	**0.429**
	R-square	*0.992*	*0.985*	*0.989*	*0.993*	*0.997*	*0.993*	***0.992***
8d Nail 1/2" (12.70mm)	*a*	887	507	716	553	688	757	**685**
	b	831	397	630	538	621	673	**615**
	c	0.723	0.714	0.653	0.691	0.705	0.781	**0.711**
	R-square	*0.993*	*0.965*	*0.993*	*1.000*	*0.997*	*0.996*	***0.991***
8d Nail 5/8" (15.88mm)	*a*	514	515	615	453	683	589	**561**
	b	442	443	564	380	572	561	**494**
	c	0.808	0.706	0.746	0.645	0.782	0.776	**0.744**
	R-square	*0.997*	*0.992*	*0.996*	*0.996*	*0.987*	*1.000*	***0.995***
10d Nail 0" (0.00mm)	*a*	756	1563	1418	1716	1567	1311	**1389**
	b	601	1369	1443	1606	1472	1097	**1265**
	c	0.404	0.344	0.603	0.480	0.414	0.423	**0.445**
	R-square	*0.980*	*0.994*	*0.996*	*0.996*	*0.996*	*0.990*	***0.992***
10d Nail 1/2" (12.70mm)	*a*	658	752	739	797	719	936	**767**
	b	528	679	694	705	657	774	**673**
	c	0.526	0.528	0.543	0.443	0.592	0.566	**0.533**
	R-square	*0.993*	*0.996*	*0.990*	*0.989*	*0.998*	*0.992*	***0.993***
10d Nail 5/8" (15.88mm)	*a*	761	715	743	724	935	783	**777**
	b	655	589	641	608	827	695	**669**
	c	0.647	0.640	0.643	0.644	0.732	0.719	**0.671**
	R-square	*0.994*	*0.993*	*0.998*	*0.989*	*0.994*	*0.994*	***0.994***

APPENDIX D: Experimental data for specimens with insulation

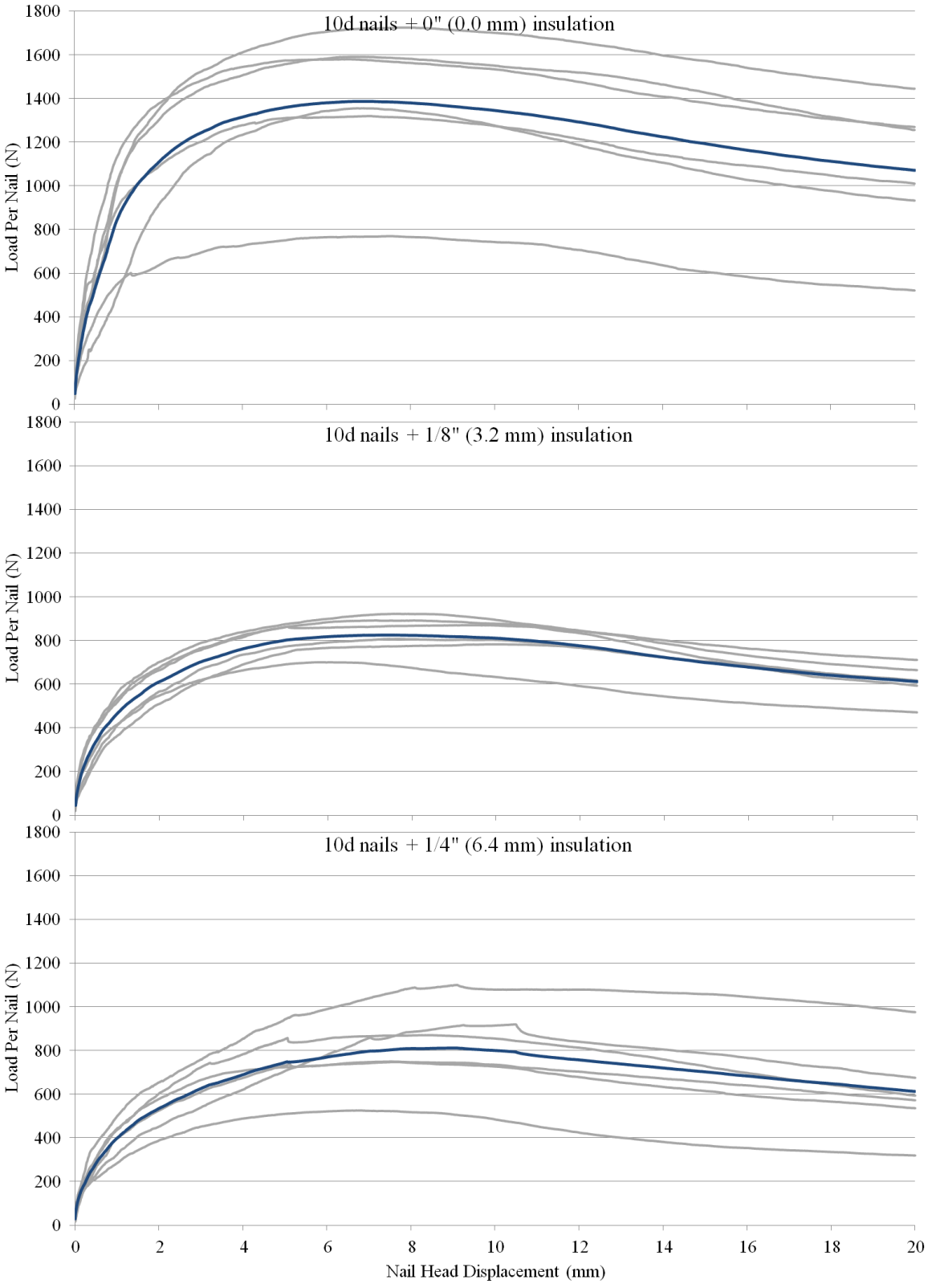

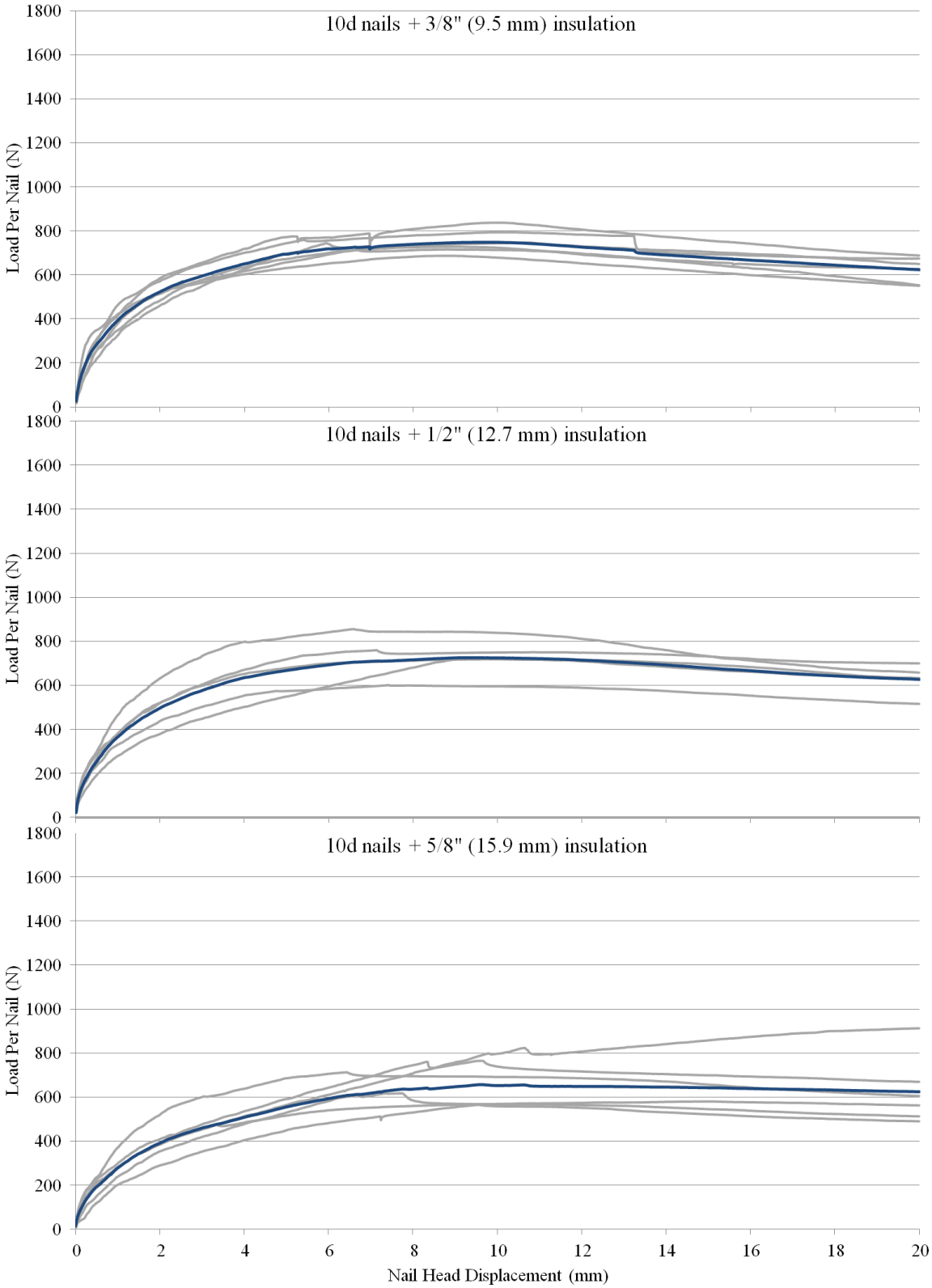
10d nails + 3/8" (9.5 mm) insulation
10d nails + 1/2" (12.7 mm) insulation
10d nails + 5/8" (15.9 mm) insulation
Load Per Nail (N)
0
200
400
600
800
1000
1200
1400
1600
1800
0
2
4
6
8
10
12
14
16
18
20
Nail Head Displacement (mm)

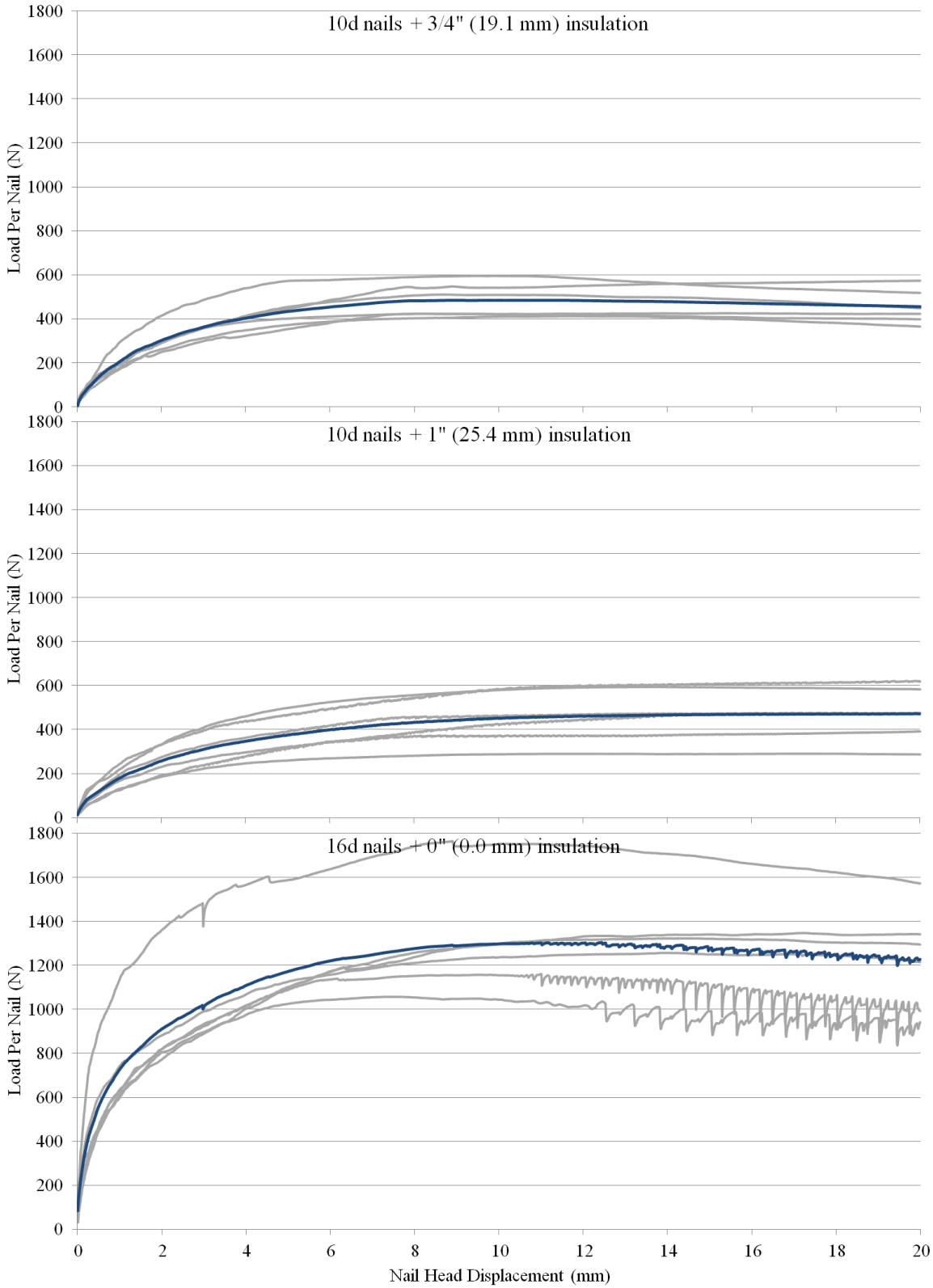
10d nails + 3/4" (19.1 mm) insulation
10d nails + 1" (25.4 mm) insulation
16d nails + 0" (0.0 mm) insulation
Load Per Nail (N)
0
200
400
600
800
1000
1200
1400
1600
1800
0
2
4
6
8
10
12
14
16
18
20
Nail Head Displacement (mm)

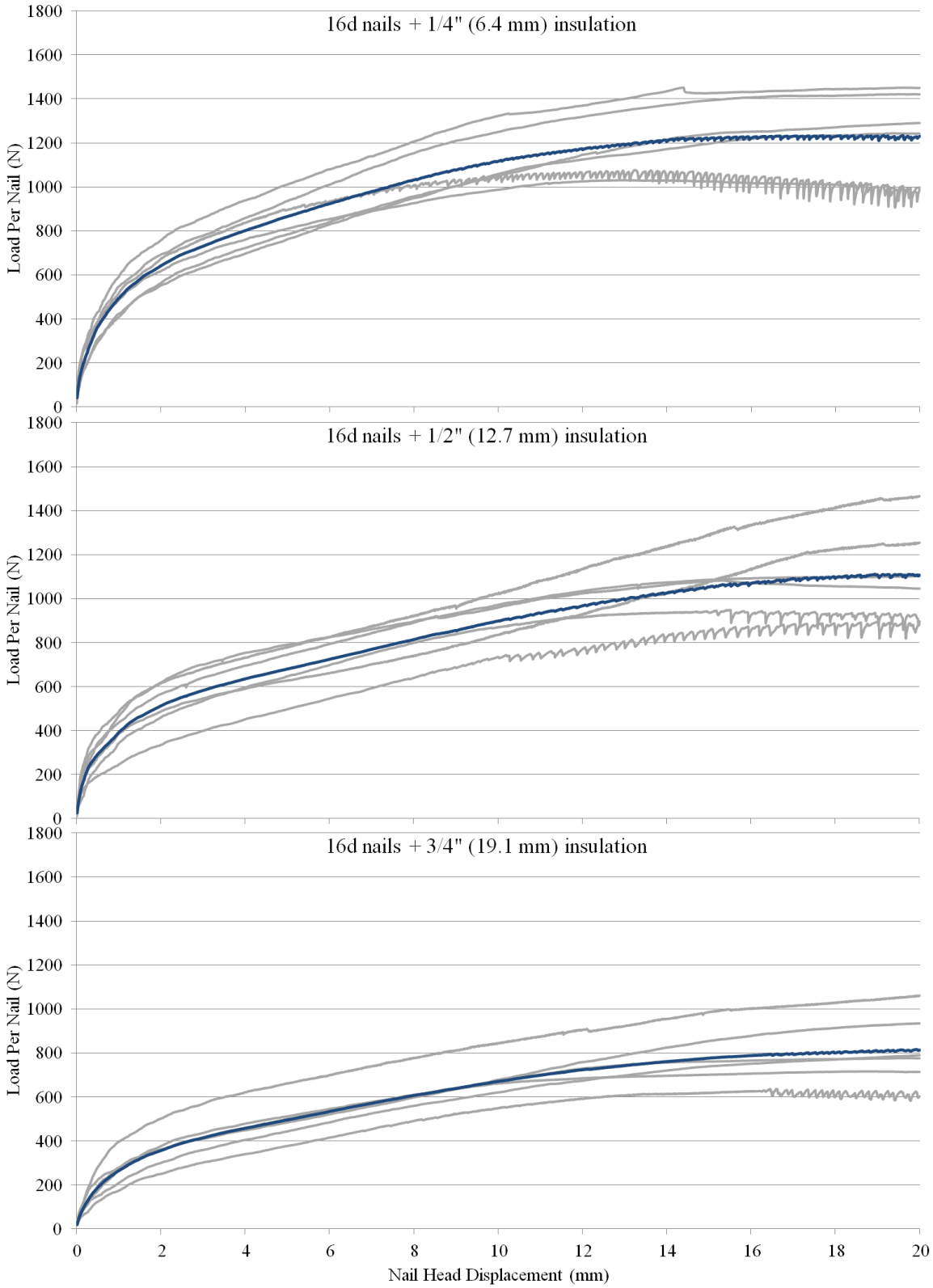
16d nails + 1/4" (6.4 mm) insulation
16d nails + 1/2" (12.7 mm) insulation
16d nails + 3/4" (19.1 mm) insulation
Load Per Nail (N)
0
200
400
600
800
1000
1200
1400
1600
1800
0
2
4
6
8
10
12
14
16
18
20
Nail Head Displacement (mm)

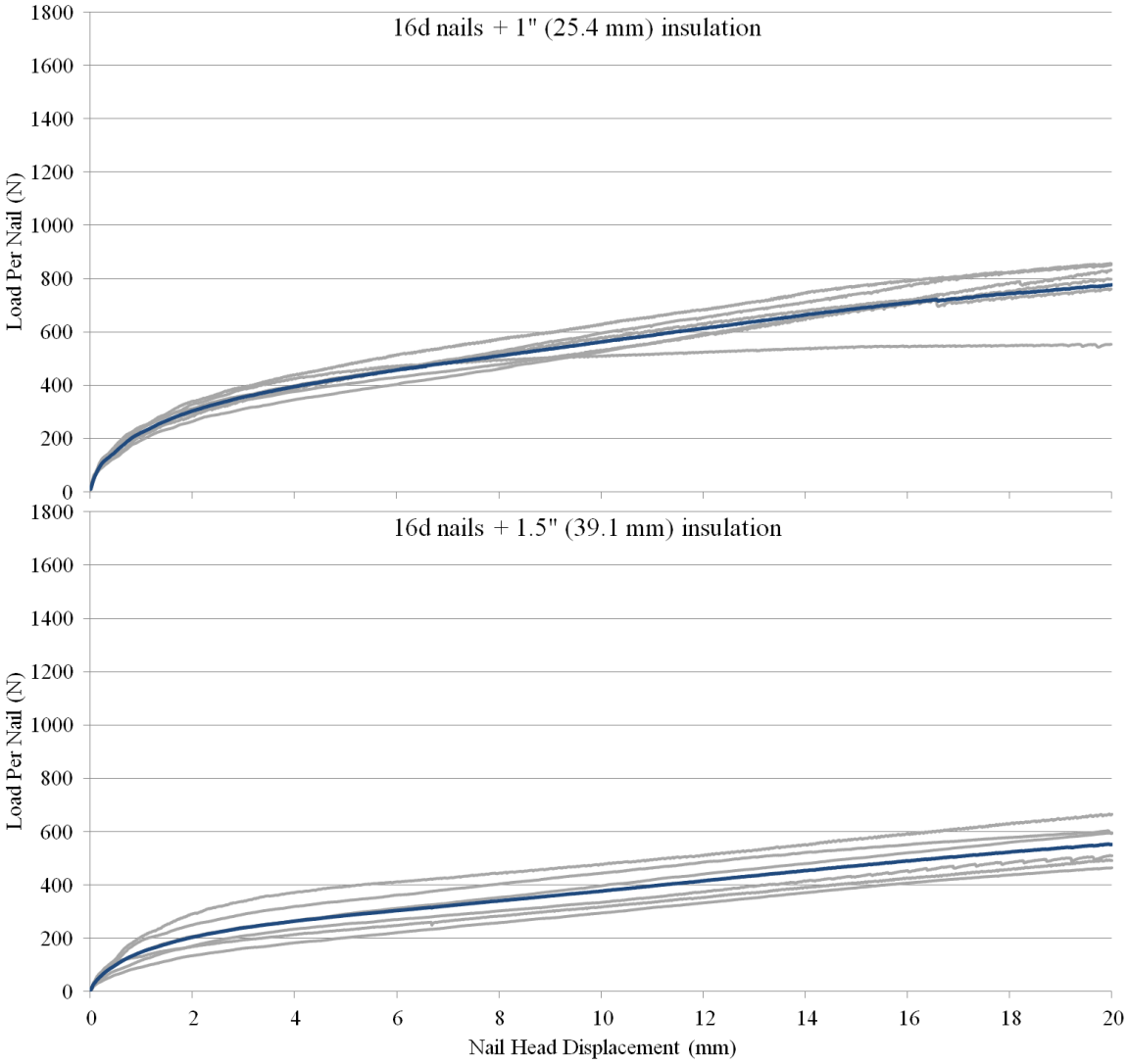

Note: Highlighted lines show mean response

Yield Point Calculation for Tests With Insulation

K&C Method

Nail Size + Insulation	Gap (mm)	Test 1	Test 2	Test 3	Test 4	Test 5	Test 6	Mean	St. Dev.
Yield Strength (N)									
10d + 0	*0.0*	385.3	789.5	677.5	862.3	794.7	659.3	**694.8**	169.9
10d + 1/8"	*3.2*	391.8	350.5	434.7	461.0	404.2	445.3	**414.6**	40.6
10d + 1/4"	*6.4*	435.1	374.8	262.3	549.4	373.4	459.1	**409.0**	96.8
10d + 3/8"	*9.5*	418.5	371.5	364.5	396.3	343.9	373.6	**378.0**	26.0
10d + 1/2"	*12.7*	-	300.6	379.3	361.4	360.0	427.2	**365.7**	45.4
10d + 5/8"	*15.9*	282.4	283.5	456.4	381.9	308.5	355.8	**344.8**	67.7
10d + 3/4"	*19.1*	255.6	211.2	286.9	205.8	213.5	298.0	**245.2**	40.9
10d + 1"	*25.4*	310.8	237.8	236.4	297.1	144.5	196.0	**237.1**	62.1
16d + 0	*0.0*	672.9	628.0	882.3	579.8	529.1	661.1	**658.9**	121.8
16d + 1/4"	*6.4*	622.2	515.6	725.6	538.0	645.3	710.4	**626.2**	86.5
16d + 1/2"	*12.7*	551.7	474.6	542.0	733.4	447.4	627.2	**562.7**	104.8
16d + 3/4"	*19.1*	358.5	388.1	530.2	394.9	467.0	318.2	**409.5**	76.8
16d + 1"	*25.4*	416.7	277.1	381.0	429.0	399.9	426.7	**382.7**	57.4
16d + 1.5"	*38.1*	232.5	302.3	297.9	255.2	246.5	333.2	**277.9**	39.0
Secant Stiffness (N/mm)									
10d + 0	*0.0*	804.8	1583.3	490.0	990.9	1085.9	1199.7	**1025.8**	369.3
10d + 1/8"	*3.2*	337.1	454.7	663.7	704.5	442.0	705.0	**551.2**	159.3
10d + 1/4"	*6.4*	441.7	423.7	313.1	447.7	533.0	220.5	**396.6**	111.3
10d + 3/8"	*9.5*	506.3	296.2	333.6	446.3	408.5	525.9	**419.5**	92.0
10d + 1/2"	*12.7*	-	382.0	382.0	207.9	404.6	498.7	**375.0**	105.1
10d + 5/8"	*15.9*	149.3	311.7	150.2	199.9	192.6	380.7	**230.7**	94.4
10d + 3/4"	*19.1*	165.3	196.9	154.3	164.4	153.0	286.3	**186.7**	51.3
10d + 1"	*25.4*	175.1	111.4	161.2	177.5	108.6	92.3	**137.7**	37.8
16d + No	*0.0*	565.6	1099.7	1891.3	732.5	754.3	525.4	**928.1**	513.7
16d + 1/4"	*6.4*	218.9	447.4	414.5	495.6	223.0	318.0	**352.9**	117.6
16d + 1/2"	*12.7*	399.7	221.1	305.4	181.5	114.1	126.1	**224.6**	110.4
16d + 3/4"	*19.1*	174.9	182.6	227.4	104.8	103.7	92.0	**147.6**	55.1
16d + 1"	*25.4*	76.7	198.0	98.7	88.8	68.4	114.7	**113.7**	47.2
16d + 1.5"	38.1	35.5	90.3	56.5	50.0	41.8	117.4	**65.2**	31.9

CEN Method

Nail Size + Insulation	Gap (mm)	Test 1	Test 2	Test 3	Test 4	Test 5	Test 6	Mean	St. Dev.
Yield Strength (N)									
10d + 0	*0.0*	494.0	1047.2	1129.4	1332.5	1153.9	749.4	**984.4**	306.8
10d + 1/8"	*3.2*	529.3	474.8	499.3	528.0	511.2	480.6	**503.9**	23.2
10d + 1/4"	*6.4*	594.9	494.1	333.2	650.5	488.9	695.5	**542.8**	131.8
10d + 3/8"	*9.5*	413.6	536.7	448.1	491.7	473.6	404.6	**461.4**	49.9
10d + 1/2"	*12.7*	-	371.5	454.6	471.7	471.1	601.1	**474.0**	82.3
10d + 5/8"	*15.9*	381.6	339.6	627.4	548.6	463.6	507.8	**478.1**	106.6
10d + 3/4"	*19.1*	386.6	301.7	400.4	295.9	284.4	414.6	**347.3**	59.3
10d + 1"	*25.4*	364.5	287.2	308.8	421.5	202.9	302.2	**314.5**	73.9
16d + 0	*0.0*	718.5	632.2	881.0	674.9	641.4	696.9	**707.5**	91.0
16d + 1/4"	*6.4*	705.1	525.4	722.0	592.1	733.2	720.4	**666.4**	86.4
16d + 1/2"	*12.7*	594.6	530.4	539.2	742.1	652.4	809.9	**644.8**	112.7
16d + 3/4"	*19.1*	409.0	401.7	506.4	547.0	622.0	466.9	**492.2**	84.6
16d + 1"	*25.4*	602.2	334.4	512.3	588.5	636.7	506.0	**515.6**	108.8
16d + 1.5"	*38.1*	405.0	303.2	440.1	371.1	389.2	334.3	**373.8**	49.3
Secant Stiffness (N/mm)									
10d + 0	*0.0*	924.0	1757.8	453.0	872.7	1084.3	1744.0	**1139.3**	517.6
10d + 1/8"	*3.2*	405.7	497.0	909.1	877.2	538.3	910.2	**689.6**	233.5
10d + 1/4"	*6.4*	493.3	432.1	388.2	530.4	570.1	256.2	**445.1**	113.4
10d + 3/8"	*9.5*	823.9	323.6	438.3	535.2	413.2	622.1	**526.1**	178.6
10d + 1/2"	*12.7*	-	424.5	497.7	240.7	461.8	498.1	**424.6**	107.2
10d + 5/8"	*15.9*	170.0	416.7	185.3	233.8	213.0	375.2	**265.7**	104.1
10d + 3/4"	*19.1*	167.4	226.1	174.6	163.8	159.9	310.0	**200.3**	59.0
10d + 1"	*25.4*	220.3	124.4	178.9	188.1	123.0	99.1	**155.6**	47.0
16d + 0	*0.0*	744.8	1459.3	2701.4	862.1	876.1	701.8	**1224.2**	773.6
16d + 1/4"	*6.4*	317.6	613.5	580.6	602.2	301.9	471.6	**481.2**	142.1
16d + 1/2"	*12.7*	455.4	295.0	420.7	320.4	139.5	207.7	**306.5**	121.0
16d + 3/4"	*19.1*	223.2	237.1	329.2	124.5	149.7	110.0	**195.6**	83.5
16d + 1"	*25.4*	108.2	241.0	121.9	123.0	86.7	157.3	**146.0**	54.7
16d + 1.5"	38.1	40.0	128.4	74.5	65.1	54.7	153.3	**86.0**	44.7

CSIRO Method

Nail Size + Insulation	Gap (mm)	Test 1	Test 2	Test 3	Test 4	Test 5	Test 6	Mean	St. Dev.
Yield Strength (N)									
10d + 0	*0.0*	340.4	703.2	678.3	887.7	761.0	556.7	**654.6**	188.1
10d + 1/8"	*3.2*	345.6	325.9	376.9	397.6	365.2	403.5	**369.1**	30.0
10d + 1/4"	*6.4*	395.1	343.7	228.5	491.3	339.6	415.7	**369.0**	88.4
10d + 3/8"	*9.5*	349.5	339.4	316.9	353.9	321.8	328.7	**335.0**	15.0
10d + 1/2"	*12.7*	-	265.3	332.3	322.9	327.3	401.1	**329.8**	48.2
10d + 5/8"	*15.9*	252.7	245.6	402.8	342.2	278.4	335.4	**309.5**	61.2
10d + 3/4"	*19.1*	243.9	186.4	263.2	191.0	196.4	268.9	**225.0**	38.0
10d + 1"	*25.4*	278.9	215.3	219.6	271.4	133.4	176.4	**215.8**	55.6
16d + 0	*0.0*	599.0	555.4	766.4	521.0	479.7	586.2	**584.6**	99.1
16d + 1/4"	*6.4*	532.2	449.8	641.2	475.6	561.8	609.8	**545.1**	74.6
16d + 1/2"	*12.7*	497.4	410.0	472.0	629.6	389.4	534.2	**488.8**	87.6
16d + 3/4"	*19.1*	321.0	338.3	459.6	352.5	404.1	283.6	**359.9**	62.8
16d + 1"	*25.4*	359.0	246.3	334.6	367.4	349.4	369.3	**333.4**	46.5
16d + 1.5"	*38.1*	206.1	262.2	255.9	222.6	213.4	293.5	**242.3**	33.9
Secant Stiffness (N/mm)									
10d + 0	*0.0*	892.0	1687.4	490.2	996.3	1133.3	1545.7	**1124.1**	439.8
10d + 1/8"	*3.2*	390.5	503.4	854.2	809.9	534.6	875.4	**661.3**	209.5
10d + 1/4"	*6.4*	486.2	425.9	373.6	507.3	573.4	264.1	**438.4**	109.6
10d + 3/8"	*9.5*	713.8	324.4	400.9	519.7	422.2	577.5	**493.1**	140.4
10d + 1/2"	*12.7*	-	405.7	470.9	234.3	462.9	513.1	**417.4**	109.3
10d + 5/8"	*15.9*	157.8	386.6	181.8	228.4	209.0	389.9	**258.9**	103.0
10d + 3/4"	*19.1*	173.8	216.3	173.0	168.5	156.7	299.0	**197.9**	53.5
10d + 1"	*25.4*	211.8	121.3	182.4	188.2	125.2	97.4	**154.4**	45.6
16d + 0	*0.0*	703.1	1369.9	2448.7	846.5	852.8	652.6	**1145.6**	687.4
16d + 1/4"	*6.4*	290.7	562.4	540.7	568.0	282.3	424.3	**444.7**	133.2
16d + 1/2"	*12.7*	436.2	268.3	383.0	291.1	137.7	195.5	**285.3**	111.8
16d + 3/4"	*19.1*	211.7	217.3	294.1	123.8	143.8	108.3	**183.2**	70.6
16d + 1"	*25.4*	103.7	228.3	118.3	116.5	85.6	146.6	**139.1**	50.7
16d + 1.5"	38.1	40.1	114.9	71.7	62.5	53.7	140.5	**80.6**	38.8

Y&K Method

Nail Size + Insulation	Gap (mm)	Test 1	Test 2	Test 3	Test 4	Test 5	Test 6	Mean	St. Dev.
Yield Strength (N)									
10d + 0	*0.0*	486.4	953.9	901.6	1171.2	1014.9	751.5	**879.9**	236.8
10d + 1/8"	*3.2*	393.4	398.8	481.7	515.3	412.7	477.4	**446.5**	51.3
10d + 1/4"	*6.4*	461.7	406.8	277.2	553.0	408.0	412.3	**419.8**	89.7
10d + 3/8"	*9.5*	438.3	375.4	388.3	454.9	432.7	424.5	**419.0**	30.7
10d + 1/2"	*12.7*	-	320.9	399.3	360.1	393.7	471.8	**389.2**	55.8
10d + 5/8"	*15.9*	292.2	332.1	503.0	377.5	312.9	434.6	**375.4**	80.6
10d + 3/4"	*19.1*	269.1	235.7	296.1	234.7	234.6	323.5	**265.6**	37.7
10d + 1"	*25.4*	346.3	245.1	256.7	345.7	164.9	205.4	**260.7**	73.6
16d + 0	*0.0*	731.2	685.4	1069.8	632.6	589.6	659.1	**728.0**	174.1
16d + 1/4"	*6.4*	577.5	558.4	713.9	592.3	608.3	675.4	**621.0**	60.7
16d + 1/2"	*12.7*	609.2	454.1	530.6	622.9	464.8	528.3	**535.0**	70.4
16d + 3/4"	*19.1*	355.3	384.5	521.4	382.5	397.4	298.9	**390.0**	73.4
16d + 1"	*25.4*	346.4	332.6	363.4	366.2	340.6	398.0	**360.2**	23.6
16d + 1.5"	*38.1*	191.3	280.2	251.9	217.5	202.7	333.3	**246.2**	53.8
Secant Stiffness (N/mm)									
10d + 0	*0.0*	646.4	1294.9	457.6	860.6	1002.8	1017.9	**880.0**	296.5
10d + 1/8"	*3.2*	335.9	419.4	599.3	598.1	421.2	588.9	**493.8**	115.6
10d + 1/4"	*6.4*	408.5	382.6	289.4	444.3	496.6	267.0	**381.4**	88.9
10d + 3/8"	*9.5*	493.7	293.4	315.8	389.2	339.6	418.9	**375.1**	74.3
10d + 1/2"	*12.7*	-	351.4	363.0	209.2	361.4	456.8	**348.4**	88.8
10d + 5/8"	*15.9*	143.0	270.1	131.6	203.2	192.3	325.1	**210.9**	74.6
10d + 3/4"	*19.1*	150.3	192.7	148.6	146.6	129.4	266.2	**172.3**	50.5
10d + 1"	*25.4*	158.9	101.5	145.1	163.8	101.8	86.9	**126.3**	33.4
16d + 0	*0.0*	500.6	850.6	1240.8	614.7	611.9	527.7	**724.4**	281.4
16d + 1/4"	*6.4*	252.5	387.6	429.5	402.9	256.8	365.8	**349.2**	76.1
16d + 1/2"	*12.7*	319.1	233.3	316.0	298.8	109.3	203.6	**246.7**	82.0
16d + 3/4"	*19.1*	176.8	184.2	234.5	109.0	148.7	102.1	**159.2**	50.0
16d + 1"	*25.4*	149.7	162.3	106.3	118.0	88.8	126.3	**120.4**	27.2
16d + 1.5"	38.1	42.8	102.8	74.2	64.9	58.8	117.3	**76.8**	28.1

5% Diameter Method

Nail Size + Insulation	Gap (mm)	Test 1	Test 2	Test 3	Test 4	Test 5	Test 6	Mean	St. Dev.
Yield Strength (N)									
10d + 0	*0.0*	440.7	907.2	934.1	1204.0	1042.4	626.4	**859.1**	279.2
10d + 1/8"	*3.2*	364.0	378.7	424.0	471.4	394.2	447.8	**413.4**	41.6
10d + 1/4"	*6.4*	438.0	405.4	254.2	522.1	410.7	420.3	**408.4**	86.9
10d + 3/8"	*9.5*	364.0	367.6	341.6	391.9	395.1	389.0	**374.9**	20.9
10d + 1/2"	*12.7*	-	315.7	348.3	331.2	359.9	477.1	**366.4**	64.1
10d + 5/8"	*15.9*	257.3	268.7	393.0	347.2	297.8	398.6	**327.1**	61.7
10d + 3/4"	*19.1*	258.7	201.0	268.8	215.0	219.8	309.8	**245.5**	41.0
10d + 1"	*25.4*	282.8	217.3	229.1	283.8	138.8	185.0	**222.8**	56.3
16d + 0	*0.0*	636.5	645.6	918.7	589.3	549.8	623.0	**660.5**	131.3
16d + 1/4"	*6.4*	525.6	470.0	661.0	517.1	550.5	609.7	**555.6**	69.0
16d + 1/2"	*12.7*	537.8	409.7	484.8	617.9	375.6	522.4	**491.4**	88.6
16d + 3/4"	*19.1*	326.0	339.1	457.4	345.6	392.1	277.8	**356.3**	61.6
16d + 1"	*25.4*	415.1	261.6	322.2	356.3	330.7	356.2	**325.4**	50.4
16d + 1.5"	*38.1*	190.4	258.0	244.6	212.3	202.8	293.6	**233.6**	39.0
Secant Stiffness (N/mm)									
10d + 0	*0.0*	711.3	1369.8	446.7	844.2	979.4	1192.8	**924.0**	332.7
10d + 1/8"	*3.2*	361.9	429.3	692.5	688.1	463.9	693.3	**554.8**	153.1
10d + 1/4"	*6.4*	437.2	384.3	328.1	473.4	492.1	258.9	**395.7**	90.0
10d + 3/8"	*9.5*	597.5	301.7	369.7	457.4	373.1	501.5	**433.5**	106.9
10d + 1/2"	*12.7*	-	363.2	418.9	228.9	404.7	451.7	**373.5**	86.8
10d + 5/8"	*15.9*	156.7	342.6	188.1	224.8	202.6	347.5	**243.7**	81.6
10d + 3/4"	*19.1*	161.3	200.4	167.0	157.2	149.1	277.2	**185.4**	48.3
10d + 1"	*25.4*	203.8	120.4	169.7	182.0	115.1	97.4	**148.1**	42.8
16d + 0	*0.0*	630.9	1041.6	1737.0	711.7	698.6	593.6	**902.2**	438.8
16d + 1/4"	*6.4*	300.3	504.6	515.1	513.6	289.7	424.5	**424.6**	106.0
16d + 1/2"	*12.7*	409.4	269.1	371.4	305.1	145.7	210.7	**285.2**	98.5
16d + 3/4"	*19.1*	206.1	216.8	294.7	128.2	153.0	111.6	**185.1**	68.0
16d + 1"	*25.4*	113.7	214.2	124.3	126.3	92.4	153.3	**142.1**	42.5
16d + 1.5"	38.1	43.2	120.1	78.0	67.1	58.4	144.4	**85.2**	38.9

Curve Fitting Parameters for Tests With Insulation

3-Parameter Exponential Model

Nail size + Insulation Thickness	Parameter	Test 1	Test 2	Test 3	Test 4	Test 5	Test 6	Mean
10d Nail + 0" (0.00mm)	k_1	-23.3	-36.8	69.7	-25.0	-34.3	-37.5	**-14.5**
	k_0	1206	2236	654	1468	1637	1718	**1487**
	p_1	623	1375	1968	1550	1380	1097	**1332**
	R-square	*0.985*	*0.993*	*0.997*	*0.996*	*0.998*	*0.985*	***0.992***
10d Nail + 1/8" (3.18mm)	k_1	-5.5	-31.9	-15.0	-35.7	-30.2	-44.4	**-27.1**
	k_0	452	696	911	1093	666	1097	**819**
	p_1	739	532	754	680	605	617	**655**
	R-square	*0.988*	*0.996*	*0.964*	*0.983*	*0.979*	*0.977*	***0.981***
10d Nail + 1/4" (6.35mm)	k_1	-16.8	-27.8	-24.7	-60.4	-17.2	-49.8	**-32.8**
	k_0	601	589	515	880	735	429	**625**
	p_1	750	566	378	604	629	459	**564**
	R-square	*0.990*	*0.990*	*0.973*	*0.986*	*0.983*	*0.981*	***0.984***
10d Nail + 3/8" (9.53mm)	k_1	-25.7	-70.5	-19.4	-16.5	-20.6	-24.9	**-29.6**
	k_0	834	588	508	660	662	804	**676**
	p_1	605	339	576	645	523	520	**535**
	R-square	*0.967*	*0.997*	*0.989*	*0.985*	*0.993*	*0.979*	***0.985***
10d Nail + 1/2" (12.70mm)	k_1	-	-22.1	-43.7	-45.3	-11.9	-30.5	**-30.7**
	k_0	-	546	689	477	564	734	**602**
	p_1	-	453	482	320	619	665	**508**
	R-square	-	*0.984*	*0.984*	*0.998*	*0.987*	*0.992*	***0.989***
10d Nail + 5/8" (15.88mm)	k_1	-26.6	-16.3	-17.6	-45.6	-43.2	-32.2	**-30.2**
	k_0	248	517	258	413	344	597	**396**
	p_1	319	427	591	360	311	516	**421**
	R-square	*0.997*	*0.983*	*0.979*	*0.992*	*0.996*	*0.995*	***0.99***
10d Nail + 3/4" (19.05mm)	k_1	-13.6	-6.3	-2.4	-4.6	-1.9	-4.4	**-5.5**
	k_0	236	300	209	228	184	380	**256**
	p_1	406	375	527	364	404	559	**439**
	R-square	*0.996*	*0.994*	*0.989*	*0.993*	*0.984*	*0.997*	***0.992***
10d Nail + 1" (25.40mm)	k_1	-7.2	-13.1	-5.7	-8.6	-1.2	-0.1	**-6.0**
	k_0	256	193	220	269	154	134	**205**
	p_1	494	278	401	492	272	381	**386**
	R-square	*0.978*	*0.988*	*0.988*	*0.994*	*0.993*	*0.992*	***0.989***
16d Nail + 0" (0.00mm)	k_1	-20.5	-23.9	-58.1	-21.7	-38.8	-25.5	**-31.4**
	k_0	783	1334	2818	942	1070	719	**1277**
	p_1	1050	980	1288	961	806	1015	**1017**
	R-square	*0.967*	*0.943*	*0.977*	*0.963*	*0.985*	*0.968*	***0.967***
16d Nail + 1/4" (6.35mm)	k_1	-32.9	-34.9	-52.4	-25.3	-34.5	-32.2	**-35.4**
	k_0	441	889	1004	737	471	561	**684**
	p_1	687	628	753	772	683	883	**734**

	R-square	*0.976*	*0.981*	*0.986*	*0.980*	*0.980*	*0.969*	***0.979***
16d Nail + 1/2" (12.70mm)	k_1	-23.4	-29.8	-37.5	-49.5	-25.7	-45.1	**-35.2**
	k_0	664	407	741	1214	239	905	**695**
	p_1	710	541	564	531	444	396	**531**
	R-square	*0.973*	*0.982*	*0.987*	*0.997*	*0.978*	*0.997*	***0.986***
16d Nail + 3/4" (19.05mm)	k_1	-12.0	-18.5	-28.3	-21.2	-33.6	-19.8	**-22.2**
	k_0	259	320	568	210	545	173	**346**
	p_1	521	467	540	402	326	335	**432**
	R-square	*0.978*	*0.974*	*0.99*	*0.987*	*0.990*	*0.984*	***0.984***
16d Nail + 1" (25.40mm)	k_1	-28.8	-6.3	-22.1	-30.1	-29.3	-26.3	**-23.8**
	k_0	405	294	229	426	321	325	**333**
	p_1	253	444	349	286	231	361	**321**
	R-square	*0.998*	*0.99*	*0.989*	*0.997*	*0.999*	*0.995*	***0.995***
16d Nail + 1.5" (38.10mm)	k_1	-18.1	-18.2	-20.8	-17.8	-17.7	-18.1	**-18.5**
	k_0	143	265	252	177	327	313	**246**
	p_1	114	257	187	162	140	300	**193**
	R-square	*0.999*	*0.997*	*0.999*	*0.999*	*0.999*	*0.999*	***0.999***

Asymptotic Model

Nail size + Insulation Thickness	**Parameter**	**Test 1**	**Test 2**	**Test 3**	**Test 4**	**Test 5**	**Test 6**	**Mean**
10d Nail + 0" (0.00mm)	*a*	756	1563	1418	1716	1567	1311	**1389**
	b	601	1369	1443	1605	1472	1097	**1264**
	c	0.405	0.344	0.603	0.48	0.414	0.423	**0.445**
	R-square	*0.981*	*0.994*	*0.996*	*0.996*	*0.996*	*0.990*	***0.992***
10d Nail + 1/8" (3.18mm)	*a*	796	703	871	911	826	898	**834**
	b	716	628	683	721	687	699	**689**
	c	0.621	0.492	0.519	0.534	0.609	0.568	**0.557**
	R-square	*0.996*	*0.997*	*0.994*	*0.989*	*0.996*	*0.989*	***0.993***
10d Nail + 1/4" (6.35mm)	*a*	884	761	537	1150	745	1061	**856**
	b	792	669	434	931	626	916	**728**
	c	0.587	0.588	0.584	0.74	0.504	0.823	**0.638**
	R-square	*0.997*	*0.994*	*0.996*	*0.989*	*0.997*	*0.995*	***0.995***
10d Nail + 3/8" (9.53mm)	*a*	820	813	737	784	671	744	**761**
	b	618	714	641	650	564	552	**623**
	c	0.624	0.705	0.619	0.579	0.542	0.658	**0.621**
	R-square	*0.985*	*0.993*	*0.996*	*0.995*	*0.988*	*0.974*	***0.988***
10d Nail + 1/2" (12.70mm)	*a*	-	601	783	798	719	854	**751**
	b	-	505	646	670	614	755	**638**
	c	-	0.565	0.639	0.808	0.568	0.537	**0.623**
	R-square	-	*0.995*	*0.994*	*0.987*	*0.998*	*0.998*	***0.994***
10d Nail + 5/8" (15.88mm)	*a*	591	562	945	848	685	713	**724**
	b	539	448	790	734	617	634	**627**
	c	0.762	0.607	0.859	0.801	0.75	0.556	**0.722**
	R-square	*0.995*	*0.988*	*0.994*	*0.992*	*0.994*	*0.996*	***0.993***

10d Nail + 3/4" (19.05mm)	*a*	535	423	569	413	432	597	**495**
	b	497	385	512	369	388	564	**453**
	c	0.702	0.558	0.736	0.643	0.699	0.566	**0.651**
	R-square	*0.999*	*0.998*	*0.995*	*0.999*	*0.991*	*0.998*	***0.997***
10d Nail + 1" (25.40mm)	*a*	618	494	474	596	288	385	**476**
	b	504	406	416	533	258	364	**414**
	c	0.775	0.839	0.707	0.707	0.64	0.721	**0.732**
	R-square	*0.992*	*0.989*	*0.996*	*0.998*	*0.999*	*0.994*	***0.995***
16d Nail + 0" (0.00mm)	*a*	1345	1246	1691	1166	1062	1343	**1309**
	b	1028	845.5	1195	916	880.4	1074	**990**
	c	0.741	0.664	0.527	0.618	0.544	0.738	**0.639**
	R-square	*0.990*	*0.984*	*0.965*	*0.992*	*0.993*	*0.991*	***0.986***
16d Nail + 1/4" (6.35mm)	*a*	1338	1048	1514	1058	1393	1487	**1306**
	b	1089	759.3	1148	830	1128	1176	**1022**
	c	0.875	0.781	0.841	0.707	0.883	0.852	**0.823**
	R-square	*0.992*	*0.980*	*0.984*	*0.987*	*0.991*	*0.990*	***0.987***
16d Nail + 1/2" (12.70mm)	*a*	1126	1003	1143	2342	1004	3043	**1610**
	b	812.3	827.2	863.1	1931	852.1	2717	**1334**
	c	0.836	0.835	0.851	0.961	0.897	0.979	**0.893**
	R-square	*0.975*	*0.990*	*0.982*	*0.985*	*0.995*	*0.984*	***0.985***
16d Nail + 3/4" (19.05mm)	*a*	730	814	1116	869	1285	709	**920**
	b	604.8	646.6	842.6	740	1075	620.4	**755**
	c	0.813	0.855	0.887	0.894	0.943	0.876	**0.878**
	R-square	*0.991*	*0.985*	*0.979*	*0.996*	*0.991*	*0.994*	***0.989***
16d Nail + 1" (25.40mm)	*a*	1616	539	839	1223	1277	978	**1079**
	b	1426	439	706.4	1036	1127	801.9	**923**
	c	0.972	0.718	0.901	0.949	0.959	0.915	**0.902**
	R-square	*0.982*	*0.987*	*0.992*	*0.989*	*0.991*	*0.987*	***0.988***
16d Nail + 1.5" (38.10mm)	*a*	834	678	883	743	994	719	**808**
	b	763.7	545.6	761.5	646	883.6	553	**692**
	c	0.964	0.913	0.954	0.952	0.973	0.912	**0.945**
	R-square	*0.994*	*0.979*	*0.989*	*0.984*	*0.990*	*0.958*	***0.982***

APPENDIX E: Finite Element model in OpenSees

Load-deformation response curves for all tests of the FE model

Intermediate gap thicknesses for tests of the FE model were incremented as follows:

- 1/16" (1 node) from 0" to 3/4"
- 1/8" (2 nodes) from 3/4" to 1.5"
- 1/4" (4 nodes) from 1.5" to 2"

The FE model was tested up to the following upper limits on intermediate material thickness:

- For 6d nails, up to 1"
- For 8d nails, up to 1.5"
- For 10d nails, up to 1.5"
- For 16d nails, up to 2"

Labeling on the following figures indicates intermediate material thickness in inches.

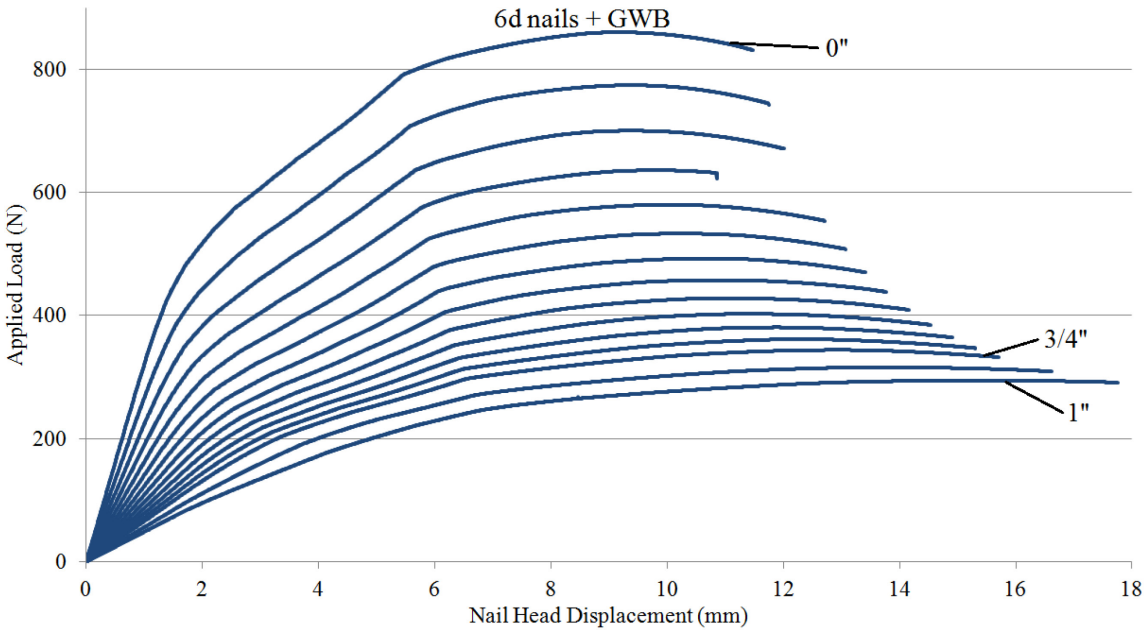

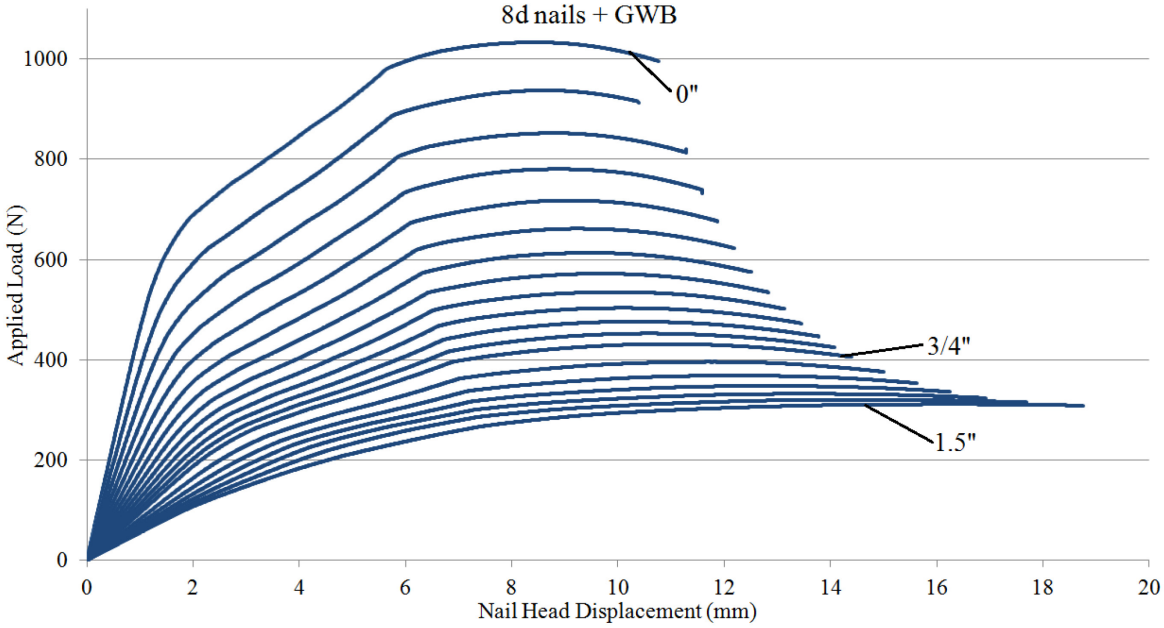
8d nails + GWB
0"
3/4"
1.5"
Applied Load (N)
Nail Head Displacement (mm)
0
200
400
600
800
1000
0
2
4
6
8
10
12
14
16
18
20

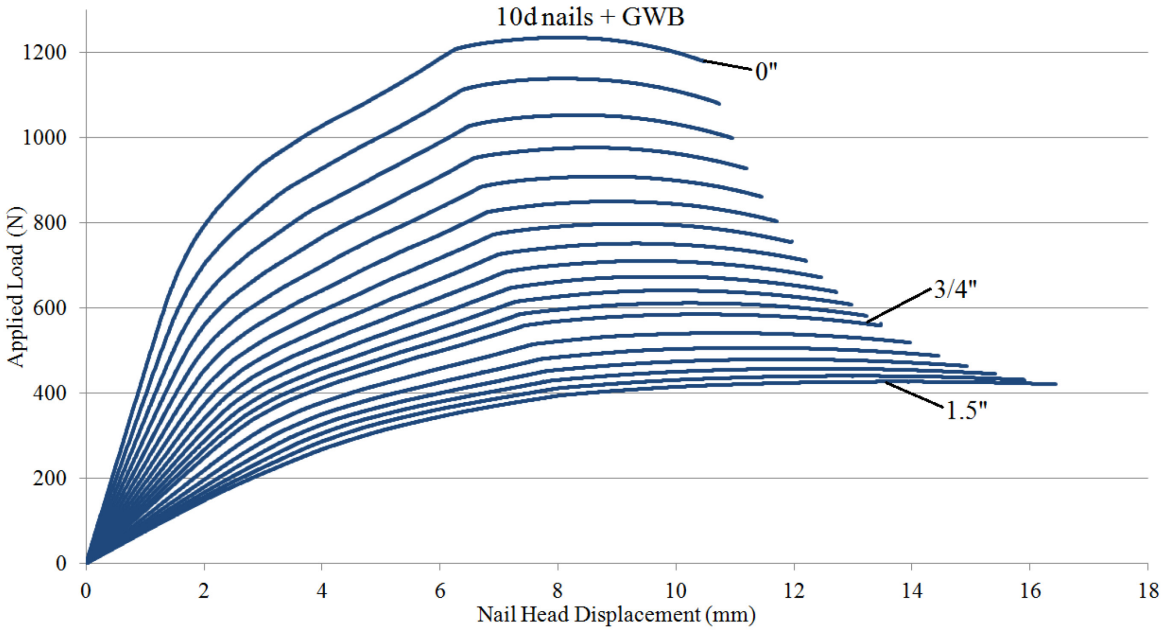
10d nails + GWB
0"
3/4"
1.5"
Applied Load (N)
Nail Head Displacement (mm)
0
200
400
600
800
1000
1200
0
2
4
6
8
10
12
14
16
18

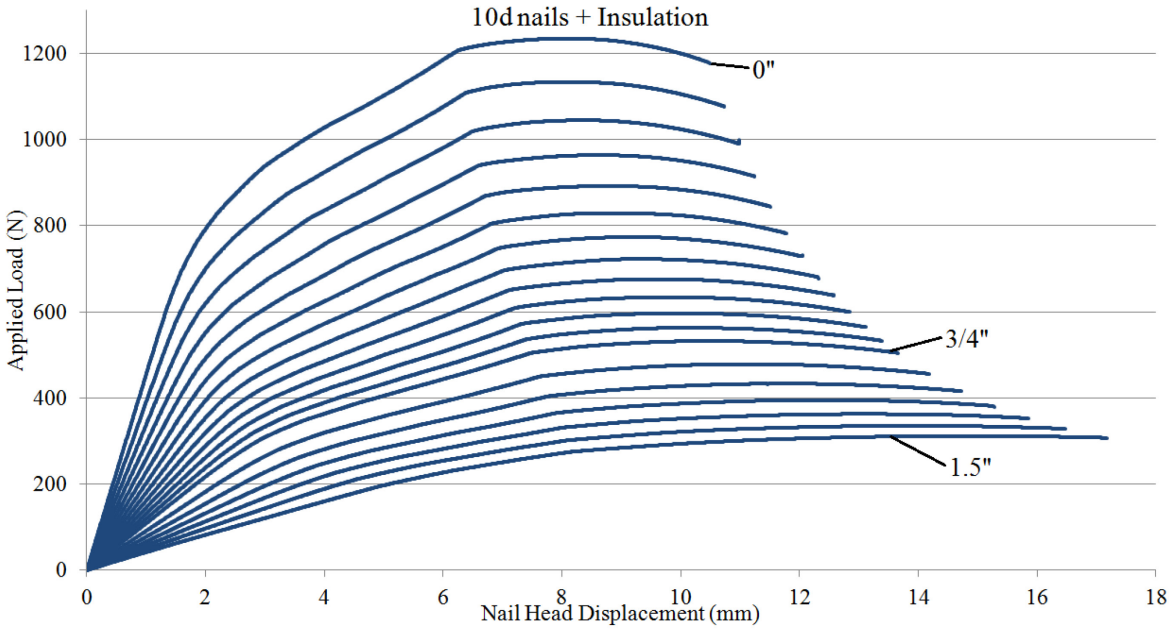
10d nails + Insulation
Applied Load (N)
Nail Head Displacement (mm)
0"
3/4"
1.5"
0
200
400
600
800
1000
1200
0
2
4
6
8
10
12
14
16
18

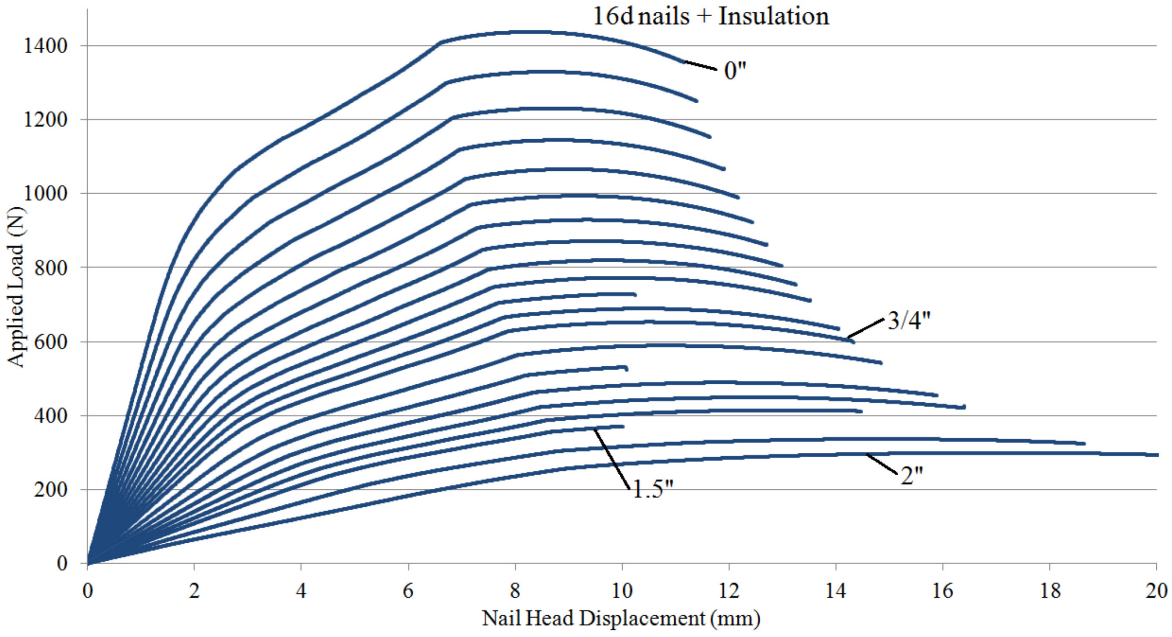
16d nails + Insulation
Applied Load (N)
Nail Head Displacement (mm)
0"
3/4"
1.5"
2"
0
200
400
600
800
1000
1200
1400
0
2
4
6
8
10
12
14
16
18
20

Yield load determination for all tests in the FE model

Yield loads shown in N,

Secant stiffness shown in N/mm

6d Nail with GWB

Gap Thickness (mm)	K&C Method		CEN Method		CSIRO Method		Y&K Method		5% Diam. Method	
	Yield Load	Secant Stiff.	Yield Load	Secant Stiff.	Yield Load	Secant Stiff.	Yield Load	Secant Stiff.	Yield Load	Secant Stiff.
0.0	430	305	602	319	416	309	463	291	462	291
1.6	387	249	557	263	372	253	400	243	405	241
3.2	350	206	516	219	335	210	354	205	359	202
4.8	318	174	479	186	303	178	316	174	324	172
6.4	290	149	443	159	277	152	285	150	294	148
7.9	267	130	412	138	255	132	261	131	270	129
9.5	246	114	383	121	236	117	243	115	250	114
11.1	229	102	358	108	220	104	228	102	233	101
12.7	214	92	335	97	206	93	217	91	220	91
14.3	201	83	315	87	195	84	207	82	209	82
15.9	190	76	298	79	185	77	200	75	200	75
17.5	181	69	285	72	176	70	195	68	192	68
19.1	172	64	273	65	168	64	190	62	186	62
22.2	158	53	256	55	154	53	184	52	172	52
25.4	147	44	242	46	142	44	175	43	148	44

8d Nail with GWB

Gap Thickness (mm)	K&C Method		CEN Method		CSIRO Method		Y&K Method		5% Diam. Method	
	Yield Load	Secant Stiff.	Yield Load	Secant Stiff.	Yield Load		Yield Load	Secant Stiff.	Yield Load	Secant Stiff.
0.0	517	452	653	464	505	454	604	415	606	413
1.6	469	367	626	382	455	371	523	345	528	342
3.2	426	303	594	318	411	307	460	291	467	287
4.8	390	254	560	268	375	258	412	247	420	243
6.4	359	216	529	229	344	220	371	212	380	209
7.9	331	186	499	198	317	190	338	184	347	181
9.5	307	163	470	173	294	166	312	161	321	159
11.1	286	144	445	152	275	147	291	143	299	141
12.7	267	129	422	136	258	131	274	128	282	126
14.3	252	117	400	123	243	119	261	116	267	114
15.9	238	107	380	111	231	108	249	105	255	104
17.5	226	99	362	102	220	99	239	97	244	96
19.1	216	91	346	94	210	92	231	89	236	88
22.2	198	80	320	82	194	80	218	78	221	77
25.4	184	71	301	73	180	71	209	69	209	69
28.6	174	64	286	66	169	64	202	62	196	62
31.8	166	58	274	60	161	58	192	56	180	57
34.9	160	53	264	55	154	53	180	51	162	53
38.1	155	48	252	51	148	49	168	47	150	49

10d Nail with GWB

Gap Thickness (mm)	K&C Method		CEN Method		CSIRO Method		Y&K Method		5% Diam. Method	
	Yield Load	Secant Stiff.	Yield Load	Secant Stiff.	Yield Load		Yield Load	Secant Stiff.	Yield Load	Secant Stiff.
0.0	617	450	881	454	612	450	743	419	766	409
1.6	569	387	835	391	563	387	669	363	692	354
3.2	526	335	791	340	520	336	607	318	630	309
4.8	488	293	750	298	481	294	557	280	579	272
6.4	454	258	709	263	447	259	515	247	536	241
7.9	425	229	672	234	418	230	478	221	499	215
9.5	398	206	637	209	392	206	447	198	467	194
11.1	375	185	606	189	370	186	421	179	440	175
12.7	355	169	577	172	350	169	400	163	417	160
14.3	337	154	550	157	332	155	381	150	398	146
15.9	320	142	527	144	316	142	366	138	382	135
17.5	305	132	506	133	302	132	352	128	367	125
19.1	292	123	486	124	289	123	339	119	354	117
22.2	270	108	452	109	268	108	319	105	333	103
25.4	253	97	425	98	251	97	304	94	315	93
28.6	239	88	402	89	236	88	290	86	299	85
31.8	229	81	384	83	224	81	276	79	281	79
34.9	220	75	370	77	215	76	262	73	257	73
38.1	213	70	357	73	207	71	244	68	234	69

10d Nail with Insulation

Gap Thickness (mm)	K&C Method		CEN Method		CSIRO Method		Y&K Method		5% Diam. Method	
	Yield Load	Secant Stiff.	Yield Load	Secant Stiff.	Yield Load		Yield Load	Secant Stiff.	Yield Load	Secant Stiff.
0.0	617	450	881	454	612	450	743	419	766	409
1.6	567	385	833	390	561	386	667	362	690	353
3.2	522	332	785	337	516	333	603	316	626	307
4.8	482	289	740	294	475	290	551	276	572	268
6.4	446	253	697	258	439	254	506	242	527	236
7.9	415	223	656	227	408	224	466	215	487	209
9.5	387	198	618	202	380	198	432	191	451	186
11.1	361	176	583	180	355	177	402	171	420	167
12.7	338	158	551	161	332	159	377	154	393	150
14.3	317	143	522	145	312	143	355	139	370	135
15.9	298	129	494	131	294	129	334	126	349	123
17.5	281	117	467	119	277	118	316	114	330	112
19.1	266	107	443	109	262	107	299	104	313	102
22.2	239	90	401	91	236	90	270	88	285	86
25.4	217	76	366	77	214	76	247	75	262	73
28.6	197	65	336	66	196	65	228	64	243	63
31.8	181	56	311	56	180	56	213	55	228	54
34.9	168	48	290	48	166	48	201	47	216	46
38.1	156	40	273	40	155	40	195	40	208	39

16d Nail with Insulation

Gap Thickness (mm)	K&C Method		CEN Method		CSIRO Method		Y&K Method		5% Diam. Method	
	Yield Load	Secant Stiff.	Yield Load	Secant Stiff.	Yield Load		Yield Load	Secant Stiff.	Yield Load	Secant Stiff.
0.0	719	526	992	529	714	526	886	484	909	473
1.6	665	453	945	457	659	453	799	421	825	411
3.2	615	392	903	397	609	393	726	368	752	359
4.8	572	342	859	347	565	343	663	324	688	315
6.4	533	301	815	306	525	301	610	287	634	278
7.9	497	266	776	271	489	266	563	254	588	247
9.5	465	236	738	241	457	237	522	227	548	221
11.1	436	211	700	215	429	212	487	204	511	198
12.7	410	190	664	193	403	190	456	184	479	179
14.3	386	171	632	174	380	172	429	166	451	162
15.9	365	155	602	158	359	156	405	151	426	147
17.5	345	141	574	144	340	142	384	138	403	134
19.1	326	129	547	131	322	129	364	126	383	123
22.2	295	109	499	110	291	109	330	106	349	104
25.4	266	93	456	94	263	93	301	91	320	89
28.6	245	80	420	81	242	80	277	78	297	77
31.8	225	70	389	70	223	70	258	68	277	67
34.9	207	61	361	61	206	61	241	60	260	59
38.1	186	54	337	54	184	54	223	53	245	52
44.5	168	41	298	41	167	41	203	41	224	40
50.8	150	31	270	30	148	31	202	30	214	30

Curve Fitting for all tests in the FE model

6d Nail with GWB

Gap Thickness (mm)	Maximum Load (N)	3-Parameter Exponential Model				Asymptotic Model			
		k_1	k_0	p_1	R-square	*a*	*b*	*c*	R-square
0.0	**860**	-22.5	406	681	*0.996*	882	858	0.672	*0.994*
1.6	**774**	-17.6	324	637	*0.996*	807	788	0.700	*0.995*
3.2	**700**	-15.1	266	587	*0.996*	742	727	0.723	*0.996*
4.8	**636**	-7.2	219	598	*0.996*	679	669	0.736	*0.996*
6.4	**580**	-1.6	186	603	*0.996*	623	618	0.747	*0.996*
7.9	**533**	0.0	161	575	*0.997*	576	574	0.758	*0.997*
9.5	**493**	3.9	141	582	*0.997*	532	533	0.763	*0.997*
11.1	**457**	5.8	126	573	*0.998*	495	498	0.769	*0.997*
12.7	**428**	6.3	113	552	*0.998*	463	468	0.773	*0.998*
14.3	**402**	7.1	103	537	*0.999*	434	441	0.776	*0.999*
15.9	**381**	8.6	94	538	*0.999*	407	416	0.777	*0.999*
17.5	**361**	10.2	87	545	*0.999*	384	396	0.778	*0.999*
19.1	**344**	11.5	80	551	*0.999*	364	377	0.778	*0.999*
22.2	**315**	14.5	68	591	*0.999*	333	350	0.786	*0.998*
25.4	**294**	14.6	57	600	*0.998*	311	327	0.802	*0.997*

8d Nail with GWB

Gap Thickness (mm)	Maximum Load (N)	3-Parameter Exponential Model				Asymptotic Model			
		k_1	k_0	p_1	R-square	*a*	*b*	*c*	R-square
0.0	**1033**	-40.3	645	731	*0.994*	1039	990	0.623	*0.985*
1.6	**938**	-35.7	512	663	*0.994*	957	915	0.659	*0.989*
3.2	**852**	-31.8	415	606	*0.994*	884	850	0.686	*0.991*
4.8	**780**	-29.8	345	548	*0.995*	822	794	0.709	*0.992*
6.4	**718**	-25.9	289	513	*0.995*	765	743	0.727	*0.993*
7.9	**661**	-21.3	246	495	*0.995*	713	697	0.741	*0.994*
9.5	**613**	-16.2	211	491	*0.995*	667	655	0.751	*0.995*
11.1	**572**	-12.6	185	483	*0.996*	625	618	0.760	*0.995*
12.7	**535**	-5.9	163	515	*0.996*	586	583	0.764	*0.996*
14.3	**503**	-2.5	147	522	*0.996*	552	552	0.769	*0.996*
15.9	**476**	0.2	133	526	*0.997*	522	525	0.772	*0.997*
17.5	**452**	4.5	122	557	*0.998*	494	499	0.773	*0.998*
19.1	**431**	8.0	113	584	*0.998*	468	476	0.773	*0.998*
22.2	**396**	14.5	98	645	*0.999*	424	437	0.770	*0.998*
25.4	**368**	17.7	88	675	*0.999*	393	409	0.771	*0.999*
28.6	**347**	19.3	80	690	*0.999*	369	387	0.772	*0.998*
31.8	**332**	19.4	74	689	*0.999*	351	369	0.777	*0.998*
34.9	**320**	16.6	68	642	*0.999*	338	354	0.786	*0.997*
38.1	**311**	9.8	63	517	*1.000*	327	339	0.802	*0.998*

10d Nail with GWB

Gap Thickness (mm)	Maximum Load (N)	3-Parameter Exponential Model				Asymptotic Model			
		k_1	k_0	p_1	R-square	a	b	c	R-square
0.0	**1235**	-28.9	619	1032	*0.996*	1254	1266	0.627	*0.995*
1.6	**1138**	-29.0	527	937	*0.997*	1170	1179	0.654	*0.995*
3.2	**1052**	-24.2	449	888	*0.997*	1095	1102	0.677	*0.996*
4.8	**976**	-19.7	387	849	*0.997*	1026	1034	0.695	*0.996*
6.4	**908**	-15.3	338	820	*0.997*	964	972	0.711	*0.997*
7.9	**850**	-12.6	298	787	*0.997*	909	918	0.724	*0.997*
9.5	**797**	-5.7	263	802	*0.997*	858	868	0.734	*0.997*
11.1	**751**	-2.6	236	791	*0.997*	813	825	0.744	*0.997*
12.7	**710**	0.9	214	791	*0.997*	773	786	0.751	*0.998*
14.3	**673**	6.4	194	822	*0.998*	734	749	0.757	*0.998*
15.9	**641**	11.2	178	854	*0.998*	700	716	0.762	*0.998*
17.5	**611**	18.7	163	930	*0.998*	666	685	0.764	*0.998*
19.1	**585**	23.7	152	983	*0.998*	638	658	0.767	*0.998*
22.2	**541**	32.8	133	1096	*0.998*	590	612	0.772	*0.998*
25.4	**506**	39.4	119	1189	*0.999*	550	574	0.774	*0.998*
28.6	**479**	43.3	109	1250	*0.999*	519	544	0.777	*0.998*
31.8	**457**	45.2	101	1284	*0.999*	494	519	0.780	*0.997*
34.9	**440**	41.0	94	1216	*0.999*	473	498	0.784	*0.997*
38.1	**427**	33.2	88	1078	*0.999*	456	480	0.789	*0.997*

10d Nail with Insulation

Gap Thickness (mm)	Maximum Load (N)	3-Parameter Exponential Model				Asymptotic Model			
		k_1	k_0	p_1	R-square	a	b	c	R-square
0.0	**1235**	-28.9	619	1032	*0.996*	1254	1266	0.627	*0.995*
1.6	**1134**	-28.7	525	935	*0.997*	1166	1175	0.654	*0.995*
3.2	**1045**	-23.8	446	882	*0.997*	1086	1094	0.677	*0.996*
4.8	**964**	-18.8	382	843	*0.997*	1013	1020	0.695	*0.996*
6.4	**892**	-14.8	331	807	*0.997*	947	955	0.711	*0.997*
7.9	**829**	-13.1	290	759	*0.997*	889	897	0.726	*0.997*
9.5	**773**	-6.8	254	765	*0.997*	833	843	0.737	*0.997*
11.1	**723**	-5.2	225	732	*0.997*	785	795	0.749	*0.997*
12.7	**676**	1.7	199	765	*0.997*	738	749	0.757	*0.998*
14.3	**634**	5.5	178	775	*0.997*	697	709	0.765	*0.998*
15.9	**596**	8.9	160	786	*0.998*	660	673	0.773	*0.998*
17.5	**563**	12.8	145	813	*0.998*	625	639	0.780	*0.998*
19.1	**532**	17.3	131	857	*0.998*	593	607	0.785	*0.998*
22.2	**478**	32.6	108	1075	*0.999*	531	548	0.791	*0.998*
25.4	**433**	46.0	91	1314	*0.999*	482	500	0.799	*0.998*
28.6	**395**	61.9	78	1654	*0.999*	438	457	0.805	*0.998*
31.8	**363**	94.0	67	2406	*0.999*	403	423	0.814	*0.997*
34.9	**335**	215.5	57	5418	*0.999*	374	395	0.824	*0.996*
38.1	**312**	-304.8	48	-7668	*0.998*	350	371	0.837	*0.994*

16d Nail with Insulation

Gap Thickness (mm)	Maximum Load (N)	3-Parameter Exponential Model				Asymptotic Model			
		k_1	k_0	p_1	R-square	*a*	*b*	*c*	R-square
0.0	**1437**	-42.7	748	1113	*0.995*	1442	1448	0.625	*0.992*
1.6	**1329**	-38.2	633	1035	*0.995*	1350	1352	0.653	*0.993*
3.2	**1231**	-36.2	542	952	*0.996*	1265	1267	0.676	*0.994*
4.8	**1145**	-33.6	468	886	*0.996*	1190	1191	0.697	*0.994*
6.4	**1066**	-29.8	406	837	*0.996*	1121	1123	0.715	*0.995*
7.9	**994**	-25.0	353	807	*0.996*	1057	1061	0.730	*0.996*
9.5	**929**	-21.2	311	778	*0.997*	999	1004	0.743	*0.996*
11.1	**871**	-17.2	275	759	*0.997*	946	952	0.755	*0.996*
12.7	**820**	-12.9	244	751	*0.997*	897	904	0.765	*0.997*
14.3	**772**	-5.8	217	784	*0.997*	850	859	0.773	*0.997*
15.9	**729**	0.4	195	820	*0.997*	807	818	0.780	*0.997*
17.5	**689**	6.4	175	865	*0.997*	767	780	0.787	*0.997*
19.1	**653**	10.0	159	890	*0.997*	733	747	0.794	*0.998*
22.2	**589**	22.0	132	1038	*0.998*	669	685	0.806	*0.998*
25.4	**531**	22.4	112	1028	*0.998*	629	642	0.823	*0.999*
28.6	**489**	77.0	94	2103	*0.999*	560	579	0.820	*0.998*
31.8	**449**	147.9	81	3719	*0.999*	511	532	0.823	*0.997*
34.9	**415**	562.5	71	13567	*0.999*	473	495	0.829	*0.997*
38.1	**371**	-66.5	60	-1292	*0.999*	506	518	0.869	*0.999*
44.5	**336**	-82.1	48	-1971	*0.999*	387	409	0.848	*0.994*
50.8	**299**	-35.6	35	-916	*0.997*	350	370	0.871	*0.990*